ISSN 0021-9673

VOL. 542 NO. 1 MARCH 29, 1991

JOURNAL OF CHROMATOGRAPHY

INCLUDING ELECTROPHORESIS AND OTHER SEPARATION METHODS

ELSEVIER

JOURNAL OF CHROMATOGRAPHY

Scope. The *Journal of Chromatography* publishes papers on all aspects of chromatography, electrophoresis and related methods. Contributions consist mainly of research papers dealing with chromatographic theory, instrumental development and their applications. The section *Biomedical Applications*, which is under separate editorship, deals with the following aspects: developments in and applications of chromatographic and electrophoretic techniques related to clinical diagnosis or alterations during medical treatment; screening and profiling of body fluids or tissues with special reference to metabolic disorders; results from basic medical research with direct consequences in clinical practice; drug level monitoring and pharmacokinetic studies; clinical toxicology; analytical studies in occupational medicine.

Submission of Papers. Manuscripts (in English; *four* copies are required) should be submitted to: Editorial Office of *Journal of Chromatography*, P.O. Box 681, 1000 AR Amsterdam, The Netherlands, Telefax (+31-20) 5862 304, or to: The Editor of *Journal of Chromatography, Biomedical Applications*, P.O. Box 681, 1000 AR Amsterdam, The Netherlands. Review articles are invited or proposed by letter to the Editors. An outline of the proposed review should first be forwarded to the Editors for preliminary discussion prior to preparation. Submission of an article is understood to imply that the article is original and unpublished and is not being considered for publication elsewhere. For copyright regulations, see below.

Subscription Orders. Subscription orders should be sent to: Elsevier Science Publishers B.V., P.O. Box 211, 1000 AE Amsterdam, The Netherlands, Tel. (+31-20) 5803 911, Telex 18582 ESPA NL, Telefax (+31-20) 5803 598. The *Journal of Chromatography* and the *Biomedical Applications* section can be subscribed to separately.

Publication. The *Journal of Chromatography* (incl. *Biomedical Applications*) has 38 volumes in 1991. The subscription prices for 1991 are:

J. Chromatogr. (incl. *Cum. Indexes, Vols. 501–550*) + *Biomed. Appl.* (Vols. 535–572):
Dfl. 7220.00 plus Dfl. 1140.00 (p.p.h.) (total *ca.* US$ 4976.25)

J. Chromatogr. (incl. *Cum. Indexes, Vols. 501–550*) only (Vols. 535–561):
Dfl. 5859.00 plus Dfl. 810.00 (p.p.h.) (total *ca.* US$ 3969.75)

Biomed. Appl. only (Vols. 562–572):
Dfl. 2387.00 plus Dfl. 330.00 (p.p.h.) (total *ca.* US$ 1617.25).

Our p.p.h. (postage, package and handling) charge includes surface delivery of all issues, except to subscribers in Argentina, Australia, Brasil, Canada, China, Hong Kong, India, Israel, Malaysia, Mexico, New Zealand, Pakistan, Singapore, South Africa, South Korea, Taiwan, Thailand and the U.S.A. who receive all issues by air delivery (S.A.L. — Surface Air Lifted) at no extra cost. For Japan, air delivery requires 50% additional charge; for all other countries airmail and S.A.L. charges are available upon request. Back volumes of the *Journal of Chromatography* (Vols. 1–534) are available at Dfl. 208.00 (plus postage). Claims for missing issues will be honoured, free of charge, within three months after publication of the issue. Customers in the U.S.A. and Canada wishing information on this and other Elsevier journals, please contact Journal Information Center, Elsevier Science Publishing Co. Inc., 655 Avenue of the Americas, New York, NY 10010, U.S.A., Tel. (+1-212) 633 3750, Telefax (+1-212) 633 3990.

Abstracts/Contents Lists published in Analytical Abstracts, Biochemical Abstracts, Biological Abstracts, Chemical Abstracts, Chemical Titles, Chromatography Abstracts, Clinical Chemistry Lookout, Current Contents/Life Sciences, Current Contents/Physical, Chemical & Earth Sciences, Deep-Sea Research/Part B: Oceanographic Literature Review, Excerpta Medica, Index Medicus, Mass Spectrometry Bulletin, PASCAL-CNRS, Pharmaceutical Abstracts, Referativnyi Zhurnal, Research Alert, Science Citation Index and Trends in Biotechnology.

See inside back cover for Publication Schedule, Information for Authors and information on Advertisements.

0021-9673/91/$03.50

Printed in The Netherlands

CONTENTS

(Abstracts/Contents Lists published in Analytical Abstracts, Biochemical Abstracts, Biological Abstracts, Chemical Abstracts, Chemical Titles, Chromatography Abstracts, Current Contents/Life Sciences, Current Contents/Physical, Chemical & Earth Sciences, Deep-Sea Research/Part B: Oceanographic Literature Review, Excerpta Medica, Index Medicus, Mass Spectrometry Bulletin, PASCAL-CNRS, Referativnyi Zhurnal, Research Alert and Science Citation Index)

REGULAR PAPERS

Column Liquid Chromatography

(Continued overleaf)

In articles with more than one author, the name of the author to whom correspondence should be addressed is indicated in the article heading by a 6-pointed asterisk (*)

Computer-Assisted Method Development for High-Performance Liquid Chromatography

edited by J.L. Glajch *and* L.R. Snyder

(Spin-off from the Journal of Chromatography Vol. 485 plus an additional chapter, index and glossary)

This book deals with the use of the computer as an aid in selecting adequate or optimum conditions for a given analytical separation. Originally published as Volume 485 of the Journal of Chromatography, it has now been reprinted in book form, since the information is so useful that many chromatographers want a copy readily available in the lab.
An extensive Introduction is added to the book edition. This surveys the field and refers to the pages where particular items are discussed in the book. The addition of a Glossary of Terms, an Author Index and a Subject Index make this book an invaluable source of easily consulted information for the practising chromatographer.
For the purpose of this book, computer-assisted method development will be limited to specific procedures which are intended to be used with a computer - rather than their manually applied precursors. In that sense, the subject can be considered to have begun around 1980.
The ongoing, intense research activity into various forms of computer assisted HPLC method development provides the assurance that this approach can really assist the practical chromatographer working in an industrial laboratory.

1990 xxx + 676 pages
Price: US$ 79.75 / Dfl. 175.00
ISBN 0-444-88748-2

Elsevier Science Publishers
P.O. Box 330, 1000 AH Amsterdam, The Netherlands
In the USA / Canada: P.O. Box 882, Madison Square Station, New York, NY 10159, USA

Ion Chromatography

Principles and Applications

by **P.R. Haddad,** *University of New South Wales, Kensington, N.S.W., Australia and* **P.E. Jackson,** *Waters Chromatography Division, Milford, MA, USA*

(Journal of Chromatography Library, 46)

Ion chromatography (IC) was first introduced in 1975 for the determination of inorganic anions and cations and water soluble organic acids and bases. Since then, the technique has grown in usage at a phenomenal rate. The growth of IC has been accompanied by a blurring of the original definition of the technique, so that it now embraces a very wide range of separation and detection methods, many of which bear little resemblance to the initial concept of ion-exchange separation coupled with conductivity detection.

Ion Chromatography is the first book to provide a comprehensive treatise on all aspects of ion chromatography. Ion-exchange, ion-interaction, ion-exclusion and other pertinent separation modes are included, whilst the detection methods discussed include conductivity, amperometry, potentiometry, spectroscopic methods (both molecular and atomic) and post-column reactions. The theoretical background and operating principles of each separation and detection mode are discussed in detail. A unique extensive compilation of practical applications of IC (1250 literature citations) is presented in tabular form. All relevant details of each application are given to accommodate reproduction of the method in the laboratory without access to the original publication.

This truly comprehensive text on ion chromatography should prove to be the standard reference work for researchers and those involved in the use of the subject in practical situations.

1990 798 pages
Price: US$ 191.50 / Dfl. 335.00
ISBN 0-444-88232-4

Elsevier Science Publishers
P.O. Box 211, 1000 AE Amsterdam, The Netherlands
P.O. Box 882, Madison Square Station, New York, NY 10159, USA

JOURNAL OF CHROMATOGRAPHY

VOL. 542 (1991)

JOURNAL of CHROMATOGRAPHY

INCLUDING ELECTROPHORESIS AND OTHER SEPARATION METHODS

ELSEVIER
AMSTERDAM — OXFORD — NEW YORK — TOKYO

J. Chromatogr., Vol. 542 (1991)

0021-9673/91/$03.50

Printed in The Netherlands

Journal of Chromatography, 542 (1991) 1–18
Elsevier Science Publishers B.V., Amsterdam

CHROM. 23 015

Influence of the choice of the boundary conditions on the results of the dynamic chromatography model

BINGCHANG LIN, ZIDU MA and GEORGES GUIOCHON*

* *Department of Chemistry, University of Tennessee, Knoxville, TN 37996-1600, and Division of Analytical Chemistry, Oak Ridge National Laboratory, Oak Ridge, TN 37831-6120 (U.S.A.)*

(First received February 23rd, 1990; revised manuscript received September 27th, 1990)

ABSTRACT

An investigation of the influence of the choice of the boundary conditions on the shape of the band profile obtained by simulation of the elution process using the classical model of semi-ideal chromatography is presented. As the boundary condition represents the perturbation created at the column inlet, it influences the response of the column. It is shown that the peak area is conservative only if certain conditions are satisfied. Among other approximations, the Houghton equation does not fulfil these requirements. Contour plots are used to illustrate the band migration process and the properties of these bands in non-linear chromatography.

INTRODUCTION

The choice of the boundary conditions for the integration of the partial differential equations which constitute the dynamic model of chromatography is important. These conditions must represent correctly the physical phenomena involved in the introduction of the sample. The boundary condition at the column inlet translates into mathematical terms the injection profile of the sample. At the column outlet, the boundary condition indicates whether and how reflection of the propagating wave takes place.

In this paper, we present an analysis of the influence of the boundary conditions on the zeroth-order moment of the elution of the band, *i.e.*, on its area. A discussion of the travelling character of the band during the elution process inside the column is also included. The results obtained by a series of computer simulations and a comparison with various experimental results are also described.

As the boundary condition represents the perturbation created at the column inlet by the injection of the feed, different boundary conditions must result in different band profiles. The mathematical and physical aspects of the problem are investigated and compared.

0021-9673/91/$03.50

MASS OF A COMPOUND AND THE ZEROTH MOMENT OF ITS BAND

Mass balance equation

The mass balance for a compound in a slice of a chromatographic column (slice thickness, dx), can be derived from the principle of continuity [1], which is written as

$$\frac{\partial \rho}{\partial t} + \text{div}\, \vec{J} = 0 \tag{1}$$

where ρ is the total concentration of the compound in the slice considered:

$$\rho = C + Fq \tag{2}$$

C is the concentration in the mobile phase, q the concentration in the stationary phase and F the phase ratio, *i.e.*, the ratio $(1-\varepsilon)/\varepsilon$, where ε is the porosity of the column packing. $\vec{J}$ is given by

$$\vec{J} = \vec{u}C - D\nabla C \rightarrow uC - D\frac{\partial C}{\partial x} \tag{3}$$

Further discussion of the properties of this equation requires a relationship between the mobile and stationary phase concentrations of the compound studied. It is most convenient here to continue the discussion within the framework of the semi-equilibrium models. The ideal model assumes constant equilibrium between the two phases, which is tantamount to assuming that the column has an infinite efficiency. In practice, it has been shown that the results obtained with the ideal model are an excellent first approximation of the chromatograms actually observed [2]. It has been shown also, both theoretically [3–5] and experimentally [6,7], that excellent band profile predictions are obtained with a mass balance equation which assumes constant equilibrium between the two phases and corrects for the finite efficiency of the real column by using a proper value of the coefficient of axial dispersion. This apparent diffusion coefficient, D_a, is equal to $Hu/2$, where H is the height equivalent to a theoretical plate of the real column and u the velocity of the mobile phase.

This semi-equilibrium model of chromatography permits an accurate description of the behavior of a band in a chromatographic system, its migration, broadening and change in profile, as long as the mass transfer kinetics are not very slow [2,8,9]. In this case, we have the following equation system:

$$\frac{\partial C}{\partial t} + F\frac{\partial q}{\partial t} + u\frac{\partial C}{\partial x} = D_a\frac{\partial^2 C}{\partial x^2} \tag{4}$$

with

$$q = f(C) \tag{5}$$

where $f(C)$ is the equilibrium isotherm of the compound studied between the two phases. The combination of eqns. 4 and 5 is the classical mass balance equation of the semi-ideal model of chromatography.

Mass and zeroth-order moment

The mass, m, of substance contained in the column can be derived from eqn. 2 and is given by

$$m = \int \rho dv = S \int_0^L (C + Fq)\mathrm{d}x \tag{6}$$

where v is the volume of mobile phase, L is the column length and S the cross-sectional area of the column fraction accessible to the solute, *i.e.*, the product of the geometrical volume and the total column porosity. The mass flow across a section perpendicular to the column axis is

$$S\left(uC - D_a \frac{\partial C}{\partial x}\right) \tag{7}$$

Integrating eqn. 1 or 4 along the column gives

$$\frac{\mathrm{d}m}{\mathrm{d}t} = S\left(uC - D_a \frac{\partial C}{\partial x}\right)_0 - S\left(uC - D_a \frac{\partial C}{\partial x}\right)_L \tag{8}$$

which is exactly the integrated mass balance for the whole column. Since at the end of an experiment the column is usually left under the same conditions as it was at the beginning, we have $m(t = \infty) - m(t = 0) = 0$, which can be written as

$$S \int_0^\infty \left(uC - D_a \frac{\partial C}{\partial x}\right)_0 \mathrm{d}t = S \int_0^\infty \left(uC - D_a \frac{\partial C}{\partial x}\right)_L \mathrm{d}t \tag{9}$$

Equation 9 indicates that, if we wait long enough, the whole sample will be washed out of the column.

In the particular case when the mobile phase velocity is constant and $D_a = 0$, the mass of compound injected is

$$Su \int_0^\infty C\mathrm{d}t\,|_{x=0} \tag{10}$$

and the mass of the same compound eluted from the column is

$$Su \int_0^\infty C\mathrm{d}t\,|_{x=L} \tag{11}$$

In this case, the area of the injected profile, the area of the profile $C(t)$ recorded at any position along the column and the area of the elution profile are all equal and proportional to the sample mass. In other words, when the diffusion coefficient is 0 and u is constant, the zeroth moment is conserved and is proportional to the sample mass. In liquid chromatography, the molecular diffusion coefficient, D_m, is of the order of $1 \cdot 10^{-5}$ cm^2/s, but the apparent dispersion coefficient is larger, typically of the order of $1 \cdot 10^{-3}$ cm^2/s and u is kept constant, so the condition stated above applies, and the previous analysis holds for the real world of liquid chromatography.

When D_a is significantly different from 0, however, a more complicated analysis of the implications of the classical boundary and initial conditions is required.

VARIATION OF PEAK AREA WITH COLUMN LENGTH

Eqn. 4 is a second-order partial differential equation. The solution of a well posed problem involving such an equation requires an initial and a boundary condition. In fact, the main difficulty in the use of a dispersion model of chromatography is in choosing a proper set of initial and boundary conditions which describe properly the actual physical problem. Three types of boundary conditions are used most often [10]:

First type: the injection profile is given by the equation

$$C(x = 0, t) = \psi_1(t) \tag{12}$$

Second type: the derivative of the injection profile is given by

$$\left.\frac{\partial C}{\partial x}\right|_{x=0} = \psi_2(t) \tag{13}$$

Third type: the following condition applies:

$$\alpha C(x = 0, t) + \beta \left.\frac{\partial C}{\partial x}\right|_{x=0} = \Psi_3(t) \tag{14}$$

From the uniqueness theorem, one knows that any one of these conditons can be used to determine a solution of the eqn. 4, and that the solution obtained is unique. If one attempts to use two or more conditions simultaneously, the problem is overdetermined and has no solution.

In the case of chromatography modeling, the following initial conditions are most often preferred:

$$C(x, t = 0) = q(x, t = 0) = 0 \tag{15}$$

and the boundary conditions are of the first or the third class.

As pointed out by Danckwerts [10], a boundary condition of the third class must be used when the diffusion coefficient, D_a, is not zero, and the column length is finite. A boundary condition of the first class may be used only if the column length is long enough so that the condition: $4D_a/Lu \ll 1$ is satisfied. Kreft and Zuber [11] introduced two definitions of the concentration (the resident and the flux concentrations), both at injection and detection, to specify the various initial and boundary conditions. Jönsson [12] discussed several assumptions and compared the solutions of the mass balance equation in linear chromatography for two types of first class boundary conditions, an infinitely sharp pulse in the time domain and an infinitely sharp pulse in the space (*i.e.*, column) domain.

In the following, we derive the value of the zeroth-order moment of the elution profile obtained as solution of eqn. 4 when using a boundary condition of the third or the first class, and we discuss the meaning of the result obtained.

General properties of the peak area

Integrating eqn. 4 with respect to time, from the beginning of the experiment (*i.e.*, between $t = 0$ and $t = \infty$), gives

$$\int_0^\infty \frac{\partial C}{\partial t}\,dt + F\int_0^\infty \frac{\partial q}{\partial t}\,dt + u\int_0^\infty \frac{\partial C}{\partial x}\,dt = D_a\int_0^\infty \frac{\partial^2 C}{\partial x^2}\,dt \tag{16}$$

or

$$(C + Fq)|_\infty - (C + Fq)|_0 + u\frac{dA(x)}{dx} = D_a\frac{d^2A(x)}{dx^2} \tag{17}$$

where

$$A(x) = \int_0^\infty C(x,t)dt \tag{18}$$

$A(x)$ is the local peak area. Our problem now is to show that it is independent of x, under certain conditions.

Since

$$(C + Fq) = 0 \text{ when } t = \infty \tag{19}$$

and

$$(C + Fq) = g_i(x) \text{ when } t = 0 \tag{20}$$

where $g_i(x)$ is the initial condition. Eqn. 17 becomes

$$-g_i(x) + u\frac{dA}{dx} = D_a\frac{d^2A}{dx^2} \tag{21}$$

$g_i(x)$ represents the initial distribution of the compound in the column, before the injection is made. If $g_i(x) = 0$, the condition is called homogenized. This is the condition which applies in almost all practical aplications of chromatography.

The solution of eqn. 21 is

$$A(x) = C_1(x)\exp(ux/D_a) + C_2(x) \tag{22}$$

Using the classical method of the variation of constant, we obtain

$$\frac{dC_1(x)}{dx}\frac{u}{D_a}\exp(ux/D_a) = -\frac{g_i(x)}{D} \tag{23}$$

and:

$$\frac{dC_1(x)}{dx}\exp(ux/D_a) + \frac{d}{dx}C_2(x) = 0 \tag{24}$$

The solutions of eqns. 23 and 24 are

$$C_1(x) = -\frac{1}{u}\int_0^x g_i(x)\exp(-ux/D_a)dx + C_{1,0} \tag{25}$$

and

$$C_2(x) = \frac{1}{u}\int_0^x g_i(x)dx + C_{2,0} \tag{26}$$

Combining eqns. 22, 25 and 26 gives

$$A(x) = C_{1,0}\exp(-ux/D_a) + C_{2,0} - \frac{1}{u}\exp(ux/D_a)\int_0^x g_i(x)\exp(-ux/Da)dx + \\ + \frac{1}{u}\int_0^x g_i(x)dx \tag{27}$$

Eqn. 27 is the fundamental result in this paper. It represents the variation of the peak area during its migration along the column. It shows that the peak area depends on the boundary conditions, through the constants $C_{1,0}$ and $C_{2,0}$, and on the initial condition, through $g_i(x)$. In fact, $S\int_0^L g_i(x)dx = m(t=0)$.

Peak area under third class boundary condition

The boundary conditions used in this case are formulated as follows, at the column inlet:

$$uC - D_a\frac{\partial C}{\partial x} = uC_k,\ x = 0 \tag{28}$$

and at the column outlet:

$$\frac{\partial C}{\partial x} = 0,\ x = L \tag{29}$$

where C_k is a constant concentration. This is the Danckwerts boundary condition [10]. Integrating eqn. 28 between the beginning and the end of the experiment gives

$$D_a\frac{dA(x)}{dx}\bigg|_{x=0} = uA(0) - uA_k \tag{30}$$

where $A_k = \int_0^\infty C_k \mathrm{d}t$. Integrating the other boundary condition (eqn. 29) gives

$$\left.\frac{\mathrm{d}A}{\mathrm{d}x}\right|_{x=L} = 0 \tag{31}$$

Combining eqns. 27, 28, 30 and 31 permits the calculation of the constants $C_{1,0}$ and $C_{2,0}$ in eqns. 25 and 26:

$$C_{1,0} = \frac{1}{u}\int_0^L g_i(x)\exp(-ux/D_a)\mathrm{d}x \tag{32}$$

and

$$C_{2,0} = A_k \tag{33}$$

Finally, equation 27 becomes:

$$A(x) = \frac{1}{u}\exp(ux/D_a)\int_x^L g_i(x)\exp(-ux/D_a)\mathrm{d}x + \frac{1}{u}\int_0^x g_i(x)\mathrm{d}x + A_k \tag{34}$$

From eqn. 34, we can derive the value of the function A at both ends of the column:

$$A(0) = A_k + \frac{1}{u}\int_0^L g_i(x)\exp(-ux/D_a)\mathrm{d}x \tag{35}$$

and

$$A(L) = A_k + \frac{1}{u}\int_0^L g_i(x)\mathrm{d}x \tag{36}$$

Accordingly,

$$A(L) - A(0) = \frac{1}{u}\int_0^L g_i(x)[1 - \exp(-ux/D_a)]\mathrm{d}x \tag{37}$$

Obviously, when $g_i(x) = 0$, which is true in chromatography, we have $A(L) = A(0)$. This demonstrates that the zeroth-order moment of the band remains constant during its migration throughout the column if the initial condition is homogeneous (*i.e.*, if dthere is nothing in the column before the injection is made).

Peak area under first class boundary condition

The boundary conditions are now written as follows, at the column inlet:

$$c(x,t) = \psi(t),\ x = 0 \tag{38}$$

and at the column outlet, for an infinitely long column:

$$c(x,t) \text{ is finite when } x \to \infty \tag{39}$$

From eqn. 38, we have

$$A(0) = \int_0^\infty \psi(t)\mathrm{d}t \tag{40}$$

Combining eqns. 27 and 40 gives (see also eqn. 22):

$$C_{1,0} + C_{2,0} = \int_0^\infty \psi(t)\mathrm{d}t \tag{41}$$

From eqns. 27 and 39, it results that, in order to have $C(x,t)$ and hence $A(x)$ finite, we *must have*

$$C_{1,0} = 0 \tag{42}$$

and

$$C_{2,0} = \int_0^\infty \psi(t)\mathrm{d}t \tag{43}$$

Combination of eqns. 27, 42 and 43 gives

$$A(x) = \int_0^\infty \psi(t)\mathrm{d}t - \frac{1}{u}\exp(ux/D_a)\int_0^x g_i(x)\exp(-ux/D_a)\mathrm{d}x + \frac{1}{u}\int_0^x g_i(x)\mathrm{d}x \tag{44}$$

From eqn. 44, we derive the value of A at both ends of the column:

$$A(L) = \int_0^\infty \psi(t)\mathrm{d}t - \frac{1}{u}\exp(uL/D_a)\int_0^L g_i(x)\exp(-ux/D_a)\mathrm{d}x + \frac{1}{u}\int_0^L g_i(x)\mathrm{d}x \tag{45}$$

and

$$A(0) = \int_0^\infty \psi(t)\mathrm{d}t \tag{46}$$

and, finally,

$$A(L) - A(0) = -\frac{1}{u}\exp(uL/D_a)\int_0^L g_i(x)\exp(-ux/D_a)\mathrm{d}x + \frac{1}{u}\int_0^L g_i(x)\mathrm{d}x \tag{47}$$

Eqn. 47 is identical with eqn. 37. We have

$$A(L) = A(0), \text{ if } g_i(x) = 0$$

In chromatography, the zeroth-order moment remains constant all along the column if the initial condition is homogeneous.

Peak area in the case of the Houghton approximate equation

Houghton [13] obtained an analytical solution of the mass balance equation of chromatography (eqn. 4) by making two assumptions. First, he assumed a parabolic isotherm, *i.e.*, replaced the isotherm by its three-term expansion around the origin (see eqn. 53). Second, he used the Cole–Hopf transform [1] in order to replace the mass balance equation (eqn. 4) by a Burger equation, for which an analytical solution can be obtained [13–16]. This requires, however, another assumption, that the factor $(1 + \lambda C)^{-1}$ (see eqn. 50) in the mass balance equation can be replaced by 1. As a consequence of these two assumptions, the analytical solution obtained has physical significance only for small concentrations. Potentially more troublesome, however, is the fact that the Burger equation (*i.e.*, the equation really solved) has lost the conservation property of eqn. 4, because of the simplification made. Since the non-conservation behavior of the Houghton equation has been reported [17,18], it is interesting to apply the same analysis as above and to investigate the extent of the variation of the zeroth-order moment of the band profile during the band migration. The equation derived by Houghton [13] may be written as

$$\frac{\partial C}{\partial t} - \lambda U C \frac{\partial C}{\partial \xi} = E_0 \frac{\partial^2 C}{\partial \xi^2} \tag{48}$$

with

$$U = \frac{u}{1 + \dfrac{K_1}{\varepsilon}} \tag{49}$$

$$\lambda = \frac{2K_2/\varepsilon}{1 + \dfrac{K_1}{\varepsilon}} \tag{50}$$

$$E_0 = \frac{D_a}{1 + \dfrac{K_1}{\varepsilon}} \tag{51}$$

$$\xi = x - Ut;\ x = \xi + Ut \tag{52}$$

where $1/\varepsilon = F$ and K_1 and K_2 are the coefficients of the parabolic adsorption isotherm, which is used for the investigation of the onset of column overload behavior. This isotherm is written as

$$q = K_0 + K_1 C + K_2 C^2 \tag{53}$$

where K_0 is constant and usually equal to 0. The initial and boundary conditions assumed by Houghton [13] are

$$\begin{aligned} C(0,x) &= g_{1,i}(x) = C_0 \text{ if } |x| < L_0/2 \\ C(0,x) &= 0 \text{ if } |x| > L_0/2 \end{aligned} \tag{54}$$

and

$$\begin{aligned} q(0,x) &= g_{2,i}(x) = K_1 C_0 + K_2 C_0^2 \text{ if } |x| < L_0/2 \\ q(0,x) &= g_{2,i}(x) = 0 \text{ if } |x| > L_0/2 \end{aligned} \tag{55}$$

In eqn. 48, we have $\partial C/\partial t = \partial C/\partial t|_{\xi=\text{constant}}$. Further, we know that

$$\left.\frac{\partial C}{\partial t}\right|_{\xi} = \left.\frac{\partial C}{\partial t}\right|_{x} + U \frac{\partial C}{\partial x} \tag{56}$$

and

$$\left.\frac{\partial C}{\partial x}\right|_{t} = \left.\frac{\partial C}{\partial \xi}\right|_{t} \tag{57}$$

Combining eqns. 48, 56 and 57 gives

$$\left(1 + \frac{K_1}{\varepsilon}\right)\frac{\partial C}{\partial t} + u\frac{\partial C}{\partial x} - \lambda u C \frac{\partial C}{\partial x} = D_a \frac{\partial^2 C}{\partial x^2} \tag{58}$$

Eqn. 58 is the Houghton approximate equation in the (x, t) space coordinate. Hence the differential of the mass density represented by the Houghton equation can be written as

$$\frac{\partial \rho}{\partial t} = \left(1 + \frac{K_1}{\varepsilon} + \frac{2K_2 C}{\varepsilon}\right)\frac{\partial C}{\partial t} \tag{59}$$

Combining eqns. 58 and 59 gives

$$\frac{\partial \rho}{\partial t} = -u\frac{\partial C}{\partial x} + D_a \frac{\partial^2 C}{\partial x^2} + \lambda^2 u C^2 \frac{\partial C}{\partial x} + \lambda D_a C \frac{\partial^2 C}{\partial x^2} \tag{60}$$

It is obvious that the solution of the Houghton equation is different from that of the mass balance equation (eqn. 1). The difference is due to the terms $\lambda^2 uC^2\ \partial C/\partial x$ and $\lambda DC\ \partial^2 C/\partial x^2$. Since $\lambda C \ll 1$, $\lambda^2 C^2$ is still smaller and the term in $\lambda^2 C^2$ can be ignored.

Integrating eqn. 60 with respect to x and t, multiplying the two sides by the cross-sectional area, S, and ignoring the term in $\lambda^2 C^2$, we obtain

$$m(t = \infty) - m(t = 0) = Su[A(L) - A(0)] + \\ + SuD_a \int_0^\infty \left[\left(\frac{\partial C}{\partial x} \right)\Big|_L - \left(\frac{\partial C}{\partial x} \right)\Big|_0 \right] dt + Su\lambda D_a \int_0^\infty \int_0^L C \frac{\partial^2 C}{\partial x^2} dx dt \quad (61)$$

From partial integration of eqn. 61, we obtain

$$\int_0^L C \frac{\partial^2 C}{\partial x^2} dx = \int_0^L C d \frac{\partial C}{\partial x} = \left(C \frac{\partial C}{\partial x} \right)\Big|_0^L - \int_0^L \left(\frac{\partial C}{\partial x} \right)^2 dx \quad (62)$$

We combine eqns. 61 and 62 and consider that $m(\infty) - m(0) = 0$. Since in the case of the Houghton equation the injection is very narrow, $L_0/2$ is small and the initial condition is still a Dirac δ pulse. Therefore, we may integrate from $x = L_0/2$ and the boundary condition is still homogeneous. Thus, we have

$$A(L) - A(0) = D_a \int_0^\infty \left[\left(\frac{\partial C}{\partial x} \right)\Big|_L - \left(\frac{\partial C}{\partial x} \right)\Big|_0 \right] dt + \\ + \lambda D_a \int_0^\infty \left(C \frac{\partial C}{\partial x} \right)\Big|_0^L dt - \lambda D_a \int_0^\infty \int_0^L \left(\frac{\partial C}{\partial x} \right)^2 dx dt \quad (63)$$

For the finite column, the Danckwerts condition (eqns. 28 and 29) can be considered. This gives

$$A(L) - A(0) = -D_a \int_0^\infty \left(\frac{\partial C}{\partial x} \right)\Big|_{x=0} (1 - \lambda C_0) dt - \lambda \int_0^\infty \int_0^L \left(\frac{\partial C}{\partial x} \right)^2 dx dt \quad (64)$$

Since we have $\lambda C \ll 1$, we can write:

$$A(L) - A(0) = -D_a \int_0^L \lambda \int_0^L \left(\frac{\partial C}{\partial x} \right)^2 dx dt - D_a \int_0^\infty \left(\frac{\partial C}{\partial x} \right)_0 dt \quad (65)$$

Usually, $\partial C/\partial x$ is large in non-linear chromatography, at least in some concentration range, *e.g.*, on the front of elution bands when the isotherm is Langmuirian. Thus, we may expect the absolute value of the term $\lambda \int_0^L (\partial C/\partial x)^2 dx$ to be larger than that of $(\partial C/\partial x)_{x=0}$. Therefore, the sign of the difference $A(L) - A(0)$ is determined by the sign of λ.

When the isotherm is convex, such as with a Langmuir isotherm, $\lambda < 0$ and the eluted band has a lower area than the injected band. In fact, the area of the eluted band decreases with increasing column length [5]. The opposite is true for a concave or an S-shaped isotherm. This loss or gain of zeroth moment, which should not be mistaken

for an apparent loss or gain in sample mass, occurs because the analytical solution of eqn. 48 is not a solution of eqn. 4, owing to the simplification introduced in the derivation of eqn. 48.

When $\lambda = 0$, we have linear chromatography and eqn. 58 is identical with eqn. 4. Comparison between eqn. 9 and eqns. 37 and 47 shows that when $g_i(x) = 0$,

$$\int_0^\infty \left(\frac{\partial C}{\partial x}\right)\Big|_0 dt = \int_0^\infty \left(\frac{\partial C}{\partial x}\right)\Big|_L dt$$

and, from eqn. 63, we have always $A(L) = A(0)$.

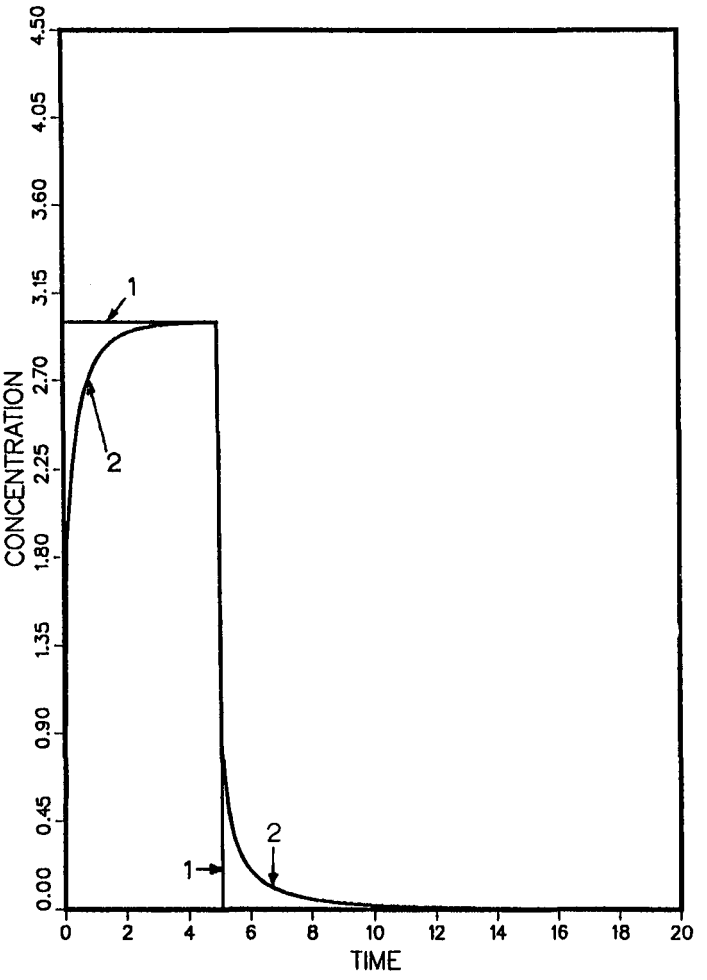

Fig. 1. Injection profiles corresponding to two different boundary conditions. 1 = plug (first kind) condition; 2 = Danckwerts (third type) conditions. Time in seconds, concentrations in mM.

INFLUENCE OF BOUNDARY CONDITIONS ON BAND MIGRATION

The previous discussion has shown that the peak area (*i.e.*, the zeroth-order moment) is not necessarily a quantity conserved by eqn. 4, contrary to general belief. Even for rigorous solutions of eqn. 4, the zeroth moment may change and this change still remains consistent with the mass conservation law. Hence the peak area does not always represent the mass of the compound analyzed. The band area is related to the mass of compound injected, however, and under certain conditions it remains constant during the migration of the band.

The choice of the boundary conditions has an effect on the retention time and the profile of the eluted band. Fig. 1 shows the injection profiles corresponding to the pulse (first type) and the Danckwerts (third type) boundary conditions. In the latter instance, the boundary condition includes a diffusion term (see eqn. 28), and Fig. 1 shows the plot of $C(t)$ at the column inlet which corresponds to that condition. The differences in the front and tail of the injection profiles are significant and explain why different profiles may be recorded for the injection of the same amount of sample using one boundary condition or the other, if the width of the injection pulse profile and especially the rise and decay times of the Danckwerts boundary condition are significant compared with the retention time. The Danckwerts condition is certainly much more realistic than the pulse condition.

To illustrate the influence of the boundary conditions, we determined the contour plots of the band migration, using a computer program previously developed to calculate numerical solutions of eqn. 4 [19] and suitably modified to include the boundary conditions required. These contour plots are the isoconcentration contours projected on a (t, x) plane. A section of these plots by a vertical plane at t = constant gives the concentration profile of the band inside the column at that given time. A section of the same contour plot by a vertical plane at x = constant gives the elution profile through the column section at that abscissa. The contour plot gives the trail of a concentration wavelet in the column, from its entrance to its exit.

Fig. 2 shows the contour plot for a very small diffusion coefficient and a linear isotherm. Then the wavelet moves linearly. The slope of the trajectories of the different wavelets are the same, as they have all the same velocity. Figs. 3–5 show the contours in the case of a non-linear isotherm. Fig. 3 corresponds to a plug injection (first type of boundary conditions), and Figs. 4 and 5 correspond to the same Dankwerts boundary condition and to different values of the axial dispersion coefficient in the column. As the isotherm is not linear, the velocity of a wavelet, *i.e.*, the velocity associated with a concentration [20], depends on this concentration and the trails are not linear. The parallel lines in the upper part of the figures correspond to the migration of the shock layer of the band [20]. The lines which leave the time axis beyond *ca.* 1 min and diverge correspond to the band tail, *i.e.*, the non-sharpening part of the profile. In each instance, the inner curvilinear triangle, at the bottom left of the figures, corresponds to the decay of the injection profile plateau. Beyond that first profile, the apex of each curvilinear triangle corresponds to a band maximum. These apices mark the trajectory of the band maximum and its decay.

The location of the countour lines in Figs. 3 and 4, which differ only by the boundary condition, are slightly different and the overall effect is small. The influence of the axial dispersion on the contour map is illustrated by a comparison between Figs.

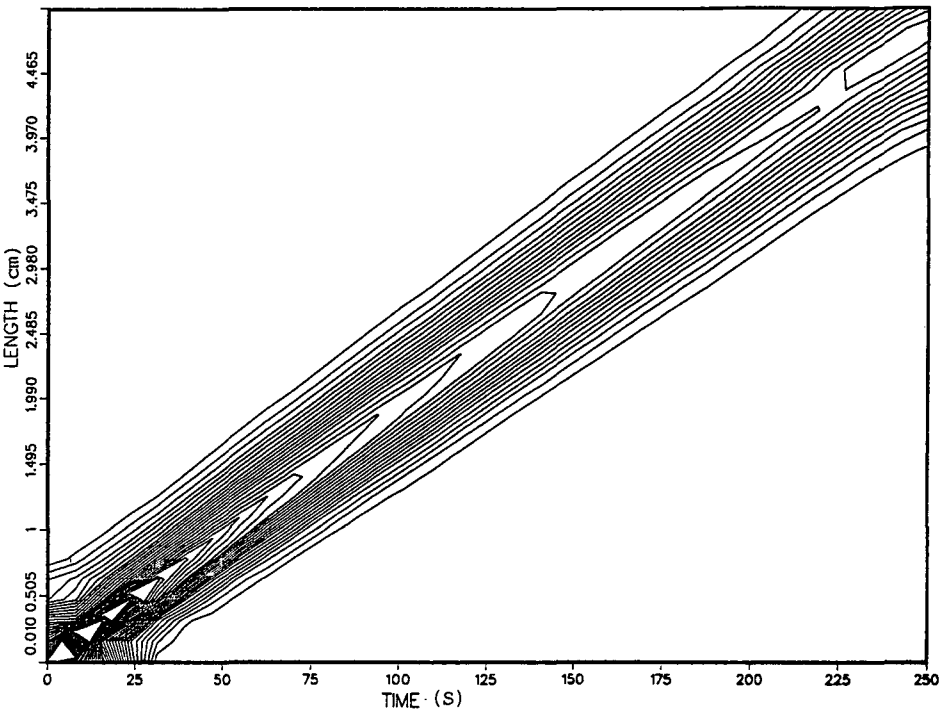

Fig. 2. Concentration contour plots corresponding to a linear isotherm. The moire effect around the origin is a graph artefact. Note the parallel lines corresponding to isokinetic concentration trajectories. Pulse injection (see Fig. 1). Apparent dispersion coefficient, $D_a = 0.0012$ cm^2/s.

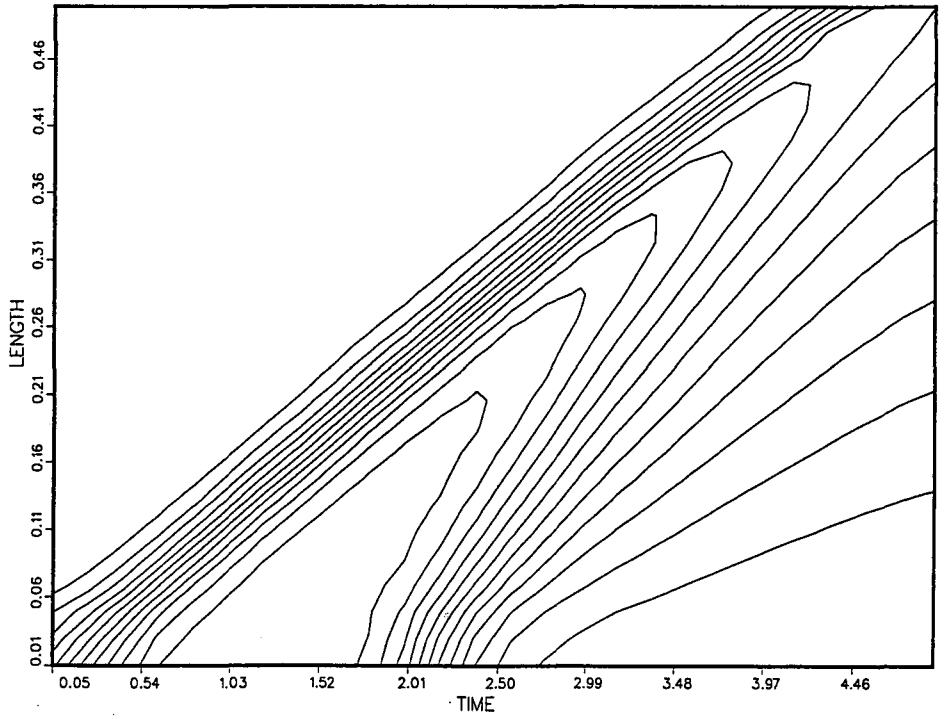

Fig. 3. Concentration contour plots corresponding to a non-linear isotherm and to a first type inlet boundary condition (see Fig. 1). Same conditions as for Fig. 2.

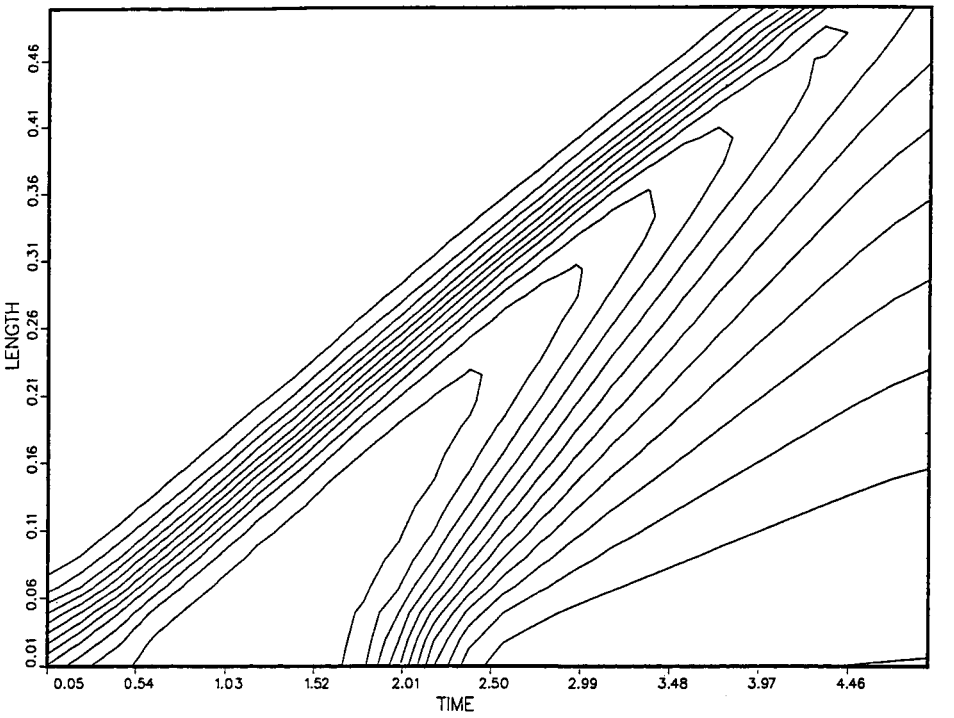

Fig. 4. Concentration contour plots corresponding to a non-linear isotherm and to a third type (Danckwerts) inlet boundary condition (see Fig. 1). Same conditions as for Fig. 2.

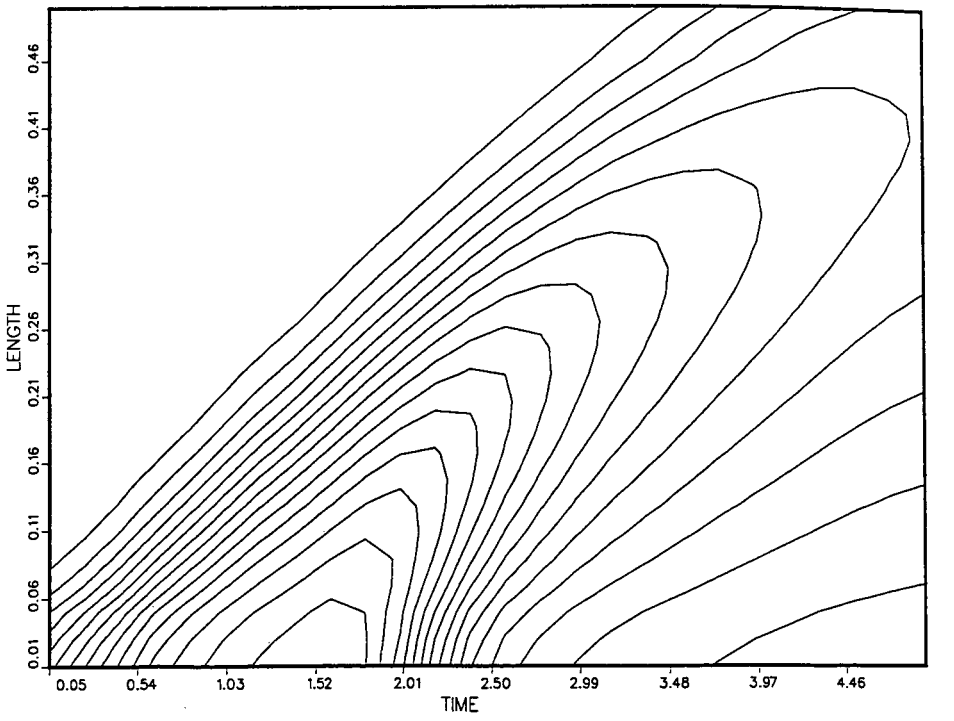

Fig. 5. Concentration contour plots corresponding to a non-linear isotherm and to a third type (Danckwerts) inlet boundary condition. Same conditions as for Fig. 2, except $D_a = 0.012$ cm^2/s.

4 and 5. In the latter figure (axial dispersion ten times as large as for Fig. 4), the self-sharpening effect on the band front is much less acute than in Fig. 4. The shock layer is much thicker.

Fig. 6 shows the elution profiles corresponding to the two boundary conditions at the end of a 5-cm long column (see injection profile in Fig. 1). The effect is important. The retention time is longer and the profile is wider, shorter and tails longer with the Danckwerts boundary condition than with the pulse injection. Such an effect should be expected on comparing the two profiles in Fig. 1. This phenomenon arises because of the influence of diffusion on the injection profile. In practice, the Danckwerts injection is a more realistic model than the plug injection.

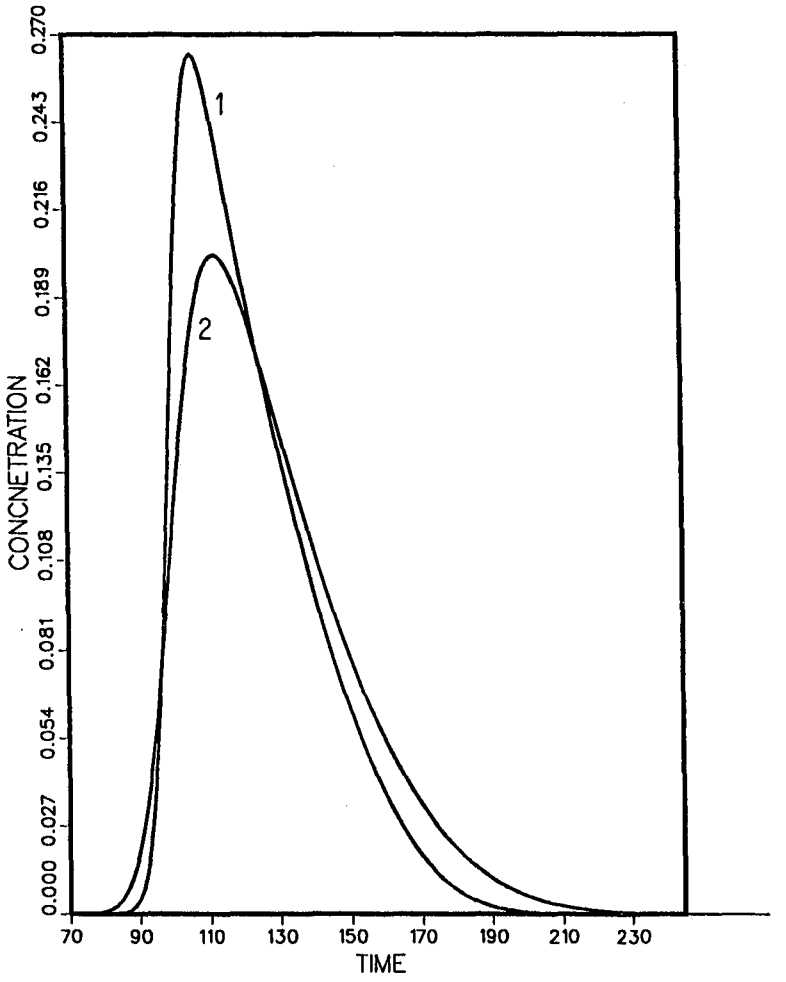

Fig. 6. Effect of the nature of the inlet boundary condition on the retention time and the shape of the elution profile. Both profiles were generated with $h = 0.01$ cm, $\tau = 0.01$ s, $L = 5$ cm. See injection profiles in Fig. 1. 1 = Plug injection; 2 = Danckwerts condition.

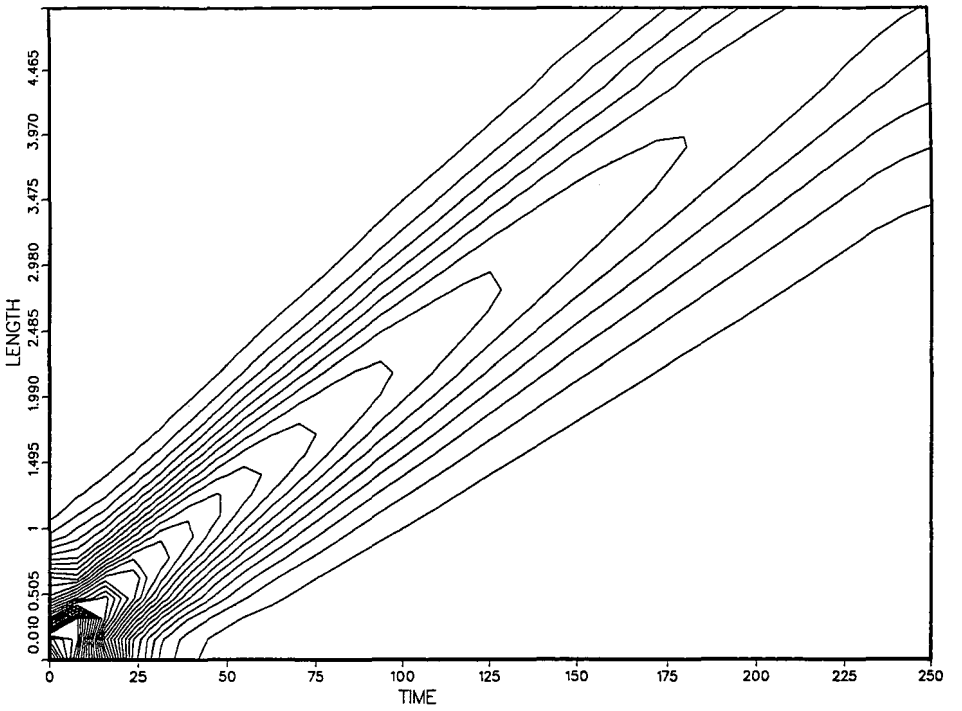

Fig. 7. Same as Fig. 2, except infinite outlet boundary condition.

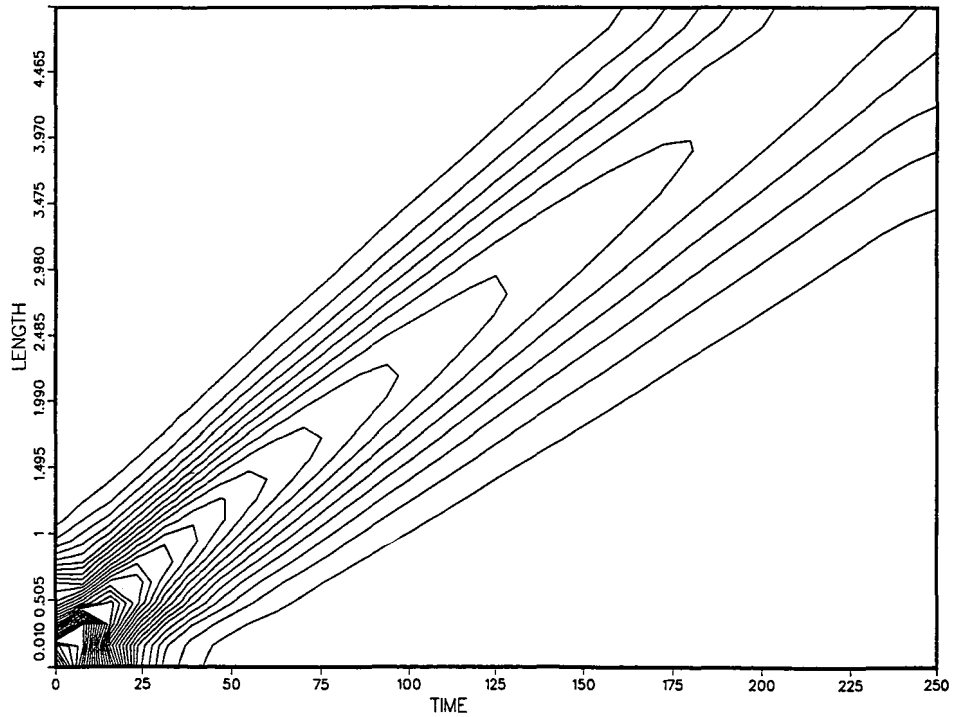

Fig. 8. Same as Fig. 2, except finite outlet boundary condition.

Finally, Figs. 7 and 8 compare the effects of the outlet boundary conditions. In Fig. 7 the boundary condition assumes an infinite column length. In Fig. 8, the column length is finite, *i.e.*, $\partial C/\mathrm{d}x|_L = 0$. In the latter instance, the contour lines are bent upwards near the column exit. The choice of a correct outlet boundary condition appears to be relevant when simulating the behavior of chromatographic columns and looking for the determination of the optimum column length for maximum production under some constraint of product purity [21].

ACKNOWLEDGEMENTS

This work was supported in part by Grant CHE-8901382 of the National Science Foundation and by the cooperative agreement between the University of Tennessee and the Oak Ridge National Laboratory. We acknowledge support of our computational effort by the University of Tennessee Computing Center.

REFERENCES

1 J. H. Seinfeld and L. Lapidus, *Mathematical Methods in Chemial Engineering*, Vol. 3, Prentice-Hall, Englewood Cliffs, NJ, 1974.
2 S. Golshan-Shirazi and G. Guiochon, *Anal. Chem.*, 60 (1988) 2364.
3 P. C. Haarhoff and H. J. Van der Linde, *Anal. Chem.*, 38 (1966) 573.
4 G. Guiochon, S. Golshan-Shirazi and A. Jaulmes, *Anal. Chem.*, 60 (1988) 1856.
5 S. Golshan-Shirazi and G. Guiochon, *J. Chromatogr.*, 506 (1990) 495.
6 S. Golshan-Shirazi, S. Ghodbane and G. Guiochon, *Anal. Chem.*, 60 (1988) 2630.
7 S. Golshan-Shirazi and G. Guiochon, *Anal. Chem.*, 60 (1988) 2634.
8 J. J. Van Deemter, F. J. Zuiderweg and A. Klinkenberg, *Chem. Eng. Sci.*, 5 (1956) 271.
9 J. C. Giddings, *The Dynamics of Chromatography*, Marcel Dekker, New York, 1964.
10 P. V. Danckwerts, *Chem. Eng. Sci.*, 2 (1953) 1.
11 A. Kreft and A. Zuber, *Chem. Eng. Sci.*, 33 (1978) 1471.
12 J. Å. Jönsson, *Chromatographia*, 18 (1984) 427.
13 G. Houghton, *J. Phys. Chem.*, 67 (1963) 84.
14 G. B. Whitham, *Linear and Non-Linear Waves*, Wiley, New York, 1974.
15 G. V. Yaroshenkova, S. A. Volkov and K. Z. Sakodynski, *J. Chromatogr.*, 198 (1980) 377.
16 A. Jaulmes, C. Vidal-Madjar, A. Ladurelli and G. Guiochon, *J. Chem. Phys.*, 88 (1984) 5379.
17 A. Jaulmes, C. Vidal-Madjar, H. Colin and G. Guiochon, *J. Chem. Phys.*, 90 (1986) 207.
18 A. Jaulmes, J. M. Gonzales, C. Vidal-Madjar and G. Guiochon, *J. Chromatogr.*, 387 (1987) 41.
19 B. Lin, Z. Ma and G. Guiochon, *Sep. Sci. Technol.*, 24 (1989) 809.
20 B. Lin, S. Golshan-Shirazi and G. Guiochon, *Anal. Chem.*, 60 (1988) 2647.
21 S. Golshan-Shirazi and G. Guiochon, *Anal. Chem.*, 61 (1989) 1368 and 2464.

Journal of Chromatography, 542 (1991) 19–28
Elsevier Science Publishers B.V., Amsterdam

CHROM. 23 056

Equilibria of biomolecules on ion-exchange adsorbents

E. A. JAMES and D. D. DO*
Department of Chemical Engineering, The University of Queensland, Queensland 4072 (Australia)
(First received August 14th, 1990; revised manuscript received December 18th, 1990)

ABSTRACT

Equilibrium adsorption isotherms of bovine serum albumin on DEAE-Sepharose Fast Flow ion exchanger were studied with different salt concentrations and buffer strengths at varying pH using a batch method. An extended Langmuir–Freundlich isotherm equation was used to fit these data and other experimental data taken from the literature. It was found that the model correctly approximates the adsorption of various proteins and amino acids at different salt concentrations using a single set of parameters.

INTRODUCTION

Ion-exchange chromatography continues to play a major role in the recovery and purification of biomolecules in the biotechnology industry. Optimisation of chromatographic operations such as adsorption, selective elution and regeneration becomes increasingly important as systems are scaled up. Currently, considerable work is being done to characterize and model the fundamental adsorption processes occurring in bioseparation systems. Studies of adsorption isotherms have been applied as a method of characterizing the ion-exchange adsorption of biomolecules at different pH values and mobile phase ionic strengths. Measurements of protein equilibria tend to be correlated differently to those of amino acids. The equilibrium dissociation reactions of amino acids are well characterized, and have been incorporated into ion-exchange equilibria models using the mass action law. Carta *et al.* [1] examined the equilibrium uptake of amino acids by a strong cation exchanger and found an excellent fit of binary exchange data. Similar results were obtained by Yu *et al.* [2] and also by Sanders *et al.* [3].

Protein ion exchange operates on the same principle as amino acid adsorption; however, due to the extreme complexity of the interactions involved, a more empirical approach must be used. Huang and Horváth [4] used the Langmuir adsorption model for fitting equilibrium isotherms of proteins on cation exchangers. Huang *et al.* [5] found the Langmuir equation inadequate for some proteins due to the extremely steep initial slope of the adsorption isotherm. These isotherms were better approximated with a Langmuir equation which incorporated two types of non-cooperative independent adsorption sites. Whitley *et al.* [6] fit protein adsorption data using the Langmuir isotherm, but also used a model incorporating mass action parameters to allow for dependence on salt concentration.

0021-9673/91/$03.50

In this article, we incorporate salt concentration into an extended form of the Langmuir–Freundlich equation to predict the dependence of salt on ion-exchange adsorption isotherms for both amino acids and proteins.

THEORY

The simplest theoretical model for monolayer adsorption was proposed by Langmuir [7] to describe the adsorption of gases on surfaces. This convenient model (eqn. 1) is based on the assumption that the adsorbed molecule is held at localized sites and the energy of adsorption is constant over all sites. It is often used to describe adsorption phenomena in biological systems even though the parameters may lose some of their physical meaning. Experimental adsorption data are typically fitted for a particular mobile phase composition:

$$q = \frac{q_{\max}\ b\ C}{1 + b\ C} \tag{1}$$

where q = adsorbed solute concentration (mol/unit adsorbent), $q_{\max}$ = maximum concentration of adsorbed solute (mol/unit adsorbent), b = Langmuir equilibrium constant and C = liquid phase concentration (mol/unit solution).

Another well known adsorption model is derived from the Langmuir equation but uses a distribution of adsorption energies for the surface sites. Using an exponential decay function to represent this distribution, Zeldowitsch [8] derived an approximate solution (eqn. 2) known as the Freundlich isotherm. For values of η (power term of Freundlich isotherm) greater than 1 the isotherm shape is favorable (convex), and for values of η less than 1 the isotherm shape is unfavorable (concave). When η equals 1 the isotherm is linear.

$$q = K\ C^{1/\eta} \tag{2}$$

where K = Freundlich equilibrium constant.

A limitation of Freundlich isotherm is that the amount adsorbed increases indefinitely with the concentration in solution. To solve this inadequacy the Langmuir and Freundlich isotherms may be combined (eqn. 3). Because this equation contains two fitting terms, it is much better for approximating adsorption of a heterogeneous nature.

$$q = \frac{q_{\max}\ b\ C^{1/\eta}}{1 + b\ C^{1/\eta}} \tag{3}$$

The Langmuir isotherm can be readily extended to an n-component mixuture, and has been used to describe mixed gas adsorption by Markham and Benton [9]. For gaseous systems, the equation implies a competition for free homogeneous sites on the adsorbent surface.

$$q_i = \frac{q_{\max i}\ b_i\ C_i}{1 + \sum_{j=1}^{n} b_j\ C_j} \tag{4}$$

When the extended Langmuir model may proves inadequate in prediction of mixture equilibria, the equation can be modified by the introduction of a power law of the Freundlich form [10], also commonly known as a loading ratio:

$$q_i = \frac{q_{maxi}\ b_i\ C_i^{1/\eta_i}}{1 + \sum_{j=1}^{n} b_j\ C_j^{1/\eta_j}} \tag{5}$$

It should be noted that these equations are not thermodynamically consistent and cannot then be expected to apply over the entire concentration range. Nevertheless, the expressions have been shown to provide a reasonably good empirical correlation of binary equilibrium data,

EXPERIMENTAL

Materials

DEAE-Sepharose Fast Flow, a weak anion exchanger, was purchased from Sigma (St. Louis, MO, U.S.A.). This ion exchanger is a macroporous gel composed of agarose which has been used in large-scale applications because of its cost and good stability. Protein used in this study, bovine serum albumin (A-7906), was purchased from Sigma. The two buffers, tris(hydroxymethyl)aminomethane (Tris) adjusted with hydrochloric acid to the required pH and sodium acetate adjusted with acetic acid were also purchased from Sigma. Sodium chloride was purchased from BDH (Kilsyth, Australia).

Batch experiments

For measurements by the batch method, a series of protein solutions having different concentrations was prepared and placed in individual microcentrifuge tubes with the anion exchanger. The tubes were gently rotated end-over-end for 4 h. Afterwards, the slurry was centrifuged, and the protein concentration of the supernatant was measured by analytical high-performance liquid chromatography (HPLC) at 280 nm.

Equipment and HPLC analysis

For HPLC analysis of proteins a Backman System Gold chromatographic system (San Ramon, CA, U.S.A.), consisting of a Model 126 dual-pump programmable solvent module, a Model 167 scanning detector module-167 and a Model 210A sample injection valve, was used. Sample sizes of 20 μl were analysed using a 75 mm $\times$ 7.5 mm TSK-DEAE-5PW column from Toya Soda (Tanda, Japan) with 10 m*M* Tris–HCl buffer (pH 7.8), containing 50 m*M* sodium chloride as the mobile phase.

RESULTS AND DISCUSSION

Analysis

For our purposes, we treat the adsorption of a biomolecule in the presence of a salt as a binary equilibria system (eqn. 4). Experimental isotherm data and isotherm

data from the literature were analysed using a non-linear curve-fitting program in SigmaPlot 4.01 (Jandel Scientific). A single set of best-fit parameter values were found for adsorption data at different salt concentrations.

$$q_{bio} = \frac{q_{max}\ b_{bio}\ C_{bio}^{1/\eta_{bio}}}{1 + b_{bio}\ C_{bio}^{1/\eta_{bio}} + b_{salt}\ C_{salt}^{1/\eta_{salt}}} \tag{6}$$

The subscripts "bio" and "salt" stand for biomolecule and displacing salt molecule, respectively.

Alternatively, eqn. 6 may be rearranged (eqn. 7), to give a single component Langmuir–Freundlich isotherm.

$$q_{bio} = \frac{q_{max}\ b^*\ C_{bio}^{1/\eta_{bio}}}{1 + b^*\ C_{bio}^{1/\eta_{bio}}} \tag{7}$$

If the experimental data is analyzed using this more traditional method, the equilibrium constant b^* should show the following dependence on salt concentration:

$$b^* = \frac{b_{bio}}{1 + b_{salt}\ C_{salt}^{1/\eta_{salt}}} \tag{8}$$

Experimental isotherms

The equilibrium binding isotherms for bovine serum albumin (BSA) were measured at different salt concentration on DEAE-Sepharose Fast Flow. Isotherms

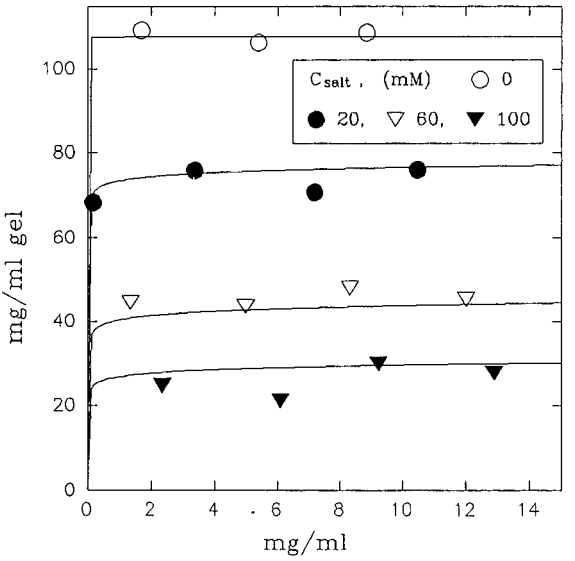

Fig. 1. Extended Langmuir–Freundlich isotherms for the uptake of BSA on the weak anion exchanger (DEAE-Sepharose Fast Flow), in Tris–HCl buffer (12 m*M*) at pH 9.1, at various sodium chloride concentrations.

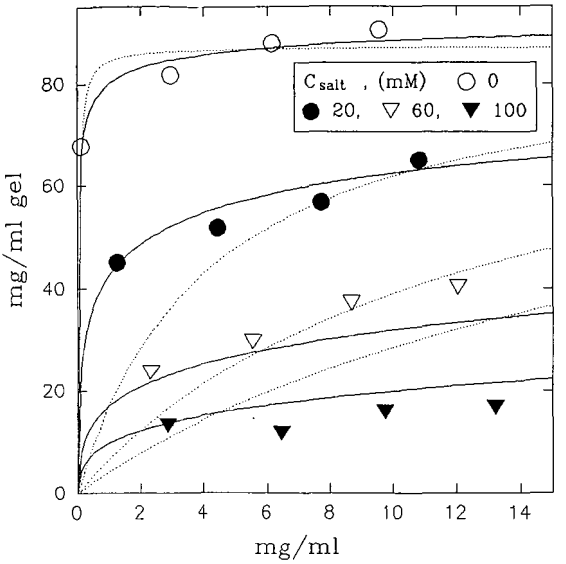

Fig. 2. Extended Langmuir–Freundlich isotherms for the uptake of BSA on the weak anion exchanger (DEAE-Sepharose Fast Flow), in sodium acetate–acetic acid buffer (12 m*M*) at pH 5.8, at various sodium chloride concentrations.

for different pH values and buffer strengths are shown in Figs. 1–3. At a pH of 9.1 and low buffer strength, BSA has very strong affinity for the anion exchanger. Data in Fig. 1 show very rectangular isotherms which decrease in total capacity with increasing salt

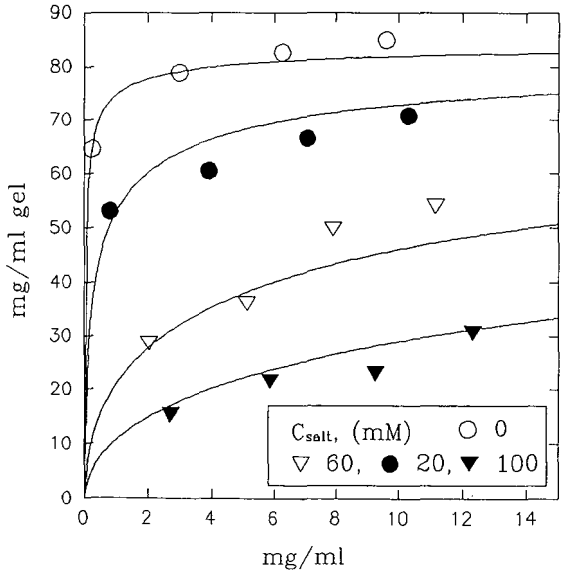

Fig. 3. Extended Langmuir–Freundlich isotherms for the uptake of BSA on DEAE-Sepharose Fast Flow, in Tris–HCl buffer (45 m*M*) at pH 8.1, at various sodium chloride concentrations.

TABLE I

PARAMETER VALUES FOR EXPERIMENTAL ISOTHERMS

Fig.	Protein	pH	Buffer (mM)	b_{bio} ($M^{-\eta_{bio}}$)	b_{salt} ($M^{-\eta_{bio}}$)	q_{max} (mg/ml)	η_{salt}	η_{bio}
1	BSA	9.1	12	$1.2 \cdot 10^8$	$8.1 \cdot 10^4$	107.8	0.86	16.6
2	BSA	5.8	12	$3.3 \cdot 10^5$	$9.0 \cdot 10^2$	95.8	0.76	2.70
2	BSA	5.8	12	$1.9 \cdot 10^6$	$5.9 \cdot 10^3$	87.2	1.00	1.00
3	BSA	8.1	45	$4.7 \cdot 10^5$	$2.3 \cdot 10^3$	85.1	0.60	1.78

concentration. When the pH is lowered to 5.8, approximately 1 pH unit above the isoelectric point of BSA, the protein affinity decreases and the isotherms become less rectangular.

Best-fit parameter values using the binary Langmuir–Freundlich isotherm (eqn. 6) are shown in Table I. For each case the model provides a good fit to all the experimental data using one set of parameters. Fig. 2 shows a comparison with the simple binary Langmuir isotherm were η_{bio} and η_{salt} both equal 1. It is not surprising to see that Freundlich parameters deviate from 1 and vary with pH. BSA is a large protein (mol. wt. 66000) known to have a number of different binding sites. Also, weak ion-exchange adsorbents like DEAE contain a range of molecules having different ionization constants that could form a heterogeneous binding surface.

Isotherm data from Carta et al. [1]

Carta *et al.* [1] studied the equilibrium uptake of the amino acids phenylalanine

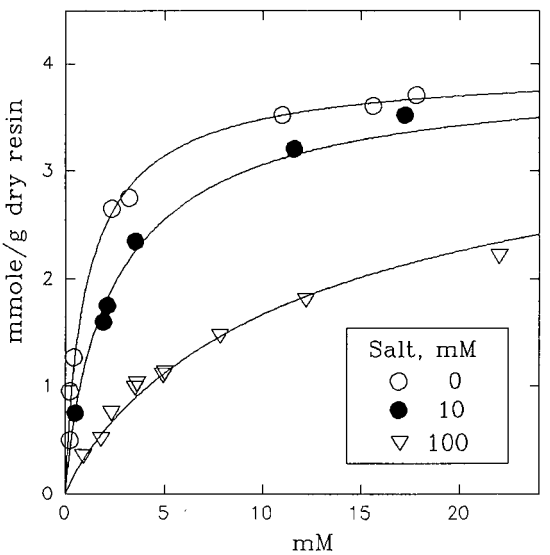

Fig. 4. Extended Langmuir isotherms for the uptake of phenylalanine on the strong cation exchanger (Amberlite 252), in no buffer between pH 1.61 and 2.90, at various chloride ion concentrations (Carta *et al.* [1]).

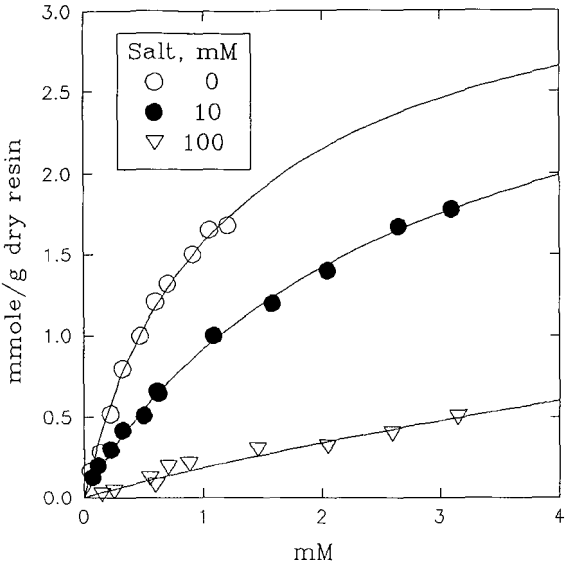

Fig. 5. Extended Langmuir isotherms for the uptake of tyrosine on the strong cation exchanger (Amberlite 252), in no buffer between pH 2.09 and 3.2, at various chloride ion concentrations (Carta *et al.* [1]).

and tyrosine by Amberlite 252, a strongly acidic, cation-exchange resin. Since amino acids were adsorbed in the absence of buffer, pH did not remain constant. Isotherms in Figs. 4 and 5 show equilibrium binding which is much weaker than that of BSA.

Best-fit parameter values using the extended Langmuir–Freundlich equation are shown in Table II. The model again provides a good fit to the experimental data for all concentrations of salt. For both amino acids the Freundlich parameters are nearly equal to 1. In this case the model reduces to a multicomponent Langmuir isotherm which may indicate adsorption of a homogeneous nature.

Isotherm data from Huang and Horváth [4]

Huang and Horváth [4] studied the equilibrium uptake of the proteins lysozyme (mol.wt. 14 400), α-chymotrypsinogen (25 000) and RNase A (13 700) on both strong and weak cation exchangers with silica support. All equilibrium binding isotherms were measured at pH 7.0 and are shown in Figs. 6–8. Using the extended Langmuir–Freundlich equation to find best fit parameters listed in Table III, the

TABLE II

PARAMETER VALUES FOR ISOTHERMS OF CARTA *et al.* [1]

Fig.	Amino acid	pH	b_{bio} ($M^{-\eta_{bio}}$)	b_{salt} ($M^{-\eta_{salt}}$)	q_{max} (mM/ml)	η_{salt}	η_{bio}
4	Phenylalanine	1.6 to 2.9	362	66	4.0	1.12	1.15
5	Tyrosine	2.1 to 3.2	464	134	3.6	0.99	1.08

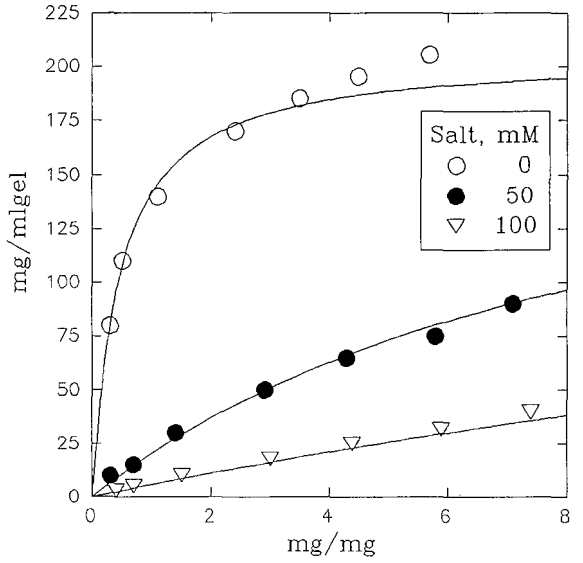

Fig. 6. Extended Langmuir–Freundlich isotherms for the uptake of α-chymotrypsinogen on the strong cation exchanger (SCX-300), in sodium phosphate buffer (25 m*M*) at pH 7.0, at various ammonium sulfate concentrations (Huang and Horváth [4]).

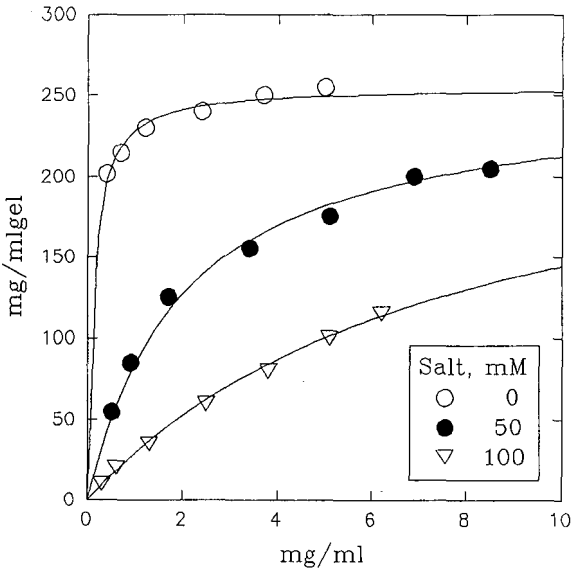

Fig. 7. Extended Langmuir–Freundlich isotherms for the uptake of lysozyme on the weak cation exchanger (WCX-300H), in sodium phosphate buffer (25 m*M*) at pH 7.0, at various ammonium sulfate concentrations (Huang and Horváth [4]).

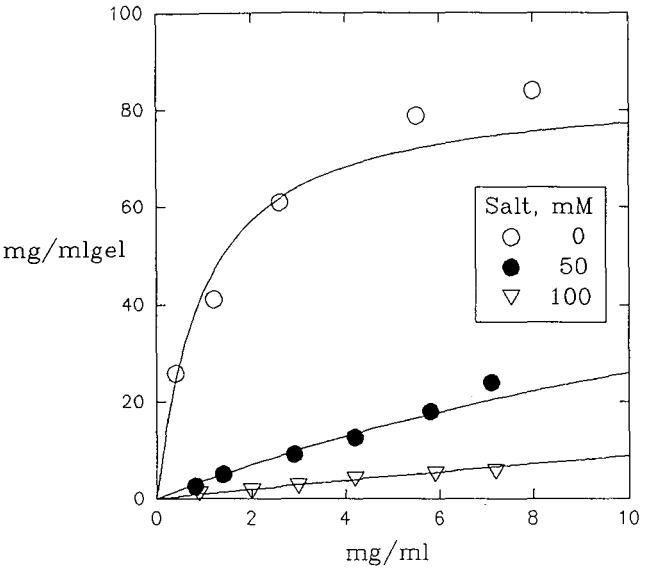

Fig. 8. Extended Langmuir–Freundlich isotherms for the uptake of RNase A on the weak cation exchanger (WCK-300H), in sodium phosphate buffer (25 mM) at pH 7.0, at various ammonium sulfate concentrations (Huang and Horváth [4]).

model again provides an excellent approximation of the data. It is also interesting to see that for all three proteins the Freundlich parameters η_{bio} and η_{salt} are approximately equal to 0.5 and 1.0, respectively. This may suggest that the binding sites of these proteins interact similarly with the ion exchange surface.

CONCLUSIONS

A simple multicomponent model has been shown to predict the dependence of salt concentration on the equilibrium adsorption of amino acids and proteins to an ion exchanger. This model could be easily incorporated into a fixed-bed model to predict the effect of different salt gradients on the elution of proteins using ion-exchange chromatography. Although empirical, the extended Langmuir–Freundlich isotherm

TABLE III

PARAMETER VALUES FOR ISOTHERMS OF HUANG AND HORVÁTH [4]

Fig.	Protein	pH	Buffer (mM)	b_{bio} ($M^{-\eta_{bio}}$)	b_{salt} ($M^{-\eta_{salt}}$)	q_{max} (mg/ml gel)	η_{salt}	η_{bio}
6	Lysozyme	7.0	25	$1.2 \cdot 10^5$	$6.7 \cdot 10^3$	255	0.49	1.06
7	α-Chymotrypsinogen	7.0	25	$5.7 \cdot 10^4$	$4.9 \cdot 10^3$	205	0.55	0.95
8	RNase A	7.0	25	$1.3 \cdot 10^4$	$2.6 \cdot 10^4$	85	0.44	0.81

provides a good fit to several different sets of equilibrium isotherm data. It has been proposed that Freundlich parameters deviating from 1 may indicate heterogeneous adsorption sites on the adsorbent surface and or the adsorbate. However, further studies are needed to test the applicability of this model and the validity of these theories.

ACKNOWLEDGEMENTS

Financial support from the Excellence Grant Scheme of The University of Queensland is gratefully acknowledged.

REFERENCES

1 G. Carta, M. S. Saunders and J. B. Vierow, *AIChE J.*, 35 (1989) 53.
2 Q. Yu, J. Yang and N.-H. L. Wang, *React. Polym.*, 6 (1987) 33.
3 S. J. Sanders, M. Rafal, D. M. Clark, R. D. Young, N. C. Scrivner, R. A. Pease, S. L. Grise and R. B. Diemer, *Chem. Eng. Prog.*, 84 (1988) 47.
4 J. X. Huang and Cs. Horváth, *J. Chromatogr.*, 406 (1987) 285.
5 J. X. Huang, G. Guiochon and J. Schudel, *J. Chromatogr.*, 504 (1990) 335.
6 R. D. Whitley, N.-H. L. Wang, R. Wacheter and F. Liu, *J. Chromatogr.*, 465 (1989) 137.
7 I. Langmuir, *J. Chem. Soc.*, 40 (1918) 1361.
8 J. Zeldowitsch, *Acta Physicochim. U.R.S.S.*, 1 (1934) 961.
9 E. C. Markham and A. F. Benton, *J. Am. Chem. Soc.*, 53 (1931) 497.
10 R. Sips, *J. Chem. Phys.*, 16 (1948) 490.

Journal of Chromatography, 542 (1991) 29–40
Elsevier Science Publishers B.V., Amsterdam

CHROM. 23 046

Solute retention in micellar liquid chromatography

BARRY K. LAVINE*, ANDREW J. WHITE and JIAN HWA HAN
Department of Chemistry, Clarkson University, Potsdam, NY 13699-5810 (U.S.A.)
(First received August 17th, 1990; revised manuscript received November 27th, 1990)

ABSTRACT

A study of the retention behavior of aromatic compounds in micellar and hydro-organic mobile phases was undertaken to better understand the differences in retention and selectivity between micellar liquid chromatography (MLC) and reversed-phase liquid chromatography. The capacity factor for 21 aromatic compounds was measured on Microsorb C_{18} using both micellar and hydro-organic mobile phases. Through correlation analysis it was shown that solute retention in MLC is influenced in some measure by the net surface charge of the stationary phase as well as by the unusual nature of the micelle–solute interaction.

INTRODUCTION

In 1980, Armstrong and Henry [1] demonstrated that aqueous micellar solutions can be used as mobile phases in reversed-phase liquid chromatography (RPLC). They called this technique pseudo-phase or micellar liquid chromatography (MLC). Since the first report by Armstrong and Henry, a number of articles have appeared in the chemical literature focusing on the unique capabilities of MLC, *e.g.*, rapid gradient capability, enhanced luminescence detection, simultaneous separation of charged and neutral compounds, and low toxicity and cost, to name a few [2–8]. More than a hundred papers to date have been published on this subject.

Retention in MLC has been shown to be correlated to surfactant type and to the concentration of the surfactant (above the critical micelle concentration) in the mobile phase [9,10]. Solute retention in MLC generally decreases with increasing surfactant (*i.e.*, micelle) concentration, but the rate of decrease can vary considerably from one organic solute to the next. Equations relating the capacity factor (k') to the concentration of the micelles in the mobile phase have been developed by Armstrong and Nome [11] and Cline-Love and Arunyanart [12] based on a three-way partition model. The equations by Armstrong and Nome [11] and Cline-Love and Arunyanart [12] have been verified experimentally [13–15] for a large number of organic solutes.

As in RPLC, selectivity in MLC is controlled primarily by manipulation of the mobile phase composition. However, mobile phase–solute interactions in MLC are very different in nature from those in RPLC. To better understand the differences in retention and selectivity between the two techniques, a study of the retention behavior

0021-9673/91/$03.50

of aromatic compounds in micellar and hydro-organic mobile phases was undertaken. This paper, as a preliminary report of an on-going investigation, stresses the importance of solute–stationary phase interactions in MLC. Using a set of 21 aromatic compounds as retention probes (see Table I), we will show that differences in retention and selectivity do, in fact, exist between the two techniques. However, these differences can be attributed in some measure to changes in the net surface charge of the stationary phase caused by adsorbed surfactant.

EXPERIMENTAL

All high-performance liquid chromatographic (HPLC) measurements were made with a Rainin 81-20 M analytical HPLC system which incorporates two Rainin Rabbit HP pumps (Rainin Instruments, Woburn, MA, U.S.A.), an Apple Macintosh computer as the controller, a Model 7125 Rheodyne injection valve, and a Rainin Dynamax mixer. The detector was a Knauer variable-wavelength UV–visible spectrometer (Berlin, Germany). The analytical columns used were Rainin Microsorb 3-μm octyldecyldimethylsilane ODS (50 mm $\times$ 4.6 mm I.D.). A silica precolumn placed between the injector and the pumps was used to saturate the mobile phase with silicates. The analytical column and the mobile phase reservoir were water-jacketed and temperature-controlled.

The 21 mono-, di- and trisubstituted benzenes were obtained from Aldrich and were used as received. Sodium dodecylsulphate (SDS) and cetyltrimethylammonium bromide (CTAB) were obtained from BDH (99% purity). SDS was recrystallized in ethanol and dried in an oven at 65°C prior to chromatographic use, whereas, CTAB was used as received. HPLC-grade distilled water, HPLC-grade methanol and 1-propanol were obtained from J. T. Baker.

The micellar solutions were prepared in HPLC-grade distilled water. The methanol–water mobile phase was also prepared with HPLC-grade solvents. Both the micellar solutions and the methanol–water mobile phase were filtered twice through a 0.45-μm Nylon membrane filter to remove particulate matter. The solutions were also degassed prior to use. pH measurements on these solutions were made using a ChemTrix pH meter. The pH of each solution was approximately 6.30.

TABLE I

THE AROMATIC DATA SET

(1) Benzyl alcohol	(12) Chlorobenzene
(2) Benzaldehyde	(13) Bromobenzene
(3) 2,4-Dinitrophenol	(14) Ethylbenzene
(4) Benzonitrile	(15) Resorcinol
(5) Acetophenone	(16) Catechol
(6) Nitrobenzene	(17) Phenol
(7) *p*-Nitroanisole	(18) *p*-Nitrophenol
(8) Methylbenzoate	(19) *o*-Chlorophenol
(9) Anisole	(20) *o*-Bromophenol
(10) Benzene	(21) 2,4-Dichlorophenol
(11) Toluene	

The void volume of the system was determined by injecting different solutions such as methanol, methanol–water, or water onto the Microsorb columns. Void volume measurements obtained for micellar mobile phases were comparable to the values obtained for methanol–water mobile phases. This volume, approximately 0.55 ml, was used for all k' calculations. The k' values determined in this study were averages of at least triplicate determinations. All capacity factor measurements were made at a flow-rate of 1.0 ml/min. The k' values were measured at 25°C for SDS and 35°C for CTAB. (Since the Kraft point of CTAB is 23°C, it was necessary to carry out the CTAB studies at a higher temperature.)

During the course of this study, solutions of surfactant containing small amounts of organic modifier, *e.g.*, 2% 1-propanol or 20% 1-propanol (v/v), were used as mobile phases. The presence or absence of surfactant aggregation (*i.e.*, micelles) in these so-called hybrid mobile phases was determined by conductometric titration [16]. Distilled water or distilled water with 2% 1-propanol or 20% 1-propanol was added to a thermostated and stirred cell. A surfactant solution prepared in the same medium was titrated against the solution in the cell. Conductance measurements were then taken periodically after addition of the titrant using a dipping electrode (nominal cell constant of 1 cm^{-1}) and a Cole-Palmer conductivity meter. If the titration curve had a sharp endpoint, the presence of micelles was so indicated in the medium. The endpoint presumably denotes the critical micelle concentration (CMC) of the surfactant in the medium (see Table II).

RESULTS AND DISCUSSION

The first step in the study was to characterize the retention behavior of the 21 aromatic compounds on Microsorb C_{18} using a hydro-organic mobile phase [methanol–water (50:50, v/v)] and a micellar mobile phase [0.05 *M* SDS with 2% 1-propanol (v/v)]. Propanol was added to the SDS solution to improve the chromatographic efficiency of the C_{18} column. It is known that poor column efficiency in MLC is caused by slow mass transfer due to poor wetting of the stationary phase [17]. This is an especially troublesome problem for C_{18} columns. The presence of an organic solvent such as 1-propanol in the mobile phase is known to provide the wetting that is needed for good mass transfer. For SDS mobile phases, small amounts of 1-propanol or an equivalent organic solvent are crucial to ensure reproducible

TABLE II

SUMMARY OF THE RESULTS FROM THE CONDUCTOMETRIC TITRATION EXPERIMENTS PERFORMED USING MICELLAR AND TERNARY (*I.E.*, HYBRID) MOBILE PHASES

System	Temperature (°C)	Detectable endpoint	CMC (*M*)
0.05 *M* SDS	25	Yes	0.0082
0.05 *M* SDS with 2% *n*-propanol	25	Yes	0.0040
0.05 *M* CTAB	35	Yes	0.0019
0.05 *M* CTAB with 2% *n*-propanol	35	Yes	0.0016
0.05 *M* CTAB with 20% *n*-propanol	35	No	–

chromatography. (In fact, workers in our laboratory were unable to generate reliable retention data on short Microsorb C_{18} columns using SDS micellar solutions that did not contain small amounts of 1-propanol.) With regard to this so-called hybrid mobile phase, it was evident on the basis of conductivity measurements (see Table II) that micelles were present in the surfactant solution. In fact, McGreevy and Schecter [18] have found that micelle size is not affected by the addition of long-chain alcohols, *e.g.*, 1-butanol, over the concentration range 0–0.162 *M*.

The retention data generated with the methanol–water mobile phase and the SDS micellar mobile phase were analyzed using a form of the Collander equation. In Fig. 1, log *P* (the log of the octanol–water partition coefficient) is plotted against log *k'* for the methanol–water mixture. The log *P* values were obtained from the Pomona College Medicinal Chemistry Data Bank [19]. An examination of Fig. 1 reveals a very interesting result: the compounds in the data set can be divided into two groups. The first group of compounds (*i.e.*, group B) consists entirely of phenols (numbers 15–21), whereas the second group (*i.e.*, group A) is mainly mono-substituted benzenes (numbers 1, 2 and 4–14). When the correlation coefficient was computed for each group, the r^2 value was 0.97 for group A and 0.98 for group B. The r^2 value for the whole data set (excluding 2,4-dinitrophenol) was 0.86. Compound 3 (2,4-dinitrophenol) has a pK_a of 4.07. Because the pH of the mobile phase is 6.30, we would expect 2,4-dinitrophenol to exist principally in the anionic form. Therefore, 2,4-dinitrophenol would be too polar to partition into the stationary phase and would be expected to elute off the column with the dead marker.

The degree of correlation between log *P* and log *k'* was also determined for the compounds using the SDS mobile phase. In Fig. 2, a plot of log *P versus* log *k'* is shown

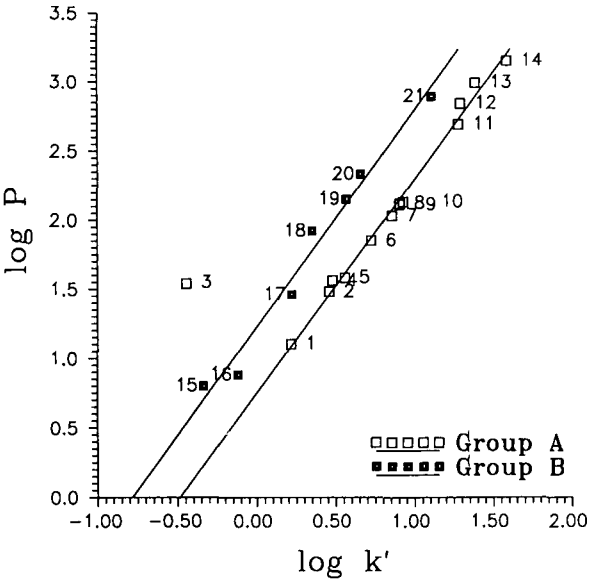

Fig. 1. Plot of log *P versus* log *k'* for the 21 aromatics, *e.g.*, 1 is benzyl alcohol, 2 is benzaldehyde (see Table I). The mobile phase consisted of methanol–water (50:50).

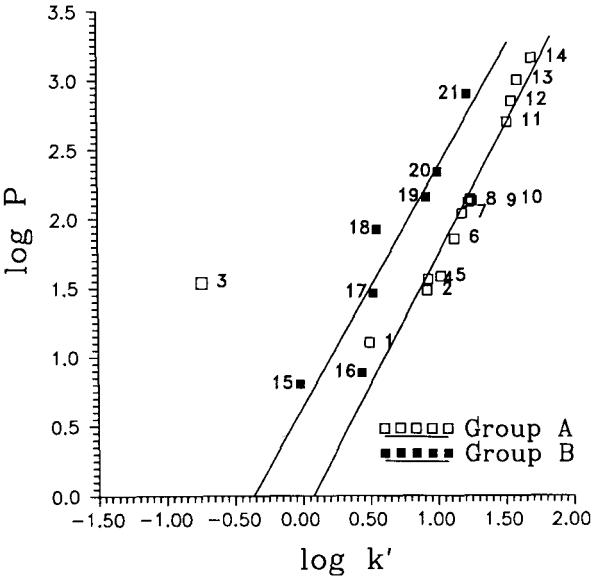

Fig. 2. Plot of log *P versus* log *k'* for the 21 aromatics. The mobile phase consisted of 0.05 *M* SDS and 2% 1-propanol (v/v).

for the 21 aromatic compounds. Again, the aromatics can be divided into two groups; 2,4-dinitrophenol again elutes off the column with the dead marker. In fact, the only difference between the two data sets is that catechol lies in group A instead of group B. (There is no difference in the elution order of the compounds and the same type of dichotomy exists in the data.) Table III provides a statistical summary of these results. The slopes of the lines drawn through the sets of points are approximately equal for each data set.

The similarity between the two data sets is surprising in view of the reported differences in selectivity between micellar mobile phases and hydro-organic mobile phases [20,21]. To better understand the reasons for the similar results, we measured *k'* on a C_{18} Microsorb column for the aromatic compounds using five different SDS

TABLE III

STATISTICAL SUMMARY OF THE RESULTS OBTAINED FROM THE METHANOL–WATER AND SDS DATA SETS

Mobile phase	Group	Slope	Intercept	r^2
Methanol–water	A	1.54	0.75	0.97[a]
	B	1.56	1.22	0.98
SDS	A	1.87	−0.14	0.98[a]
	B	1.73	0.63	0.84

[a] 2,4-Dinitrophenol was excluded from the calculation.

mobile phases: (1) 0.01 *M* SDS with 2% 1-propanol; (2) 0.025 *M* SDS with 2% 1-propanol; (3) 0.05 *M* SDS with 2% 1-propanol; (4) 0.10 *M* SDS with 2% 1-propanol; and (5) 0.15 *M* SDS with 2% 1-propanol. Next, we correlated k' to surfactant concentration using the equation developed by Cline-Love and Arunyanart [12]:

$$\frac{1}{k'} = \frac{[\mathrm{M}]K_2}{\varphi[\mathrm{L_s}]K_1} + \frac{1}{\varphi[\mathrm{L_s}]K_1} \tag{1}$$

where [M] is the concentration of surfactant, K_2 is the solute–micelle binding constant, φ is the chromatographic phase ratio, $[\mathrm{L_s}]$ is the concentration of ligate on the stationary phase, and K_1 is the solute–stationary phase binding constant. A plot of $1/k'$ *versus* [M] should result in a straight line. In fact, excellent linearity was observed for 20 of the 21 aromatic compounds ($r^2 > 0.985$). (The exception, of course, was 2,4-dinitrophenol which came out with the dead marker.) Table IV lists the values for K_2 and the intercepts, *i.e.*, $\varphi[\mathrm{L_s}]K_1$, for 20 of the 21 aromatic compounds. (K_2 was obtained by dividing the slope by the intercept and multiplying by the aggregation number.) The values obtained for K_2 were, by and large, in good agreement with previously published literature values [22].

Treiner [23] has previously reported that an excellent linear correlation exists between log *P* and log K_2 for aliphatic compounds. Therefore, we attempted to correlate log *P* to log K_2 for the aromatics. In Fig. 3, a plot of log *P* *versus* log K_2 is shown for the aromatic compounds. A nice straight line can be drawn through the data

TABLE IV

SODIUM DODECYLSULPHATE WITH 2% 1-PROPANOL

Compound	Slope	Intercept	K_2[a]	$\varphi[\mathrm{L_s}]K_1$
Benzyl alcohol	1.5	0.19	520	5.2
Benzaldehyde	0.77	0.65	780	15
Benzonitrile	0.86	0.07	810	14
Acetophenone	0.69	0.043	1100	23
Nitrobenzene	0.70	0.41	1120	25
p-Nitroanisole	0.77	0.026	2000	39
Methyl benzoate	0.62	0.020	2040	50
Anisole	0.67	0.028	1600	36
Benzene	0.72	0.020	2400	51
Toluene	0.51	0.0078	4300	130
Chlorobenzene	0.49	0.0068	4700	150
Bromobenzene	0.47	0.0045	7000	220
Ethylbenzene	0.42	0.0022	13 000	450
Resorcinol	4.3	1.1	260	0.89
Catechol	1.7	0.36	300	2.7
Phenol	1.5	0.20	500	4.9
p-Nitrophenol	1.9	0.13	980	7.7
o-Chlorophenol	1.2	0.055	1500	18.2
Bromophenol	1.2	0.037	2100	27
2,4-Dichlorophenol	1.0	0.007	9000	140

[a] K_2 is computed by multiplying 66 (the aggregation number for SDS) by the ratio of the slope to the intercept.

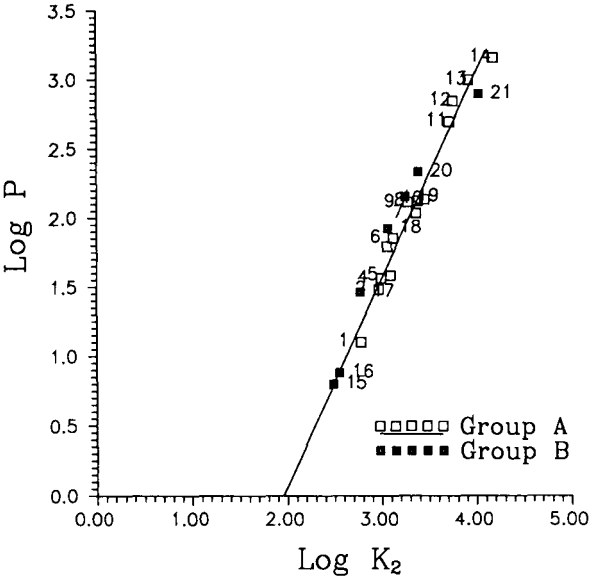

Fig. 3. Plot of log P *versus* log K_2 for the 21 aromatics. SDS was the surfactant.

points ($r^2 = 0.96$). Evidently, the dichotomy present in the log P *versus* log k' plot of SDS cannot be attributed to a mobile phase effect, *i.e.*, selectivity by the surfactant aggregate towards the phenols. Nor can the differences in the chromatographic behavior of the phenols from that of the other aromatic compounds tested be explained on the basis of ion-interaction or ion-pair chromatography [24,25]. With the exception of 2,4-dinitrophenol, the k' value of the other phenols did not change when the pH of the 0.05 M SDS mobile phase was adjusted to 4.30 or 3.00, via addition of small amounts of H_2SO_4.

In all likelihood, the silanol groups on the bonded phase surface are responsible for the differences in the chromatographic behavior between the phenols and the other aromatic compounds tested. Minick *et al.* [26] have observed this effect in RPLC with C_{18} and C_8 columns and have shown that it can be minimized by adding trace quantities of *n*-decylamine and 1-octanol to the hydro-organic eluent. Indeed, the sensitivity of the alkyl bonded phase to differences in hydrogen bonding properties of the solutes [27–29] is quite pronounced, more so than for the octanol–water system.

If the dichotomy of results observed for SDS is also due to unhindered silanol groups on C_{18}, then one should expect the same dichotomy from the plot of log P *versus* log K_1. In Fig. 4, a plot of log P *versus* log $\varphi[L_s]K_1$ is shown for the 21 aromatic compounds. The phase ratio and the concentration of the ligate on the stationary phase are constants that are characteristic of the chromatographic system. Therefore, this plot defines the relationship between the octanol–water partition coefficient and the solute–stationary phase binding constant. The similarity between Figs. 2 and 4 is truly remarkable. Therefore, we conclude that the stationary phase is responsible for the dichotomy present in the log P *versus* log k' plots shown.

Our studies of micellar mobile phases in RPLC, however, were not limited to

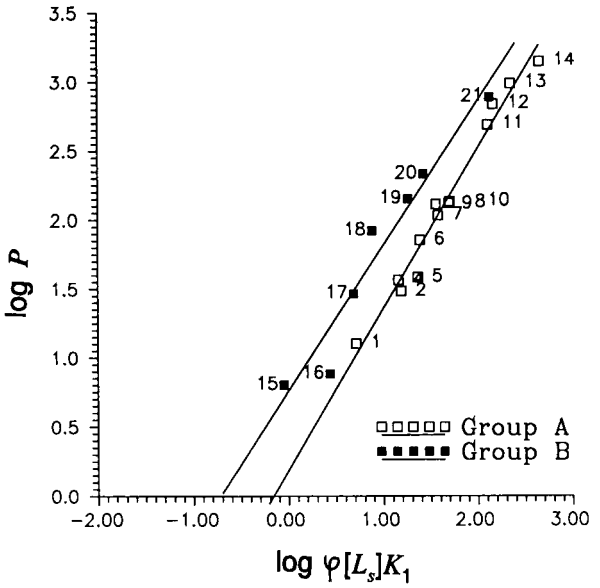

Fig 4. Plot of log P *versus* log $\varphi[L_s]K_1$ for the 21 aromatics. SDS was the surfactant.

only anionic surfactants. In Fig. 5, a plot of log P *versus* log k' is shown for the 21 aromatic compounds using a 0.05 M CTAB solution as the mobile phase. (1-Propanol was not added to the 0.05 M CTAB solution because poor column efficiency was not as serious a problem.) From Figs. 2 and 5, it is evident that the plot of log P *versus* log k'

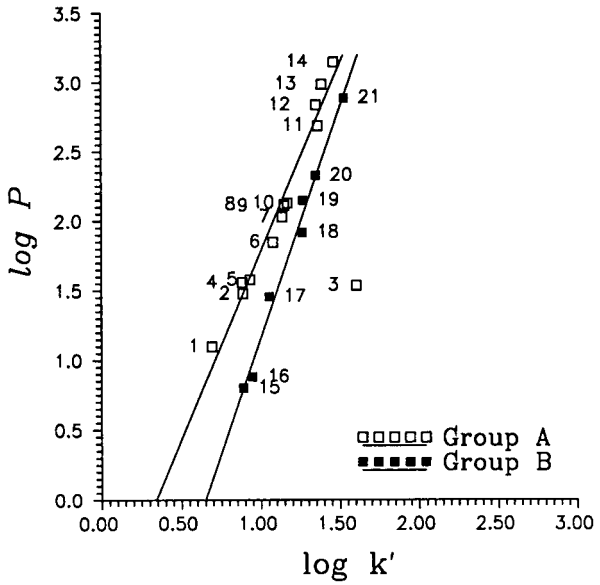

Fig. 5. Plot of log P *versus* log k' for the 21 aromatics. The mobile phase consisted of 0.05 M CTAB.

for SDS (see Fig. 2) is different from the plot of log P *versus* log k' for CTAB. In the case of CTAB, group A is on the left and group B is on the right. For SDS, group A is on the right and group B is on the left. In addition, for CTAB, 2,4-dinitrophenol is strongly retained by the column, probably due to ion pairing with the adsorbed surfactant.

To better understand the reasons for the differences between SDS and CTAB, we again found it necessary to measure k' on C_{18} Microsorb for the aromatic compounds using a set of six different mobile phases: (1) 0.005 M CTAB; (2) 0.01 M CTAB; (3) 0.25 M CTAB; (4) 0.05 M CTAB; (5) 0.10 M CTAB; and (6) 0.20 M CTAB. Again, k' was correlated to surfactant concentration using the equation developed by Cline-Love and Arunyanart [12]. The agreement between $1/k'$ and [M] was very good. (In fact, $r^2 > 0.985$ for all 21 aromatic compounds.) Table V lists the values for K_2 and $\varphi[L_s]K_1$. Again, the values that were obtained for K_2 were, by and large, in good agreement with previously published literature values [22].

We again correlated log P to log K_2 for the aromatics. In Fig. 6, a plot of log P *versus* log K_2 is shown. The similarity between Figs. 6 and 5 is striking. Evidently, the differences in chromatographic behavior between the phenols and the other aromatic compounds tested can be attributed to a mobile phase effect, *i.e.*, selectivity by the surfactant aggregate towards the phenols. This selectivity is probably the result of a secondary equilibrium process involving the transfer of a proton from the phenol to the water molecules in the Stern region of the micelle. It is well known that the charge

TABLE V

CETYLTRIMETHYLAMMONIUM BROMIDE

Compound	Slope	Intercept	K_2[a]	$\varphi[L_s]K_1$
Benzyl alcohol	1.2	0.089	1000	11
Benzaldehyde	0.86	0.054	1200	18
2,4-Dinitrophenol	0.73	0.0021	28 000	490
Benzonitrile	0.89	0.050	1400	20
Acetophenone	0.82	0.045	1400	22
Nitrobenzene	0.82	0.025	2600	41
p-Nitroanisole	0.84	0.014	4500	70
Methyl benzoate	0.77	0.019	3200	52
Anisole	0.77	0.020	2900	49
Benzene	0.75	0.021	2800	48
Toluene	0.66	0.0078	6500	130
Chlorobenzene	0.67	0.0065	8100	150
Bromobenzene	0.67	0.0039	13 000	250
Ethylbenzene	0.58	0.0038	12 000	260
Resorcinol	1.3	0.036	2700	28
Catechol	1.05	0.028	2900	35
Phenol	0.93	0.024	3000	41
p-Nitrophenol	0.72	0.0043	13 000	230
o-Chlorophenol	0.69	0.0058	9200	170
Bromophenol	0.69	0.0029	19 000	340
2,4-Dichlorophenol	0.52	0.00037	110 000	2700

[a] K_2 is computed by mutiplying 78 (the aggregation number for CTAB) by the ratio of the slope to the intercept.

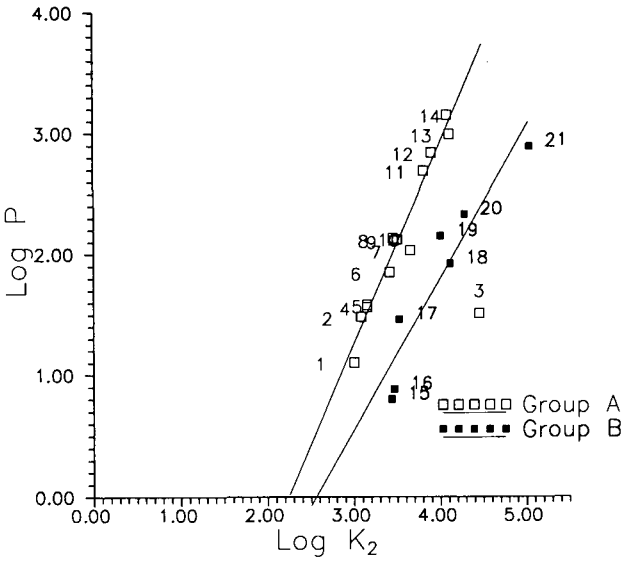

Fig. 6. Plot log P *versus* log K_2 for the 21 aromatics. CTAB was the surfactant.

on a cationic surfactant micelle will influence the pK_a value of an incorporated guest molecule [30]. A decrease of 0.5 to 3.0 in the pK_a value of dissociable amphiphiles will occur. (For anionic surfactants, the situation is reversed. In other words, an increase of 0.5 to 3.0 in the pK_a value will occur.) These shifts can be rationalized using simple electrostatic theory, *e.g.*, surface potential, low dielectric constant at the micellar surface [31].

However, the differences in selectivity between CTAB and SDS for the compounds tested cannot be attributed only to a shift in the pK_a values of the phenols. Fig. 7 shows a plot of log P *versus* log $\varphi[L_s]K_1$ for the CTAB data: the similarity between Figs. 7 and 5 is evident. When Fig. 7 is compared to Fig. 4, one has to conclude that the interaction of the solute with a CTAB-coated C_{18} phase is different from that of a SDS-coated C_{18} phase. This difference is probably due to a change in the surface charge of the stationary phase. In the case of CTAB, the chromatographic surface possesses a net positive charge due to the adsorbed CTAB monomer, whereas, in the case of SDS, the overall charge on the C_{18} surface is negative due to adsorbed SDS.

Although the role of the surfactant in the mobile phase has been extensively studied, the modification of the stationary phase by adsorbed surfactant has been investigated to a lesser extent [32–34]. Borgerding and Hinze [35] have observed that surfactant modification can cause changes in the selectivity and polarity of the stationary phase. Perhaps surface modification is also responsible for the similarity between aqueous micellar solutions and surfactant–water–propanol ternary mixtures with respect to the retention behavior of an homologous series. For example, Khaledi [20] noted that the addition of up to 20% of 2-propanol (v/v) to an SDS micellar mobile phase has a negligible effect on the hydrophobic selectivity of this mobile phase. However, we know that micelles will not be present in a solution of 0.05 M SDS with 20% 1-propanol (see Table II). Perhaps the similarity between aqueous micellar

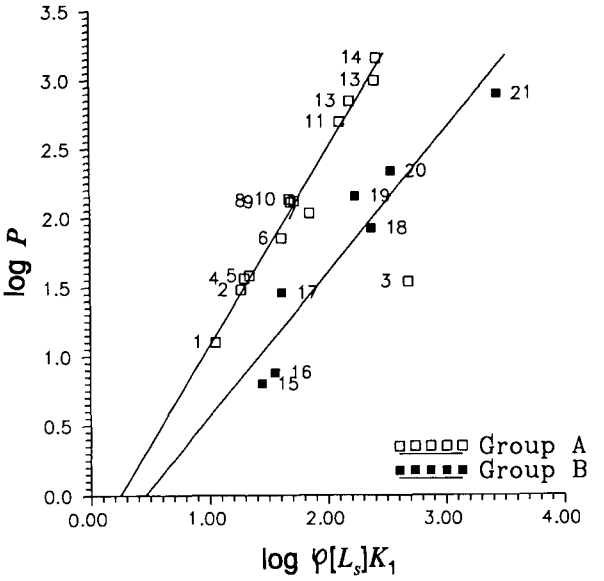

Fig. 7. Plot of log P *versus* log $\varphi[L_s]K_1$ for the 21 aromatics. CTAB was the surfactant.

solutions and the ternary mixtures is due in some measure to a modification of the surface of the stationary phase by the adsorbed surfactant.

CONCLUSION

Solute–stationary phase interactions in MLC are very important. It is possible that some of the reported differences in selectivity between MLC and RPLC with hydro-organic mobile phases are due in some measure to the modification of the surface of the stationary phase by adsorbed surfactant. The surface charge, as well as the structure of the C_{18} stationary phase, is altered by the adsorbed surfactant monomer. The results of this study also demonstrate that differences do exist in selectivity between micellar mobile phases and traditional hydro-organic mobile phases due to the unusual nature of the micelle–solute interaction.

ACKNOWLEDGEMENTS

B.K.L. acknowledges the financial support of the Reynolds Tobacco Company. Critical discussions on amphiphilic association structures with Professor Stig Friberg are acknowledged. Professor Anthony J. I. Ward's group at University College at Dublin provided the conductometric titration data on the SDS and CTAB solutions.

REFERENCES

1 D. W. Armstrong and S. J. Henry, *J. Liq. Chromatogr.*, 3 (1980) 657.
2 D. W. Armstrong and G. Y. Stine, *Anal. Chem.*, 55 (1983) 2317.
3 H. N. Singh and W. L. Hinze, *Analyst*, 107 (1982) 1073.

4 J. S. Landy and J. G. Dorsey, *J. Chromatogr. Sci.*, 22 (1984) 68.
5 L. J. Cline-Love, J. G. Habarta and J. G. Dorsey, *Anal. Chem.*, 56 (1984) 1132A.
6 D. W. Armstrong, *Sep. Purif. Methods*, 14 (1985) 213.
7 M. Khaledi and J. G. Dorsey, *Anal. Chem.*, 57 (1985) 2190.
8 J. G. Dorsey, *Adv. Chromatogr.*, 27 (1987) 167.
9 P. Yarmchuk, R. Weinberger, R. F. Hirsch and L. J. Cline-Love, *Anal. Chem.*, 54 (1984) 2233.
10 M. Arunyanart and L. J. Cline-Love, *J. Chromatogr.*, 342 (1985) 293.
11 D. W. Armstrong and F. Nome, *Anal. Chem.*, 53 (1981) 1662.
12 M. Arunyanart and L. J. Cline-Love, *Anal. Chem.*, 56 (1984) 1557.
13 E. Pramauro, G. Saini and E. Pelizzetti, *Anal. Chim. Acta*, 166 (1984) 233.
14 E. Pelizzetti and E. Pramauro, *J. Phys. Chem.*, 88 (1984) 990.
15 M. F. Borgerding, F. H. Quina, W. L. Hinze, J. Bowermaster and H. M. McNair, *Anal. Chem.*, 60 (1988) 2520.
16 M. J. Rosen, *Surfactants and Interfacial Phenomena*, Wiley, New York, 2nd ed., 1988.
17 J. G. Dorsey, M. T. DeEchegaray and J. S. Landy, *Anal. Chem.*, 55 (1983) 924.
18 R. J. McGreevy and R. S. Schechter, *J. Colloid Interface Sci.*, 127 (1989) 209.
19 *Med. Chem. Software*, *Version 3.52*, Pomona Medicinal Chemistry Project, Pomona College, Claremont, CA.
20 M. G. Khaledi, *Anal. Chem.*, 60 (1988) 876.
21 M. G. Khaledi, E. Peuler and J. Ngeh,-Ngwainbi, *Anal. Chem.*, 59 (1987) 2738.
22 J. P. Foley, *Anal. Chim. Acta*, 231 (1990) 237.
23 C. J. Treiner, *J. Colloid Interface Sci.*, 93 (1986) 93.
24 J. C. Kraak, K. M. Jonker and J. F. K. Huber, *J. Chromatogr.*, 142 (1977) 283.
25 E. Tomlinson, T. M. Jefferies and C. M. Riley, *J. Chromatogr.*, 159 (1978) 315.
26 D. J. Minick, J. H. Frenz, M. A. Patrick and D. A. Brent, *J. Med. Chem.*, 31 (1988) 1923.
27 J. Haky and A. M. Young, *J. Liq. Chromatogr.*, 7 (1984) 675.
28 F. Gaspari and M. Bonati, *J. Pharm. Pharmacol.*, 39 (1987) 252.
29 S. H. Unger, J. R. Cook and J. S. Hollenberg, *J. Pharm. Sci.*, 67 (1978) 1364.
30 G. S. Hartley, *Trans. Faraday Soc.*, 30 (1934) 444.
31 A. L. Underwood, *Anal. Chim. Acta*, 140 (1982) 89.
32 A. Berthod, I. Girard and C. Gonnet, *Anal. Chem.*, 58 (1986) 1356.
33 A. Berthod, I. Girard and C. Gonnet, *Anal. Chem.*, 58 (1986) 1362.
34 A. Berthod and A. Roussel, *J. Chromatogr.*, 449 (1988) 349.
35 M. F. Borgerding and W. L. Hinze, *Anal. Chem.*, 57 (1985) 2183.

Journal of Chromatography, 542 (1991) 41–54
Elsevier Science Publishers B.V., Amsterdam

CHROM. 23 031

Comparison of site-specific coupling chemistry for antibody immobilization on different solid supports

JINN-NAN LIN*

Department of Bioengineering, College of Engineering and Department of Pharmaceutics, College of Pharmacy, University of Utah, Salt Lake City, UT 84112 (U.S.A.)*

I-NAN CHANG

Department of Material Science and Engineering, College of Engineering, University of Utah, Salt Lake City, UT 84112 (U.S.A.)

JOSEPH D. ANDRADE

Departments of Bioengineering and Material Science and Engineering, College of Engineering, University of Utah, Salt Lake City, UT 84112 (U.S.A.)

JAMES N. HERRON

Department of Pharmaceutics, College of Pharmacy, University of Utah, Salt Lake City, UT 84112 (U.S.A.)

and

DOUGLAS A. CHRISTENSEN

Department of Electrical Engineering, College of Engineering, University of Utah, Salt Lake City, UT 84112 (U.S.A.)

(First received August 15th, 1990; revised manuscript received December 6th, 1990)

ABSTRACT

Silica is an important chromatographic support for high-performance affinity chromatography due to its high mechanical stability. However, silica is very different from traditional gel chromatographic materials, such as agarose, dextran, and polyacrylamide, with respect to many chemical and physical properties. Thus, it is expected that different immobilization techniques must be used for orienting the immobilized ligand on the surfaces of the two substrates. In this study, a site-specific coupling chemistry for immobilization of antibodies on modified silica surfaces and on agarose gels was investigated. The effects of substrates on the orientations of immobilized native and partially denatured antibodies was deduced. An important conclusion is that non-covalent interactions (physical adsorption) dominate the orientation of immobilized antibodies on silica surfaces.

INTRODUCTION

Due to their high specificity, antibodies immobilized on chromatographic supports have been widely used for purification of molecules since the early 1970s [1]. Numerous coupling chemistries for the immobilization of antibodies have been developed and reviewed [2,3]. Most coupling chemistries rely on the random coupling of antibodies through the amino groups of lysine residues. This often results in a decrease in antigen binding capacity (AgBC) due to improper orientation of the

0021-9673/91/$03.50

antibody molecules on the solid surfaces. To overcome these problems, two approaches for site-specific immobilization of antibodies have been reported recently. In the first approach, antibodies are immobilized to hydrazide-activated supports via their oxidized carbohydrates by forming covalent hydrazone bonds. Immunoglobulins contain carbohydrate moieties linked to the CH_2 domain of the Fc fragments. Under mild conditions, the hydroxyl groups of the carbohydrates can be oxidized to aldehyde groups by sodium periodate without significantly impairing the active sites of the antibody [4–6]. Another method is to immobilize Fab′ fragments via thiol groups at the hinge region [6–8]. This can be done by first making $F(ab)'_2$ with pepsin digestion, followed by reduction of the disulfide bond which links the two Fab′ fragments by dithiothreitol. The free thiol groups can then be coupled to maleimide-activated supports.

When antibodies are immobilized to agarose gels, both site-specific coupling methods result in an increase in AgBC over non-selective coupling methods. However, agarose gel is not an ideal support for high-performance affinity chromatography (HPAC) because of its low mechanical stability. Recently, it has been suggested that silica is a promising material for HPAC due to its inherent mechanical stability, which provides good flow characteristics even under high pressure [9].

However, silica and agarose exhibit completely different chemical and physical properties. For example, agarose gel is a soft organic material with high water content, while silica is a hard inorganic material. From the point of view of antibody immobilization, there is one important difference between the two materials which has been ignored so far and needs to be examined, protein adsorption or resistance properties. Why are these properties important for site-specific couping of antibodies? Examine Fig. 1.

In the upper part of Fig. 1, materials used for chromatographic supports are roughly classified into three categories, according to their protein resistance properties. The first category includes natural and synthetic uncharged hydrogels, such as agarose, dextran, and polyacrylamide, which exhibit low protein adsorption properties. Although a number of explanations have been offered as to why proteins exhibit weak interactions with these materials[10], the exact mechanism is still unclear. The second category includes materials such as silica, polystyrene, and polyethylene, which exhibit strong protein adsorption. Depending on the nature of the surface, protein, and solution medium, the protein is adsorbed via ionic interactions, hydrophobic effects, polar–polar interactions, Van der Waals forces, or, most probably, a combination of all such interactions [10,11]. An enormous amount of work has been reported in the literature on the protein adsorption to various substrates [11,12]. The third category consists of the materials which have the protein adsorption properties somewhat between the two types of materials discussed above.

Site-specific coupling of a protein to agarose (left) and silica (right) surfaces is schematically shown in the lower part of Fig. 1. Examine the agarose situation first: the open circle on the hydrogel surface represents a functional group which can form a covalent bond with a specific site on the protein (shown by the closed circle on the protein). Our hypothetical protein is a single polypeptide chain and consists of two domains, whose surface includes regions of hydrophobic, charged, or polar character. According to the collision theory of bimolecular reactions, the protein molecule must first approach and collide with the surface before the covalent bond can be formed.

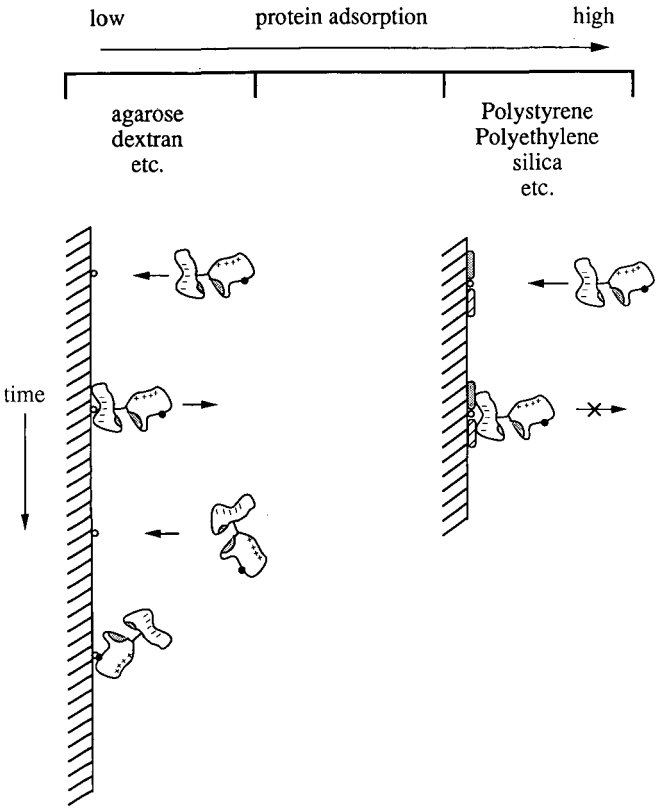

Fig. 1. Schematic representation for the concept of antibody immobilization on different types of solid supports.

The first collision may not be of proper orientation for the formation of a covalent bond. Since agarose has very weak non-covalent interactions with the protein, the protein will then diffuse away from the surface and other proteins will collide with the surface in different orientations. After a number of collisions, protein finally approaches the surface with an orientation suitable for formation of chemical bonds. This surface coupling process is similar to solution reactions except that one of the reactants is a stationary phase.

In the case of silica (right, Fig. 1), non-covalent adsorption sites (represented by the filled squares) are presented on the silica surface, and probably influence the site-specific coupling of the protein. Therefore, in order to understand site-specific coupling to silica surfaces, protein adsorption must be examined. The general concepts of protein adsorption currently accepted have recently been reviewed by Andrade and co-workers [10–12]. In summary, for a one-component system, a protein of given bulk concentration diffuses to and collides with the interface. If the interaction forces and contact area are large enough, the protein stays on the surface for a certain residence time, probably in the range of milliseconds to seconds, while on the surface, the protein may begin surface "denaturation". With increasing contact time, the probability for

desorption decreases. Eventually, the protein may become irreversibly adsorbed on the surface in a completely or partially denatured conformation. Therefore, one could expect that on the silica surfaces the formation of chemical bonds is secondary to physical adsorption.

From the above discussion, it seems that, depending on the types of substrates, different immobilization strategies should be employed for controlling the orientation of the immobilized protein. But, how can we experimentally prove it? We have previously shown that the immobilization of the partially denatured antibodies on silanized silica surfaces resulted in higher AgBC and higher antibody surface concentrations than for the native antibody [13]. The antibody immobilization methods used in the previous study were physical adsorption and non-site-specific chemical coupling. In this study we have immobilized antibodies on different supports to investigate the substrate effect on the site-specific coupling for antibody immobilization. Hydrazide-derivatized agarose and silica were used to immobilize oxidized and non-oxidized native and partially denatured antibodies.

EXPERIMENTAL

Cleaning of silica samples

All silica samples were cut from 2.5 cm × 2.5 cm × 0.1 cm fused-silica slides (CO grade, ESCO) and the edges were finely polished. The size of the sample was 1.1 cm × 0.95 cm × 0.1 cm and fits into a 13 × 75 mm culture tube (Fisher) in which all surface reactions took place at room temperature. Cleaning of the silica samples has been described elsewhere [13].

Silanization of cleaned silica samples

Two silane reagents were used in this study: γ-glycidoxypropyltrimethoxysilane (GOPS, Aldrich) and dimethyldichlorosilane (DDS, Petrarch). The silica chips were reacted with a dry toluene solution of GOPS (2% GOPS, 0.2% triethylamine and 97.8% dry toluene, v/v) [14] or dry toluene solution of DDS (10% DDS and 90% dry toluene, v/v) for 1 h and 30 min at room temperature, respectively. The GOPS samples were rinsed with dry acetone and the DDS samples were rinsed with absolute ethanol. The chips were then cured in a vacuum oven (which has been flushed with nitrogen three times) at 120–130°C for 1 h. The epoxide groups of GOPS on the silica surfaces were then reacted with a 10% hydrazine solution (E. Merck) in methanol for 3.5 h at room temperature, followed by rinsing with deionized water first and then absolute ethanol and dried in a vacuum oven for 1 h at 120–130°C. The hydrazide-treated silica (Si-Hz) surfaces were analyzed by electron spectroscopy for chemical analysis (ESCA) to confirm the occurrence of the surface modification.

Antibody and antigen system

The polyclonal goat anti-human serum albumin (anti-HSA) immunoglobulin G (IgG) fraction was purchased from Cappel Labs. Crystallized human serum albumin (HSA) was purchsed from Miles Diagnostics.

Radiolabelling of proteins

The anti-HSA or HSA was labelled with carrier-free ^{125}I (100 mCi/ml,

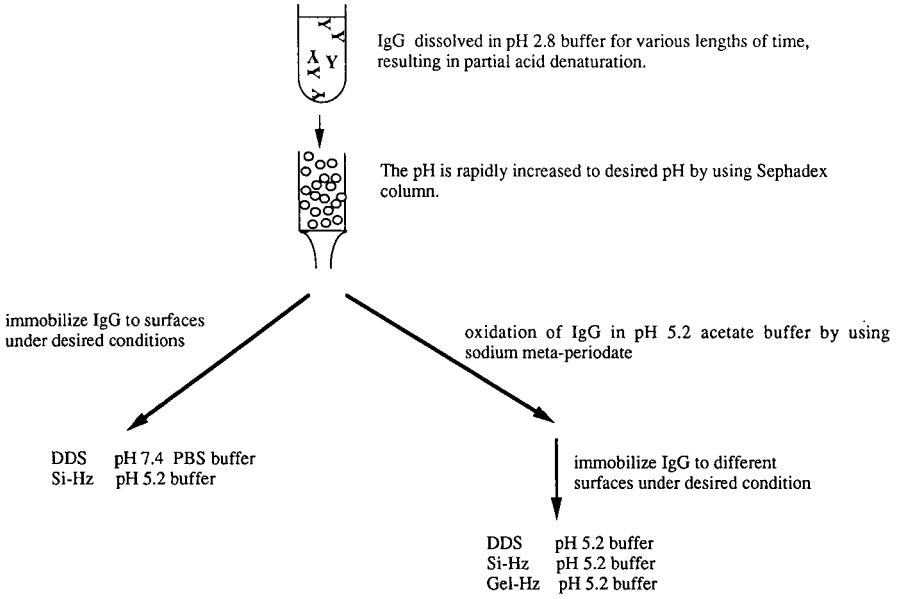

Fig. 2. Schematic representation of the antibody denaturation and immobilization procedures. DDS = dimethyldichlorosilane-treated silica surface; Si-HZ = hydrazide-treated silica surface; Gel-Hz = hydrazide-treated agarose gel.

Amersham) by the chloramine-T method as described by Lin *et al.* [13]. The final concentration of [^{125}I]protein solution was measured in a UV–visible spectrophotometer (Beckman, Model 35) at 280 nm. Values of 0.54 and 66,000 were used for the absorption extinction coefficient ($E^{0.1\%}$) and molecular weight (MW) of HSA, respectively, while for IgG the values of $E^{0.1\%}$ and MW used were 1.35 and 150,000, respectively. Labelling efficiency was determined by precipitating proteins with 20% trichloroacetic acid (TCA, Sigma) in the presence of bovine serum albumin (BSA) as carrier protein. The amount of iodide bound to protein was determined by subtracting the counts in the supernatant from the total counts in solution.

Preparation of the partially denatured antibodies

Antibody was partially denatured by dissolving approximately 5 mg of anti-HSA in 0.5 ml of 0.1 *M* citric acid–phosphate buffer (pH 2.8) for various lengths of time: 1, 20, 60 and 300 min (Fig. 2). The pH of the antibody solution was then increased by using a PD-10 column (Pharmacia) which has been equilibrated with the buffer used for antibody immobilization.

Oxidation antibodies

The native or partially denatured antibodies were oxidized by sodium meta-periodate (J. T. Baker) in 0.1 *M* acetate buffer pH 5.2 (Fig. 2). Sodium meta-periodate stock solution (30 mg/ml) was added to antibody solution (3 mg/ml) at one tenth the final volume. The mixture was gently mixed for various lengths of time (20, 40 and 60 min) at room temperature and the sodium meta-periodate was then removed using

a desalting column which had been washed and equilibrated with diluted coupling buffer, pH 5.2 acetate buffer.

Immobilization antibodies

Silica. Oxidized or non-oxidized samples of native or partially denatured anti-HSA antibodies were immobilized via either physical adsorption or site-specific chemical coupling. For physical adsorption, three experiments were performed: (1) non-oxidized antibodies in 0.15 *M* phosphate-buffered saline (PBS, pH 7.4) adsorbed onto DDS silica surfaces; (2) non-oxidized antibodies in 0.1 *M* acetate buffer (pH 5.2) adsorbed onto S-Hz surfaces; and (3) the oxidized antibodies in 0.1 *M* acetate buffer (pH 5.2) adsorbed onto DDS silica surfaces. For site-specific coupling, the oxidized antibodies were reacted with the Si-Hz surfaces in 0.1 *M* acetate buffer (pH 5.2.). The adsorption or reaction time for all experiments was 3 h at room temperature followed by rinsing with buffer. The concentration of antibody solutions ranged from 0.7 to 0.9 mg/ml. Surface concentrations of the immobilized antibodies were determined by radiolabelling technique.

Agarose gel. The Affi-Gel hydrazide agarose gel (gel-Hz) purchased from Bio-Rad was used to immobilize anti-HSA antibodies. The gel contained hydrazide groups, and coupling procedures have been described elsewhere [15,16]. Solution concentrations of antibodies ranged from 0.8 to 1.1 mg/ml. The amount of antibody immobilized on the gel beads was determined by measuring the depletion of antibody in bulk solution with a UV–VIS spectrophotometer.

Antibody–antigen binding experiments

The anti-HSA-coated silica and hydrogel samples were incubated with an excess amount of iodinated HSA in PBS for 1 and 2 h at room temperature, respectively. The silica samples were held by forceps and rinsed with PBS gently to remove the weakly adsorbed antigen solution layer. The hydrogel samples were rinsed with PBS more than five times until no iodinated HSA was detected in the rinsing solution. In all antigen binding experiments, an excess amount of BSA was added to the HSA solution to minimize non-specific adsorption. The amount of BSA added was 70–100 times higher than that of HSA.

Fluorescence measurement

Conformation changes of the antibodies resulted from acid treatment or oxidation were characterized by 4,4′-bis[8-(phenylamino)naphthalene-1-sulfonate] (bis-ANS, Molecular Probes). Bis-ANS fluoresces strongly with an emission peak at 515 nm when bound to hydrophobic regions of proteins, whereas the unbound dye is virtually non-fluorescent in aqueous buffer [17,18]. For non-oxidized antibodies, the final concentrations of the antibodies and bis-ANS in PBS were $3 \cdot 10^{-6}$ and $1 \cdot 10^{-5}$ *M*, respectively. For oxidized antibodies, the fluorescence measurements were performed in pH 5.2 acetate buffer in which cross-linking between antibody molecules was prevented. The final concentrations of the antibodies and bis-ANS were $6 \cdot 10^{-6}$ and $1 \cdot 10^{-5}$ *M*, respectively. The fluorescence experiments were performed in a Greg-200 multifrequency fluorometer (ISS, Champaign, IL, U.S.A.). The sample solutions were excited with plane-polarized light at 400 nm from a broadband 200-W xenon high-pressure lamp. The fluorescence at 515 nm was collected at 90° with respect to the incident light.

RESULTS

The AgBC of oxidized and non-oxidized antibodies immobilized on DDS silica surfaces are shown in Fig. 3 as a function of antibody denaturation time. The zero time point is for the native antibody, immobilized without low-pH treatment. Denaturation of antibody in low-pH buffer for 1 min, 20 min, 1 h and 5 h were performed (Fig. 2). Prior to immobilization, the low-pH buffer was exchanged with pH 7.4 PBS buffer for the non-oxidized antibodies or pH 5.2 acetate buffer for the oxidized antibodies.

For non-oxidized antibody, the AgBC after 20 min exposure to low-pH buffer is approximately two times higher than that of the native antibody (0 min) case (Fig. 3a). This increase in antigen binding is probably due to specific interactions because BSA was used to reduce non-specific binding. Furthermore, the AgBC decreases dramatically with increasing denaturation time. After 5 h of exposure to low-pH buffer, the AgBC is slightly lower than that of the native case. Although this set of results has been published previously, it is listed here again for the purpose of comparison [13]. A similar trend was also observed for antibodies which had been oxidized with sodium meta-periodate (Fig. 3b). The AgBC increased with increasing antibody denaturation

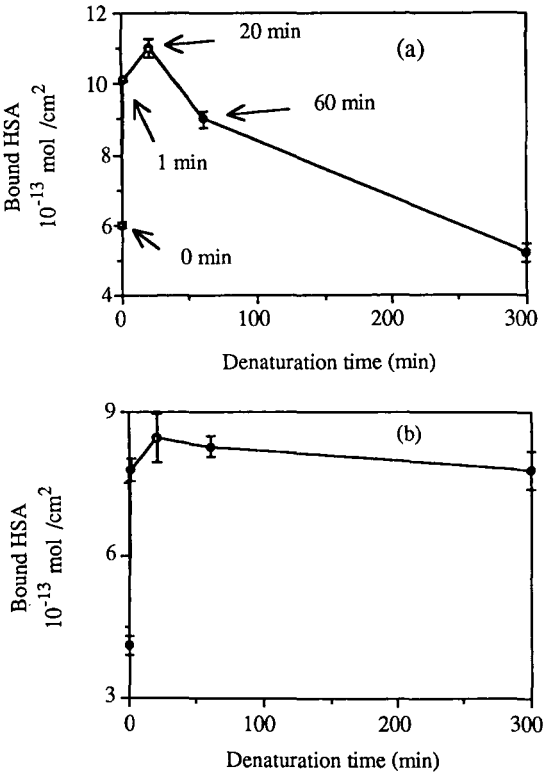

Fig. 3. Antigen binding capacity of immobilized antibody on DDS surfaces as a function of antibody denaturation time: (a) non-oxidized antibody ($n = 3$) (from ref. 13); (b) oxidized antibody ($n > 4$) (n = number of samples). The zero time point is for the native antibody, immobilized without low-pH treatment.

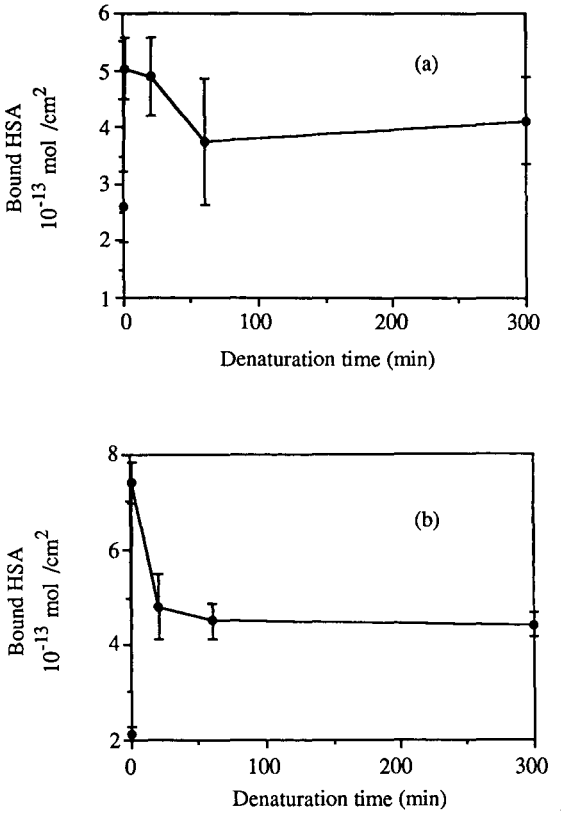

Fig. 4. Antigen binding capacity of immobilized antibody on Si-Hz surfaces as a function of antibody denaturation time: (a) non-oxidized antibody ($n=3$); (b) oxidized antibody ($n=8$).

time and reached a maximum after 20 min. The AgBC was approximately two times higher than that of the native case. At longer times, the AgBC decreased slightly with further denaturation time.

The AgBC of oxidized and non-oxidized antibodies immobilized on Si-Hz surfaces are shown in Fig. 4. The results were similar to those observed on DDS surfaces. The maximum AgBC of both antibodies on Si-HZ surfaces occur after 1 min of low-pH treatment, and they are about two to three times higher than those of the native antibodies. The surface concentrations of non-oxidized and oxidized antibodies immobilized on DDS and Si-Hz surfaces were also determined as a function of antibody denaturation time (Figs. 5 and 6, respectively). In all cases, exposure of antibodies to low-pH solution prior to immobilization dramatically increased antibody surface concentrations.

In contrast to modified silica surfaces, the hydrogel exhibited very good protein resistance [13]. In other words, the antibodies did not adsorb to agarose and can only be immobilized to the beads through covalent bonds. This was demonstrated by incubation of the hydrogel beads with iodinated non-oxidized native and partially

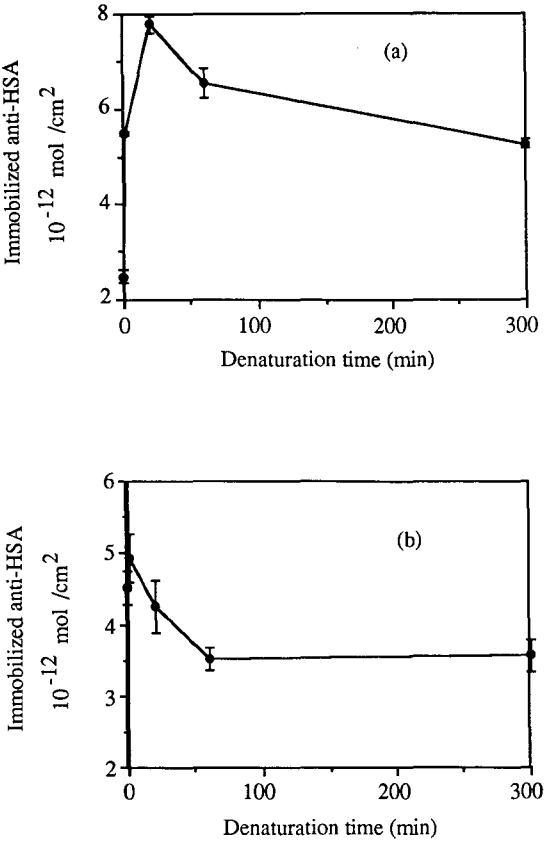

Fig. 5. Surface concentrations of anti-HSA on DDS surfaces as a function of antibody denaturation time: (a) non-oxidized antibody ($n = 3$); (b) oxidized antibody ($n > 4$).

denatured antibodies (5-h acid treatment). In principle, formation of covalent bonding is not possible in this case. After incubation and extensive rinsing, the beads were counted for antibody surface concentrations. The results show that only a trace of antibody bound to the beads. Therefore, the hydrogel beads were used as control for a surface which exhibits little or no protein adsorption.

The amount of oxidized antibodies and their AgBC immobilized on the Affi-Gel beads were determined as a function of antibody denaturation time (Fig. 7). The results showed that the AgBC and antibody surface concentrations decreased concomitantly with increasing antibody denaturation time. This suggested that the decrease in AgBC is caused by the decrease in antibody surface concentration, rather than the orientation of the immobilized anibody. Furthermore, the initial increase in the AgBC that was observed with short denaturation time on silica samples (Figs. 2–4) was not observed with hydrogel beads, suggesting that different mechanisms were involved in antibody immobilization on the two different types of materials.

It is well known that proteins in low-pH solution undergo conformational

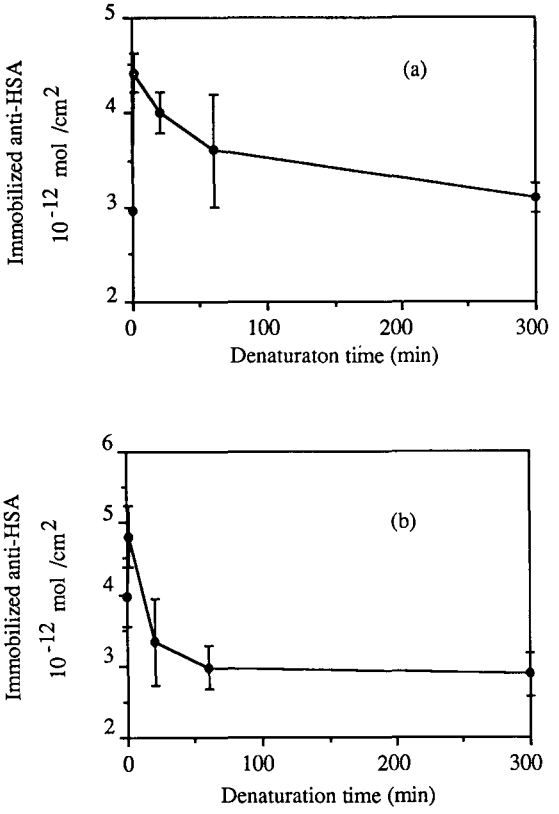

Fig. 6. Surface concentrations of anti-HSA on Si-Hz surfaces as a function of antibody denaturation time: (a) non-oxidized antibody ($n=3$); (b) oxidized antibody ($n=7$).

changes, which in turn affect their adsorption properties. The conformational changes of the partially denatured antibodies were characterized using a fluorescent hydrophobic probe, bis-ANS. The fluorescence spectra of bis-ANS in different antibody solutions are shown in Fig. 8. It can be seen that the fluorescence intensity of bis-ANS increases with increasing antibody denaturation time, indicating conformational changes of the Abs. In Fig. 8, data for the antibody with acid treatment for 5 h are not shown because the fluorescence intensity was too high to measure. The effect of oxidation time on the conformation of antibodies was also characterized by bis-ANS (Fig. 9). The fluorescence spectra for the antibodies oxidized by sodium periodate for 20, 40 and 60 min (curve c and d) overlap each other and are higher than that for the non-oxidized antibody (curve b). This indicates that oxidation processes have changed the conformation of certain parts of the antibody molecule and that the kinetics of the conformational changes are relatively fast (less than 20 min).

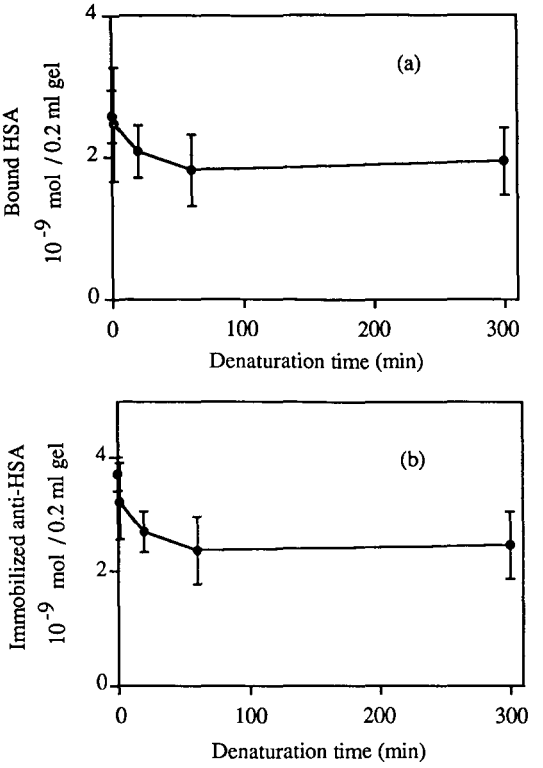

Fig. 7. (a) Antigen binding capacity of immobilized antibody; (b) surface concentrations of anti-HSA on agarose gel as a function of antibody denaturation time; $n=4$ in both experiments.

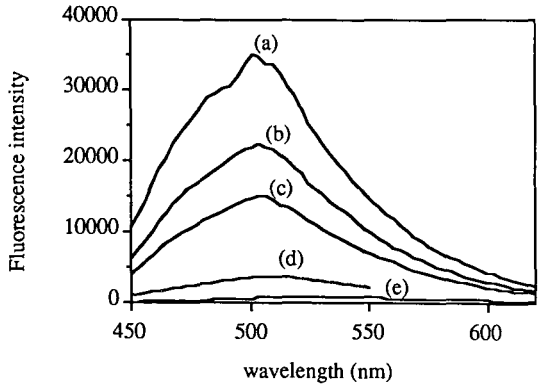

Fig. 8. Fluorescence spectra of bis-ANS binding to the non-oxidized native and partially denatured antibodies in pH 7.4 PBS; bis-ANS in (a) anti-HSA acid treated for 60 min, (b) anti-HSA acid treated for 20 min, (c) anti-HSA acid treated for 1 min, (d) native anti-HSA and (e) PBS.

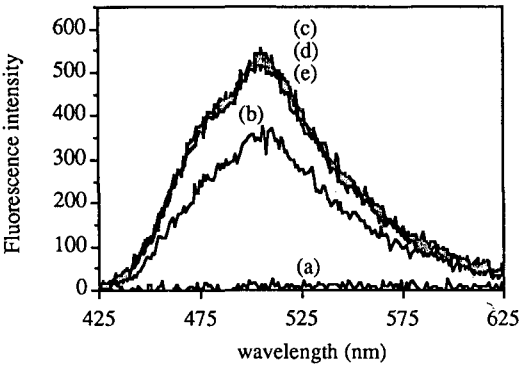

Fig. 9. Fluorescence spectra of bis-ANS binding to anti-HSA as a function of oxidation time in pH 5.2 acetate buffer; bis-ANS in (a) buffer, (b) non-oxidized native anti-HSA and (c–e) anti-HSA oxidized for 20, 40 and 60 min, respectively.

DISCUSSION

Oxidized or non-oxidized native and partially denatured antibodies were immobilized on three different surfaces via physical adsorption or chemical coupling. From the chemistry point of view, the hydrazide on the surfaces can react with aldehyde groups of oxidized carbohydrates in Fc fragments, resulting in site-specific coupling. Our results indicate that this chemistry works very well on the agarose gels. First, since only oxidized antibodies could be immobilized to agarose gels, immobilization was due exclusively to covalent coupling (Fig. 7). Second, the apparent activities of all immobilized antibodies using hydrazide chemistry on the agarose gels were 75 $\pm$ 3%, calculated assuming that only half of the IgG is the specific antibody, according to the specification provided by the company (Fig. 7). This value is consistent with other researchers' finding and is generally two to four times higher than that of non-site-specific coupling methods, such as cyanogen bromide-activated and N-hydroxysuccinimide ester-activated agarose gels [4,5].

Does hydrazide chemistry work as well on silica surfaces as on the agarose gels? From the results shown in Fig. 4b and 6b, the apparent activities of the immobilized oxidized antibodies on Si-Hz surfaces exhibited values ranging from 5 to 15%, which are substantially lower than that on the agarose gels. This is because the orientation of the antibodies on Si-Hz surfaces was controlled by the non-covalent interactions between the surfaces and antibodies rather than by site-specific coupling chemistry. This hypothesis is supported by the following experimental observations. First, in the control experiments for Si-Hz surfaces (Fig. 4a and 6a), the non-oxidized antibodies were strongly adsorbed onto the surfaces and showed approximately the same degree of AgBC as oxidized antibodies. This means that even though chemical bonds were formed between the antibody and the surfaces, the rest of the antibody molecule could still interact with non-specific adsorption sites on the surface and may have undergone surface denaturation. As a consequence, there is no advantage of using site-specific coupling with silica surfaces. Furthermore, since antibodies tend to adsorb irreversibly to silica surfaces, the chance of the adsorbed molecule having the right orientation for

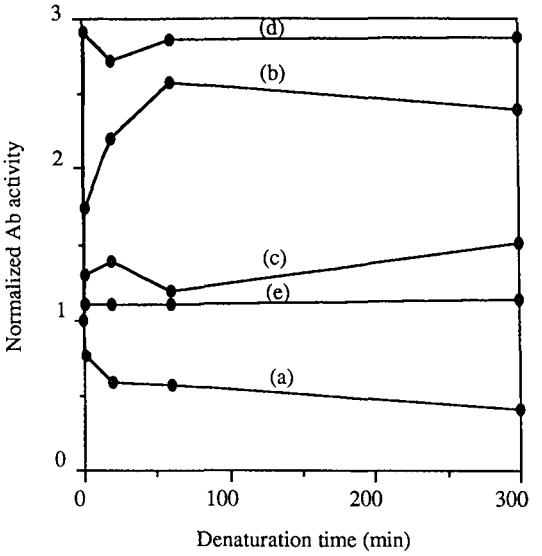

Fig. 10. Normalized antibody (Ab) activity on five different surfaces: (a) non-oxidized anti-HSA immobilized on DDS surfaces; (b) oxidized anti-HSA immobilized on DDS surfaces; (c) non-oxidized anti-HSA immobilized on Si-Hz surfaces; (d) oxidized anti-HSA immobilized on Si-Hz surfaces; (e) oxidized anti-HSA immobilized on Affi-Hz gel.

site-specific coupling is low. Thus, most of the antibodies were immobilized primarily via physical adsorption.

Second, if physical adsorption dominates the orientation of the antibody on silica surfaces, in principle it is possible to manipulate the orientation by altering the adsorption properties of the antibody. This concept is demonstrated by using the partially denatured antibodies. From the fluorescence experiments (Fig. 8), the results show that exposure of hydrophobic regions of the antibody increases with increasing acid denaturation time. As a result, acid treatment prior to immobilization has a significant influence on both antibody surface concentrations and AgBC, as shown in Figs. 2–5. Oxidation can also change the conformation of antibodies (Fig. 9), which in turn affects their adsorption properties, as observed on the non-functionalized DDS surfaces (Figs. 3 and 5). We have previously suggested that the increase in antibody surface concentrations was due to the high affinity of the denatured regions for the surfaces [13]. This phenomenon is analogous to the "Vroman effect" competitive adsorption between proteins [10]. In our case, the competitive adsorption is between the denatured and non-denatured regions of the antibody.

On the agarose gels, antibody surface concentration decreases with increasing denaturation time (Fig. 7). Since non-oxidized antibodies did not adsorb to agarose gels, we believe that the decrease in amount of immobilized antibody is due to the decrease in accessibility of the carbohydrate groups after acid treatment.

Finally, Fig. 10 shows the plot of normalized activity of immobilized antibody as a function of antibody denaturation time for all immobilization experiments. The normalized values were calculated by

$$\text{normalized activity} = \frac{([\text{Ag}]/[\text{Ab}])_{\text{N or D}}}{([\text{Ag}]/[\text{Ab}])_{\text{N}}}$$

where [Ag] and [AL] are the surface concentrations of antigen and antibody, respectively, and the subscripts N and D represent native and denatured antibody cases, respectively. Values greater than 1 indicate that the apparent AgBC of the immobilized antibodies is higher than that of the native antibody. For agarose gels all values are close to 1 as expected, because the orientation of immobilized antibody was controlled by chemical coupling. Thus, it has the least dependence on the conformational changes. However, on silica surfaces all cases exhibit some degree of dependence on the adsorption properties of the antibodies. Positive orientational effects (cases b, c and d) and negative influences (case a) are observed.

In summary, we have demonstrated that exposure of antibodies to a low-pH buffer prior to immobilization results in an increase in AgBC of the immobilized antibody on silica surfaces. This can be a useful method to improve the column capacity in immunoaffinity chromatography. Another very important conclusion is that physical adsorption dominates the orientation of immobilized antibodies on silica surfaces. Although chemical bonds may be useful in providing stable linkages between the antibody and surface, they do not affect orientation of the antibody on the surface. This concept is applicable to all materials that have high non-specific adsorption sites for proteins, including antibodies and enzymes. Therefore, when such materials are chosen as the solid supports for affinity chromatography, one should not approach the problem totally on the basis of trial and error. Instead, one can either modify the antibody molecules in such a way that active sites have a low interaction energy to the surface, or modify the surface to preferentially interact with only certain parts of the antibody.

ACKNOWLEDGEMENTS

This work has been supported in part by US Army Research Office Contract ARO 25539-LS and by AKZO Corporate Research America, Inc. We thank Dr. Hlady for valuable advice.

REFERENCES

1 P. Mohr and K. Pommerening, *Affinity Chromatography: Practical and Theoretical Aspects*, Marcel Dekker, New York, 1985.
2 K. Ernst-Cabrera and M. Wilchek, *Trends Anal. Chem.*, 7 (1988) 58.
3 P. W. Carr, A. F. Bergold, D. A. Hanggi and A. J. Muller, *Chromatogr. Forum*, Sept. (1986) 31.
4 W. L. Hoffman and D. J. O'Shannessy, *J. Immunol. Methods*, 112 (1988) 113.
5 D. J. O'Shannessy and W. L. Hoffman, *Biotechnol. Appl. Biochem.*, 9 (1987) 488.
6 V. S. Prisyazhony, M. Fusek and Y. B. Alakhov, *J. Chromatogr.*, 424 (1988) 243.
7 U. Jonsson, M. Malmovist, G. Olofsson and I. Ronnbery, *Methods Enzymol.*, 137 (1986) 381.
8 Y. Jimbo and M. Saito, *J. Mol. Electron.*, 4 (1988) 111.
9 K. Ernst-Cabrera and M. Wilchek, *Anal. Biochem.*, 159 (1986) 267.
10 J. D. Andrade, in J. D. Andrade (Editor), *Surface and Interfacial Aspects of Biomedical Polymers*, Vol. 2, Plenum Press, New York, 1985, Ch. 1, p. 2.
11 J. D. Andrade and V. Hlady, *Ann. N.Y. Acad. Sci.*, 516 (1987) 158.
12 J. D. Andrade, S. Nagaoka, S. Cooper, T. Okano and S. W. Kim, *ASAIO J.*, 10 (1987) 75.
13 J. N. Lin, J. D. Andrade and I. N. Chang, *J. Immunol. Methods*, 125 (1989) 67.
14 P. O. Larsson, M. Glad, L. Hansson, M. O. Masson, S. Ohlson and K. Mosbach, *Adv. Chromatogr.*, 21 (1983) 359.
15 R. S. Matson and M. C. Little, *J. Chromatogr.*, 458 (1988) 67.
16 M. C. Little, C. J. Siebert and R. S. Matson, *BioChromatography*, 3 (1988) 156.
17 G. Musci, G. D. Metz, H. Tsunematsu and L. J. Berliner, *Biochemistry*, 24 (1985) 2034.
18 A. R. S. Prasad, R. F. Lueuena and P. M. Horowitz, *Biochemistry*, 25 (1986) 3536.

Journal of Chromatography, 542 (1991) 55–64
Elsevier Science Publishers B.V., Amsterdam

CHROM. 23 018

Properties of supports for the partition chromatography of proteins[a]

A. WALSDORF and M. R. KULA
Institut für Enzymtechnologie, Heinrich Heine Universität Düsseldorf, Postfach 2050, D-5170 Jülich (Germany)

(First received March 21st, 1990; revised manuscript received August 14th, 1990)

ABSTRACT

LiParGel 650 and 750 were investigated as supports for the partition chromatography of proteins using aqueous two-phase systems. It was found that the elution pattern of the column is not determined solely by partitioning. Size exclusion properties and interactions with negatively charged residues on the support and hydrophobic effects, typical of polymer matrices, may strongly influence the migration rate of single components. In order to calculate elution volumes from partition coefficients and *vice versa*, the volumes of the stationary and mobile phases, V_s and V_m, respectively, were determined using a set of standards for calibration and a computer fit to correlate the data. The observed deviations from ideality are due to the broad pore-size distribution and unspecific side affinities of the support material, but do not affect the general applicability of the support materials for the chromatographic separation of proteins.

INTRODUCTION

In recent years, several attempts have been made to immobilize the dextran (Dx)-rich bottom phase of an aqueous polyethylene glycol (PEG)–dextran two-phase system and in this way to combine the favourable properties of aqueous phase systems with the advantages of column chromatography [1–3]. The main difficulty in finding a suitable support for this purpose arises from the similarity of the physico-chemical properties of the two phases and their low interfacial tension. This problem was finally solved by Müller [4], combining the incompatibility of polyacrylamide towards PEG with the mechanical strength of silica gel or a hydrophilic methacrylated polymer. Using a method described by Mino and Kaizerman [5], Müller grafted linear polyacrylamide chains of 15–25 monomer units to the hydroxylated support, which was then wetted preferentially by the dextran-rich phase. As long as the corresponding PEG-rich phase is used as the mobile phase the dextran-rich bottom phase is retained as a stationary phase and liquid–liquid partition chromatography can be performed. We examined the general properties of the newly developed material for partition chromatography.

[a] The results presented in this paper are part of the doctoral thesis of A. Walsdorf submitted to the Heinrich Heine Universität Düsseldorf.

0021-9673/91/$03.50

EXPERIMENTAL

Materials

The support materials LiParGel 650 and 750 were a gift from E. Merck (Darmstadt, Germany). Merck also provided experimental samples of polyacrylated LiChrospher Diol 1000/10, a porous spherical silica with 1000-Å pores and 10-μm particle size. The triazine dye Procion Red HE3b was a gift from ICI Germany. PEG 20 000 was obtained from Merck Schuchard (München/Hohenbrunn, Germany and monomethoxy-PEG 5000 from Fluka (Neu Ulm, Germany). Dextran Pl 500 (MW $5 \cdot 10^5$ dalton) and Vc 40 (MW $4 \cdot 10^4$ dalton) were bought from Pfeifer und Langen (Dormagen, Germany). The proteins were purchased from the following sources: albumin and peroxidase (E. Merck), ferritin, thyroglobulin (Pharmacia, Uppsala, Sweden), transferrin, myoglobin (Serva, Heidelberg, Germany), α-chymotrypsinogen A Type II (Sigma, St. Louis, MO, U.S.A.), lysozyme from egg white (Fluka) and formate dehydrogenase (Boehringer, Mannheim, Germany). Dextran blue was obtained from Pharmacia and glycyl-L-tyrosine from Serva. The monoclonal antibody directed against peroxidase was a gift from Dr. Eran Hadas (Department of Biotechnology, University of Tel Aviv, Israel). All other chemicals were of analytical-reagent grade.

Preparation of PEG–dye derivatives

The triazine dye Procion Red HE3b was coupled to monomethoxy-PEG 5000 and PEG 20 000 according to Cordes and Kula [6].

Phase preparation

The concentration of PEG and dextran in various phase systems used for partition chromatography were taken from phase diagrams established by Albertsson [7]. The PEG- and dextran-rich phases were prepared, mixing the polymers with water and salts in the appropriate amounts for 1 h. The pH was adjusted by adding concentrated phosphoric acid or potassium hydroxide solutions. The phases were allowed to settle under gravity in a separating funnel, and after 1–2 h the phases were separated. The PEG-rich phase was left standing to obtain a totally clear top phase, removing a small amount of bottom phase that settled over several days. In order to prevent oxidative degradation of the PEG, the mobile phase was stored under nitrogen.

Preparation of columns

The polyacrylated support particles LiParGel 650 or 750 and LiChrospher Diol 1000/10 were equilibrated with the phase system and packed into the chromatographic columns (Superformance system; E. Merck) according to Müller [4].

Column chromatography

The chromatography columns were integrated into a Pharmacia FPLC system. The fractions were collected using a Frac 100 fraction collector (Pharmacia).

Sample preparation

Exactly weighed amounts of the substances to be analysed were dissolved in the

mobile phase and centrifuged (3000 *g*, 5 min) to remove undissolved solid material. The samples were applied to the column using an MV 7 valve (Pharmacia).

The isoelectric points of the different proteins were determined using the Pharmacia Phast System with Phast gel IEF 3–9. The isoelectric points of chymotrypsinogen A and lysozyme were taken from the literature [8].

To determine the partition coefficient k, the individual proteins were mixed with equal volumes of top and bottom phases. The phases were separated by low-speed centrifugation (1800 *g*, 10 min) and the protein concentation determined in each phase measuring the absorbance at 280 nm (Shimadzu, UV 160). The activity of formate dehydrogenase was determined according to Schütte *et al.* [9] by an enzymatic assay. The k value was calculated as the ratio of the absorbances or enzyme activities in the top and bottom phases according to the equation [7]

$$\frac{C_T}{C_B} = \frac{f_T}{f_B} = k = \text{constant} \tag{1}$$

where k = partition coefficient, C_T and C_B = concentration of the component in the top and bottom phase, respectively, and f_T and f_B = activity of the component in the top and bottom phase, respectively.

RESULTS

Calibration of the column

Liquid–liquid partition chromatography (LLPC) was developed by Martin and Synge [10] and the following equations can be derived to calculate the elution volume of a given substance from the known partition coefficient in the phase system used and *vice versa*:

$$V_s = \frac{V_{el(2)} - V_{el(1)}}{1/k_{(2)} - 1/k_{(1)}} \tag{2}$$

$$V_m = V_{el(1)} - V_s(1/k_{(1)}) \tag{3}$$

$$V_{el} = V_s/k + V_m \tag{4}$$

$$k_{(n)} = V_s/(V_{el} - V_m) \tag{5}$$

where $V_{el(1,2)}$ elution volume of components 1 and 2, V_s = volume of the stationary phase, V_m = volume of the mobile phase and $k_{(n)}$ = partition coefficient.

To do so, the volumes of the stationary phase, V_s, and mobile phase, v_m, in the column must be known. Fig. 1 illustrates the relationship between the partition coefficient and elution volume in liquid–liquid partition chromatography, which is a hyperbolic function described by eqn. 4. At high k values the term V_s/k tends to zero and $V_{el} = V_m$. To determine V_s and V_m (eqns. 2 and 3) the elution volume of at least two substances in the column and their respective partition coefficients in the given phase system are required. The latter are determined by independent batch experiments.

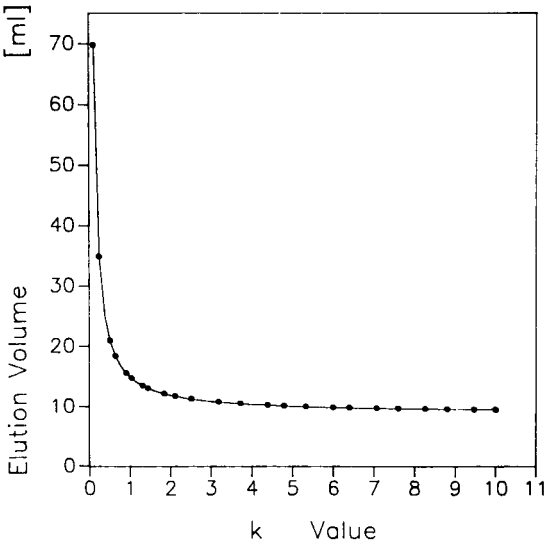

Fig. 1. Relationship between elution volume and partition coefficient in liquid–liquid partition chromatography. The hyperbolic function is derived by the equation $V_{el} = V_s/k + V_m$, where V_{el} is the elution volume, V_s the volume of the stationary phase, V_m the volume of the mobile phase and k the partition coefficient. In this example the column has the dimensions 30 × 1 cm I.D., with V_s = 5 ml and V_m = 10 ml.

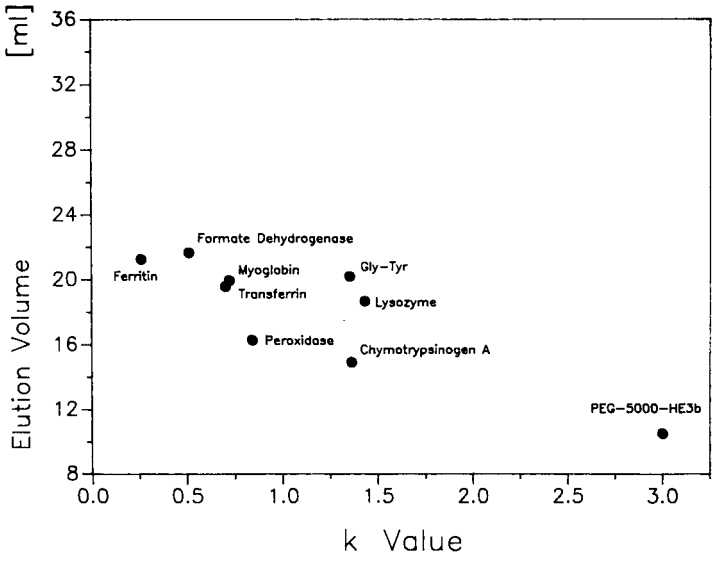

Fig. 2. Relationship between partition coefficient and elution volume of a set of standard proteins the dipeptide glycyl-L-tyrosine and a PEG-5000 triazine dye derivative in a LiParGel 750 column (30 × 1 cm I.D.). The system composition was 2.7% PEG 20000, 4.5% dextran Pl 500, 75 m*M* KBr and 10 m*M* phosphate buffer (pH 7). The temperature was 30°C and the flow-rate 1 ml/min.

TABLE I

MOLECULAR PROPERTIES OF MODEL PROTEINS USED FOR CALIBRATION, REPRODUCIBILITY OF ELUTION VOLUME BY PARTITION CHROMATOGRAPHY

The isoelectric points (IEP) in the range 3–9 were determined by isoelectric focusing using a Pharmacia Phast-gel pH gradient of 3–9. The IEP of chymotrypsinogen A and lysozyme were taken from the literature [8]. The partition coefficient k and relative standard deviation of the elution volume ($n = 10$) were determined in a phase system composed of 5.4% PEG 6000–9% dextran Vc 40, 100 mM NaCl and 50 mM phosphate (pH 7.5). The column (30 × 0.5 cm I.D.) had V_s = 1.2 ml and V_m = 2.3 ml and was operated at 23°C.

Protein	MW (dalton)	IEP	k	Standard deviation of elution volume (%)
Chymotrypsinogen A	23 000	9.5	1.0	4.3
Ferritin	440 000	7.0	0.38	6.1
Formate dehydrogenase	76 000	5.0	0.29	5.2
Lysozyme	14 600	11.0	0.76	2.8
Myoglobin	17 600	7.0	0.65	4.8
Peroxidase	40 000	8.7	0.89	3.1
Transferrin	80 000	5.6	0.43	10.0

Gel filtration of proteins in the absence of liquid–liquid partition

We started the experiments using LiParGel 750 in a gel bed of 30 × 1 cm. Using different pairs of proteins for calibration we could not obtain constant values of V_s and V_m. To compare the elution behaviour of the column with the theoretical curve in Fig. 1 we chose a set of standard proteins with k values in the range 0.2–3 and applied them

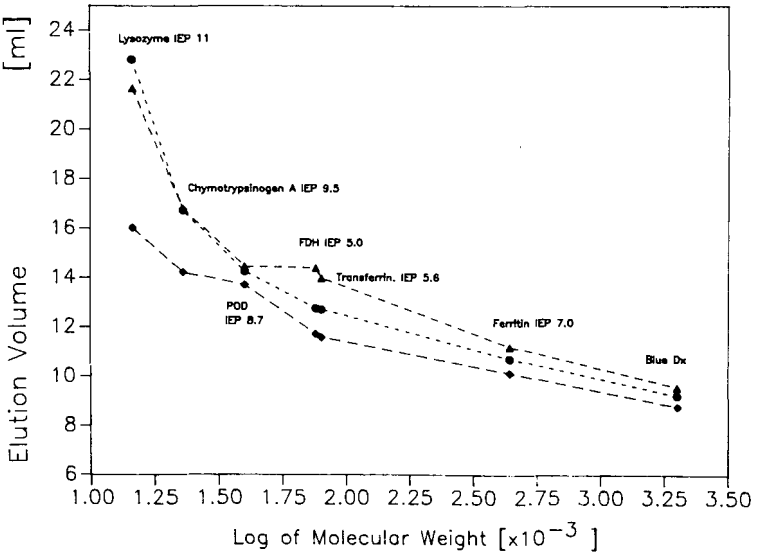

Fig. 3. Elution volume of a set of standard proteins during gel filtration on LiParGel 750 omitting the phase-forming polymers (30 × 1 cm I.D. column). The column was equilibrated against aqueous buffer (50 mM) of various pH values. The elution volume is plotted as a function of the molecular weight of the substances. Dextran blue was injected as an internal standard to determine the void volume of the column at the different pH values. The flow-rate was 1 ml/min. pH: ● = 7; ▲ = 4; ◆ = 10.

to the column. Fig. 2 shows the elution volume in the column in relation to k. The data do not follow the ideal hyperbolic function shown in Fig. 1, and it was also not possible to determine V_s and V_m unequivocally from these results. The reproducibility of the partition chromatography was fairly good, as can be judged by the standard deviation of the elution volume reported in Table I.

To establish whether the support material has any influence on the elution behaviour of the standard proteins, we prepared a column of LiParGel 750 but omitted the phase-forming polymers. The column was equilibrated against aqueous buffer of various pH and gel filtration carried out. The results are shown in Fig. 3. The elution volumes are plotted as a function of the molecular weight of the proteins. Data for the isoelectric points and the molecular weight of the standard proteins are included in Table I. Dextran blue with a molecular weight of $2 \cdot 10^6$ dalton was injected as an internal standard to determine the void volume of the column at the different pH values.

Considering the different isoelectric points, the observed shift in elution volume with pH may be interpreted as follows. The gel matrix is carrying negatively charged residues which interact with positively charged proteins. With decreasing pH any positively charged protein is more and more retained by the gel matrix and the elution volumes are increased.

The dipeptide glycyltyrosine, also injected at the different pH values, could not be eluted from the gel matrix under the conditions employed, suggesting that in addition hydrophobic interactions or π-electron effects between the tyrosine residue and the gel matrix might also play a role.

Effects of size exclusion on partition chromatography

Neglecting the basic protein lysozyme strongly affected by the matrix and the dipeptide, we used a computer fit to determine the desired values of V_s and V_m in the experimental column using the partition coefficient k and the corresponding elution volumes:

$$Y = \frac{B_2}{X} + B_1$$

where Y = elution volume, X = partition coefficient, B_1 = volume of the stationary phase and B_2 = volume of the mobile phase. The resulting graph obtained from the computer fit is shown in Fig. 4. Closer inspection reveals that ferritin is eluted significantly earlier than calculated. To establish whether mass transfer limitations due to diffusion or lack of equilibrium in partition are responsible for the unusual elution behaviour of the large molecule ferritin (MW $4.4 \cdot 10^5$ dalton), we reduced the flow-rate stepwise to one tenth of the original value. The elution volume of ferritin, however, remained constant (Fig. 5). This result led to the conclusion that the premature elution is a consequence of size exclusion effects of the matric LiParGel 750. Apparently the available volume of the stationary phase V_s is not a constant for all molecules, reflecting a broader pore size distribution typical of the polymeric resin. Large proteins cannot penetrate into the total dextran phase retained by the matrix and therefore are eluted earlier. This effect is necessarily more pronounced if dextran of higher molecular weight is used in the stationary phase, which may block access to the limiting pores for larger analytes.

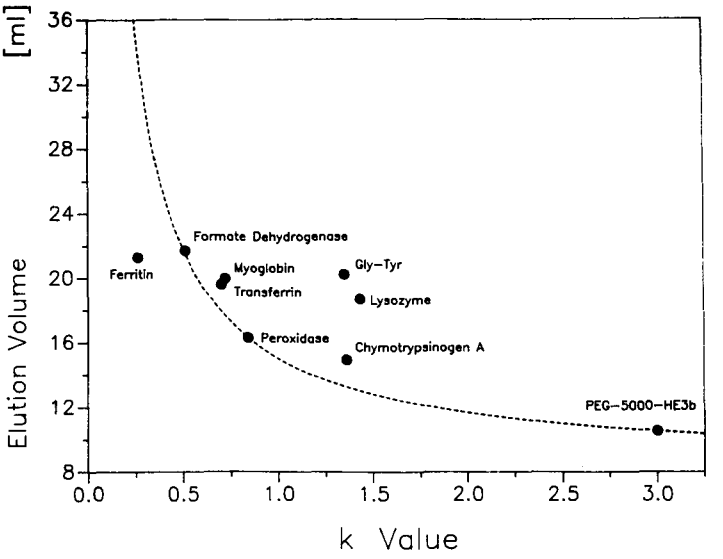

Fig. 4. Experimental results in Fig. 2 (●) replotted together with the computer-derived hyperbola (dashed line) illustrating the ideal elution curve of the column. (V_s = 7.2 ml, V_m = 8.37 ml). The values for glycyl-L-tyrosine and lysozyme were omitted in calculating V_s and V_m.

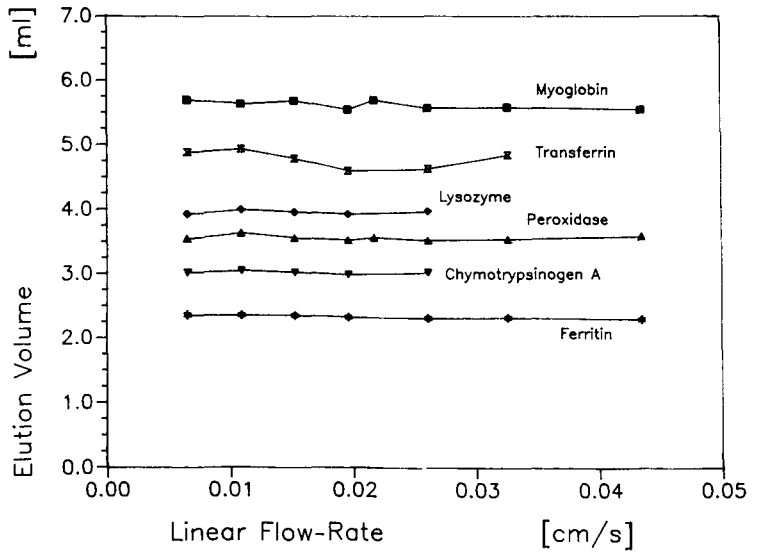

Fig. 5. Elution volume of the standard proteins from a column of LiParGel 750 as a function of the linear flow-rate. Column: 30 × 0.5 cm I.D.). System composition: 2.7% PEG 20 000, 4.5% dextran Pl 500, 75 m*M* KBr, 10 m*M* phosphate buffer (pH 7); temperature, 30°C.

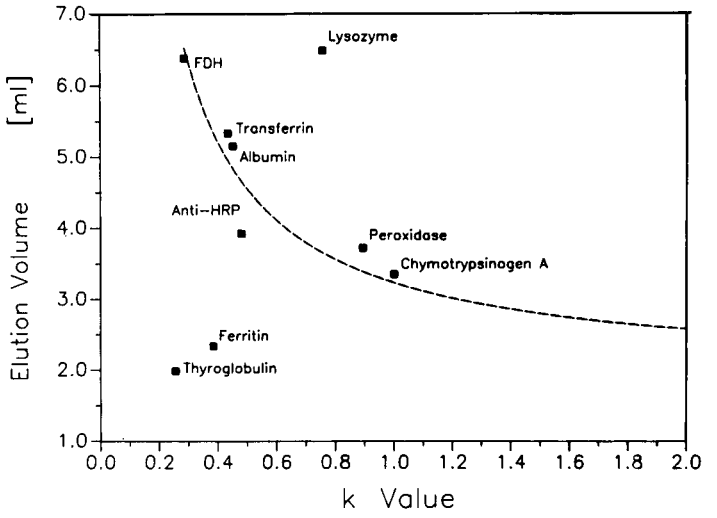

Fig. 6. Elution behaviour of the LiParGel 650. Column: 30 × 0.5 cm I.D. System composition: 5.45% PEG 6000, 9.75% dextran Vc 40, 100 m*M* NaCl, 50 m*M* phosphate buffer (pH 7.5). The temperature was 23°C and the flow-rate 0.15 ml/min. ● = Measured elution volume. The graph (dashed line) is a result of a computer fit omitting data for lysozyme, ferritin and thyroglobulin for evaluation. The calculated values for V_s and V_m are 1.31 and 1.92 ml, respectively.

To confirm the size exclusion properties of the support material, we tested LiParGel 650, which is based on the Fractogel TSK HW 65 (s) and recommended by the manufcturer for proteins smaller than $8 \cdot 10^4$ dalton. We also injected two other large protein molecules: a monoclonal antibody (MW $1.5 \cdot 10^5$ dalton) and thyroglobulin (MW $6.69 \cdot 10^5$ dalton). To exclude any influence of the phase composition on the results, we equilibrated the LiParGel 650 with a phase system of PEG 6000 and dextran V_c 40 (MW $4 \cdot 10^4$). Again a computer fit was used to correlate the data obtained. The results are presented in Fig. 6.

Lysozyme is eluted again much too late, corresponding to our previous observations. The premature elution of thyroglobulin, ferritin and the antibody follows their increasing molecular weight and verifies the assumption of a size exclusion effect of the support material. The largest molecule, thyroglobulin, shows the largest difference with regard to the calculated elution volumes and the antibody the smallest difference. We again reduced the flow-rate in this experiment to exclude mass transport problems and limitation in diffusion, and no change in the elution positions of thyroglobulin, ferritin and the antibody was observed (data not shown).

Polyacrylated LiChrospher Diol as support material

The next experiments were carried out with polyacrylated LiChrospher Diol 1000/10 as support material. The material was a research sample, based on silica beads of 10-μm diameter and selected for the large pore size of 100 nm. We equilibrated the column with the same phase system as in the experiments in Fig. 2 and chromatographed the same set of standards. Fitting was performed neglecting the experimental value for lysozyme, and the results are shown in Fig. 7.

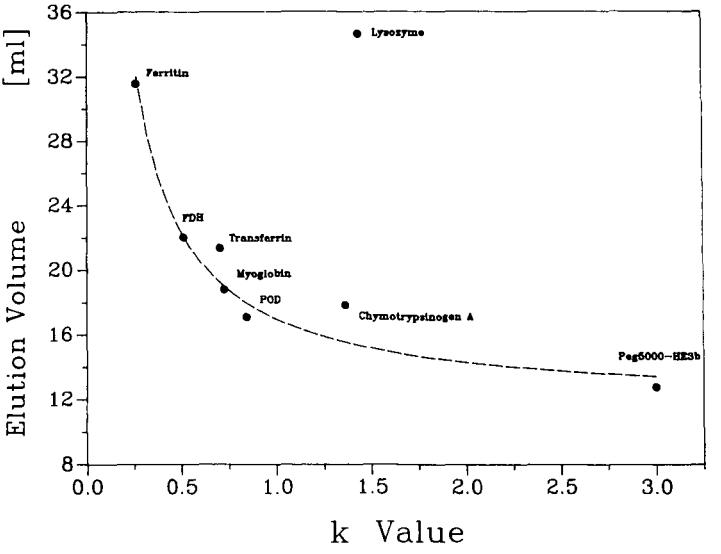

Fig. 7. Elution volume of the standard proteins and the PEG-5000 triazine dye derivative from a column of LiChrospher Diol 1000/10 (30 × 1 cm I.D.). System composition: 2.7% PEG 20 000, 4.5% dextran Pl 500, 75 m*M* KBr, 10 m*M* phosphate buffer (pH 7). The temperature was 30°C and the flow-rate 0.35 ml/min. ● = Measured elution volume. The graph (dashed line) is the result of a computer fit omitting the data for lysozyme. The calculated values for V_s and V_m are 5.75 and 10 ml, respectively.

The silica-based support shows no size exclusion properties indicated by the elution behaviour of ferritin, where the experimental elution volume is idential with the calculated value. The difference between the calculated and the experimental elution positions of lysozyme is even larger than that obtained with LiParGel. This result was not unexpected, as it was known that the starting material contained negatively charged groups. Other interactions might contribute to the observed result, but could not be differentiated.

DISCUSSION

It is obvious that in liquid–liquid partition chromatography using LiParGel 650 and 750 to retain the dextran-rich bottom phase of an aqueous phase system, the elution volume of a given substance may be a function of at least four different superimposed effects: the partition coefficient in the phase system, interactions of the analyte with hydrophobic and/or negatively charged residues and size exclusion properties of the support material. With LiChrospher Diol 1000/10, the pore size of the material seems to be sufficient to avoid size exclusion effects, at least up to molecular weights of *ca.* $5 \cdot 10^5$ dalton. The equations derived from the basic experiments of Martin and Synge [10] to calculate the volumes of stationary and mobile phase of a given column are valid only for true partitioning in the absence of other strong interactions. As the latter requirement is difficult to judge beforehand, a set of standards and a computer fit of the experimental data will yield more accurate values for V_s and V_m than calculations based on two components only.

Changing the ionic strength or pH of the phases employed will suppress interactions due to the charge [11], but the size exclusion properties can only be avoided by employing support material with larger pore sizes and to some extent also by lowering the molecular weight of the polymers forming the phase system. This conclusion does not affect the general applicability of the support material for partition chromatography. Liquid–liquid partition chromatography is well suited to solve difficult separation problems [11–16]. Some of the additional interactions described here might even be used with advantage to achieve a desired separation.

ACKNOWLEDGEMENTS

We thank Professor W. Müller and Mr. D. Forciniti for stimulating disscussions and E. Merck for the Superformance system and supplying LiParGel and polyacrylated LiChrospher Diol. A.W. was supported by a fellowship within the BMFT programme Applied Biology and Biotechnology by DECHEMA.

REFERENCES

1 C. J. O. R. Morris, *Protides Biol. Fluids, Proc. Colloq.*, 10 (1963) 325.
2 W. Müller, H. J. Schütz, C. Guerrier-Tanaka, P. E. Cole and R. Potts, *Nucleic Acids Res.*, 7 (1979) 2483.
3 W. Müller and G. Kütemeier, *Eur. J. Biochem.*, 128 (1982) 231.
4 W. Müller, *Eur. J. Biochem.*, 155 (1986) 213.
5 G. Mino and S. Kaizerman, *J. Polym. Sci.*, 31 (1958) 242.
6 A. Cordes and M.-R. Kula, *J. Chromatogr.*, 376 (1986) 375.
7 P. A. Albertsson, *Partition of Cell Particles and Macromolecules*, Wiley-Interscience, New York, 3rd ed., 1986.
8 A. Lehninger, *Biochemie*, Verlag Chemie, Weinheim, 1st ed., 1975.
9 H. Schütte, J. Flossdorf, H. Sahm and M.-R. Kula, *Eur. J. Biochem.*, 62 (1976) 151.
10 A. J. P. Martin and R. L. M. Synge, *Biochem. J.*, 35 (1941) 1358.
11 W. Müller, *Kontakte (Darmstadt)*, No. 3 (1986) 3.
12 W. Müller, *Kontakte (Darmstadt)*, No. 1 (1987) 45.
13 W. Müller, *Kontakte (Darmstadt)*, No. 1 (1988) 54.
14 M. R. Kula, A. Walsdorf and C. Cordes, *Ber. Bunsenges. Phys. Chem.*, 93 (1989) 968.
15 A. Heubner, O. Belowsky, W. Müller, W. Grill and K. Pollow, *J. Chromatogr.*, 397 (1987) 419.
16 A. Heubner, M. Juchem, W. Müller and K. Pollow, in D. Fisher and I. A. Sutherland (Editors), *Separations Using Aqueous Phase Systems*, Plenum Press, New York and London, 1989, p. 393.

Journal of Chromatography, 542 (1991) 65–81
Elsevier Science Publishers B.V., Amsterdam

CHROM. 23 016

Use of polymeric reversed-phase columns for the characterization of polypeptides extracted from human pancreata

I. Effect of the mobile phase

BENNY S. WELINDER* and SUSANNE LINDE
Hagedorn Research Laboratory, 6 Niels Steensensvej, DK-2820 Gentofte (Denmark)
(First received August 20th, 1990; revised manuscript received November 23rd, 1990)

ABSTRACT

The high-performance liquid chromatographic (HPLC) behaviour of two different styrene–divinylbenzene-based reversed-phase (RP) columns was evaluated using crude acetic acid extracts from normal and diabetic human pancreata as samples. Acetic acid gradients in water and acetonitrile gradients in triethylammonium phosphate (TEAP) and trifluoroacetic acid (TFA) were used as mobile phases, and comparisons were made with a silica-based C_4 column. When two different polymeric RP columns were eluted with acetic acid gradients in water, surprisingly similar HPLC profiles of the pancreatic extracts were obtained. Elution of the polymer-based columns with acetonitrile gradients in TFA or TEAP resulted in changes in the polypeptide selectivity of these columns, in parallel with that of a silica-based C_4 column eluted under similar conditions, indicating the general usability of polymeric columns for RP-HPLC of peptides and proteins. The pronounced difference in composition between normal and diabetic samples, which also was demonstrated after size-exclusion chromatography (SEC) on a silica-based and an agarose-based high-performance SEC column, was found to be related to the different ischaemia times for the two types of pancreata.

INTRODUCTION

We have recently demonstrated that several polypeptides, including insulin and growth hormone, could be eluted from a divinylbenzene-based polymeric reversed-phase (RP) column eluted with an acetic acid gradient in water. The peak shapes were excellent, and the recoveries were comparable to those obtained after elution with acetic acid-based mobile phases containing "classical" organic modifiers (*i.e.*, acetonitrile or 2-propanol) [1]. This stationary phase–mobile phase combination was also found to be very useful for the RP high-performance liquid chromatographic (HPLC) characterization of crude acetic acid extracts of normal and diabetic human pancreas. Almost identical UV profiles were obtained for acetic acid gradients in acetonitrile, 2-propanol or water, and the elution patterns after RP-HPLC utilizing acetic acid gradients in water were found to be similar to those obtained when a silica-based C_4

0021-9673/91/$03.50

column was eluted with acetonitrile gradients in trifluoroacetic acid (TFA) [2].

The elution patterns from the normal and the diabetic human pancreas were very different. Considerably smaller amounts of polypeptides could be extracted from the diabetic than from the normal pancreas, and the polypeptides detected after RP-HPLC were shifted significantly towards lower molecular weight and/or hydrophobicity. This finding might reflect that the normal pancreata were removed and frozen shortly after clinical death whereas the diabetic glands were taken out after more than 6 h ischaemia time (according to the Danish death criteria), leaving sufficient time for the digestive enzymes in the exocrine pancreas to carry into effect a pronounced proteolytic degradation.

In order to explain this point, we analysed the acetic acid-extractable polypeptides obtained from a number of diabetic and normal human pancreatic glands with similar ischaemia times, and the effect on "fresh", normal pancreata of a 6-h time period at room temperature before extraction. Protein determinations and insulin analyses [radioimmunoassay (RIA)] of the extracts were performed as well.

The performance of silica-based alkyl RP columns in polypeptide analyses is highly dependent on the actual mobile phase, especially the buffer components. Further, columns supposed to be identical (*e.g.*, "end-capped" C_{18} columns from different manufacturers, or from the same manufacturer but from different batches) may behave differently after elution with identical mobile phases [3–5].

As the potential value of polymeric columns for RP-HPLC of polypeptides remains largely untested [3], we performed the analyses with acetic acid gradients in water on two different polymeric RP columns (based on polymerized divinylbenzene or styrene). With acetic acid extracts of a normal and a diabetic human pancreas as model samples, one of the polymer columns was further eluted with acetonitrile gradients in TFA and triethylammonium phosphate (TEAP), and the results were compared with those of similar separations performed on a silica-based C_4 column.

EXPERIMENTAL

Apparatus

Commercially available HPLC equipment and columns were used throughout: pumps, Waters Assoc. M510 and M6000A, Gynkotek 300C; sample injectors, U6K, WISP 710A and B (Waters Assoc.), 7125 (Rheodyne); UV detectors, Linear UVIS 200, Hitachi L4200; integrator, Hitachi L2500; and gradient controllers, Waters Assoc. M660, Gynkotek 250B and 480.

Asahipak ODP-50 (150 × 4.6 mm I.D.), C8P-50 and C4P-50 (250 × 4.6 mm I.D.), Chrompack 8P 300 RP (150 × 4.6 mm I.D.), 300 Å Nucleosil C_4 (5 μm, 250 × 4.0 mm I.D.), TSK Phenyl 5PW RP+ (75 × 4.6 mm I.D.), Tosoh octadecyl 4PW (150 × 4.6 mm I.D.) and Tosoh octadecyl NPR (35 × 4.6 mm I.D.) columns were obtained prepacked. Dynospheres PD-102-RE was obtained as a 10-μm packing material from Dyno Particles; 250 and 30 × 4.6 mm I.D. columns were slurry-packed in methanol in our laboratory (maximum pressure 150 bar). Zorbax Bio Series GF-250 and 450 columns (250 × 9.6 mm I.D.) and a 300 × 10.0 mm I.D. Superose 12 column were obtained from DuPont and Pharmacia, respectively.

Chemicals

Acetonitrile was obtained form Rathburn (HPLC grade S), acetic acid (analytical-reagent grade) from Merck and TFA (sequential grade) from Applied Biosystems. All other chemicals were of analytical-reagent, sequential or similar purity. Water was drawn from a Millipore Milli-Q plant. The mobile phases were Millipore-filtered (0.45 μm) and degassed (vacuum/ultrasound) before use. During chromatography, the mobile phases were degassed continuously by passage through an ERMA ERC 3310 or a Shodex KT-35S degasser.

HPLC separations

All separations were performed at room temperature. Detailed descriptions of the stationary and mobile phases used are given in the figure legends.

Polypeptide standards

Highly purified human insulin and human proinsulin were obtained from Novo-Nordisk and crystalline porcine glucagon (same amino acid sequence as human glucagon) from Sigma.

Samples

Pancreatic glands were obtained from the University Hospital, Copenhagen. From normal subjects classified as kidney donors, the pancreas was removed and frozen shortly after death. Only non-identified parts (40–140 g frozen weight, 10–37 g after lyophilization) of these pancreata were available for this study. A number of normal and insulin-dependent diabetic human glands [obtained in their entirety, age and duration of insulin-dependent diabetes mellitus (IDDM) unknown] were obtained after 6–8 h ischaemia time.

Sample preparation was performed essentially as described [2]. Briefly, the pancreas was lyophilized, minced and extracted with 3 *M* acetic acid at 4°C. The acetic acid extract was analysed as such, or after lyophilization. Redissolved lyophilized pancreatic extracts were subjected to gel chromatography (Sephadex G-50 eluted with 3 *M* acetic acid at 4°C), and two major fractions were obtained: peak I [molecular weight (MW) >6000 dalton] containing the major pancreatic digestion enzymes, albumin and globulins and peak II (MW $\leqslant 6000$ dalton, salts being excluded). Peak I and II materials were isolated from the column eluate by lyophilization.

Sodium dodecyl sulphate–polyacrylamide gel electrophoresis (SDS-PAGE)

SDS-PAGE was performed in a PhastGel apparatus (Pharmacia) with 8–25% gradient gels. Electrophoresis and silver staining were performed as described by the manufacturer (Pharmacia Bulletins Nos. 110 and 210).

Protein determinations

The protein content in the extracts was measured in the BCA protein assay (Pierce) with bovine serum albumin as standard. Before analysis, the extracts were diluted to 0.1 *M* acetic acid.

Insulin determinations

In order to avoid unspecific binding of insulin, the pancreatic extracts were diluted 1:10 with 6 *M* urea and left for 1 h in this solvent before further dilution.

Insulin RIA was performed essentially as described [6]. Monoiodinated insulin tracer was obtained from Novo-Nordisk.

RESULTS

The RP-HPLC separations of raw acetic acid extracts of a normal and a diabetic human pancreas using two different polymeric columns (Dynospheres PD-102-RE and Chrompack 8P 300RP) are shown in Fig. 1. The columns were eluted with 60-min linear acetic acid gradients in water (from 34 to 90% acetic acid), and the elution patterns were surprisingly similar. However, whereas insulin and glucagon coeluted from the Dynospheres column, they were separated on the Chrompack column.

We have recently shown that the elution patterns of extractable polypeptides from diabetic pancreata were very different from those from normal subjects, and

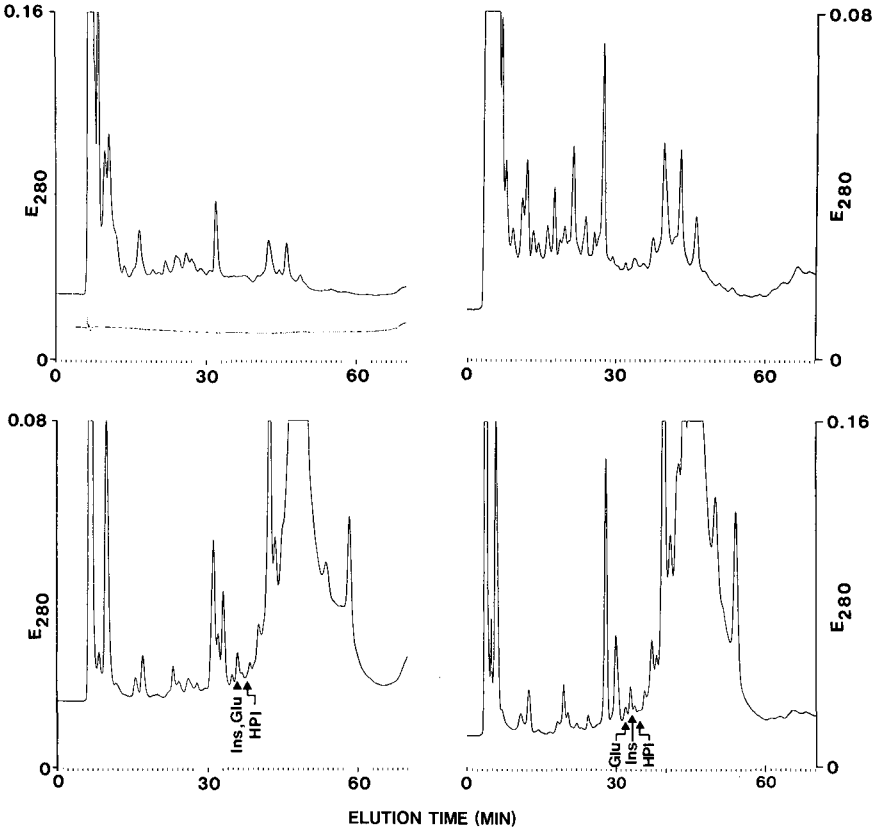

Fig. 1. RP-HPLC of 50 μl of acetic acid extract of a normal human pancreas (H93, bottom) and a diabetic human pancreas (H56, top) using a 250 × 4.6 mm I.D. Dynospheres PD-102-RE column (left) or a 150 × 4.6 mm I.D. Chrompack 8P 300 RP column (right) eluted with an acetic acid gradient (from 34% to 90% acetic acid linearly for 60 min, followed by 10 min isocratically at 90% acetic acid) at 0.5 ml/min. The elution positions of authentic human insulin (Ins), proinsulin (HPI) and glucagon (Glu), obtained after chromatography of the extracts spiked with the corresponding hormones, are marked.

that greater individual variations were found between the compositions of extracts from a few individual diabetic than from a few normal pancreatic glands [2]. We therefore extracted five different diabetic glands and analysed the extractable polypeptides on both polymeric RP columns. Two representative extracts are shown in Fig. 2. When these UV profiles are compared with those of a normal extract (lower curves in Fig. 1), it is evident that the dominant sample constituents in the normal extract (eluted in the last third of the chromatograms) are virtually absent from all diabetic extracts. Although similar in the outline, the elution patterns for the diabetic glands displayed a number of minor differences, and these differences are clearly and identically observed in the chromatograms from both polymeric RP columns.

The molecular size distribution in lyophilized acetic acid extracts from three normal and three diabetic pancreata were analysed on two different high-performance size-exclusion chromatography (HPSEC) columns. Typical chromatograms are shown in Fig. 3 for silica-based Zorbax GF-250 and GF-450 columns in series (right) and an agarose-based Superose 12 column (left). Although the distributions of sample components separated on the two different HPSEC columns are different, it is clearly seen that sample components with higher molecular weights were present in extracts form normal pancreata (Fig. 3, bottom) than in the extracts of diabetic glands (Fig. 3, top).

As the major difference between the handling of the normal and the diabetic glands was the ischaemia period, parts of three individual normal pancreata were thawed and kept at room temperature for 6 h before lyophilization and extraction. Two typical chromatograms obtained on the Dynospheres column are shown in Fig. 4 (top and middle). In spite of individual differences in the total amounts of extracted and eluted polypeptides, the overall distributions of sample components from the two pancreata are comparable to that of an instantly removed and frozen normal pancreas (compare with Fig. 1). Strikingly similar chromatograms were obtained for the same samples using the Chrompack column (data not shown).

Whole normal human pancreatic glands were obtained after similar ischaemia times as for the diabetic glands, and three of them were extracted and analysed as described above. The elution pattern of a single of these "normal" glands (Fig. 4, bottom) was different from that of the fresh normal gland shown in Fig. 1 and the fresh normal glands incubated for 6 h at room temperature (Fig. 4, top and middle): the UV profile was totally shifted towards that of a diabetic gland (as shown in Fig. 2) with almost total disappearance of the dominant sample components eluted in the last part of the gradient.

The protein and insulin contents in acetic acid extracts of normal glands with various time periods between removal, freezing and lyophilization/extraction are shown in Table I. As only non-identified parts of fresh normal glands were available, and as the distribution of hormone-producing cells is uneven throughout the gland [7–15], a variable insulin content in these extracts would be expected. In order to overcome this uncertain factor, a single part of a normal human pancreas was thawed, cut into several smaller pieces and mixed. Half of the pieces were lyophilized immediately and the other half were left at room temperature for 6 h before lyophilization. After extraction, the protein contents in the extracts from the two halves were found to be comparable (175 mg per g pancreas for the fresh half and 158 mg per g pancreas for the half incubated for 6 h at 22°C), whereas the insulin content was

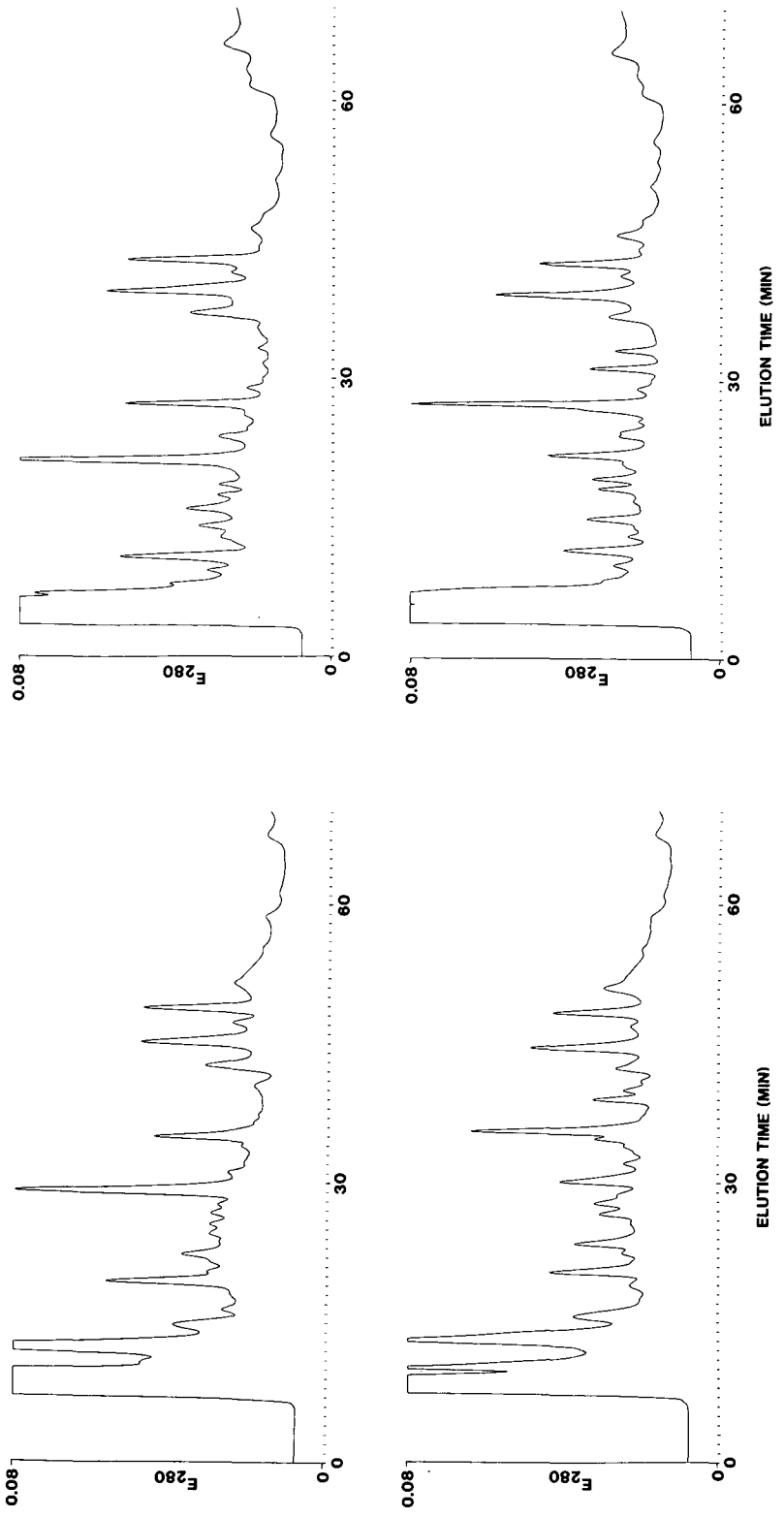

Fig. 2. RP-HPLC of 200 μl of acetic acid extract from two individual diabetic human pancreata using a 280 × 4.6 mm I.D. Dynospheres PD-102-RE column (top) or a 150 × 4.6 mm I.D. Chrompack 8P 300 RP column (bottom) eluted essentially as described in Fig. 1. The order of the two individual diabetic pancreatic glands (left, diabetic pancreas A; right, diabetic pancreas B) is identical in both the top and bottom panels.

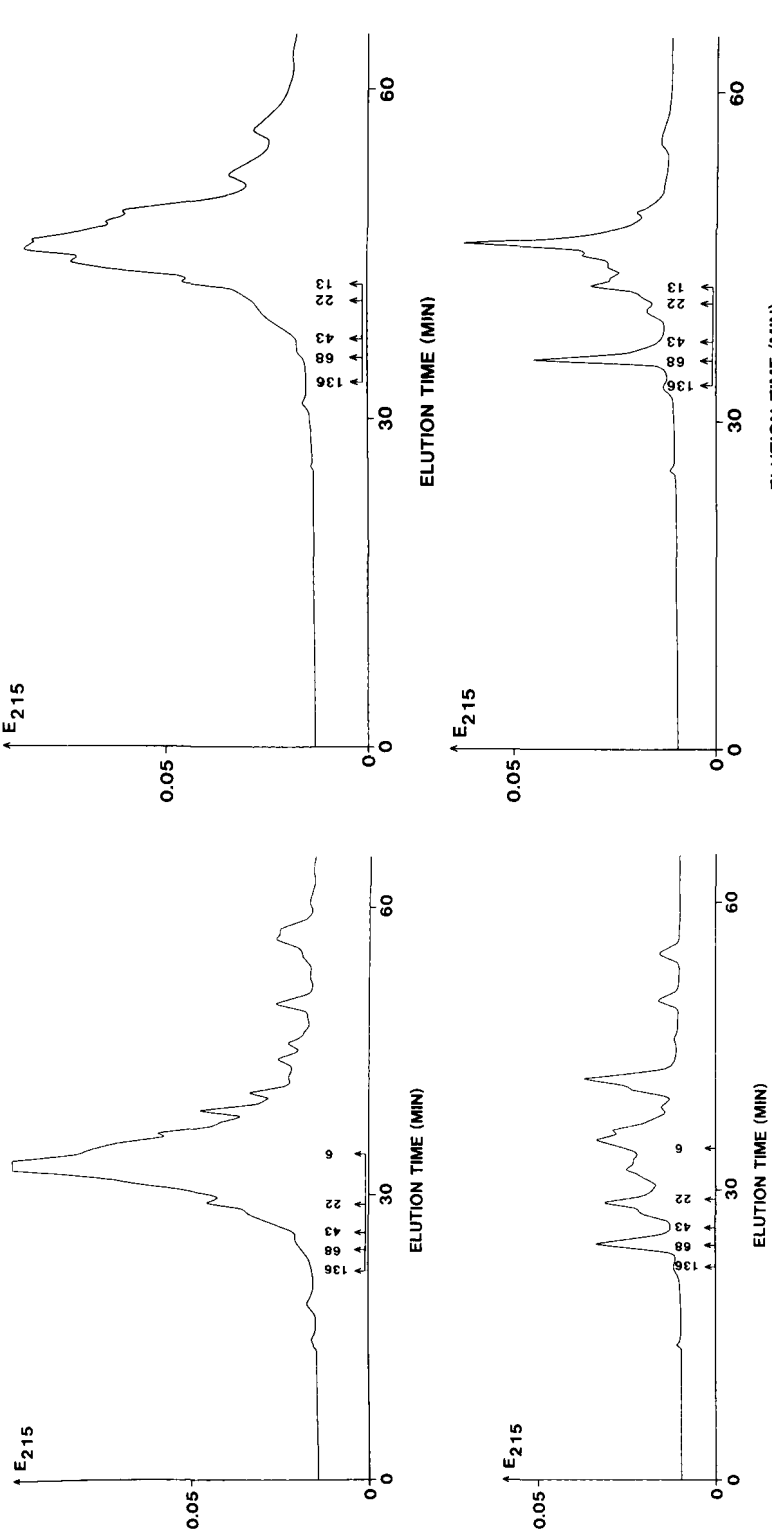

Fig. 3. HPSEC of lyophilized acetic acid extract from a diabetic (top) and a normal human pancreas (bottom) using a 300 × 10.0 mm I.D. Superose 12 column (left) or 250 × 9.4 mm I.D. Zorbax GF-250 and GF-450 columns connected in series (right). The columns were eluted at 0.5 ml/min with 0.2 *M* Na_2HPO_4 (pH 7.0). The lyophilized crude extracts were redissolved in the mobile phase to 1 mg/ml and 100 μl were applied to both columns. The elution positions of HSA dimer (136 000 dalton), HSA (68 000 dalton), ovalbumin (43 000 dalton), growth hormone (22 000 dalton), ribonuclease (13 000 dalton) and insulin (6000 dalton) are marked.

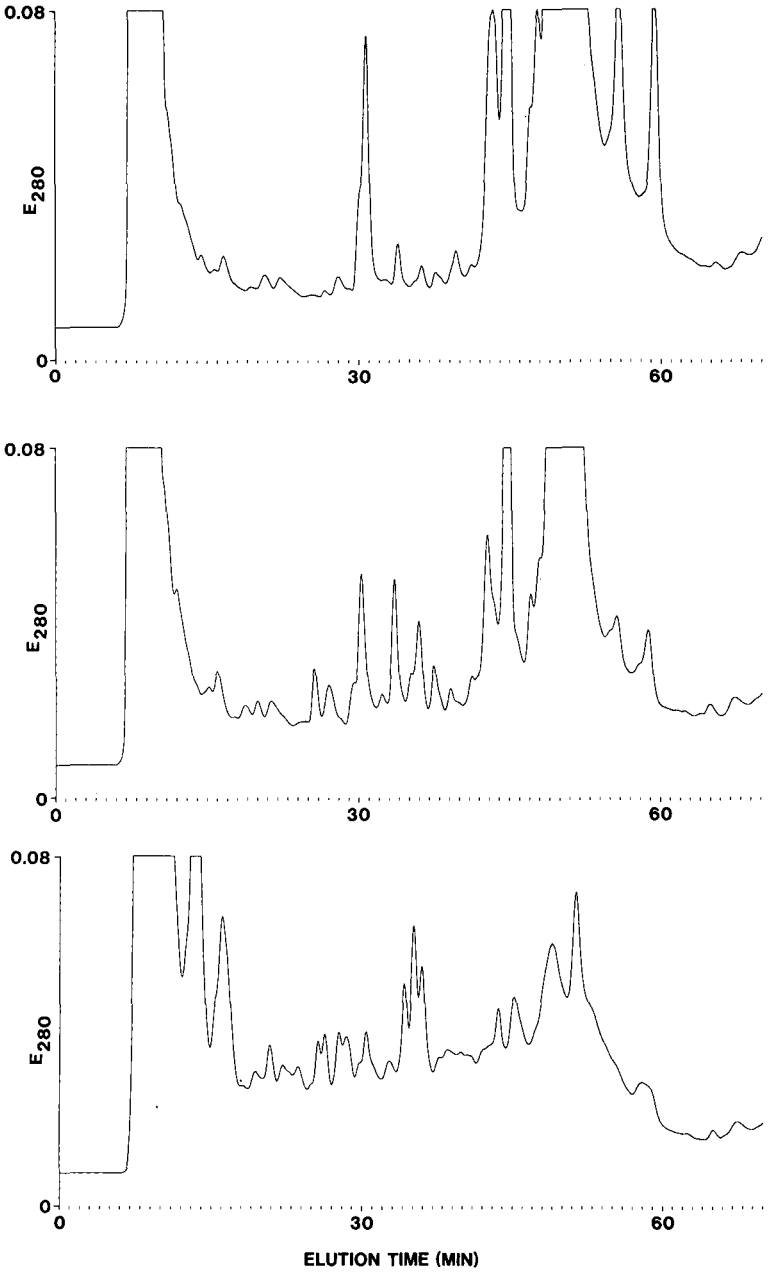

Fig. 4. Top and middle: RP-HPLC of 200 μl of acetic acid extract from two individual normal human pancreatic glands, removed and frozen shortly after death. The glands were allowed to thaw and then kept at room temperature (*ca.* 22°C) for 6 h before lyophilization and extraction. Bottom: RP-HPLC of 200 μl of acetic acid extract from a normal human pancreas gland removed after 6–8 h ischaemia time. A 280 × 4.6 mm I.D. Dynospheres PD-102-RE column was eluted essentially as in Fig. 1.

TABLE I

CONTENTS OF PROTEIN AND INSULIN (IN PARENTHESES) IN THE CRUDE ACETIC ACID EXTRACTS OF THREE FRESH NORMAL AND FIVE DIABETIC HUMAN PANCREATA, THREE FRESH NORMALS WHICH WERE THAWED AND KEPT AT ROOM TEMPERATURE FOR 6 HOURS BEFORE EXTRACTION AND OF THREE NORMALS WITH A SIMILAR ISCHAEMIA TIME AS THE FIVE DIABETIC GLANDS

The values for the fresh normals and the diabetics are reprinted from ref. 2. The protein content is calculated as mg per gram of lyophilized pancreas and the insulin content as μg per gram of lyophilized pancreas.

Fresh normal	Fresh normal, 6 h at room temperature	Normal, 6–8 h ischaemia time	Diabetic, 6–8 h ischaemia time
258 (607)	269 (9)	86 (631)	80 (37)
161 (463)	325 (14)	93 (729)	59 (38)
81 (322)	311 (1803)	94 (533)	15 (15)
			41 (19)
			53 (14)

drastically reduced after the incubation period (288 μg per g pancreas compared with 2200 μg per g pancreas for the non-incubated half).

The polypeptide profiles of the two halves (obtained after RP-HPLC using the Dynospheres column) were very similar with respect to the presence of individual sample components, and the SDS-PAGE analyses of the first, second and third extracts were almost identical (Fig. 5). However, larger amounts of most of the separated polypeptides were found in the extract from the fresh half compared with the "incubated" half, and the strongly reduced insulin content in the extracts, as measured in insulin RIA, was clearly demonstrated (Fig. 5).

In order to fully establish the potential of polymeric RP columns for polypeptide separations, acetic acid extracts of a normal and a diabetic pancreas were separated on the Dynospheres column utilizing acetonitrile as organic modifier in combination with two of the most popular mobile phase additives, TFA and TEAP. The resulting chromatograms were further compared with the separation patterns obtained for identical samples and mobile phases using a "classical" silica-based stationary phase, 5-μm 300 Å Nucleosil C_4. In order to increase the separation capacity, the gradient time was increased from 1 to *ca.* 2 h, and the separations of the normal and diabetic extracts with TEAP–acetonitrile are shown in Fig. 6 (Dynospheres) and Fig. 7 (Nucleosil).

Similar chromatograms utilizing acetonitrile gradients in TFA are shown in Fig. 8 (Dynospheres) and Fig. 9 (Nucleosil). Although the use of identical gradients resulted in closely comparable chromatograms for extracts of a normal pancreas (top), distinct differences in selectivity were observed in the separations of the diabetic extracts (middle). Several sample components eluted from the Dynospheres column with retention times between 5 and 20 min (Fig. 8, middle) seem to be eluted very early from the C_4 column, unresolved from the frontal solvent peak (Fig. 9, middle).

The use of acetic acid gradients in water as mobile phases excludes UV recording of the column eluate at 215–220 nm (as utilized in Figs. 6–9). Extracts of a normal human pancreas were therefore separated using TFA–acetonitrile as mobile

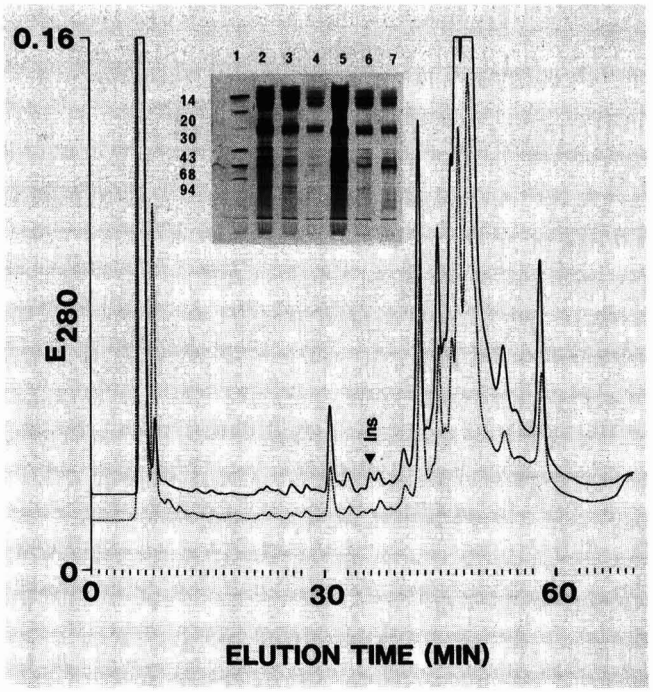

Fig. 5. RP-HPLC of two halves of a normal human pancreas removed and frozen shortly after death. One half was extracted immediately after lyophilization (solid curve) and the other half was kept at room temperature for 6 h before lyophilization/extraction (dotted curve). A 250 × 4.6 mm I.D. Dynospheres PD-102-RE column was eluted essentially as described in Fig. 1. The elution position of authentic human insulin (Ins) (obtained after chromatography of the extract spiked with insulin) is marked. SDS-PAGE of the first, second and third acetic acid extracts of the instantly extracted half (lanes 2, 3 and 4) and of the "incubated" half (lanes 5,6 and 7) is shown as an inset. Lane 1: molecular weight markers; MW in kilodaltons on the left.

phase followed by UV detection at 280 nm for the Dynospheres (Fig. 8, bottom) and the Nucleosil C_4 columns (Fig. 9, bottom). When these chromatograms are compared with those obtained after recording at 215 nm (Figs. 8 and 9, top), the chromatograms are strikingly alike. In spite of differences in light intensities for individual sample components, it appears valid to compare results obtained at different UV wavelengths.

DISCUSSION

We have recently described the use of acetic acid gradients for the analysis of acetic acid extracts of the human pancreas [2]. As the UV profiles of extracts of normal pancreata were very different from those of diabetic samples, and considering the fact that the objective for diabetes is the endocrine part (constituting *ca.* 1% of the weight of the total pancreas), the reason for this difference must originate from elsewhere.

In contrast to the parts of normal human glands (removed and frozen shortly

after death), the diabetic pancreata were obtained as whole organs, removed 6–8 h (or longer) after hospital death. Proteolytic cleavage could be expected to take place under these circumstances, as has been described for insulin, glucagon and pancreatic polypeptide in surgically removed, non-diabetic human pancreata [16–18].

When the RP-HPLC analyses of extracts of individual diabetic glands (Fig. 2) were compared with similar analyses of a normal sample (Fig. 1, bottom), it is evident that the proteolytic cleavage is not restricted to the above-mentioned pancreatic hormones (constituting less than 0.5% of the pancreatic polypeptide mass). Virtually all sample components eluted in the last half of the chromatogram (peak I material, MW >6000 dalton, normally constituting 95–98% of the extractable polypeptides [2]) were degraded. Concurrently with this disappearance, the front peak in the chromatograms increased dramatically, and this elution position would be expected for smaller peptides and amino acids.

The proteolytic degradation was also reflected in the HPSEC profiles for normal and diabetic extracts obtained on both SEC columns (Fig. 3) and in the figures

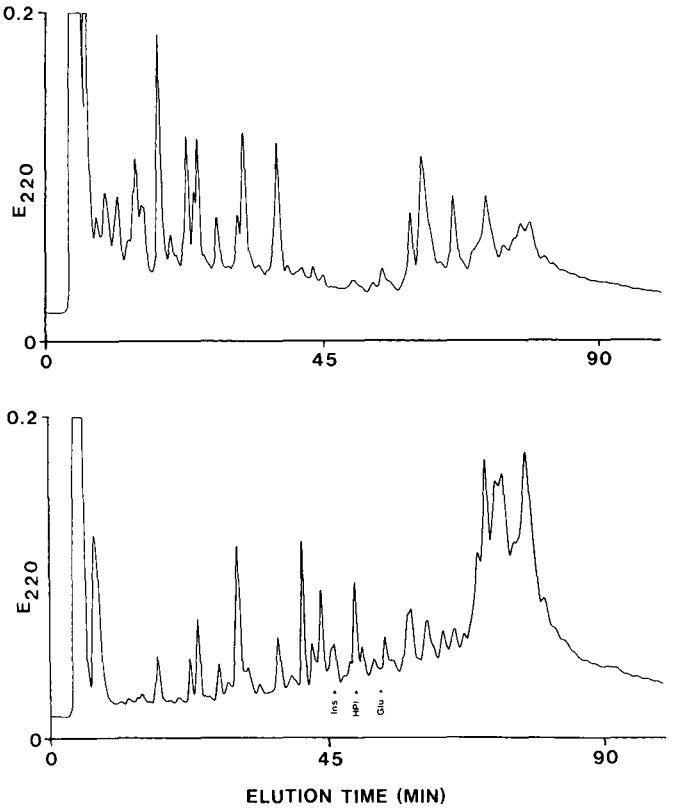

Fig. 6. RP-HPLC of 50 μl of acetic acid extract of a normal (bottom) and a diabetic, human pancreas (top) using a 250 × 4.6 mm I.D. Dynospheres PD-102-RE column eluted with an acetonitrile gradient in 25 m*M* TEAP (pH 3.0) (from 12% to 48% acetonitrile linearly for 100 min). Flow-rate, 1.0 ml/min. The extracts were similar to those analysed in Fig. 1. The elution positions of authentic human insulin (Ins), proinsulin (HPI) and glucagon (Glu) are marked.

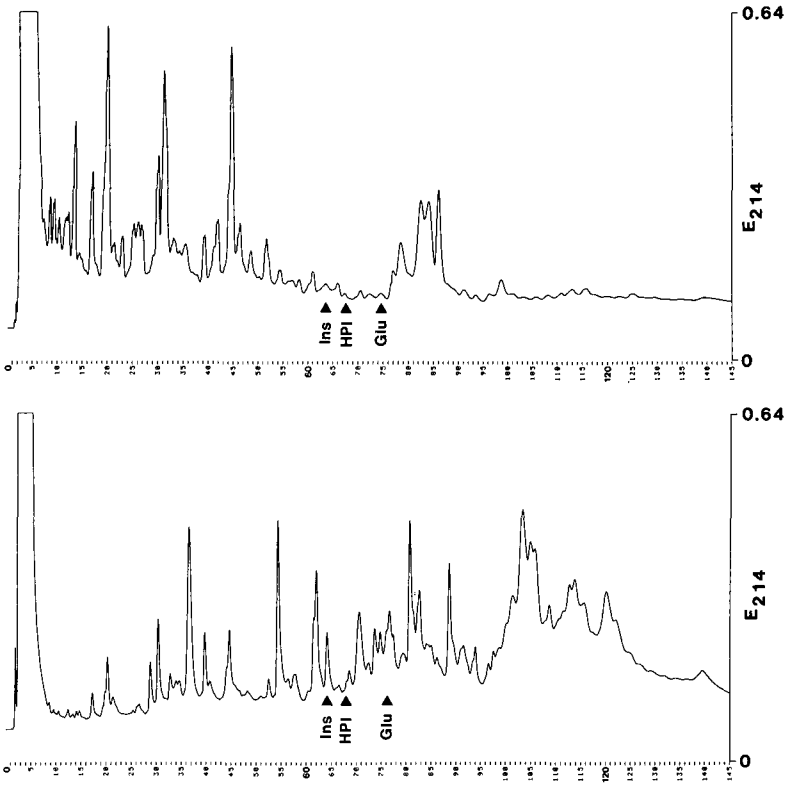

Fig. 7. RP-HPLC of 50 μl of acetic acid extract of a normal (bottom) and a diabetic human pancreas (top) using a 250 × 4.0 mm I.D. 300 Å Nucleosil C_4 (5 μm) column eluted with an acetonitrile gradient in 25 m*M* TEAP (pH 3.0) (from 12% to 45% acetonitrile linearly for 132 min followed by 45% to 60% acetonitrile linearly for 13 min). Flow-rate, 0.5 ml/min. The extracts were similar to those analysed in Fig. 1. The elution positions of authentic human insulin (Ins), proinsulin (HPI) and glucagon (Glu) are marked. Time scale in min.

for the protein contents in extracts of the five diabetic and three normal pancreatic glands (Table I), although it should be borne in mind, that large individual variations in such biological materials are likely to occur.

From the chromatograms obtained after extracting parts of individual normal pancreata which had been thawed and kept in the laboratory for 6 h at *ca.* 22°C before lyophilization and extraction (Fig. 4, top and middle), it is clear that no enzymatic cleavage comparable to that occurring in the diabetic pancreas was induced. The UV profiles were comparable to those for normal samples, and the protein contents in the raw extracts did not indicate any reduction (Table I). The differences in recoverable polypeptide mass after RP-HPLC and the difference in the size of the front peaks may be ascribed to individual variations in the sample material.

When three whole normal pancreatic glands, obtained after a similar ischaemia time to the diabetic sample, were analysed, the extractable polypeptides were found to be significantly degraded (Fig. 4, bottom). This chromatogram was very similar to those of diabetic glands (Fig. 2), *i.e.*, loss of peak I material and an abundant front peak,

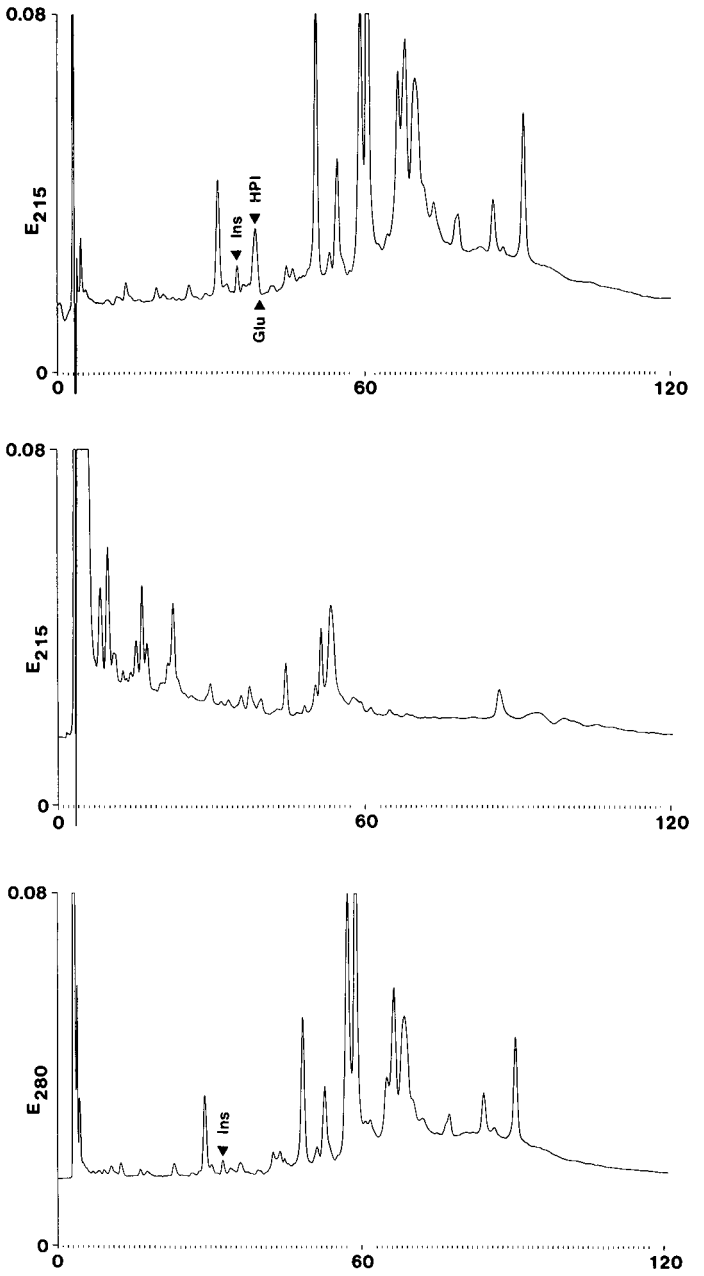

Fig. 8. RP-HPLC of 5 μl of acetic acid extract of a normal (top) and a diabetic human pancreas (middle) using a 250 × 4.6 mm I.D. Dynospheres PD-102-RE column eluted at 1.0 ml/min with an acetonitrile gradient in TFA (from 20% acetonitrile–0.075% TFA to 60% acetonitrile–0.070% TFA linearly for 120 min). Bottom: RP-HPLC of 50 μl of acetic acid extract of a normal human pancreas using a 250 × 4.6 mm I.D. Dynospheres PD-102-RE column eluted essentially as described for the top and middle panels. UV detection at 215 nm (top and middle) and 280 nm (bottom). The normal and diabetic samples were identical with those analysed in Figs. 1 and 7. The elution positions of authentic human insulin (Ins), proinsulin (HPI) and glucagon (Glu) are marked.

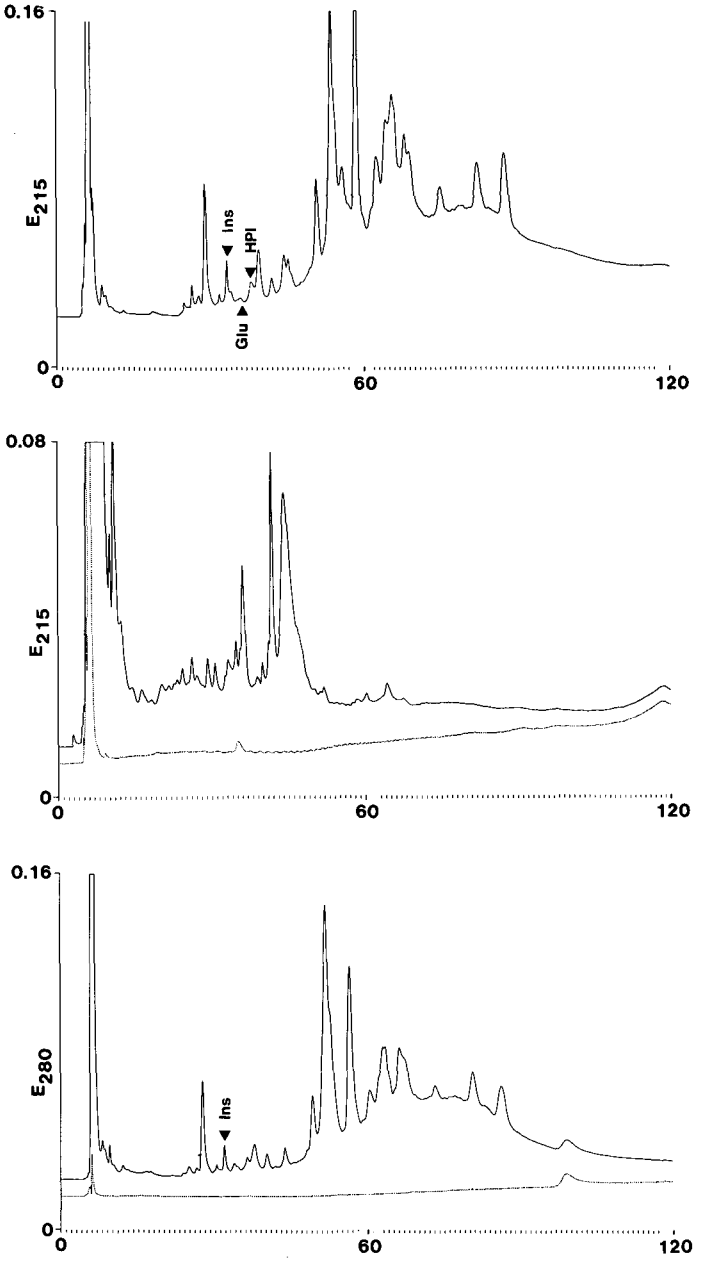

Fig. 9. RP-HPLC of 5 μl of acetic acid extract of a normal (top) and a diabetic human pancreas (middle) using a 250 × 4.0 mm I.D. 300 Å Nucleosil C_4 (5 μm) column eluted at 0.5 ml/min with essentially the same acetonitrile–TFA gradient as in Fig. 8. Bottom: RP-HPLC of 50 μl of acetic acid extract of a normal human pancreas using a 250 × 4.0 mm I.D. 300 Å Nucleosil C_4 (5 μm) column eluted essentially as described for the top and middle panels. The lower, dotted curves in the middle and bottom panels represent a blank injection (5 μl of 3 *M* acetic acid). UV detection at 215 nm (top and middle) and 280 nm (bottom). The normal and diabetic samples were identical with those analysed in Figs. 1, 7 and 8. The elution positions of authentic human insulin (Ins), proinsulin (HPI) and glucagon (Glu) are marked.

and the protein contents in the extracts were of the same order as found in the diabetic extracts (Table I).

The insulin contents in these glands were found to be similar to those of fresh, normal pancreata, whereas the values for fresh normal glands, thawed and kept at room temperature for 6 h, were extremely scattered (Table I). However, a study of 29 pancreatic glands obtained from human non-diabetics with ischaemia times from less than 1 to 24 h failed to show any correlation between the amount of extractable insulin and the corresponding ischaemia time [17]. Further, the insulin content in 32 non-diabetic human pancreata (with ischaemia times <6 h) varied from 4 to 192 μg per g wet pancreas [19], and a marked decrease in the amount of insulin extractable from fresh, immediately frozen pancreata has been reported to occur rapidly on thawing [18].

In spite of these large and expected individual differences among the various pancreata, it can be concluded that the ischaemia time is the major reason for the different UV profiles of extractable polypeptides previously observed between the normal and the diabetic pancreas. If a diabetic pancreas was removed and frozen instantly as for those from healthy persons, the sample constituents in the acetic acid extract would probably be very similar to that of a normal sample, with the exception of the insulin content.

That this difference in insulin content is actually detectable after RP-HPLC analyses using a polymeric column eluted with an acetic acid gradient in water is shown in Fig. 5. The curves represent the extracts of two equal halves of the same (part of a) normal human pancreas, the only difference being that one half was extracted immediately after thawing and the other was kept at 22°C for 6 h before extraction. The insulin content in the extract of the latter half was *ca.* 13% of that in the former, whereas the protein contents in the extracts from the two halves were similar. This difference in insulin content is clearly indicated in the chromatograms (Fig. 5) but, although the protein contents in the two raw extracts were found to be similar, less polypeptide mass is recovered after HPLC in the half left at 22°C. When analysed carefully, the two chromatograms revealed the presence of (various amounts of) identical sample components with retention times between 12 and 60 min, but the front peak was slightly broader, and the three peaks eluted immediately after the front peak were significantly more prominent in the extract from the "incubated" half. These minor differences could indicate an incipient proteolytic degradation after 6 h at room temperature.

Although the two different polymeric columns are based on different monomers (styrene *versus* divinylbenzene) and copolymerized additives (resulting in different loads of aromatics *versus* alkyl groups in the bonded phases), the chromatograms obtained after elution with acetic acid in water of these complex extracts were closely similar. When separations based on this mobile phase were compared with results obtained with an extended acetonitrile gradient in 25 m*M* TEAP, the Dynospheres column (Fig. 6) is seen to change in selectivity: for extracts from a normal pancreas, the resolution of the components in the peak I material (in the last half of the chromatogram) was poor, whereas the part of the chromatogram dedicated to separation of the polypeptides in the peak II material (MW $\leqslant$6000 dalton) became enlarged, and these components were very well resolved. In parallel with this, the extract of a diabetic pancreas showed a much higher heterogeneity than after the acetic acid gradient (compare with Fig. 1).

This change in selectivity was further increased if the polymeric column was replaced with a silica C_4 column eluted with the same mobile phase (Fig. 7): the resolution in the final part of the chromatogram of the extract from a normal pancreas was further reduced, whereas the peak shape and the separation capacity obtained for the peak II sample components (eluted in the first half of the chromatogram) were excellent (Fig. 7, bottom). Probably owing to the low hydrophobicity of the C_4 ligand, the separation of polypeptides extracted from the diabetic pancreas was less satisfactory in the last half of the chromatogram (Fig. 7, top).

Changing the mobile phase to acetonitrile in TFA resulted in selectivity changes in the opposite direction for the Dynospheres column (Fig. 8): compared with the acetic acid elution shown in Fig. 6, the initial halves of the chromatograms were alike in outline, whereas the peak I material in the last half was very well resolved (top). However, much of the material present in the extract of the diabetic pancreas was now not resolved from the front peak with this mobile phase (bottom), and this lack of resolution of polypeptides with low hydrophobicity was further emphasized when the Dynospheres column was replaced with the Nucleosil C_4 column (Fig. 9, top and middle).

When complex polypeptide mixtures are analysed using different stationary and mobile phases, the criteria for success may differ from one way of presenting the problems to another. Judged by parameters such as the ability to resolve the maximum number of components in a single analysis, whether they are characterized by high or low molecular weight and/or hydrophobicity, the use of polymeric RP columns eluted with acetic acid in water appears to be an exciting alternative to classical RP-HPLC polypeptide analyses. This work has further shown that polypeptide selectivity for a polymeric RP column can be manipulated according to documented experiences with mobile phase additives acquired for silica-based alkyl-RP columns.

Studies of the effect of various polymeric stationary phases on the resulting polypeptide selectivity using acetic acid–water and TFA–acetonitrile as mobile phases and the effect of the stationary and mobile phase on polypeptide recovery will be published separately [20].

ACKNOWLEDGEMENTS

We thank Helle Bojesen-Koefoed, Linda Larsø and Ingelise Fabrin for excellent technical assistance.

REFERENCES

1 B. S. Welinder and H. H. Sørensen, *J. Chromatogr.*, 537 (1991) 181.
2 B. S. Welinder and S. Linde, *J. Chromatogr.*, 537 (1991) 201.
3 C. T. Mant and R. S. Hodges, *J. Liq. Chromatogr.*, 12 (1989) 139.
4 K. K. Unger and K. D. Lork, *Eur. Chromatogr. News*, 2 (1988) 14.
5 B. S. Welinder, S. Linde and B. Hansen, *J. Chromatogr.*, 348 (1985) 347.
6 O. D. Madsen, L.-I. Larsson, J. H. Rehfeldt, T. W. Schwartz, Å. Lernmark, O. A. Labrecque and D. F. Steiner, *J. Cell. Biol.*, 103 (1986) 2025.
7 L. Orci, F. Malaisse-Lagae, D. Baetens and A. Perrelet, *Lancet*, ii (1978) 1201.
8 D. Baetens, F. Malaisse-Lagae, A. Perrelet and L. Orci, *Science*, 206 (1979) 1323.
9 F. Malaisse-Lagae, Y. Stefan, L. Cox, L. Perrelet and L. Orci, *Diabetologia*, 17 (1979) 361.
10 J. Rahier, J. Wallen, W. Gepts and J. Hoot, *Cell Tissue Res.*, 200 (1979) 359.

11 L. Orci and L. Perrelet, in R. H. Unger and L. Orci (Editors), *Glucagon, Physiology, Pathophysiology and Morphology of the Pancreatic A-Cell*, Elsevier, New York, 1981, p. 3.
12 E. R. Trimble, P. A. Halban, C. B. Wollheim and A. E. Renold, *J. Clin. Invest.*, 69 (1982) 405.
13 Y. Tasaka, S. Inoue, K. Marumo and Y. Hirata, *Acta Endocrinol.*, 105 (1984) 223.
14 R. L. Gingerich, P. E. Lacy, R. E. Chance and M. G. Johnson, *Diabetes*, 27 (1978) 96.
15 D. J. Gersell, R. L. Gingerich and M. H. Greider, *Diabetes*, 28 (1979) 11.
16 Y. Tasaka, S. Inoue, Y. Harata, F. Hanyu and M. Endo, *Endocrinol. Jpn.*, 28 (1981) 261.
17 J. R. Kimmel and H. G. Pollock, *Diabetes*, 16 (1967) 687.
18 G. A. Wrenshall, C. H. Best and W. S. Hartroft, *Can. J. Biochem. Physiol.*, 35 (1957) 527.
19 G. M. Rastogi, M. K. Sinha and R. J. Dash, *Diabetes*, 22 (1973) 804.
20 B. S. Welinder, *J. Chromatogr.*, 542 (1991) 83.

Journal of Chromatography, 542 (1991) 83–99
Elsevier Science Publishers B.V., Amsterdam

CHROM. 23 017

Use of polymeric reversed-phase columns for the characterization of polypeptides extracted from human pancreata

II. Effect of the stationary phase

BENNY S. WELINDER
Hagedorn Research Laboratory, 6 Niels Steensensvej, DK-2820 Gentofte (Denmark)
(First received August 20th, 1990; revised manuscript received November 23rd, 1990)

ABSTRACT

The potential value of eight commercial available polymer-based reversed-phase (RP) columns for peptide and protein separations was evaluated using crude acetic acid extracts of normal and diabetic human pancreata and mixtures of pure polypeptides as samples. All columns were characterized with acetic acid gradients in water as mobile phase, and different chromatographic profiles were obtained depending on the type of polymer column (bare or derivatized) and the type of ligand. Some of the columns were virtually free from effects related to the polymer skeleton whereas in others the separation was influenced by both the ligand and the polymeric backbone. Two selected polymeric RP columns were, together with a silica-based C_4 column, further characterized with acetonitrile gradients in trifluoroacetic acid (TFA), and the separation temperature was found to have a drastic effect on the separation efficiency for proteins with mol. wt. > 6000 dalton. No such effect was seen for polypeptides with mol. wt. < 6000 dalton.

Mixtures of pure peptides and proteins were separated using acetic acid gradients in water, acetonitrile or isopropanol, and normally the highest efficiency was found with the use of acetonitrile as mobile phase modifier. Isopropanol was less suitable as an organic modifier. The separation of the β-lactoglobulin A- and B-chains may be used to give a rapid estimate of the chromatographic usability of polymer-based RP-columns for peptide and protein separations in acetic acid gradients in water and in acetonitrile gradients. Recoveries for insulin, proinsulin, growth hormone, ovalbumin and human serum albumin were measured for several polymer-based RP columns eluted with acetic acid gradients in water and with acetonitrile-based mobile phases. The highest recoveries of serum albumin and ovalbumin were found after elution with acetic acid gradients in water.

INTRODUCTION

Although the first commercially available silica-based reversed-phase high-performance liquid chromatographic (RP-HPLC) columns were introduced more than 15 years ago, this type of stationary phase is still the main choice for RP-HPLC-based polypeptide analyses. More than 65% of the total number of HPLC analyses are performed on such columns [1], and the choice of mobile phase additives for these analyses (*e.g.*, insulin analyses) is invariably from one of three groupings: ion-pairing

0021-9673/91/$03.50

agents [alkylammonium salts, trifluoroacetic acid (TFA), phosphoric acid], salts at acidic or neutral pH (acetates, phosphates, sulphates) or chaotropic agents (*e.g.* perchlorates) in combination with acetonitrile [2].

Several polymer-based RP-HPLC columns have been available for some time, but although they in theory should offer some advantages over similar silica-based columns (higher chemical stability, no potential interfering silanol group [3]), their use for polypeptide analyses has been rare [4].

We have recently shown that polymeric RP columns eluted with acetic acid gradients (without any "organic modifier") are an interesting alternative for polypeptide analyses [5], especially for crude extracts of biological materials [6]. The separation patterns of acetic acid extracts of diabetic and normal human pancreata obtained after elution with acetic acid gradients were comparable to those resulting from the use of acetonitrile gradients in TFA or triethylammonium phosphate (TEAP), and similar results were obtained on a divinylbenzene (DVB)-based RP column and a silica C_4 column [6,7].

As the polypeptide selectivity of the DVB column could be changed in parallel with that of the silica C_4 column (*i.e.*, by changes in the mobile phase composition), and as the separation patterns after acetic acid gradient elution of a DVB-based and a styrene-based RP column were strikingly alike [7], a number of commercially available polymeric RP columns were compared with respect to their separation capacity for crude pancreatic extracts. In this work we examined several polymeric "phenyl" and "alkyl" columns with 120-min acetic acid gradients, and a few of these stationary phases were further characterized (together with a silica C_4 column) with similar samples using acetonitrile gradients in TFA.

EXPERIMENTAL

The HPLC equipment, columns and samples used were essentially as described in Part I [7]. Detailed descriptions of samples and stationary and mobile phases are given in the figure legends.

RESULTS

Fig. 1 shows the separation of crude acetic acid extracts from a normal and a diabetic human pancreas using three different polymeric RP columns [Dynospheres PD-102-RE (top, left), Chrompack 8P 300RP (top right) and TSK Phenyl 5PW RP+ (bottom)]. The three columns have aromatic groups as the principal type of bonded phase, but differ in other respects: the Dynospheres and Chrompack columns are polymerized (primarily) from DVB and styrene, respectively, whereas the TSK column has phenyl groups attached to a hydrophilic polymer backbone. The acetic acid gradients were similar in length and slope (increase of 0.45%/min of acetic acid). However, in order to obtain similar retention times for the principal sample components in the last part of the chromatograms of the normal pancreatic extracts (peak I material), the starting and ending points of the acetic acid gradient used for the elution of the TSK Phenyl column had to be adjusted from 37.5% to 90% acetic acid (used for the other two columns) to 20% to 72% acetic acid. On elution with the 37.5% to 90% acetic acid gradient, the chromatograms from the TSK Phenyl column

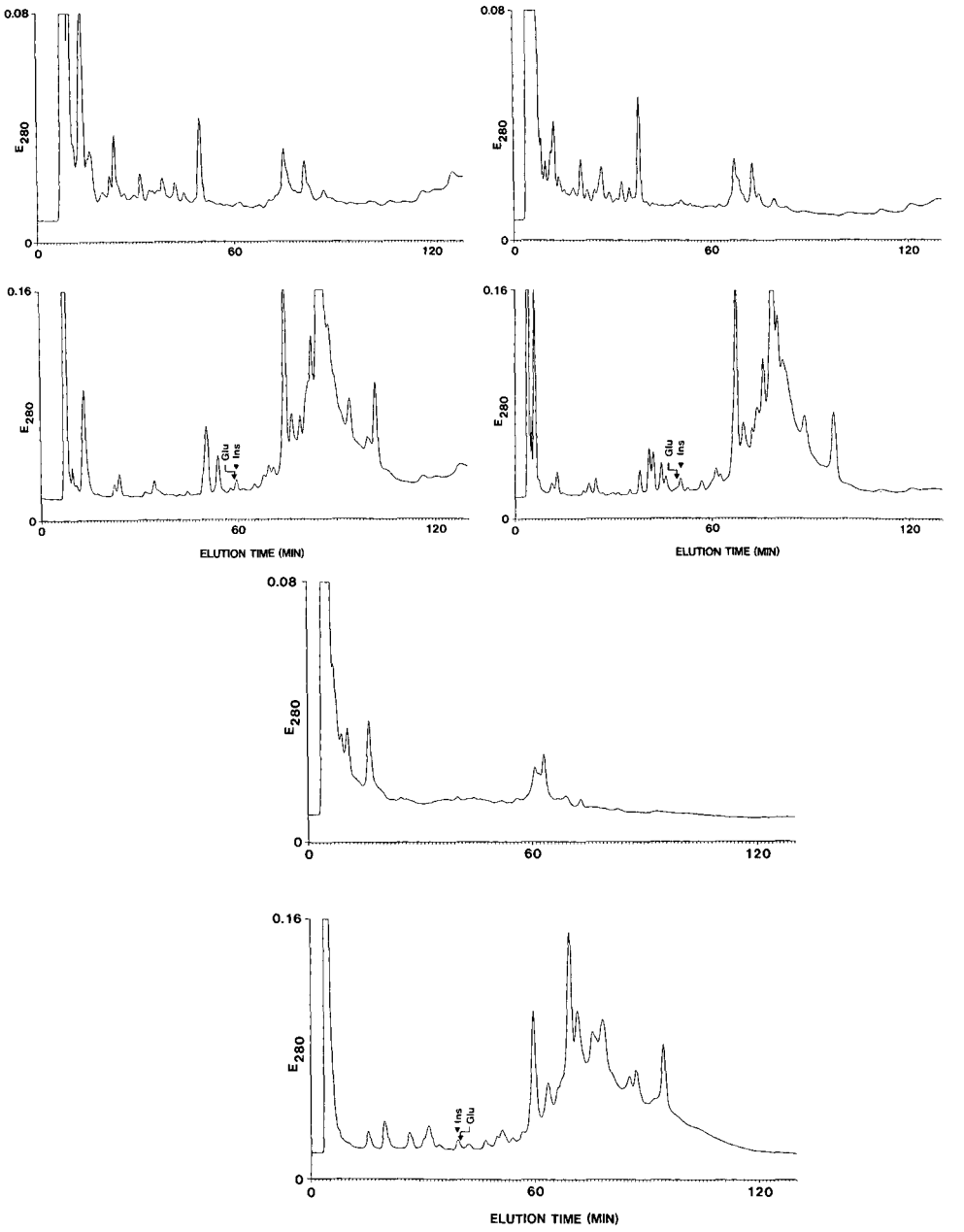

Fig. 1. RP-HPLC of 50 μl of crude acetic acid extract of a diabetic human pancreas (top) and a normal human pancreas (bottom) using a 250 × 4.6 mm I.D. Dynospheres PD-102-RE column (top left), a 150 × 4.6 mm I.D. Chrompack 8P 300 RP column (top right) or two 75 × 4.6 mm I.D. TSK Phenyl 5PW RP+ columns in series (bottom) eluted with an acetic acid gradient [from 34% to 90% acetic acid (top) or from 20% to 72% acetic acid (bottom) linearly for 120 min followed by 10 min isocratically at 90% acetic acid]. Flow-rate, 0.5 ml/min. Elution positions of authentic human insulin (Ins) and glucagon (Glu) are marked.

were unacceptably compressed and lacked all details otherwise revealed in the initial half of the chromatograms, and insulin and glucagon were not resolved from the front peak (data not shown).

The chromatograms for the Dynospheres and the Chrompack columns were remarkably similar: the chromatograms of the diabetic extract were almost replicas of each other, and they differed markedly from that obtained on the TSK Phenyl column. Further, the sharp peaks obtained on both columns in the first half of the chromatograms of extracts of a normal pancreas disappeared in the chromatogram from the TSK Phenyl column. However, the best separation of the individual components in the peak I material (composed primarily of albumin, globulin and the digestion enzymes from the exocrine pancreas [6]), eluted in the last part of the three chromatograms, was obtained with use of the TSK Phenyl 5PW RP+ column.

Separations of similar acetic acid extracts, using four different alkyl-polymer columns, are shown in Fig. 2. Three of these (the Asahipak columns) are composed of an identical poly(vinyl alcohol) matrix, to which C_4, C_8 or C_{18} groups are anchored (top left, top right and bottom left, respectively), whereas the fourth, a Tosoh octadecyl 4PW column (bottom right), has C_{18} groups attached to the same hydrophilic backbone as the TSK Phenyl 5PW RP+ column. The acetic acid gradients were of similar length and slope, but in order to obtain retention times comparable to the other three, the starting and ending points of the gradient used for the Asahipak C_4 column were reduced so as to be similar to that described above for the TSK Phenyl 5PW RP+ column.

A decreasing hydrophobicity of the bonded phases in the series C_{18} to C_4 was clearly demonstrated in the components eluted in the first half of the chromatogram of the normal pancreas [by and large corresponding to peak II material with molecular weight (MW) $<$ 6000 dalton], which were best separated on the C_{18} column (bottom left). In parallel with this, the components in the last half of the chromatograms (peak I material, MW $>$ 6000 dalton) displayed the greatest number of details on the C_4 column (top left). This column also seemed to have the best selectivity for the diabetic extract (top left, upper trace). However, the chromatograms of this extract obtained from all three columns were less detailed than those obtained using the Dynospheres or Chrompack columns (Fig. 1, top).

The separation of both extracts on the Tosoh C_{18} 4PW column (Fig. 2, bottom right) bore some resemblance to that on the TSK Phenyl 5PW RP+ column (Fig. 1, bottom): lack of most of the details from the diabetic extract and a reduced peak capacity in the first half of the chromatogram of the normal extract. However, the components with MW $>$ 6000 dalton were less well separated on this column than on the TSK Phenyl 5PW RP+ column.

The separation capacities of the seven different polymeric columns towards the extremely complex, lipid-containing pancreatic extracts were obviously very different. In order to compare the individual variations obtained with acetic acid gradients with "classical" RP-HPLC polypeptide analyses, crude extract and peak I and peak II components were separated on a Dynospheres column (Fig. 3, left), a Nucleosil C_4 column (Fig. 3, right) and an Asahipak C_8 column (Fig. 4, right) eluted with an acetonitrile gradient in TFA.

Although the chromatograms of the normal extract separated with acetic acid or acetonitrile–TFA were comparable in outline, it is evident that the latter mobile

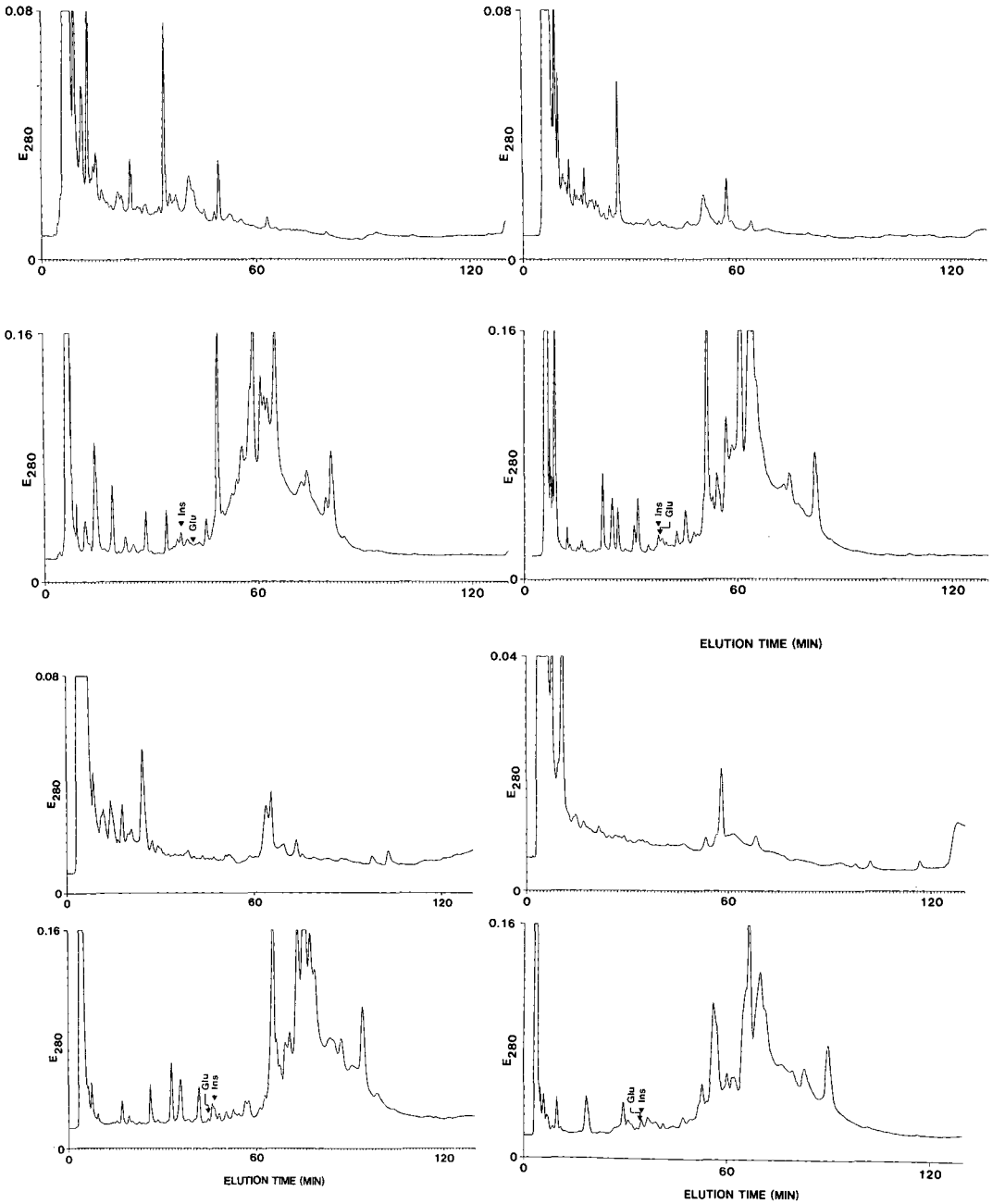

Fig. 2. RP-HPLC of 50 μl of crude acetic acid extract of a diabetic human pancreas (top) and a normal human pancreas (bottom) using a 250 × 4.6 mm I.D. Asahipak C4P column (top left), a 250 × 4.6 mm I.D. Asahipak C8P column (top right), a 150 × 4.6 mm I.D. Asahipak ODP column (bottom left) and a 150 × 4.6 mm I.D. Tosoh octadecyl 4PW column (bottom right) eluted with an acetic acid gradient [from 34% to 9% acetic acid (Asahipak C18 and C8, Tosoh octadecyl 4PW) or from 20% to 72% acetic acid (Asahipak C4) linearly for 120 min followed by 10 min isocratically at 90% acetic acid]. Flow-rate, 0.5 ml/min. Elution positions of authentic human insulin (Ins) and glucagon (Glu) are marked.

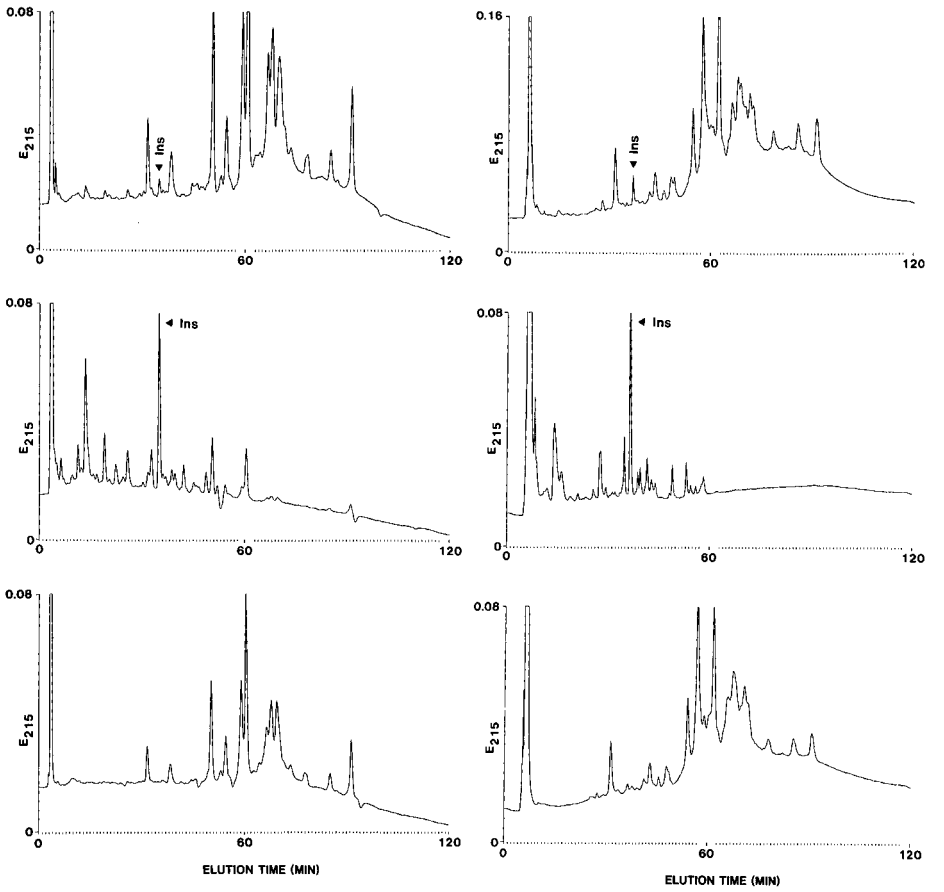

Fig. 3. RP-HPLC of 5 μl of crude acetic acid extract from a normal human pancreas (top) and 50 μl of the corresponding peak I (bottom) and peak II (middle) materials dissolved at 1 mg/ml in 3 *M* acetic acid using a 250 × 4.6 mm I.D. Dynospheres PD-102-RE column (left) or a 250 × 4.0 mm I.D. 5-μm Nucleosil 300 Å C_4 column (right) eluted with an acetonitrile gradient in TFA (from 0.075% TFA–20% acetonitrile to 0.070% TFA–60% acetonitrile linearly for 120 min). Flow-rate, 1.0 ml/min (Dynospheres) or 0.5 ml/min (Nucleosil). The elution position of authentic human insulin (added to the sample) is marked.

phase had a marked influence on especially the separation of the components with MW >6000 dalton, which were now much better separated on the Dynospheres column (compare Fig. 3, top left, with Fig. 1, top left). A more detailed separation of peak I material was not observed for the Asahipak column eluted with acetonitrile–TFA (compare Fig. 4, top right, with Fig. 2, top right).

With the exception of the effect of the difference in hydrophobicity of the bonded phases, the separation patterns of the crude extract, peak I and peak II materials using the Dynospheres column were comparable to those obtained on the Nucleosil C_4 column (Fig. 3, left and right). The separation of peak II material on the Asahipak column (Fig. 4, middle right) was superior to those obtained on the Dynospheres and Nucleosil columns (Fig. 3, middle left and right). The separation temperature had no

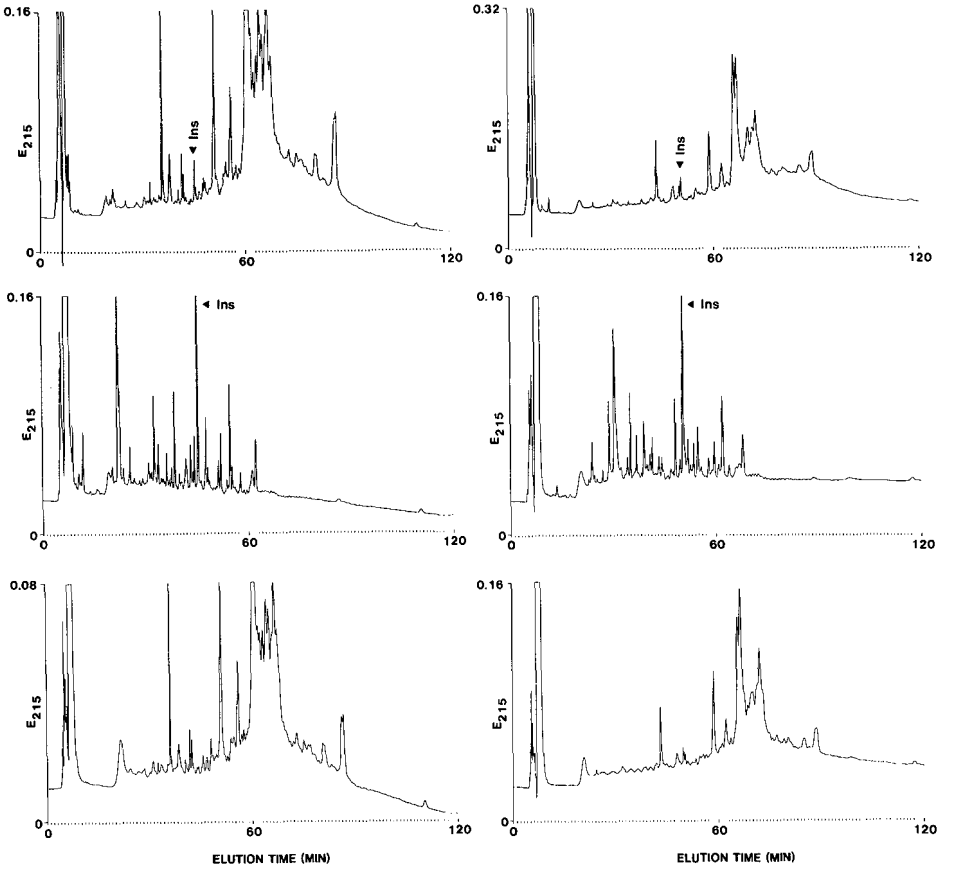

Fig. 4. RP-HPLC of 5 μl of crude acetic acid extract from a normal human pancreas (top) and 25 μl of the corresponding peak I (bottom) and peak II (middle) materials dissolved at 1 mg/ml in 3 *M* acetic acid using a 250 × 4.6 mm I.D. Asahipak C8P column eluted with an acetonitrile gradient in TFA (from 0.075% TFA–20% acetonitrile to 0.070% TFA–60% acetonitrile linearly for 120 min). Flow-rate, 0.5 ml/min. The elution position of authentic human insulin is marked. Separation temperature: room temperature (right) or 45°C (left).

major influence on this UV profile (Fig. 3, middle), whereas the separation of components with MW >6000 dalton was markedly improved when performed at 45°C (Fig. 4, bottom).

Manufacturers of RP columns dedicated to polypeptide analyses often characterize their stationary phases with a number of pure "standard" proteins. As it could be of interest to know whether information about the behaviour of a limited number of pure polypeptides might allow reliable predictions of the potential value of the stationary phase for the separation of unknown peptides and proteins or highly complex samples, utilizing identical or alternative mobile phases, the polymeric columns described above were characterized with a number of "standard" proteins eluted with acetic acid gradients in water, acetonitrile or 2-propanol. The results for two C_{18} columns are shown in Fig. 5 (Tosoh octadecyl 4PW) and Fig. 6 (Asahipak ODP-50).

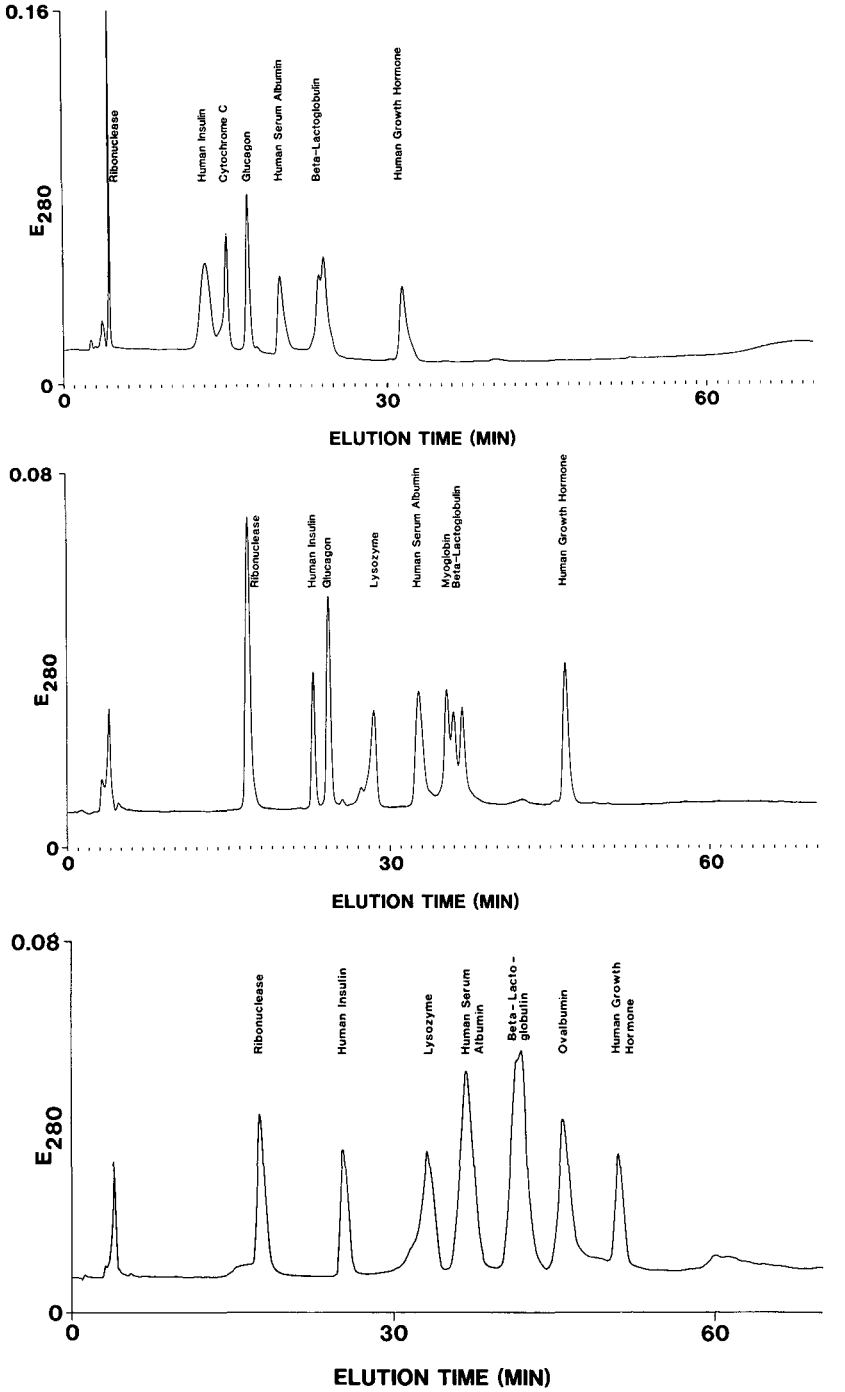

Fig. 5. RP-HPLC of a number of "standard" proteins using a 150 × 4.6 mm I.D. Tosoh octadecyl 4PW column eluted with a 2-propanol–acetic acid gradient (from 24% acetic acid–12% 2-propanol to 40% acetic acid–60% 2-propanol linearly for 60 min followed by 10 min isocratically at the final conditions; top), an acetonitrile–acetic acid gradient (from 24% acetic acid–12% acetonitrile to 40% acetic acid–60% acetonitrile linearly for 60 min followed by 10 min isocratically at the final conditions; middle) or an acetic acid gradient (from 34% to 90% acetic acid linearly for 60 min followed by 10 min isocratically at the final conditions; bottom). Flow-rate, 0.5 ml/min. Sample load, 50–100 μg of each "standard" protein.

In spite of individual variations, the majority of the polymeric RP columns analysed so far behaved in a manner identical with the Tosoh C_{18} column (Fig. 5): peak shape, selectivity and peak capacity were optimum with acetonitrile as organic modifier (middle), whereas broader peak shapes and (total or partial) loss of resolution occurred with acetic acid gradients (bottom).

Poor peak shapes of several of the more hydrophobic polypeptides were observed after elution with 2-propanol in acetic acid (Fig. 5, top, and especially Fig. 6, top). This was also observed with the use of the Chrompack column and the Asahipak C_4 and C_8 columns (data not shown).

The behaviour of the Asahipak C_{18} column was different from the average results described above (Fig. 6): equally sharp peaks were obtained for all polypeptides (including albumin, ovalbumin and lysozyme) in acetic acid–acetonitrile gradients and in acetic acid gradients in water (Fig. 6, bottom and middle), and also the resolution of the two closely related chains in β-lactoglobulin (a valuable measure for polypeptide selectivity) in acetic acid was superior to that obtained in acetonitrile. A comparable resolution of β-lactoglobulin in acetic acid gradients was only achieved with the TSK Phenyl 5PW RP+ and the Tosoh octadecyl NPR columns (Fig. 7). When the other polymeric RP columns were eluted with acetic acid gradients in water, they either lacked the ability to separate the two chains or the separation was just indicated (data not shown).

The recoveries obtained for some of the polypeptides and proteins used in the characterization of the polymeric RP columns, are listed in Table I.

DISCUSSION

Reversed-phase analyses are still the most popular type of HPLC analyses and the preferred column for such analyses, in both Europe and the U.S.A., is a 5–10-μm silica-based C_{18} column [8].

More than 200 RP-HPLC columns are available, and they all differ more or less with respect to plate numbers, peak shapes and selectivities. Further, a lack of column-to-column and batch-to-batch reproducibility is a common problem in many laboratories [8].

Polymer columns are primarily applied in gel permeation chromatographic, ion-exchange and reversed-phase analyses, and their use in RP-HPLC has recently been reported as "increasing" [1]. The main argument in favour of the polymeric RP columns is their increased chemical stability, which allows the use of alkaline mobile phases and also base washing in the case of contaminated columns. So far the potential differences between the various polymeric RP columns has not been analysed with respect to polypeptide separations.

Using our previously described alternative mobile phase of acetic acid gradients in water, we compared the chromatographic behaviour of "bare" polymer columns (Dynospheres, Chrompack) and derivatized columns (Asahipak C_4, C_8 and C_{18}, TSK Phenyl and Tosoh C_{18}) using acetic acid extracts of the normal and the diabetic pancreas as model samples (Figs. 1 and 2).

Although the two "bare" columns are polymerized from different monomers (DVB *versus* styrene) and contain different amounts of copolymerized non-aromatic compounds, their behaviours were surprisingly similar (Fig. 1, top). Almost identical

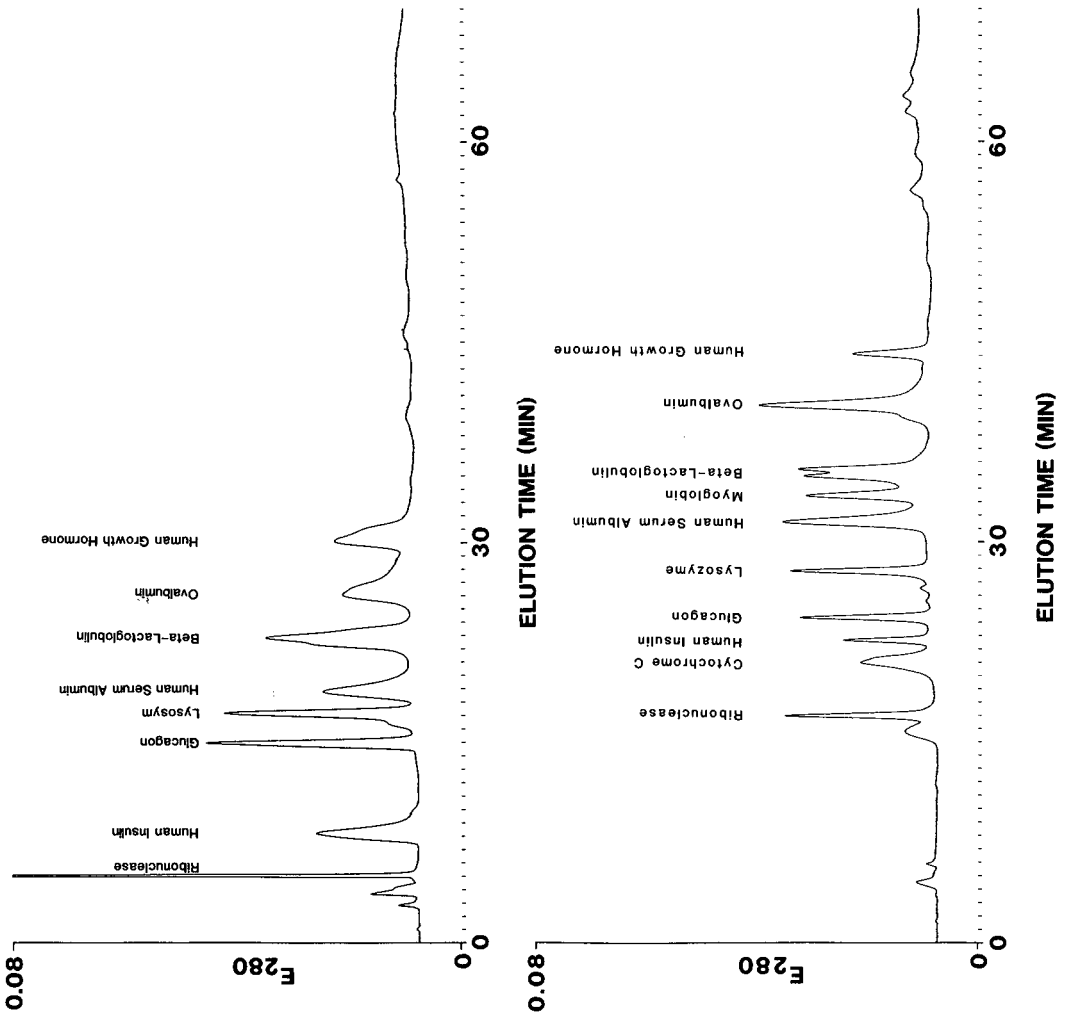
0.08
E280
0
0
30
60
ELUTION TIME (MIN)
Ribonuclease
Human Insulin
Glucagon
Lysozym
Human Serum Albumin
Beta-Lactoglobulin
Ovalbumin
Human Growth Hormone
0.08
E280
0
0
30
60
ELUTION TIME (MIN)
Ribonuclease
Cytochrome C
Human Insulin
Glucagon
Lysozyme
Human Serum Albumin
Myoglobin
Beta-Lactoglobulin
Ovalbumin
Human Growth Hormone

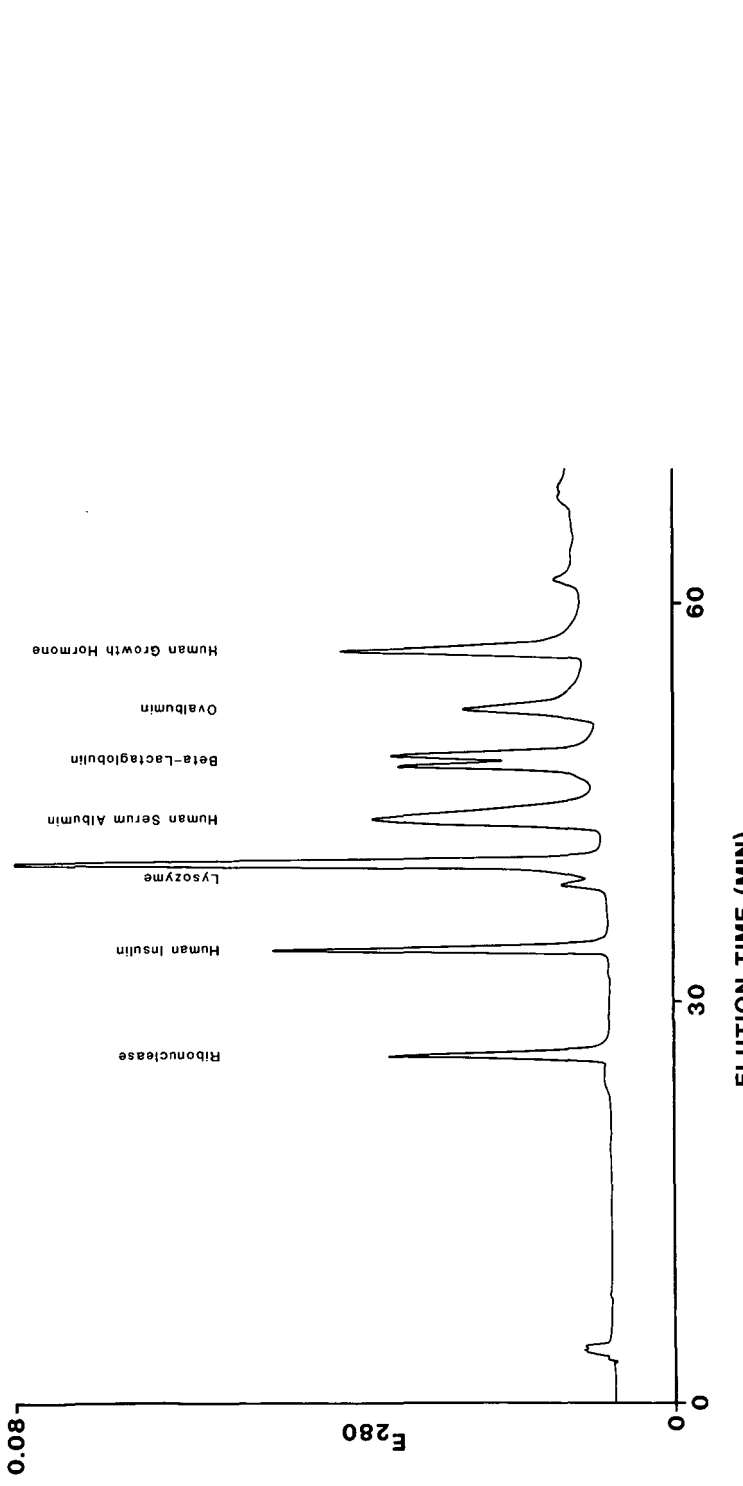

Fig. 6. RP-HPLC of a number of "standard" proteins using a 150 × 4.6 mm I.D. Asahipak ODP column eluted with a 2-propanol–acetic acid gradient (from 24% acetic acid–12% 2-propanol to 40% acetic acid–60% 2-propanol linearly for 60 min followed by 10 min isocratically at the final conditions; top), an acetonitrile–acetic acid gradient (from 24% acetic acid–12% acetonitrile to 40% acetic acid–60% acetonitrile linearly for 60 min followed by 10 min isocratically at the final conditions; middle) or an acetic acid gradient (from 34% to 90% acetic acid linearly for 60 min followed by 10 min isocratically at the final conditions; bottom). Flow-rate, 0.5 ml/min. Sample load, 50–100 μg of each "standard" protein.

TABLE I

RECOVERIES OF INSULIN (Ins), b-COMPONENT (b-comp), PROINSULIN (Proins), HUMAN GROWTH HORMONE (hGH), OVALBUMIN (Ovalb) AND HUMAN SERUM ALBUMIN (HSA) OBTAINED ON DIFFERENT SILICA- AND POLYMER-BASED RP-COLUMNS

The recoveries were calculated as the area under the UV curves (280 nm) obtained after gradient elution of the column relative to that obtained after bypassing the column with a PTFE capillary and injecting a similar sample.

RP column type	Mobile phase		pH	Ligand	Modifier	Recovery (%)					
						Ins	b-comp	Proins	hGH	Ovalb	HSA
Silica-based	$(NH_4)_2SO_4$–NaH_2PO_4–$HClO_4$[a]		2.5	C_{18}	CH_3CN	93[13]			87[13]		2–21[13]
	0.1% TFA[a,b]		2.0	C_{18}	CH_3CN	Inapplicable for recovery studies of Ins and hGH[11,15]					
	0.1% TFA[b]		2.0	C_4	CH_3CN	100[16]		100[16]	80[12]	79	90
Polymer-based	0.25 *M* TEAP	(TSK Phenyl 5PW RP+)	3.0	Phenyl	CH_3CN				68[14]		
	0.25 *M* TEAP	(PLRP-S)	3.0	Phenyl	CH_3CN				37[14]		
	$(NH_4)_2HPO_4$	(TSK Phenyl 5PW RP+)	7.0	Phenyl	CH_3CN	95[14]			68[14]		91[14]
	CH_3COOH	(TSK Phenyl 5PW RP+)	2.2	Phenyl	Water				98	86	97
	CH_3COOH	(Dynospheres)	2.2	Phenyl	Water	85			90		
	CH_3COOH	(Dynospheres)	2.2	Phenyl	CH_3CN	86			76		
	CH_3COOH	(Dynospheres)	2.2	Phenyl	2-Propanol	76			85		
	CH_3COOH	(Asahipak)	2.2	C_8	Water					64	83
	0.075% TFA	(Asahipak)	2.0	C_8	CH_3CN					38	90
	0.025 *M* TEAP	(Asahipak)	3.0	C_8	CH_3CN					12	96
	0.1% TFA	(Asahipak)	2.0	C_4	CH_3CN	100[16]		100[16]	98	63	90

[a] LiChrosorb column.
[b] Nucleosil column.

chromatograms were obtained for both samples, and these chromatograms differed from those of a derivatized phenyl column (TSK Phenyl 5PW RP+; Fig. 1, bottom) with respect to chromatographic efficiency. At first glance, this column seems to be better qualified for the separation of proteins than the two other phenyl columns, and this observation is further supported by the good peak shapes obtained for several pure proteins (including high-molecular-weight samples such as transferrin and catalase) eluted from the TSK Phenyl column with an acetic acid gradient (Fig. 7, top).

These observations could indicate an influence of the stationary phase polymeric backbone in the TSK Phenyl 5PW RP+ column on the separation, in addition to that of the bonded phenyl phase, in accordance with the general opinion that differences between various alkylsilica columns is a function of the attached ligand as well as the silica [9].

The three Asahipak alkyl columns clearly demonstrated the effect of the hydrophobicity of the attached ligand, in accordance with common experiences with alkylsilica columns. As this effect is equally distributed between sample components with high and low molecular weight, the effect of the stationary phase framework itself (polymerized vinyl alcohol) seems to be negligible.

In this series, the Tosoh 4PW C_{18} column is different from the other derivatized alkyl columns. Compared with these columns, and with the TSK Phenyl column (which has a similar polymeric backbone), the efficiency for peak I material (MW >6000 dalton) is reduced and, in accordance with this, the separation of "standard proteins" in acetic acid gradients (Fig. 5, bottom) is considerably less satisfactory than those of the TSK Phenyl column (Fig. 7, top) and the Asahipak C_{18} column (Fig. 6, bottom).

The Asahipak C_{18} column has an unusual selectivity for acetic acid gradients: the best separation of the two chains in β-lactoglobulin on this column was actually achieved with acetic acid in water, *i.e.*, it was better than that obtained with acetic acid–acetonitrile gradients (Fig. 6, middle), in contrast to the behaviour of the Dynospheres column [5], the Chrompack column (data not shown) and the Tosoh C_{18} column (Fig. 5).

Insulin was eluted with a good peak shape and with satisfactory recoveries from all polymer-based RP columns after acetic acid gradient elution, with the exception of the Tosoh C_{18} NPR column. Interestingly, serum albumin and thyroglobulin were eluted from this column with good peak shapes, and the separation of the two β-lactoglobulin chains was even better than that with the other two TSK columns (Fig. 7, bottom). The irreversible binding of insulin under these circumstances remains to be explained.

When the Asahipak C_8 column was eluted with a "classical" mobile phase for RP polypeptide analyses (TFA–acetonitrile), the major change observed is an increased plate number, especially in the first part of the chromatogram where peak II material (MW <6000 dalton) is eluted (Fig. 4, right). In the case of the Dynospheres column, the separation of peak I material is improved (contradictionary to the Asahipak column; compare with Fig. 2, top right). However, a dramatic increase in the chromatographic efficiency of the Asahipak C_8 column towards peak I material was noted when the separation temperature was increased from ambient to 45°C (Fig. 4, bottom left). A parallel increase in chromatographic efficiency for peak II material (MW <6000 dalton) was not observed, in accordance with earlier observations that

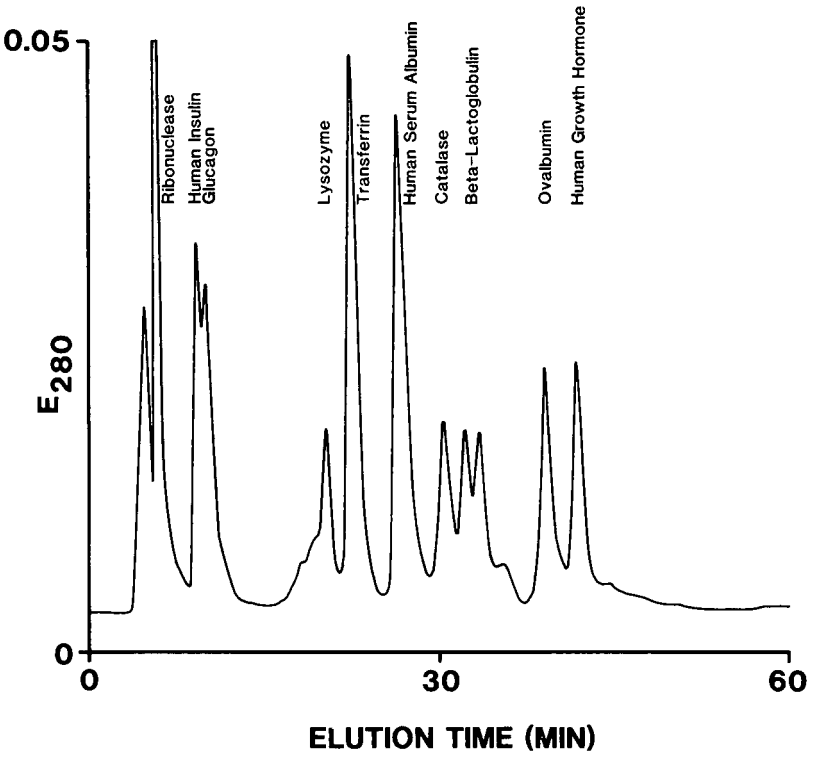
0.05
0
E_{280}
Ribonuclease
Human Insulin
Glucagon
Lysozyme
Transferrin
Human Serum Albumin
Catalase
Beta-Lactoglobulin
Ovalbumin
Human Growth Hormone
0
30
60
ELUTION TIME (MIN)

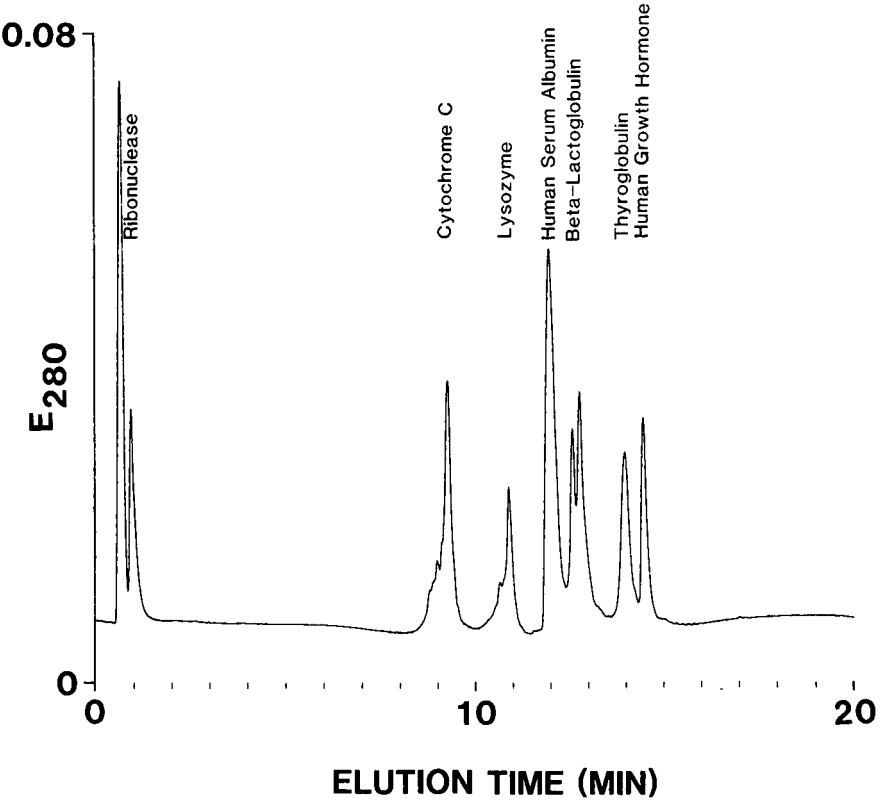
0.08
0
E_{280}
Ribonuclease
Cytochrome C
Lysozyme
Human Serum Albumin
Beta-Lactoglobulin
Thyroglobulin
Human Growth Hormone
0
10
20
ELUTION TIME (MIN)

the use of elevated temperatures seemed to be of no advantage for peptide RP-HPLC [10]. Only very limited effects were observed when the elution with acetic acid gradients was performed at elevated temperature (data not shown).

The use of a high content of acetic acid in mobile phases for polymeric RP columns is an interesting alternative to "classical" polypeptide analyses with a C_{18} column and TFA–acetonitrile as mobile phase. From this work it is clear that different groups of polymer columns under these conditions behave as differently as alkyl-silica columns eluted under comparable conditions, and that the potential value of a polymer-based column for acetic acid elution may be quickly judged by using "standard" proteins. Some of the columns seem to be virtually free from any influence from the stationary phase backbone, in contrast to the disturbing effects of free silanol groups in several silica-based RP columns. It is also noteworthy that the polypeptide selectivity of these columns can be changed with variations in the mobile phase, and that the columns with optimum performance with acetic acid maintain their superiority when they are eluted with mobile phases containing organic modifiers.

In the evaluation of the potential usability of polymeric RP columns for peptide and protein separations the recovery is an important factor. The pancreatic extracts are highly complex, containing peptides from a few amino acids to proteins with MW $>300\,000$ dalton with equally large variations in hydrophobicity. Recoveries with these extracts would be extremely difficult to measure, and the information obtainable from such analyses would be of limited scientific value with respect to the general performance of the columns. Therefore, the recoveries from various polymer-based RP columns for a number of individual polypeptides and proteins with very different molecular weights and hydrophobicities were measured using various stationary–mobile phase combinations, and the results were compared with similar values obtained for various silica-based RP columns (Table I).

For the silica C_{18} columns eluted with acetonitrile-containing mobile phases, the recovery was directly related to the molecular weight of the sample: with the exception of TFA [11,12], use of all all other mobile phases resulted in *ca.* 100% recoveries for insulin (6000 dalton). However, already for the b-component {composed primarily of proinsulin (9000 dalton) and insulin dimer (12 000 dalton) [6]} the recoveries with two of these mobile phases were reduced and for the hydrophobic growth hormone (22 000 dalton) only the use of a single mobile phase (with perchloric acid) resulted in a satisfactory recovery. The use of TEAP-acetonitrile resulted in a minimal recovery and with TFA–acetonitrile the growth hormone was irreversibly bound [12].

The effect of the silica-bound ligand on the recovery was clearly seen when a C_4 column was compared with the C_{18} columns: insulin, proinsulin, growth hormone, ovalbumin and serum albumin were now recovered in excellent yields under mobile phase conditions where these samples were irreversibly bound to C_{18} columns.

Fig. 7. RP-HPLC of a number of "standard" proteins using two 75 × 4.6 mm TSK Phenyl 5PW RP+ columns in series eluted with an acetic acid gradient (from 34% to 90% acetic acid linearly for 60 min, top), or a 35 × 4.6 mm I.D. Tosoh octadecyl NPR column eluted with an acetic acid gradient (from 34% to 90% acetic acid linearly for 10 min followed by 10 min isocratically at 90% acetic acid; bottom). Flow-rate, 0.5 ml/min. Sample load, 50–100 μg (top) or 2–10 μg (bottom) of each "standard" protein.

In contrast to the results from the silica C_{18} columns, excellent recoveries for insulin, growth hormone and serum albumin were obtained on a single polymer-based stationary phase (TSK Phenyl) eluted with ammonium phosphate–acetonitrile. However, the recoveries of growth hormone in TEAP–acetonitrile from two different polymeric phenyl columns clearly demonstrated the impact of the individual stationary phase on the recovery (compare TSK Phenyl with PLRP-S).

For the Asahipak C_8 column, the results of elution with acetic acid in water and with TFA and TEAP in acetonitrile clearly depended on the actual sample: for serum albumin the use of acetonitrile resulted in higher recovery than after elution with acetic acid, whereas the use of acetonitrile resulted in extremely low recoveries for (the notoriously difficult) ovalbumin, which was recovered in the highest yield after elution with acetic acid. With this mobile phase, the effect of the individual polymeric stationary phase again was elucidated when the recoveries of serum albumin and ovalbumin on the Asahipak C_8 column were compared with the higher values obtained on the TSK Phenyl column. Further, the very high recovery of growth hormone demonstrated the general excellence of the TSK Phenyl column for elution with acetic acid in water.

For the Dynospheres column, the effects of the individual samples on the recoveries obtained with different mobile phases were found to parallel those on the Asahipak C_8 column, although smaller.

Comparison of a silica-based C_4 and a polymeric C_4 column eluted with TFA–acetonitrile demonstrated the superiority of the polymer-based C_4 column for growth hormone, whereas ovalbumin was recovered in higher yields on the silica-based column. However, in contrast to the results obtained after elution of ovalbumin from polymer-based columns with acetic acid gradients in water (where it was eluted as a single component), elution of ovalbumin with TFA–acetonitrile resulted in two peaks from both the silica-based and the polymer-based C_4 columns and from the Asahipak C_8 column (probably owing to the formation of a native and a denatured form of ovalbumin). As the ratio between the two forms was found to differ for the two C_4 columns, and as one of these main components was eluted with severe tailing, the two recovery figures may not be directly comparable.

In general, the recoveries from the polymeric RP columns were not only excellent for insulin and proinsulin, but were equally high for growth hormone, ovalbumin and serum albumin. Similar recoveries from silica C_{18} columns could either only be obtained with a single mobile phase (growth hormone) or not at all (serum albumin). In addition, the finding that the recoveries of all samples after elution with acetic acid gradients in water were either at the same level as or higher than those obtained after elution with acetonitrile gradients remains an outstanding characteristic of the polymer-based RP columns.

For environmental, economical and toxicity reasons, replacement of acetonitrile with a less offensive solvent would be an advantage. The efficiency of polymeric columns eluted with acetic acid is at present not comparable to that obtained with acetonitrile, but future improvements in the design of the stationary phase, backbone and ligands may well change this situation.

ACKNOWLEDGEMENTS

I thank Helle Bojesen-Koefoed and Linda Larsø for excellent assistance, and Dr. Y. Kato (Tosoh) for the generous supply of Tosoh columns.

REFERENCES

1 R. E. Majors, *LC · GC Int.*, 3 (1990) 12.
2 B. S. Welinder, H. H. Sørensen, K. R. Hejnæs, S. Linde and B. Hansen, in M. T. W. Hearn (Editor), *HPLC of Proteins, Peptides and Polynucleotides*, VCH, New York, in press.
3 C. T. Wehr, in W. S. Hancock (Editor), *CRC Handbook for the HPLC Separation of Amino Acids, Peptides and Proteins*, CRC Press, Boca Raton, FL, 1984, pp. 31–57.
4 C. T. Mant and R. S. Hodges, *J. Liq. Chromatogr.*, 12 (1989) 139.
5 B. S. Welinder and H. H. Sørensen, *J. Chromatogr.*, 537 (1991) 181.
6 B. S. Welinder and S. Linde, *J. Chromatogr.*, 537 (1991) 201.
7 B. S. Welinder and S. Linde, *J. Chromatogr.*, 542 (1991) 65.
8 R. C. Majors, *LC · GC*, 7 (1989) 468.
9 J. D. Pearson, N. T. Lin and F. E. Regnier, *Anal. Biochem.*, 124 (1982) 217.
10 F. Lottspeich and A. Henschen, in A. Henschen, F. Lottspeich and W. Voelter (Editors). *High Performance Liquid Chromatography in Biochemistry*, VCH, Weinheim, 1985, p. 139.
11 B. S. Welinder, H. H. Sørensen and B. Hansen, *J. Chromatogr.*, 361 (1986) 357.
12 B. S. Welinder and H. H. Sørensen, unpublished results.
13 B. S. Welinder, H. H. Sørensen and B. Hansen, *J. Chromatogr.*, 408 (1987) 191.
14 B. S. Welinder, H. H. Sørensen and B. Hansen, *J. Chromatogr.*, 398 (1987) 309.
15 S. Linde and B. S. Welinder, *J. Chromatogr.*, 536 (1991) 43.
16 S. Linde and B. S. Welinder, presented at the *10th International Symposium on HPLC of Proteins, Peptides and Polynucleotides, Wiesbaden, October 29th–31st, 1990*, poster No. 423.

Journal of Chromatography, 542 (1991) 101–113
Elsevier Science Publishers B.V., Amsterdam

CHROM. 23 011

Naphthalenesulfonates as mobile phases for anion-exchange chromatography using indirect photometric detection

S. A. MAKI and N. D. DANIELSON*
Department of Chemistry, Miami University, Oxford, OH 45056 (U.S.A.)
(Received September 6th, 1990)

ABSTRACT

Naphthalenesulfonate mobile phases for chromatography with indirect photometric detection have been characterized for the separation and detection of common inorganic and organic anions using an ion-exchange column. The singly charged 2-naphthalenesulfonate (NMS) has shown good chromatographic performance for small singly charged inorganic anions such as F^-, Cl^-, NO_2^-, Br^- and NO_3^- with detection limits ranging from 20 to 4 ng. The doubly charged 1,5-naphthalenedisulfonate (NDS) was more efficient toward the separation and identification of small singly charged, multicharged, and large anions such as F^-, Cl^-, NO_2^-, Br^-, NO_3^-, SO_4^{2-}, $S_2O_3^{2-}$, I^- and SCN^-. Analysis of a mixture containing the above anions can be performed in less than 16 min, with detection limits in the 20–1 ng range. The linear response range of these mobile phases were from 100 ppm to the detection limits of all anions (0.05–1 ppm). Both NMS and NDS require no pH adjustment for indirect photometric detection use, and no system peak was observed in any chromatogram.

INTRODUCTION

Anion-exchange chromatography with indirect photometric detection is a simple but powerful technique for the separation and detection of non-UV-absorbing inorganic and organic anions. The crucial part of ion-exchange chromatography with indirect photometric detection chromatography (IEC–IPD) is the mobile phase, which plays roles as both an eluent and a means for detection. In IEC–IPD the ion-exchange column is first equilibrated with the light-absorbing mobile phase until a steady baseline with high absorbance background is reached. Mobile phases in IEC–IPD should have the ability of displacing the analyte ions from the stationary phase and selectively separating them. Detection in IEC–IPD is best accomplished by using an eluent which possesses a large molar absorptivity in order to achieve high sensitivity at a moderately low eluent concentration. The non-light-absorbing ions when eluted will be detected by observing the decrease in the absorbance. Negative peaks will be the result instead of the conventional positive peaks in the usual UV detection mode [1].

Most of the commonly used mobile phases in anion IEC–IPD are the salts of weak organic acids, such as phthalate, sulfobenzoate, and salicylate derivatives. These compounds possess relatively high molar absorptivities and, with their avail-

0021-9673/91/$03.50

ability in pure form, are good candidates for anion IEC–IPD. However, the elution of analyte ions will be determined by the effective charge of the eluent, which in turn is dependent upon the pH of the mobile phase. Precise control of the mobile phase pH is found to be important to ensure reproducible elution and retention times [2–5].

Another drawback of these commonly used mobile phases is the presence of one or more extraneous (system or ghost) peaks, which are not related to the analyte sample. These peaks appear either between the analyte peaks in which a distorted chromatogram is the result, or appear at the end of the chromatogram, which in turn will increase the actual analysis time. Haddad and co-workers [2,3] have reported on two occasions the presence of a large system peak at 14 min, when using potassium hydrogenphthalate as the mobile phase. Brandt *et al.* [6], on the other hand, reported a system peak eluting in the middle of the chromatogram, when muconic acid was used as the eluent at pH 4.3. Sato [7] has reported in recent work a system peak when he used the acid form of 1,2-dihydroxybenzene-3,5-disulfonic acid as the eluent, but no system peak was observed when the salt was used. We have experienced in previous work [8], using 2-naphthol-3,6-disulfonate, a system peak eluting in the middle of the chromatogram. We were successful in reducing its size by 80%, by dissolving the sample in the mobile phase before injection. The mechanism and the conditions for the formation of the system peak are not fully understood. However, a theoretical study of the formation of the system peak has been recently published [9], in which the system peak was attributed to the elution of the neutral species (undissociated form) of the weak organic acid eluent in a reversed-phase retention mode. Consequently, when the salt of a strong acid was used no system peak was observed.

Our research group has been working on characterizing several new mobile phases for anion IEC–IPD with an effective charge independent of pH. We report here the results of optimizing the chromatographic conditions of 2-naphthalenesulfonate (NMS) and 1,5-naphthalenedisulfonate (NDS) as potential eluents for anion IEC–IPD. Both of these mobile phases generate ion chromatograms free of any system peaks. Moreover, these two eluents possess very large molar absorptivities and, consequently, detection limits of the separated anions are low.

EXPERIMENTAL

Instrumentation

The liquid chromatograph used in this study consisted of: a Model 510 high-performance liquid chromatographic (HPLC) pump, a Model U6K injector, a Model 490 programmable multiwavelength detector, and an IC-PAK anion-exchange column (5 cm × 4.6 mm I.D.), all from Waters Chromatography Division (Milford, MA, U.S.A.). A Model 5000 Fisher Recordall chart recorder (Austin, TX, U.S.A.) provided the output of chromatograms. A Varian Model DMS 90 UV–VIS spectrophotometer (Sunnyvale, CA, U.S.A.) was used for measuring absorption spectra of the mobile phases.

Reagents

Three kinds of NMS were studied in this work: NMS acid and NMS salt of 99.5% purity, both purchased from Eastman Kodak (Rochester, NY, U.S.A.), and NMS salt of 90% purity obtained from Aldrich (Milwaukee, WI, U.S.A.). The di-

sodium salt of NDS of 95% purity was purchased from Aldrich. Acetonitrile, HPLC grade, was received from Fisher Scientific (Fair Lawn, NJ, U.S.A.). Salts of the common anions, reagent grade or better quality, were obtained from different suppliers. A 1000-ppm stock solution of each anion was prepared and used for further dilutions. Triply distilled, deionized water was used for preparing all solutions. The Oxford water sample was obtained from the lab faucet and used without any treatment except dilution with triply distilled, deionized water.

A 0.01 *M* stock solution of each mobile phase was prepared and used for subsequent dilutions. All final mobile phases used in this study have been diluted with acetonitrile–water (10:90, v/v). This percentage of acetonitrile was found to be effective in reducing the unwanted hydrophobic interaction between the polymeric stationary phase and the naphthalene moiety of the mobile phase and provided smooth baseline noise [8]. Although other anion-exchange columns were tried, we found the IC-PAK column to give better performance with these mobile phases. This may be because this column packing has a relatively hydrophilic polymethacrylate-type polymer backbone, which should lessen any hydrophobic effect with these aromatic mobile phases.

RESULTS AND DISCUSSION

The UV absorption spectrum from 350 to 250 nm for 0.05 m*M* NMS superimposed on that of 0.02 m*M* NDS is shown in Fig. 1. The absorption maxima of the NMS and the NDS solutions occur at 275 and 285 nm, with molar absorptivities of 5160 and 13 100 l/mol cm, respectively. The 10-nm shift in the maximum absorption wavelength and the large difference in the molar absorptivities is mainly due to the

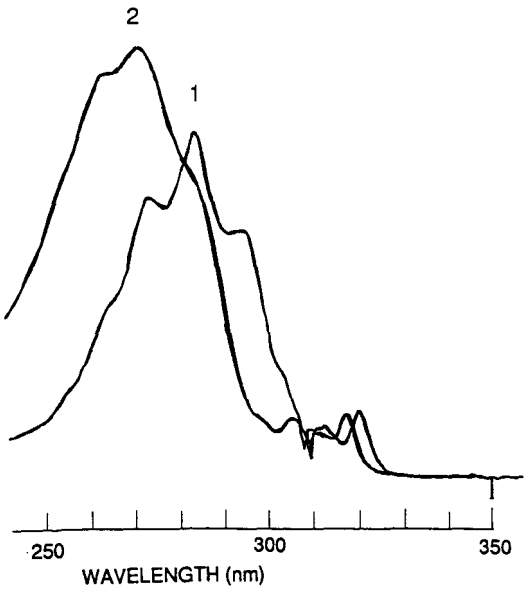

Fig. 1. UV spectra of (1) 0.02 m*M* NDS and (2) 0.05 m*M* NMS.

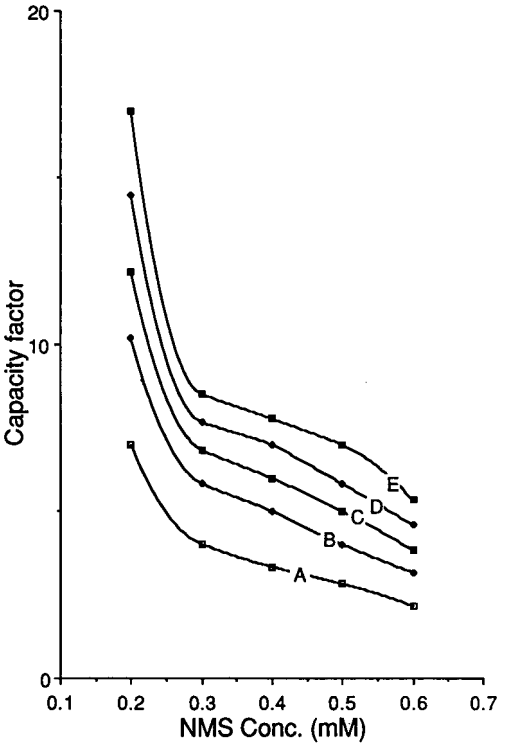

Fig. 2. Retention of inorganic analyte anions as a function of eluent concentration. Conditions: flow-rate, 1 ml/min; injection volume, 20 μl; indirect UV detection at 280 nm; ambient temperature; solute concentration, 10 ppm. (A) F^-; (B) Cl^-; (C) NO_2^-; (D) Br^-; (E) NO_3^-.

presence and position of the extra sulfonate group in NDS. Because of the common use and availability of the 280-nm filter in many UV detectors, most of this work was done at 280 nm as the detection wavelength, unless otherwise indicated. The molar absorptivities of NMS and NDS solutions at 280 nm are 4290 and 11250 l/mol cm, respectively. This represents a molar absorptivity decrease of only about 15% for both mobile phases.

The retention of fluoride, chloride, nitrite, bromide and nitrate as a function of NMS concentration is shown in Fig. 2. Larger and multicharged anions gave very long retention times and, consequently, were not studied using this mobile phase. As would be expected with all ion-exchange processes, the retention of these anions becomes shorter with increasing mobile phase concentration. The capacity factor (k') for these anions range from 2 to 7 with NMS concentration changing from 0.6 to 0.3 mM; below 0.2 mM, k' rises sharply to the range 7–17. At NMS concentrations higher than 0.6 mM, the separation of these anions becomes more difficult. Lower mobile phase concentrations provide higher sensitivities. The measured sensitivity (sensitivity = analyte peak area/its concentration) using 0.15 mM NMS is about 1.2 and 1.5 times higher than that using 0.3 and 0.6 mM NMS, respectively. This is due to the fact that small changes in absorbance can be easily detected in a low rather than a high background signal. In addition, the baseline noise level is much smaller at low

mobile phase concentrations; the peak-to-peak noise using 0.3 m*M* NMS is about one third that of 0.6 m*M* NMS, measured at 0.05 a.u.f.s. As a compromise, we have chosen 0.3 m*M* NMS–10% acetonitrile as the optimum concentration for this mobile phase. At this concentration, good sensitivity, separation performance, and reasonably short retention times can be achieved.

We have studied three kinds of NMS products. The acid form of NMS (Kodak product) was not completely soluble in water partly due to the presence of neutral impurities of naphthalene derivatives which can be easily noticed from the distinct smell. Extraction with chloroform and/or pH adjustment to 8 did not improve the solubility or the chromatographic performance of this acid. The NMS salt (Aldrich) gave a much better chromatographic performance. Analysis of a standard mixture of common inorganic anions using 0.3 m*M* NMS (Aldrich) as the mobile phase is shown in Fig. 3. All anions are well resolved, especially the fluoride ion peak which is well separated from the injection (solvent) peak and far from any interferences. However, the solubility of this product was not quite complete. Extraction with chloroform was not effective in removing the undissolved residues. A clear stock solution has been used throughout this study, after letting the impurities settle out for a few hours. The third product, NMS salt (Kodak), was very soluble in water with no residue and gave a fine chromatographic performance. Fig. 4 shows a separation of a 1-ppm standard anion mixture using 0.3 m*M* NMS (Kodak)–10% acetonitrile. The analysis time using this mobile phase is about half of that shown in Fig. 3, suggesting that the

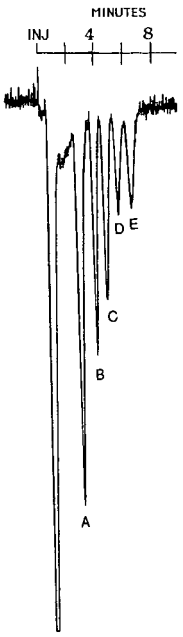

Fig. 3. Separation of a standard mixture of inorganic anions with IEC–IPD. Conditions as in Fig. 2 except: mobile phase, 0.3 m*M* NMS (Aldrich product)–10% acetonitrile; 0.05 a.u.f.s. Peak identification: 1 ppm each of (A) F^-, (B) Cl^-, (C) NO_2^-, (D) Br^-, and (E) NO_3^-.

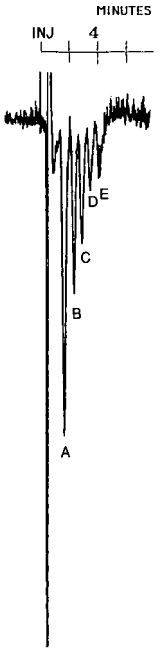

Fig. 4. Separation of a standard mixture of inorganic anions with IEC–IPD. Conditions as in Fig. 3 except: mobile phase, 0.3 m*M* NMS (Kodak product)–10% acetonitrile; detection wavelength, 280 nm, 0.05 a.u.f.s. Peak identification: 1 ppm each of (A) F^-, (B) Cl^-, (C) NO_2^-, (D) Br^-, and (E) NO_3^-.

Kodak product is higher in NMS content than the Aldrich product. This is in agreement with the supplier listing purity of 99.5 and 90%, respectively. Mobile phases using both brands of NMS salt required no pH adjustment and they showed very

TABLE I

LINEARITY RESPONSE FOR FIVE ANIONS BY IEC–IPD USING 0.3 m*M* NMS (KODAK PRODUCT)–10% ACETONITRILE AS THE MOBILE PHASE

Injected sample volume, 20 μl.

Anion	Range (ppm)	Linear least-squares equation ($y = a + bx$)[a]	Correlation coefficient
Fluoride	100–0.2	$a = 1.23 \cdot 10^{-2} \pm 6.68 \cdot 10^{-3}$	0.9999
		$b = 3.71 \cdot 10^{-2} \pm 1.56 \cdot 10^{-4}$	
Chloride	100–0.1	$a = 1.78 \cdot 10^{-2} \pm 1.46 \cdot 10^{-2}$	0.9999
		$b = 6.92 \cdot 10^{-2} \pm 3.37 \cdot 10^{-4}$	
Nitrite	100–0.5	$a = -1.86 \cdot 10^{-3} \pm 2.83 \cdot 10^{-3}$	0.9999
		$b = 1.98 \cdot 10^{-2} \pm 6.51 \cdot 10^{-5}$	
Bromide	100–1	$a = -6.16 \cdot 10^{-3} \pm 5.03 \cdot 10^{-3}$	0.9998
		$b = 1.34 \cdot 10^{-2} \pm 1.04 \cdot 10^{-4}$	
Nitrate	100–1	$a = 1.21 \cdot 10^{-2} \pm 5.59 \cdot 10^{-2}$	0.9998
		$b = 1.42 \cdot 10^{-2} \pm 1.15 \cdot 10^{-4}$	

[a] y = calculated peak area (cm^2); x = concentration (ppm).

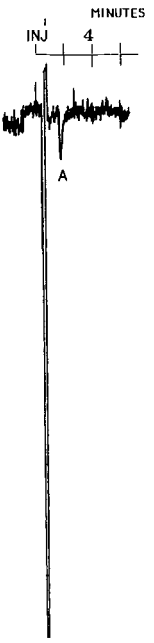

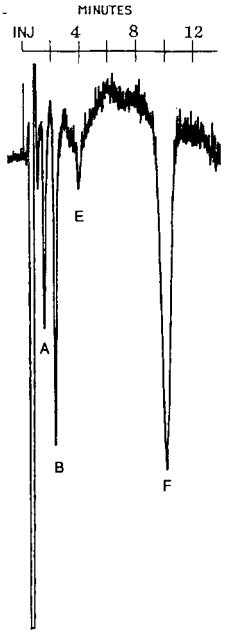

Fig. 5. Chromatogram of 0.2 ppm fluoride ion with IEC–IPD. Conditions as in Fig. 4.

Fig. 6. Chromatogram of 1% Oxford city water sample. Conditions as in Fig. 4 except: mobile phase, 0.3 m*M* NMS (Kodak product)–10% acetonitrile; detection wavelength, 275 nm; 0.02 a.u.f.s. Peak identification: A = F^-; B = Cl^-; E = NO_3^-; F = SO_4^{2-}.

reproducible performances. The average relative standard deviation (R.S.D.) in retention time was 1.1% (n = 4). Moreover, chromatograms of both mobile phases showed no extraneous peak (system peak) even after 40 min of analysis.

The linearity response for the five anions studied extended from 100 ppm to the detection limits of each anion, using the optimized NMS mobile phase (Table I). The R.S.D. of the slope ranged from 0.33 to 0.81% with an average of 0.57% for the five anions. The correlation coefficient varied from 0.9998 to 0.9999. The average R.S.D. in the calculated peak area was about 1% (n = 4). Fig. 5 shows a chromatogram of fluoride ion at its reported detection limit. The signal-to-noise ratio for this early eluted anion is more than 3.

A chromatogram of 1% tap city water is shown in Fig. 6, using 0.3 m*M* NMS (Kodak). The components of the water sample were identified and quantified using a standard mixture of all the components except fluoride. The fluoride ion quantitation was done individually because of variation of the bicarbonate ion present in the triply distilled water which we found affected the fluoride ion area calculation. To overcome this problem both samples and standards were prepared at the same time and diluted with the same triply distilled water. The concentrations of each component found in Oxford city water were 1.16 mg/l fluoride, 25.5 mg/l chloride, 2.26 mg/l nitrate and 52.6 mg/l sulfate. These results agreed well (within ± 10%) with the most recent tap water analysis data published by the city water authority.

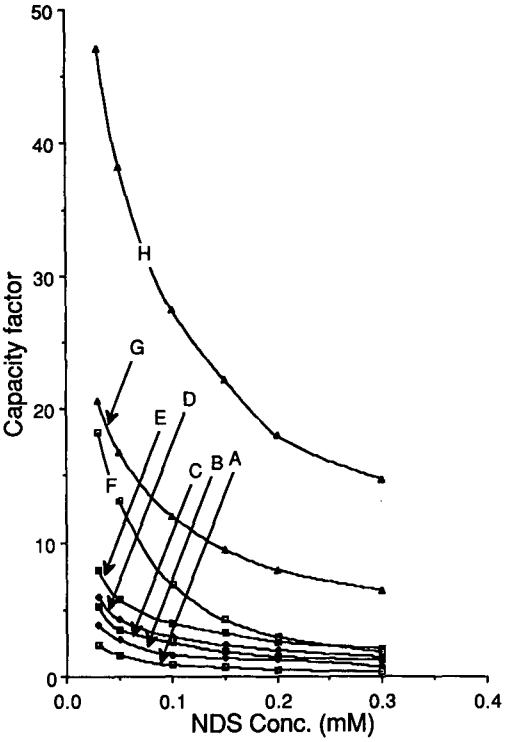

Fig. 7. Retention of inorganic anions as a function of eluent concentration. Conditions as in Fig. 2. (A) F^-; (B) Cl^-; (C) NO_2^-; (D) Br^-; (E) NO_3^-; (F) SO_4^{2-}; (G) I^-; (H) SCN^-

Another mobile phase that has been studied in this work is NDS disodium salt. The retention of various common anions as a function of NDS concentration is shown in Fig. 7. As with NMS, the capacity factors for the small singly charged anions such as F^-, Cl^-, NO_2^-, Br^-, and NO_3^- ranged from 2 to 7. For the doubly charged and large anions such as SO_4^{2-}, I^-, and SCN^-, the k' values were from 3 to 47 as the mobile phase concentration was varied between 0.3 and 0.03 m*M*. For mobile phase concentrations higher than 0.2 m*M*, separation of these anions becomes more difficult due to the overlap of the early eluting anions with the injection peak. For mobile phase concentrations lower than 0.1 m*M*, the retention of these anions becomes longer and consequently peak broadening of the late eluting anions is observed. The baseline noise measured at 0.05 a.u.f.s. was 2.7 times larger and the calculated sensitivity was 0.81 times smaller for 0.15 m*M* compared to 0.05 m*M* NDS. These results are, again, in agreement with the theory of indirect detection methods [10].

The optimized mobile phase selected, considering factors such as sensitivity, resolution, and analysis time, was 0.15 m*M* NDS–10% acetonitrile. Fig. 8 shows a typical example for the separation of a mixture containing nine monovalent and divalent anions using the optimized mobile phase. The analysis times for small monovalent anions such as F^-, Cl^-, NO_2^-, Br^-, and NO_3^- and for divalent anions such as

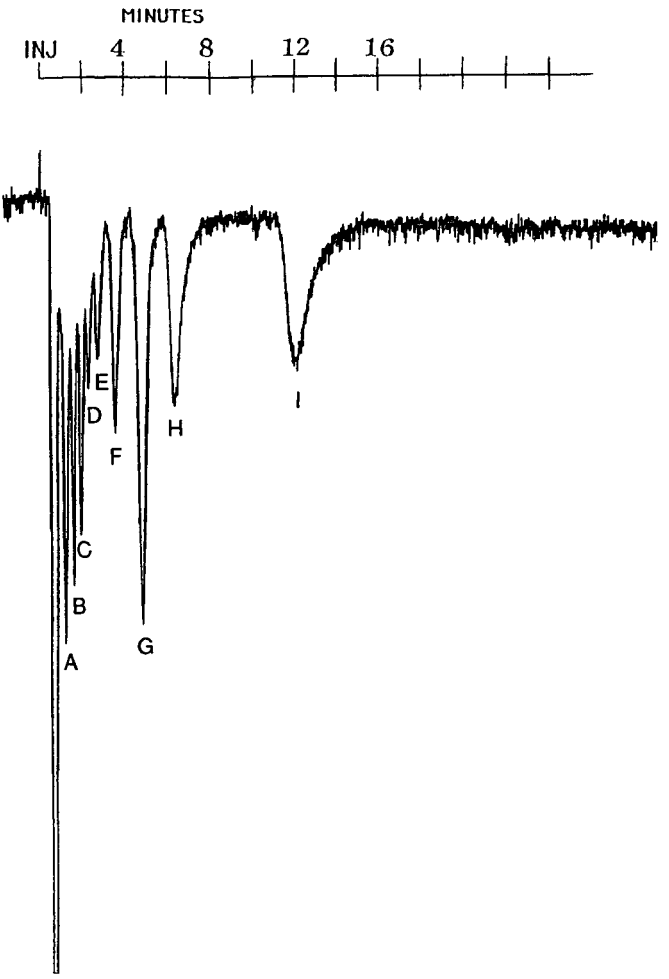

Fig. 8. Separation of a standard mixture of inorganic anions with IEC–IPD. Conditions as in Fig. 3 except: mobile phase is 0.15 m*M* NDS–10% acetonitrile. Peak identification: 0.5 ppm each of (A) F^-, (B) Cl^-, (C) NO_2^-, (D) Br^-, (E) NO_3^- and (F) SO_4^{2-} and 2.5 ppm each of (G) $S_2O_3^{2-}$, (H) I^-, and (I) SCN^-.

SO_4^{2-} and $S_2O_3^{2-}$ are less than 4 and 6 min, respectively. The retention time for large anions such as I^- and SCN^- is 14 min, which is good considering IEC–IPD of these anions is rare [11]. This overall short analysis time makes NDS a more favorable mobile phase for simultaneous separation of these three groups of anions.

Linearity response for the eight anions studied with NDS is shown in Table II. With the exception of fluoride ion, the linear response for all anions extended from 100 ppm to the detection limit of each anion. Because of its early elution, the fluoride ion peak overlapped with the injection peak especially at concentrations higher than 50 ppm, which makes the peak-area measurements inaccurate. The average R.S.D. of the calculated peak area was 0.75% (n = 4). The R.S.D. of the slope ranges from 1.4 to 0.30% with an average of 0.62%, while the correlation coefficient for all anions

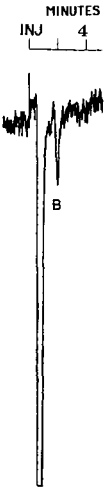

Fig. 9 Chromatogram of 0.05 ppm chloride ion. Conditions as in Fig. 8.

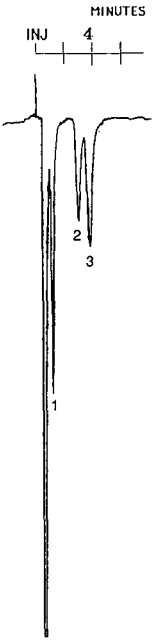

Fig. 10. Separation of an organic anion mixture with IEC–IPD. Conditions as in Fig. 8 except using 0.2 a.u.f.s. Peak identification: 5 ppm each of (1) lactic acid, (2) maleic acid, and (3) tartaric acid.

TABLE II

LINEARITY RESPONSE FOR EIGHT ANIONS BY IEC–IPD USING 0.15 m*M* NDS–10% ACETONITRILE AS THE MOBILE PHASE

Injected sample volume, 20 μl.

Anion	Range (ppm)	Linear least-squares equations ($y = a + bx$)[a]	Correlation coefficient
Fluoride	50–0.05	$a = -4.54 \cdot 10^{-2} \pm 2.65 \cdot 10^{-2}$ $b = 1.41 \cdot 10^{-1} \pm 1.39 \cdot 10^{-3}$	0.9997
Chloride	100–0.05	$a = -1.41 \cdot 10^{-2} \pm 1.52 \cdot 10^{-2}$ $b = 8.73 \cdot 10^{-2} \pm 3.67 \cdot 10^{-4}$	0.9999
Nitrite	100–0.05	$a = -1.43 \cdot 10^{-2} \pm 8.19 \cdot 10^{-3}$ $b = 7.00 \cdot 10^{-2} \pm 1.98 \cdot 10^{-4}$	0.9999
Bromide	100–0.1	$a = -1.07 \cdot 10^{-2} \pm 6.33 \cdot 10^{-3}$ $b = 3.87 \cdot 10^{-2} \pm 1.46 \cdot 10^{-4}$	0.9999
Nitrate	100–0.5	$a = -5.80 \cdot 10^{-2} \pm 2.12 \cdot 10^{-2}$ $b = 4.96 \cdot 10^{-2} \pm 4.62 \cdot 10^{-4}$	0.9997
Sulfate	100–0.1	$a = -1.18 \cdot 10^{-2} \pm 8.67 \cdot 10^{-3}$ $b = 6.07 \cdot 10^{-2} \pm 1.89 \cdot 10^{-4}$	0.9999
Iodide	100–1	$a = -7.91 \cdot 10^{-3} \pm 2.63 \cdot 10^{-3}$ $b = 1.81 \cdot 10^{-2} \pm 5.41 \cdot 10^{-5}$	0.9999
Thiocyanate	100–1	$a = -1.75 \cdot 10^{-2} \pm 3.26 \cdot 10^{-2}$ $b = 4.94 \cdot 10^{-2} \pm 6.71 \cdot 10^{-4}$	0.9995

[a] y = calculated peak area (cm^2); x = concentration (ppm).

TABLE III

DETECTION LIMIT COMPARISON FOR VARIOUS ANIONS

Signal-to-noise ratio ≥ 3; sample volume, 20 μl.

Anion	Concentration[a]			
	NMS		NDS	
	ppm	ng	ppm	ng
Fluoride	0.2	4	0.05	1
Chloride	0.1	2	0.05	1
Nitrite	0.5	10	0.05	1
Bromide	1	20	0.1	2
Nitrate	1	20	0.5	10
Sulfate	–	–	0.1	2
Iodide	–	–	1	20
Thiocyanate	–	–	1	20

[a] Using the optimized mobile phases: 0.3 m*M* NMS and 0.15 m*M* NDS both in 10% acetonitrile.

varied from 0.9997 to 0.9999. Fig. 9 shows a chromatogram of chloride ion at its detection limit of 0.05 ppm with a signal-to-noise ratio of more than 4.

A typical chromatogram for the separation of a mixture of organic anions containing lactic, maleic and tartaric acids is shown in Fig. 10. These three hydroxycarboxylic acids are well separated in the order as expected based on their size, pK_a values, and number of carboxylate groups. Lactic acid (mol. wt. 90) has a pK_a of 3.86. The diprotic maleic acid (mol. wt. 116) has pK_a values of 1.94 and 6.22, while tartaric acid (mol. wt. 150) has pK_a values of 3.22 and 4.81.

A detection limit comparison of all anions using the optimized mobile phases of NMS and NDS is shown in Table III. The detection limits of the early eluting anions range from 0.1 to 1 ppm (2–20 ng) and 0.05 to 0.5 ppm, (1–10 ng) using NMS and NDS, respectively. Lower detection limits for NDS are observed compared to that of NMS. This can be attributed to two main factors. First, the molar absorptivity of NDS is about 2.5 times larger than that of NMS. Secondly, since NDS is doubly charged, its elution tendency is much stronger, which consequently means lower mobile phase concentrations and lower baseline noise. Fig. 11 shows a slope comparison of two linearity runs for fluoride and nitrite ions using the optimized NMS and NDS mobile phases. It is quite clear that the slope for NDS is much higher than that for NMS. This trend has been consistently observed for all anions studied in this work.

Furthermore, NDS has proven to be even more favorable than the previously optimized IEC–IPD mobile phase, naphtholdisulfonate (NODS) [8], which has the same effective charge of -2. The NDS analysis time in Fig. 8 is about 5 min shorter than that using NODS, although the same mobile phase concentrations and compositions were used. The detection limits for F^-, Cl^-, NO_2^-, and Br^- are 10 times lower using NDS than those using NODS as the mobile phase, while the detection limits for larger and multicharged anions such as NO_3^-, SO_4^{2-}, I^-, and SCN^- ranged from 2 to 10 times higher. These trends can be explained by lower baseline noise using NODS

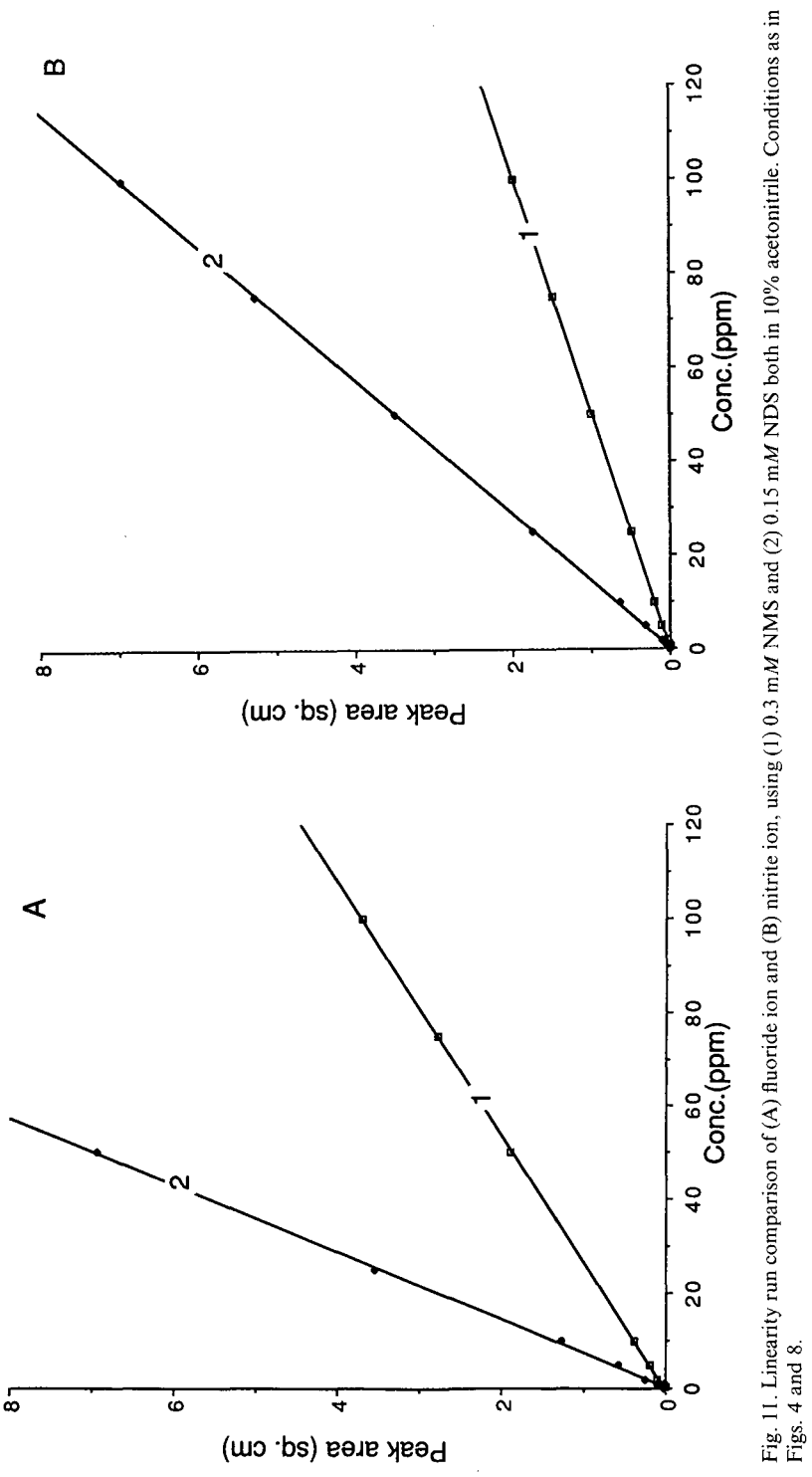

Fig. 11. Linearity run comparison of (A) fluoride ion and (B) nitrite ion, using (1) 0.3 m*M* NMS and (2) 0.15 m*M* NDS both in 10% acetonitrile. Conditions as in Figs. 4 and 8.

for the late-eluting peaks and system peak interference with the early eluting peaks with NODS. No system peak was observed with NDS and consequently no special treatment of the analyte samples was necessary before analysis. In addition, no problems were experienced with the nitrite ion separation using NDS as the mobile phase. In contrast, using NODS, the nitrite ion peak extended from the positive to the negative direction, affecting the resolution of the neighboring ions.

This work has demonstrated the applicability of NMS and NDS as potential mobile phases for anion IEC–IPD. NMS has been found quite suitable for the analysis of small and singly charged anions, with high efficiency. NDS, on the other hand can be used for the separation and identification of both small singly charged as well as large multicharged anions, with very high sensitivity. Both mobile phases required no pH adjustment and the absence of any system peak in the chromatograms allowed easy peak identification. These mobile phases, furthermore, caused no degradation of the analytical column and constant column efficiency was maintained.

ACKNOWLEDGEMENTS

We thank Waters Chromatography Division (Millipore) for their support of this research.

REFERENCES

1 H. Small and T. E. Miller, Jr., *Anal. Chem.*, 54 (1982) 462.
2 A. L. Heckenberg and P. R. Haddad, *J. Chromatogr.*, 299 (1984) 301.
3 P. E. Jackson and P. R. Haddad, *J. Chromatogr.*, 346 (1985) 25.
4 T. Okada and T. Kuwamoto, *Anal. Chem.*, 56 (1984) 2073.
5 T. Okada and T. Kuwamoto, *J. Chromatogr.*, 284 (1984) 149.
6 G. Brandt, P. Vogler and A. Kettrup, *Z. Anal. Chem.*, 325 (1986) 252.
7 H. Sato, *Anal. Chim. Acta*, 206 (1988) 281.
8 S. A. Maki and N. D. Danielson, *J. Chromatogr. Sci.*, 28 (1990) 537.
9 H. Sato, *Anal. Chem.*, 62 (1990) 1567.
10 E. S. Yeung, *Acc. Chem. Res.*, 22 (1989) 125.
11 K. Ito and H. Sunahara, *J. Chromatogr.*, 502 (1990) 121.

Journal of Chromatography, 542 (1991) 115–128
Elsevier Science Publishers B.V., Amsterdam

CHROM. 23 028

Comparative study of the reversed-phase high-performance liquid chromatography of black tea liquors with special reference to the thearubigins

R. G. BAILEY and H. E. NURSTEN
Department of Food Science and Technology, University of Reading, Whiteknights, Reading RG6 2AP (U.K.)
and
I. McDOWELL*
Natural Resources Institute, Central Avenue, Chatham Maritime, Chatham, Kent ME4 4TB (U.K.)
(First received July 13th, 1990; revised manuscript received October 23rd, 1990)

ABSTRACT

New high-performance liquid chromatographic methods for the analysis of black tea phenolic pigments, using Hypersil ODS, Hypersil octyl wide-pore, and Hamilton PRP-1 columns, and several new results arising from them are presented. Very good resolution of a wide range of phenolic tea pigments, was obtained using a Hypersil ODS column with a citrate buffer, and, for the first time, eight theaflavins were observed in a single chromatogram. Unresolved brown phenolic pigments (thearubigins), ran as a convex broad band on the Hypersil wide-pore and Hamilton PRP-1 columns, and the Hamilton PRP-1 column showed an anthocyanidin to be a significant contributor to liquor colour. The pigments were classified into three groups by chromatographic behaviour: group I, pigments running close to the void volume of the columns; group II, resolved pigments; and group III, unresolved pigments. Group II pigments were divided into four Sub-Groups by their photodiode-array UV–VIS spectra, as follows: sub-group II.1, theaflavins; sub-group II.2, theaflavic acids; sub-group II.3, type I resolved pigments; and sub-group II.4, type II resolved pigments. Pigments in sub-groups II.3 and II.4 were designated as resolved thearubigins, and those in group III as unresolved thearubigins.

INTRODUCTION

The work in this paper continues our earlier studies of the high-performance liquid chromatography (HPLC) of black tea liquors, in which the main classes of polyphenolic compound were identified, using a photodiode-array detector and associated data system as a combined chromatographic–spectroscopic technique [1]. Although many polyphenolics were separated and identified in this way, the chromatography of the thearubigins has proved to be a more difficult problem.

Two main classes of pigment are formed in black tea manufacture, the theaflavins and the thearubigins [2–5]. The theaflavins are compounds of known structure, but the thearubigins are an inhomogeneous group of phenolic pigments of unknown structure [2–5]. Roberts [2] suggested that the thearubigins were acidic brown pig-

0021-9673/91/$03.50

ments, formed by the oxidative degradation of the theaflavins. However, Berkowitz *et al.* [6] thought that they derived from theaflavic acids, and Brown *et al.* [7] suggested that they were polymeric proanthocyanidins (the chromatograms described in this paper suggested that the thearubigins studied were a mixture of phenolic pigments with different chemical structures).

Robertson and Bendall [8] used a Hypersil ODS column with isocratic elution to analyse thearubigins produced in a model system, whereas Roberts *et al.* [9] used gradient elution, to study the degradation of thearubigins on storage, but only limited separation was achieved in either case. Opie *et al.* [10] obtained better resolved chromatograms of thearubigins formed in a model system, using a Hypersil ODS 3-μm column with a non-linear gradient. They claimed, without providing supporting evidence, that decaffeination was an essential sample pretreatment step, required for the successful chromatography of the thearubigins.

The chromatography of the thearubigins is likely to be difficult for two principal reasons, firstly, they are considered to be compounds with a wide range of molecular masses (700 to 40 000 daltons) [2,3], and, secondly, they adsorb strongly onto active surfaces. Generally, chromatographic conditions optimal for compounds of lower molecular mass are not optimal for compounds of higher molecular mass [11]; therefore, one set of conditions is unlikely to be suitable for the chromatography of the full range of thearubigins. In addition to the molecular-mass problem, secondary retention [12–15], due to the interaction of the thearubigins with hydroxyl groups or metals on the surface of silica-based reversed-phase packings, is a likely cause of the peak broadening and peak tailing observed on tea chromatograms.

Three different types of reversed-phase columns were used in this study, Hypersil ODS, Hypersil octyl wide-pore, and Hamilton PRP-1. Hypersil ODS, a narrow-pore, high surface area packing, was used for its proven ability to resolve lower molecular mass polyphenolics [1]. Hypersil octyl wide-pore phase was used with the aim of obtaining improved chromatograms of higher molecular mass thearubigins. Generally, wide-pore phases are useful for the chromatography of polymers; they have a lower surface-area and are less retentive than narrow-pore phases [11,16–19], potentially valuable properties for the chromatography of the thearubigins. Hamilton PRP-1 styrene-divinylbenzene copolymer [20–22] has no surface hydroxyl groups or surface metals, and was used to study the chromatography of tea liquors in the absence of secondary retention.

Although the secondary retention encountered with silica-based phases can be eliminated by using polymer phases, these phases have a lower resolving power and different selectivity than the silica-based ones, and are not a direct replacement for them [20–22]. The secondary retention caused by the surface metals of silica-based phases has been removed by adding EDTA [23,24] or phytic acid [24] to the aqueous solvent. Therefore, the Hypersil ODS column was used with solvents containing, first, EDTA and then sodium citrate, duly resulting in greatly improved chromatograms. Photodiode-array UV–VIS spectra were extracted from 33 peaks in the citrate chromatogram, and the spectra were used to classify the resolved peaks into four groups

MATERIALS AND METHODS

Equipment

The Hewlett-Packard diode array system and standard samples were as described previously [1]. A Gilson gradient system, consisting of Model 302 pumps, Data Master, and Apple computer, with a Bryans BS600 chart recorder and ABI Spectroflow 757 UV–VIS detector, was used for off-line HPLC work. Sources for the columns are given below.

HPLC analysis methods

The columns and gradients used were as follows:

Hypersil ODS. Packing: Hypersil C_{18}, 5-μm, pore size 12 nm; column size: 25 × 0.49 cm; column source: Hichrom Excel grade: a linear gradient of 8% to 31% organic over 50 min, at a flow-rate of 1.5 ml/min, was used.

Hypersil octyl wide-pore. Packing: Hypersil C_8, 5-μm, pore size 30 nm; column size: 25 × 0.49 cm (a 15 × 0.49 cm column gave similar results); column source: HPLC Technology Ltd: a linear gradient of 0% to 26% organic over 50 min, at a flow-rate of 1.4 ml/min, was used.

Hamilton PRP-1. Packing: Hamilton PRP-1 styrene-divinylbenzene copolymer, 5-μm, pore size 7.5 nm (a 10-μm column proved less useful); column size: 15 × 0.49 cm; column source: Anachem: a linear gradient of 5% to 33% organic over 50 min, at a flow-rate of 1.0 ml/min, was used.

Two different aqueous phases were adopted for the HPLC methods, 2% acetic acid and 1% citric acid (the latter adjusted to pH 2.8 with solid sodium hydroxide). In addition, 2% acetic acid, made 2% in EDTA disodium salt, was used for method development, but, as an aqueous phase, it held no advantage over citrate. The organic phase was acetonitrile.

The tea, Clone SFS 204, was obtained from the Tea Research Foundation of Central Africa, Malawi. Tea liquors were prepared as described previously [1] and volumes of 20 μl were injected.

In our work, chromatograms were monitored at 280, 380 and 460 nm —280 nm was used to detect all polyphenolics, 380 nm to detect flavonol glycosides, theaflavins and thearubigins, and 460 nm to detect theaflavins and thearubigins without interference from flavonol glycosides [25]. In this paper, emphasis is given to chromatograms monitored at 460 nm, a wavelength used in the spectrophotometric method for the determination of thearubigins by Roberts and Smith [26,27].

RESULTS AND DISCUSSION

Hypersil ODS column

The 280 nm chromatogram of a Malawi tea, on the Hypersil ODS column with an acetic acid gradient, has been discussed previously [1]. The chromatogram of Clone SFS 204 was similar (Fig. 1), and showed peaks close to the void volume of the column, a convex broad band, and resolved and partially resolved peaks with the broad band as baseline. The 460 nm chromatogram of this tea showed few sharp well defined peaks other than the theaflavins (Fig. 2). There were minor peaks close to the void volume of the column, an unresolved broad-band spreading throughout the

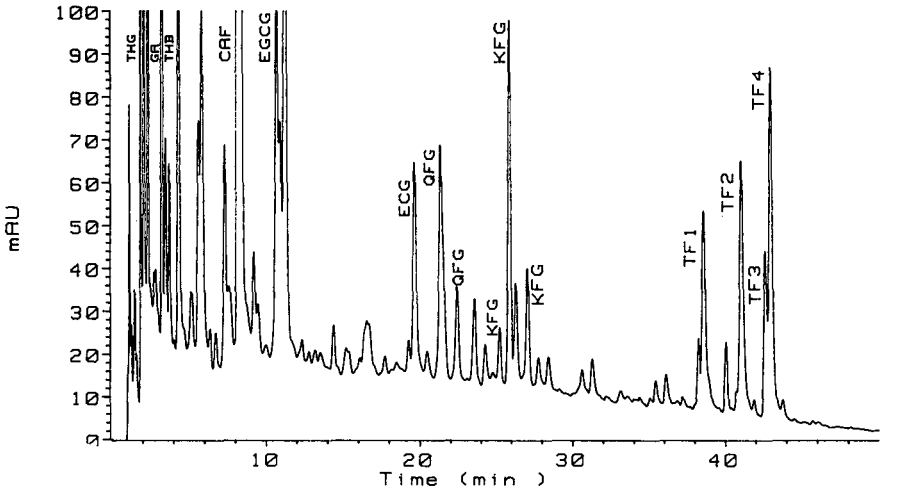

Fig. 1. Tea chromatogram (280 nm) on the Hypersil ODS column. Aqueous solvent 2% (v/v) acetic acid. Organic solvent acetonitrile. Linear gradient, 8 to 31% organic over 50 min. THG = Theogallin (5-galloylquinic acid); GA = gallic acid; THB = theobromine; CAF = caffeine; EGCG = (−)-epigallocatechin gallate; ECG = (−)-epicatechin gallate; QFG = quercetin flavonol glycoside; KFG = kaempferol flavonol glycoside; TF1 = theaflavin; TF2 = theaflavin-3-gallate; TF3 = theaflavin-3′-gallate; TF4 = theaflavin-3,3′-digallate.

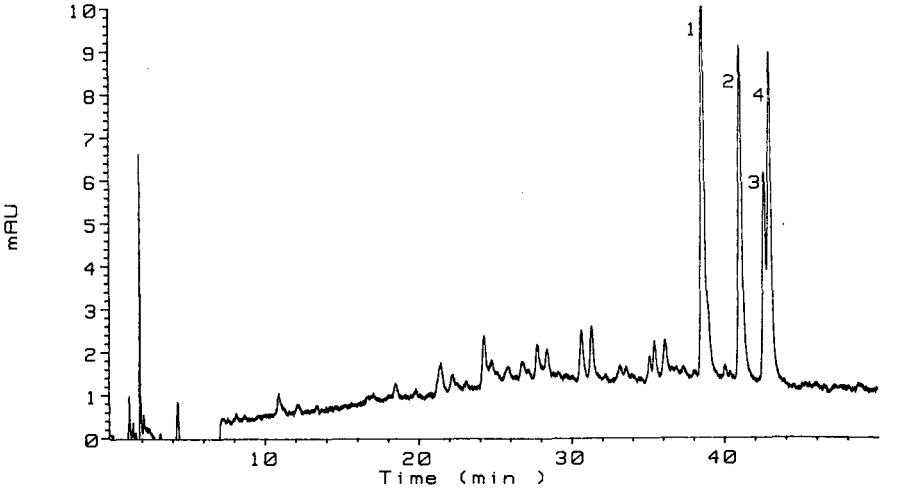

Fig. 2. Tea chromatogram (460 nm) on the Hypersil ODS column. Aqueous solvent 2% (v/v) acetic acid. Organic solvent acetonitrile. Linear gradient, 8 to 31% organic over 50 min. Peaks: 1 = theaflavin; 2 = theaflavin-3-gallate; 3 = theaflavin-3′-gallate; 4 = theaflavin-3,3′-digallate.

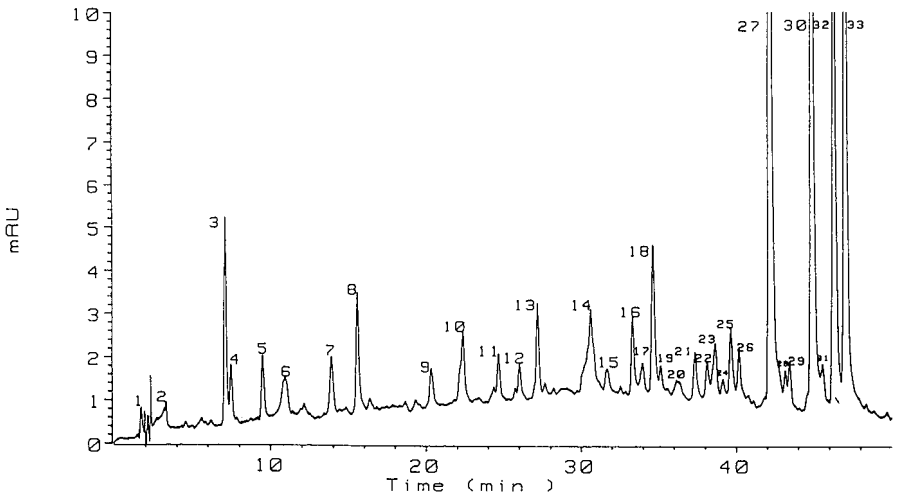

Fig. 3. Tea chromatogram (460 nm) on the Hypersil ODS column. Aqueous solvent 1% (w/v) citric acid, adjusted to pH 2.8 with solid sodium hydroxide. Organic solvent acetonitrile. Linear gradient, 8 to 31% organic over 50 min. For key see Table I.

whole chromatogram, and resolved peaks superimposed on the broad band. Peaks 1–4 in Fig. 2 were assigned to theaflavins [1], the remaining resolved peaks and the broad band remained as unassigned phenolic pigments.

In order to test the hypothesis that the chromatography of these pigments was degraded by secondary retention due to surface metals, a chromatogram was run on the Hypersil ODS column, using 2% acetic acid made 2% in EDTA. Chromatograms obtained in this way showed improvements in resolution and peak shape. However, EDTA was not very soluble in acetic acid and crystallised on standing, so citric acid, a more soluble chelating agent, was used for further work. Chromatograms, run with a citrate aqueous phase, showed further improvements in resolution and peak shape, the 460 nm chromatogram being reproduced in Fig. 3.

Irreversible and reversible improvements were observed with citrate, and, when acetic acid was used again after the use of citrate, much, but not all, of the improvement was maintained. However, the most highly resolved chromatograms were obtained with citrate. This suggested that the irreversible improvements were the result of a reduction of secondary retention, caused by the removal or masking of surface metals by the citrate. The reversible effect was probably caused by prevention of polyphenol–metal interactions by citrate. Tea liquors contain metals [28], and a wide range of polyphenol–metal interactions, some involving thearubigins [29], are theoretically possible. The prevention or removal of these interactions would require the presence of citrate. The use of the Hypersil ODS column in conjunction with citrate, was adopted as a new method for the analysis of black tea pigments.

Hypersil octyl wide-pore column

The previous acetic acid gradient did not work with the Hypersil wide-pore column, most material being eluted very rapidly in an unresolved band, reminiscent

of the polymers discussed by Snyder *et al.* [11]. However, a chromatogram with a useful level of resolution was obtained with a modified acetic acid gradient. The 280 nm tea chromatogram, using an acetic acid gradient, showed peaks close to the void volume of the column, a convex broad band, and resolved and partially resolved peaks with the broad band as baseline. The 460 nm tea chromatogram, using an acetic acid gradient (Fig. 4), showed minor peaks close to the void volume of the column, a convex broad band, and resolved and partially resolved peaks with the broad band as baseline. The baseline of a solvent blank was flat, so the broad band was not caused by refractive index changes during the gradient. The maximum of the broad band in the 460 nm chromatogram occurred at a longer retention time than in the 280 nm chromatogram. This suggested that there were two types of unresolved material in the liquor, only one of which was coloured.

The resolved peaks were less well resolved than on the Hypersil ODS column, an intelligible result of the change from a narrow-pore to a wide-pore column [11]. The broad band had a convex shape, the detector output rising to a maximum and then falling to the baseline. This type of chromatogram is characteristic of an unresolved complex mixture of compounds of lower molecular mass [30] or a polydisperse polymer [11], and the broad band in Fig. 4 could have been due to either of these. A wide-pore phase allows faster solute diffusion and favours the chromatography of polymeric material [11], but it also has a low surface area and is less likely to cause secondary retention of strongly adsorbing material. Therefore, the possibility, that the convex broad band was an unresolved complex mixture of strongly adsorbing compounds of lower molecular mass, cannot be ruled out. However, the broad band was tentatively designated as a strongly adsorbing polydisperse polymer.

When the column was used with citrate, small irreversible and reversible im-

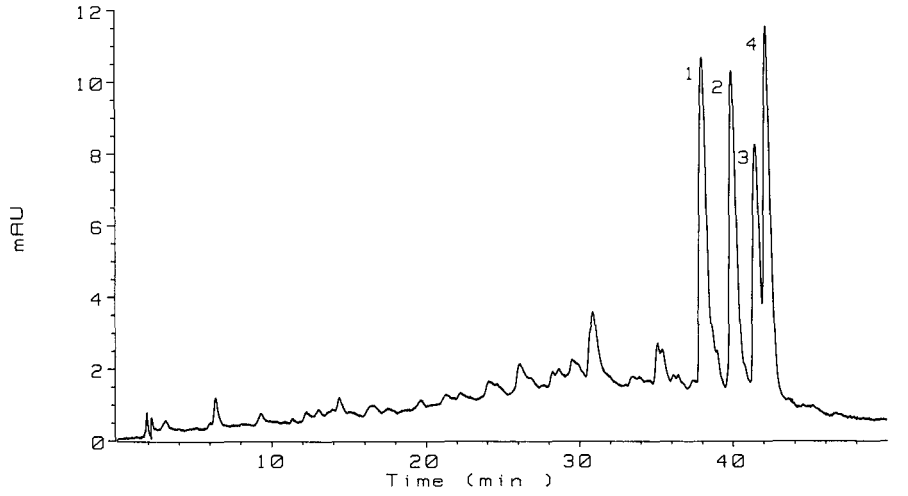

Fig. 4. Tea chromatogram (460 nm) on the Hypersil octyl wide pore column. Aqueous solvent 2% (v/v) acetic acid. Organic solvent acetonitrile. Linear gradient, 0 to 26% organic over 50 min, flow-rate 1.4 ml/min. Peaks: 1 = theaflavin; 2 = theaflavin-3-gallate; 3 = theaflavin-3′-gallate; 4 = theaflavin-3,3′-digallate.

provements were observed. The fact, that the wide-pore column gave smaller irreversible improvements than the Hypersil ODS column, probably reflected the lower surface area of its wide-pore stationary phase.

Hamilton PRP-1 column

Styrene–divinylbenzene stationary phases, such as Hamilton PRP-1, operate most efficiently with acetonitrile [21], so a linear gradient using acetonitrile and acetic acid was developed. The 280 nm tea chromatogram showed peaks near the void volume of the column, a convex broad band, and resolved and partially resolved peaks with the broad band as baseline. The 460 nm chromatogram (Fig. 5) showed minor peaks near the void volume of the column, a convex broad band, and resolved and partially resolved peaks with the broad band as baseline. As with the Hypersil wide-pore column, the maximum of the broad band occurred at a longer retention time in the 460 nm chromatogram, than in the 280 nm chromatogram.

The chromatograms obtained with this column were consistent with the properties of the Hamilton PRP-1 stationary phase, which, being narrow-pore, resolved lower-molecular-mass material better than the Hypersil wide-pore column, and, being inert, allowed strongly adsorbing material to elute more successfully than the Hypersil ODS column. Although the Hamilton PRP-1 column resolved lower molecular mass polyphenolics well, its different selectivity made it a less useful column for these compounds than the Hypersil ODS column.

Peak 1 in Fig. 5 was a very prominent peak which did not have a counterpart in the other chromatograms. A photodiode-array three-dimensional plot of the chromatogram suggested that the peak was an anthocyanidin, and the photodiode-array UV–VIS spectrum extracted from the peak (Fig. 6a) confirmed this. The position of

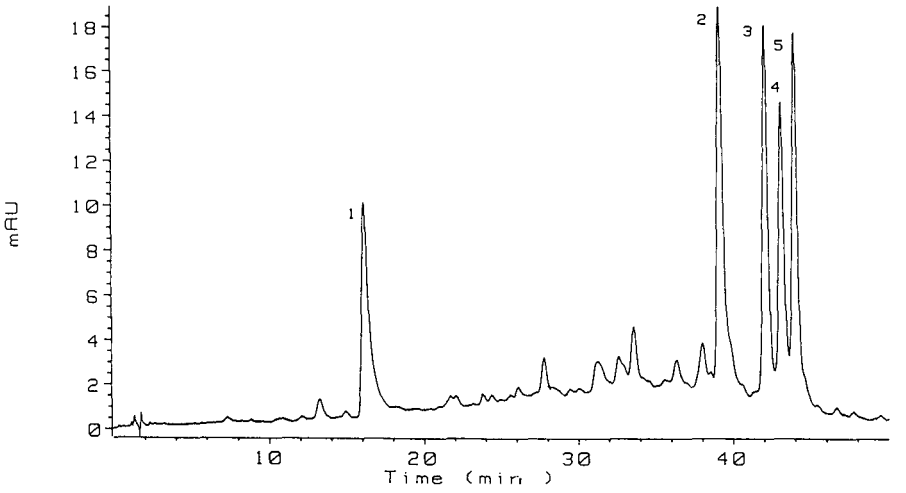

Fig. 5. Tea chromatogram (460 nm) on the Hamilton PRP-1 column. Aqueous solvent 2% (v/v) acetic acid. Organic solvent acetonitrile. Linear gradient, 5 to 33% organic over 50 min, flow-rate 1.0 ml/min. Peaks: 1 = anthocyanidin; 2 = theaflavin; 3 = theaflavin-3-gallate; 4 = theaflavin-3′-gallate; 5 = theaflavin-3,3′-digallate.

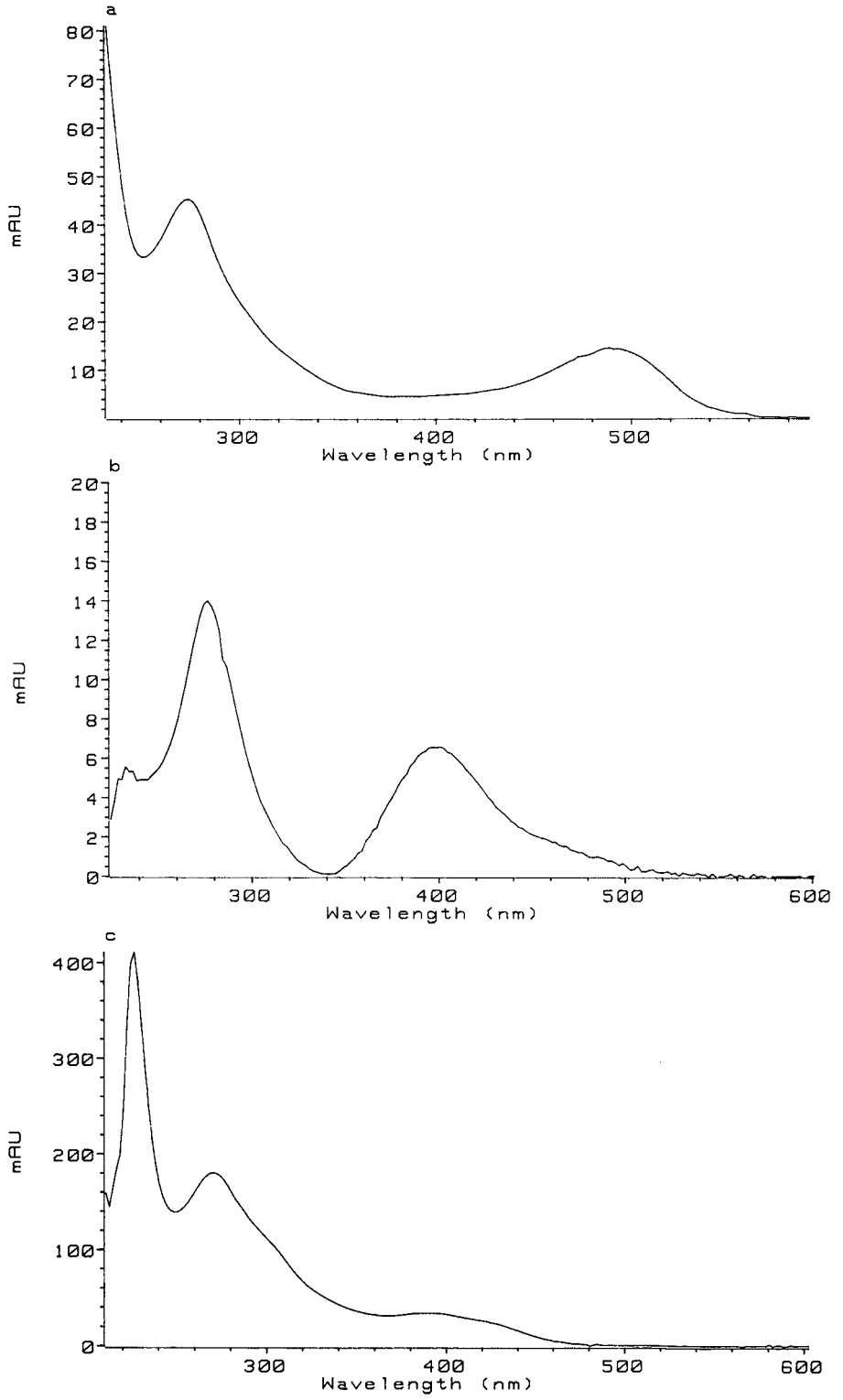
a
mAU
80
70
60
50
40
30
20
10
300
400
500
Wavelength (nm)
b
mAU
20
18
16
14
12
10
8
6
4
2
0
300
400
500
600
Wavelength (nm)
c
mAU
400
300
200
100
0
300
400
500
600
Wavelength (nm)

Fig. 6.

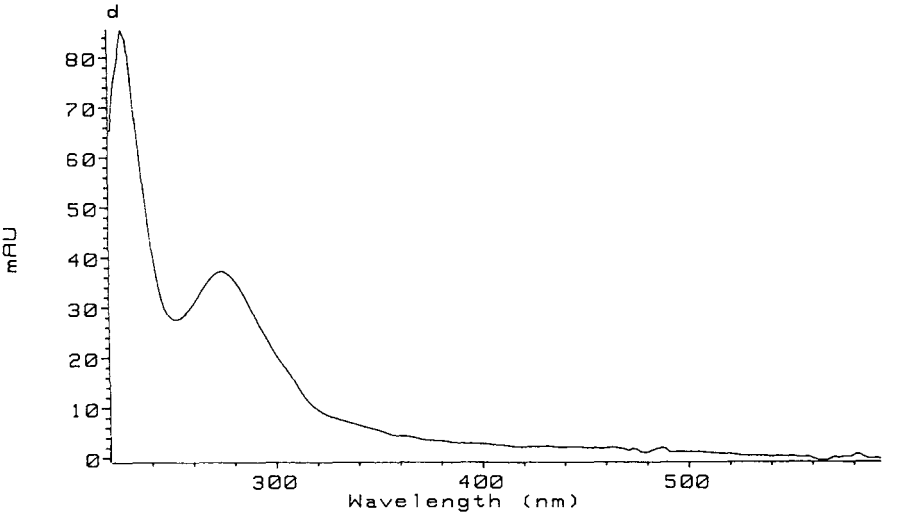

Fig. 6. Photodiode-array UV–VIS spectra. (a) Peak 1 of Fig. 5, an anthocyanidin; (b) peak 13 of Fig. 3, a theaflavic acid; (c) peak 3 of Fig. 3, a type I resolved pigment; (d) peak 7 of Fig. 3, a type II resolved pigment.

the absorption maximum (486.5 nm, in about 15% acetonitrile/85% acetic acid) was different to that of tricetinidin (520 nm, in ethanol), an anthocyanidin isolated from black tea liquors by Roberts and Williams [2,31]. However, an anthocyanidin band measured in aqueous solution is blue-shifted by 25 to 35 nm with respect to the band position measured in ethanol [32]. The difference in the absorption maxima of peak 1 and tricetinidin (33.5 nm) was within this range, so peak 1 in Fig. 5 was tentatively assigned to tricetinidin.

Small reversible improvements were observed with citrate, but no irreversible improvements. The fact, that no irreversible improvements were observed with this column, was probably due to the absence of surface metal contamination of its polymer stationary phase.

Classification of the phenolic tea pigments

From the different chromatograms on the different columns, a classification of the phenolic tea pigments was devised. The pigments were classified by their chromatographic behaviour into three groups, as follows: group I pigments, pigments which ran close to the void volume of the columns; group II pigments, resolved pigments; and group III pigments, unresolved pigments. The photodiode-array UV–VIS spectra extracted from the 33 largest peaks in the chromatogram shown in Fig. 3 (Hypersil ODS column with citrate) allowed the group II pigments to be classified further into four sub-groups (sub-groups II.1, II.2, II.3, and II.4), consisting of peaks with similar photodiode-array UV–VIS spectra (Fig. 3; Table I).

Group I pigments appeared to be totally excluded from all the columns, and ran close to the void volumes of the columns. This material may have been polymeric, hydrogen-bonded, associated, charged, or any combination of these, exclusion being

TABLE I

CLASSIFICATION OF THE GROUP II PIGMENT PEAKS FROM THE HYPERSIL ODS COLUMN BY PHOTODIODE-ARRAY UV–VIS SPECTRA

Peak	Wavelength (nm)	Classification: assignment
1	510	Anthocyanidin polymer
2	271, tailing into visible	II.4: type II resolved pigment
3	271, 387	II.3: type I resolved pigment
4	277, tailing into visible	II.4: type II resolved pigment
5	271, 379	II.3: type I resolved pigment
6	273, tailing into visible	II.4: type II resolved pigment
7	273, tailing into visible	II.4: type II resolved pigment
8	273, 387	II.3: type I resolved pigment
9	271, tailing into visible	II.4: type II resolved pigment
10	273, tailing into visible	II.4: type II resolved pigment
11	271, tailing into visible	II.4: type II resolved pigment
12	263, tailing into visible	II.4: type II resolved pigment
13	275, 395	II.2: a theaflavic acid
14	275, 395	II.2: a theaflavic acid
15	271, tailing into visible	II.4: type II resolved pigment
16	275, 389	II.2: a theaflavic acid
17	267, tailing into visible	II.4: type II resolved pigment
18	267, 371, 461	II.1: a theaflavin
19	267, tailing into visible	II.4: type II resolved pigment
20	271, 382	II.3: type I resolved pigment
21	271, 373, 445	II.1: a theaflavin
22	267, 389	II.3: type I resolved pigment
23	271, 387	II.3: type I resolved pigment
24	275, tailing into visible	II.4: type II resolved pigment
25	271, 371, 450	II.1: a theaflavin
26	271, 370, 450	II.1: a theaflavin
27	271, 371, 460	II.1: theaflavin
28	273, 415	II.3: type I resolved pigment
29	275, 301, 405	II.3: type I resolved pigment
30	269, 371, 451	II.1: theaflavin-3-gallate
31	274, tailing into visible	II.4: type II resolved pigment
32	273, 371, 451	II.1: theaflavin-3′-gallate
33	273, 373, 447	II.1: theaflavin-3,3′-digallate

by molecular size, strong electrostatic repulsion, or both. Photodiode-array three-dimensional plots of the early peaks of the Hypersil ODS tea chromatogram showed three peaks with absorption which extended across the entire spectral region (200–600 nm), which, for this reason, were thought to be brown pigments, and a peak with an absorption maximum at 510 nm, which was thought to be a anthocyanidin pigment.

Although work on the identification of these substances is continuing, some comments on their nature may be made at this point. A spectrum consisting of low-intensity absorption extending across the visible region, is characteristic of substances which are brown [33]. The non-dialysable thearubigins, isolated by Millin and co-workers [34,35] using thin-film counter-current dialysis, were brown protein-containing substances of high molecular mass, probably in the form of a protein–polyphenol complex [36]. Substances of this type could be of sufficient size to be excluded

from the HPLC columns. Somers [37] has shown that anthocyanidin pigments, charged flavanol polymers with units oxidised to the anthocyanidin level, occur in various degrees of association as pigments in red wine. If a pigment of this type were present in the tea liquor, its size and charge would cause it to elute very quickly, and this could account for the peak with the absorption band at 510 nm.

Sub-group II.1 pigments consisted of eight peaks, with spectra which showed three bands in the ranges 267–273, 371–373 and 445–451 nm. Literature theaflavin spectra [38,39] have three bands in the ranges 268–278, 372–378 and 456–461 nm (Table II). The photodiode-array UV–VIS spectra were blue-shifted compared with the literature spectra, but had retained their characteristic shape, so these peaks were assigned to theaflavins. Peaks 27, 30, 32 and 33 in Fig. 3 were assigned as before [1], but the other peaks remain to be assigned to individual theaflavins.

Bailey *et al.* [1] pointed out that nine theaflavins can be formed by the coupling of the appropriate flavanol *o*-quinones, so the assignment of eight peaks to group II.1 is not unreasonable. Some peaks were too small to give reliable spectra, and were not included in the classification; the ninth theaflavin may have been one of these peaks. Other theaflavins can be formed by the oxidation of (−)-epigallocatechin, in the presence of catechol (categallin) or pyrogallol (pyrogallin) [38,39], but the data at present are insufficient for any of the peaks in the chromatogram to be assigned to these compounds.

Sub-group II.2 pigments consisted of three peaks with spectra which showed two bands, at 275 and 389–395 nm (Fig. 6b). Literature theaflavic acid spectra [38] show two bands in the ranges 278–280 and 398–400 nm (Table II), so the three peaks were assigned to theaflavic acids. Three theaflavic acids can be formed by the reaction of the appropriate flavanol *o*-quinones with gallic acid [6,38], and this accounts for the three peaks in our chromatogram.

Sub-group II.3 pigments consisted of eight peaks, the spectra of which showed bands in the ranges 267–275 and 379–405 (Fig. 6c), and with a different absorption maxima ratio to the group II.2 pigments. Peaks with a spectrum of this type, were assigned to type I resolved pigments. They may have been thearubigins of lower

TABLE II

LITERATURE UV–VIS ABSORPTION DATA OF THE THEAFLAVINS AND RELATED COMPOUNDS

All spectra in methanol.

Compound	Wavelength (nm)	Ref.
Theaflavin	268, 378, 461	38
Theaflavin-3-gallate	272, 376, 455	38
Theaflavin-3′-gallate	278, 376, 452	38
Theaflavin-3,3′-digallate	278, 378, 455	38
Categallin	274, 373, 453	39
Pyrogallin	281, 307, 356, 425	39
Epitheaflavic acid	280, 400	38
Epitheaflavic acid-3′-gallate	279, 398	38
Theaflavic acid	278, 398	38

molecular mass, being oxidation products of theaflavins [2], of theaflavic acids [6], and/or of catechins [40].

Sub-group II.4 pigments consisted of thirteen peaks with spectra which showed an absorption maximum in the range 271–277 nm, and absorption which tailed across the entire spectral region (Fig. 6d). The spectra from peaks 12, 17, and 19 each had a band outside this range, but these were not pure peaks. Peaks with a spectrum of this type were assigned to type II resolved pigments. This spectrum is characteristic of substances which are brown [33], so type II resolved pigments were brown phenolic substances, possibly thearubigins, of lower molecular mass. They may have been oxidation products of theaflavins [2], of theaflavic acids [6], and/or of catechins [40]. However, the possibility that some of these peaks were the products of non-enzymic browning reactions, cannot be ruled out completely.

Group III pigments were unresolved pigments, which ran as a convex broad band on the Hypersil wide-pore and Hamilton PRP-1 columns. The photodiode-array UV–VIS spectra of group III pigments showed a band at about 280 nm, and absorption which tailed across the entire spectral region, indicating that they were brown phenolic pigments, possibly polymeric thearubigins. Brown *et al.* [7] suggested that some thearubigins were proanthocyanidin polymers, and indeed McMurrough [41] and Putman and Butler [24] have shown that proanthocyanidin polymers run as unresolved broad bands on an ODS column. However, tea manufacture involves a complex set of enzymic and chemical reactions capable of producing highly polydisperse polymers [2–5]. Therefore, the group III pigments may be polydisperse flavanol polymers incorporating chromophoric monomer units, rather than proanthocyanidin polymers.

This classification thus highlights that a range of pigments were present in the black tea liquor studied, some resolvable by HPLC and some, at this time, unresolvable.

CONCLUSIONS

New HPLC methods for the analysis of black tea liquor have been developed. Very good separation of phenolic tea pigments has been achieved using a Hypersil ODS column in conjuction with a citrate buffer. The suggestion was put forward, that the improved performance of this column on changing from acetic acid to citrate was mainly caused by the removal or masking of surface metals from the stationary phase by the citrate. Unresolved, probably polymeric, pigments formed a convex broad band on the Hypersil octyl wide-pore (Fig. 4) and Hamilton PRP-1 (Fig. 5) columns. The Hamilton PRP-1 column provided a method for the analysis of an anthocyanidin, and showed it to be an important contributor to liquor colour (Fig. 5).

The phenolic pigments in black tea liquor were classified by their chromatographic behaviour, as follows: group I pigments, pigments which ran close to the void volume of the HPLC columns; group II pigments, resolved pigments; and Group III pigments, unresolved pigments. Group II pigments were then further classified by photodiode-array UV–VIS spectra, into four sub-groups, as follows: sub-group II.1, three bands in the ranges 267–273, 371–373 and 445–451 nm (theaflavins); sub-group II. 2, two bands at 275 and 389–395 nm (theaflavic acids); sub-group II.3, bands in the ranges 267–275 and 379–405 nm, of different shape to sub-group II.2 spectra (type I

resolved pigments); and sub-group II.4, a band in the range 271–277 nm and absorption which tailed into the visible region (type II resolved pigments). Pigments in sub-groups II.3 and II.4 were designated as resolved thearubigins, and those in group III as unresolved thearubigins.

This work is part of a larger project, the aim of which is to obtain instrumental measures of tea quality. In parallel with the qualitative work reported here, quantitative statistical studies are in progress, the aim of which is to discover what relation, if any, the classes of pigments discussed in this paper have to tea quality. Further qualitative work will also be carried out on the identification of these pigments, and the further improvement of the analytical methods.

ACKNOWLEDGEMENT

Financial support by NRI is gratefully acknowledged.

REFERENCES

1 R. G. Bailey, I. McDowell and H. E. Nursten, *J. Sci. Food Agric.*, 52 (1990) 509.
2 E. A. H. Roberts, in T. A. Geissman (Editor), *Chemistry of Flavonoid Compounds*, Pergamon, Oxford, 1962, p. 468.
3 G. W. Sanderson, *Recent Adv. Phytochem.*, 5 (1972) 247.
4 R. L. Wickremasinghe, *Adv. Food Res.*, 24 (1978) 229.
5 M. A. Bokuchava and N. I. Skobeleva, *CRC Rev. Food Sci. Nutrition*,12 (1980) 303.
6 J. E. Berkowitz, P. Coggon and G. W. Sanderson, *Phytochemistry*, 10 (1971) 2271.
7 A. G. Brown, W. B. Eyton, A. Holmes and W. D. Ollis, *Phytochemistry*, 8 (1969) 2333.
8 A. Robertson and D. S. Bendall, *Phytochemistry*, 22 (1983) 883.
9 G. R. Roberts, R. S. S. Fernando and A. Ekanayake, *J. Food Sci. Technol.*, 18 (1981) 118.
10 S. C. Opie, A. Robertson and M. N. Clifford, *J. Sci. Food Agric.*, 50 (1990) 547.
11 L. R. Snyder, M. A. Stadalius and M. A. Quarry, *Anal. Chem.*, 55 (1983) 1412A.
12 L. R. Snyder, J. L. Glajch and J. L. Kirkland, *Practical HPLC Method Development*, Wiley, Chichester, 1988, p. 53.
13 J. W. Dolen and L. R. Snyder, *Troubleshooting LC Systems*, Humana, Clifton, NJ, 1989, p. 404.
14 V. R. Meyer, *Practical High-Performance Liquid Chromatography*, Wiley, Chichester, 1988, p. 79.
15 J. Nawrocki and B. Buszewski, *J. Chromatogr.*, 449 (1988) 1.
16 J. F. K. Huber and F. Eisenbeiss, *J. Chromatogr.*, 149 (1978) 127.
17 R. R. Walters, *J. Chromatogr.*, 249 (1982) 19.
18 J. P. Larmann, J. J. DeStefano, A. P. Goldberg, R. W. Stout, L. R. Snyder and M. A. Stadalius, *J. Chromatogr.*, 255 (1983) 163.
19 L. C. Sander and S. A. Wise, *J. Chromatogr.*, 316 (1984) 163.
20 J. G. Buta, *J. Chromatogr.*, 295 (1984) 506.
21 L. D. Bowers and S. Pedigo, *J. Chromatogr.*, 371 (1986) 243.
22 D. J. Pietrzyk, in P. R. Brown and R. A. Hartwick, (Editors), *High Performance Liquid Chromatography (Chemical Analysis*, Vol. 8), Wiley-Interscience, Chichester, 1989, p. 223.
23 S. M. Cramer, B. Nathanael and Cs. Horváth, *J. Chromatogr.*, 295 (1984) 405.
24 L. J. Putman and L. G. Butler, *J. Agric. Food Chem.*, 37 (1989) 943.
25 I. McDowell, R. G. Bailey and G. Howard, *J. Sci. Food Agric.*, 53 (1990) 411.
26 E. A. H. Roberts and R. F. Smith, *Analyst (London)*, 86 (1961) 94.
27 E. A. H. Roberts and R. F. Smith, *J. Sci. Food Agric.*, 14 (1963) 689.
28 S. Natesan and V. R. Ranganathan, *J. Sci. Food Agric.*, 51 (1990) 125.
29 G. Weber and G. Schwedt, *J. Chromatogr.*, 285 (1984) 380.
30 M. T. Gilbert, *High Performance Liquid Chromatography*, Wright, Bristol, 1987, p. 155.
31 E. A. H. Roberts and D. M. Williams, *J. Sci. Food Agric.*, 9 (1958) 217.
32 P. Ribéreau-Gayon, *Plant Phenolics*, Oliver and Boyd, Edinburgh, 1972, p. 153.

33 L. G. S. Brooker and E. J. Van Lare, *Encyclopedia of Chemical Technology,* Vol. 5, Wiley, New York, 1964, p. 763.
34 D. J. Millin, D. Swaine and P. L. Dix, *J. Sci. Food Agric.,* 20 (1969) 296.
35 D. J. Millin, D. S. Sinclair and D. Swaine, *J. Sci. Food Agric.,* 20 (1969) 305.
36 E. Haslam, *Plant Polyphenols,* Cambridge University Press, Cambridge, 1989, p. 154.
37 T. C. Somers, *Phytochemistry,* 10 (1971) 2175.
38 P. D. Collier, T. Bryce, R. Mallows, P. E. Thomas, D. J. Frost, O. Korver and C. K. Wilkins, *Tetrahedron,* 29 (1973) 125.
39 Y. Takino, A. Ferretti, V. Flanagan, M. A. Gianturco and M. Vogel, *Can. J. Chem.,* 45 (1967) 1949.
40 D. E. Hathway and J. W. T. Seakins, *J. Chem. Soc.,* (1957) 1562.
41 I. McMurrough, *J. Chromatogr.,* 218 (1981) 683.

Journal of Chromatography, 542 (1991) 129–136
Elsevier Science Publishers B.V., Amsterdam

CHROM. 23 009

High-performance liquid chromatographic determination of optical purity of planar chiral organometallic compounds resolved by enzymic transformations

YOSHIMITSU YAMAZAKI*, NOBUO MOROHASHI[a] and KUNIAKI HOSONO
Fermentation Research Institute, Agency of Industrial Science and Technology, 1–1–3 Higashi, Tsukuba, Ibaraki 305 (Japan)

(First received June 5th, 1990; revised manuscript received November 12th, 1990)

ABSTRACT

The enantiomers of planar chiral organometallic compounds, *i.e.*, 1-hydroxymethyl-2-methyl, 1-acetoxymethyl-2-methyl and 1-methoxycarbonyl-2-methyl derivatives of (η^6-benzene)tricarbonylchromium, tricarbonyl(η^5-cyclopentadienyl)manganese and ferrocene, and their 3-methyl analogues, were separated by high-performance liquid chromatography with a Chiralcel OD column. This method was useful to determine the optical purity for the above compounds formed in enzymic transformations.

INTRODUCTION

Enzymic transformation is one of the most practical methods for preparing optically active organometallics having planar chirality such as homoannularly di- or trisubstituted ferrocene derivatives [1–3] and asymmetrically substituted arenes or alkadienes complexed with tricarbonylmetal clusters [2–8]. These compounds are useful as chiral auxiliaries for asymmetric reagents or catalysts. An important problem in the study on asymmetric bioconversion is to determine the optical purity of the product as easily as possible for screening new biocatalysts or monitoring kinetic resolution.

Optical purities of planar chiral organometallics have heretofore been determined by NMR spectroscopy with a chiral shift reagent [2–6,9], by high performance liquid chromatography (HPLC) on a chiral stationary phase [1,2] or by NMR [7] or HPLC [10] after conversion to diastereomeric derivatives.

The NMR shift reagent method as well as the diastereomeric methods are too complicated to be used in routine work. Chromatographic analysis without pretreatment or derivatization is the best choice in this respect. A β-cyclodextrin-bonded column was successfully used for optical purity determination of planar chiral ferrocene derivatives [1,2], but it did not resolve (±)-tricarbonyl (η^5-1-methoxycarbonyl-2-

[a] Present address: Tsukuba Research Laboratories, Toyo Ink Mfg. Co., Ltd., 27-Wadai, Tsukuba, Ibaraki 300-42, Japan.

0021-9673/91/$03.50

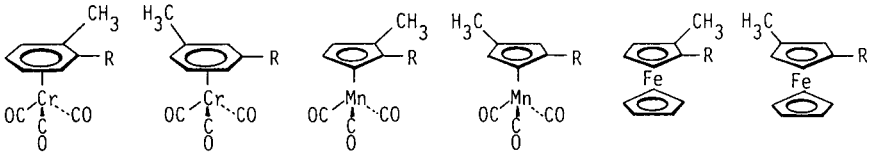

a, R = CH_2OH ; **b**, R = CHO ; **c**, R = $COOCH_3$; **d**, R = CH_2OCOCH_3 ; **e**, R = COOH

Fig. 1. Structures of compounds.

methylcyclopentadienyl)manganese (**3c**) (Fig. 1) in our preliminary experiments, so that the application of this column seems to be limited to some metallocenes [4,11] certainly with regard to the size of the cavity of β-cyclodextrin. Although several stationary phases containing cellulose derivatives [12,13] or a synthetic chiral polymer [14] had been used for the preparative resolution of planar chiral tricarbonylmetal complexes, their utility in analytical HPLC has not been reported. The HPLC analysis of organometallics [15] is still undeveloped from the point of view of treating the stereochemistry. Therefore, we tested seven types of commercially available chiral columns for the optical purity determination of 22 planar chiral organometallic compounds.

EXPERIMENTAL

Chromatographic procedure

The HPLC apparatus was constructed with a Shimadzu LC-6A pump, a Rheodyne Model 7125 injector with a 20-μl sample loop, a Shimadzu SPD-6A UV spectrophotometric detector set at 220 nm and a Shimadzu C-R6A data processor. Prepacked Chiralcel OA, OB, OC, OK and OD and Chiralpak OT(+) and OP(+) columns (250 mm × 4.6 mm I.D.) were obtained from Daicel Chemical Industries (Tokyo, Japan). The system was operated at room temperature at a flow-rate of 0.5 ± 0.02 ml/min with 0.65–2.6 *M* 2-propanol or ethanol in hexane as the mobile phase. The solvents were of JIS-guaranteed reagent grade from Wako (Osaka, Japan).

Organometallics

The following compounds were obtained in our previous work: (±)-**1a** [4], (1*S*)-(+)-**1a** [6], (±)-**1b** [4], (1*R*)-(−)-**1b** [4], (1*R*)-(+)-**2a** [6], (1*R*)-(−)-**3a** [2], (±)-**3b** [4], (±)-**4b** [5], (±)- and (1*R*)-**5a** [1], (±)-**5b** [1], (±)- and (1*R*)-**5c** [1], (±)-**6a** [1], (±)-**6b** [1] and (±)-**6c** [1]. Three $Cr(CO)_3$ complexes, (±)-**1c**, (±)-**2a** and (±)-**2c**, were prepared by complexation of methyl 2-methylbenzoate, 3-methylbenzyl alcohol and methyl 3-methylbenzoate with $Cr(CO)_6$ [16], respectively. $Mn(CO)_3$-complexed esters (±)-**3c** and (±)-**4c** were synthesized according to the literature [17]. The enantiomerically enriched methyl esters (1*R*)-**2c**, (1*S*)-**3c**, (1*S*)-**4c** and (1*R*)-**6c** were prepared by methylation of (1*R*)-(+)-**2e** [3], (1*S*)-(−)-**3e** [4], (1*S*)-(−)-**4e** [3] and (1*R*)-(−)-**6e** [3], respectively, with diazomethane. Dimethyl sulphoxide oxidation [5] of (±)-**2a** gave (±)-**2b** and $LiAlH_4$ reduction of (±)-**3b**, (±)-**4b**, (1*R*)-(+)-**4b** and

(1*R*)-**6c** gave (±)-**3a**, (±)-**4a**, (1*R*)-**4a** and (1*R*)-**6a**, respectively. The optically active aldehyde (1*R*)-(+)-**4b** was obtained as the less reactive enantiomer in horse liver alcohol dehydrogenase (HLADH)-catalysed reduction of (±)-**4b** [5] in 34% yield, $[\alpha]_D^{22}$ + 27° (*c* = 2.1, benzene). The absolute configuration of (+)-**4b** was determined by Ag_2O oxidation [5] to (1*R*)-(+)-**4e**, m.p. 182–183°C, $[\alpha]_D^{23}$ + 8.3° (*c* = 1, ethanol). Acetates (±)-**1d**, (1*S*)-**1d**, (±)-**2d**, (1*R*)-**2d**, (±)-**3d**, (1*R*)-**3d**, (±)-**4d** and (1*R*)-**4d** were prepared by treatment of the corresponding alcohols (1–2 mg) with acetic anhydride (20 μl) and pyridine (20 μl) in 100 μl of toluene and purified by preparative thin-layer chromatography (TLC) on silica gel F_{254} (0.25 mm thick) (Merck) developed with 0–10% ethyl acetate in benzene. All compounds thus prepared showed the molecular ion peak corresponding to each structure in the mass spectrum.

Optical purity determination of the products of lipase-catalysed acetylation

Lipase P (dry powder; 23 U/mg, as assayed with PVA-emulsified olive oil and reciprocal shaking [18]) was supplied by Amano Pharmaceutical (Nagoya, Japan). To 4.9 ml of toluene were added 0.1 ml of vinyl acetate, 50 mg of (±)-**1a** or (±)-**2a** and 0.15 g of lipase P. The mixtures were stirred at 4°C. Aliquots (0.3 ml) were withdrawn at time intervals and then immediately centrifuged to remove the enzyme. A 1-μl volume of each supernatant was dried under vacuum and the residue was dissolved in 1 ml of 10% ethanol in hexane for HPLC analysis (Figs. 3 and 4).

Optical purity determination of the product of HLADH-catalysed reduction

To a solution of (±)-**4b** (0.7 mg) in 50 μl of ethanol were added 0.43 ml of 0.1 *M* phosphate buffer (pH 7.5) containing 0.5 mg of NADH. The turbid mixture was cooled with ice and the reaction was started by addition of 0.04 U of HLADH (Sigma, 2 U/mg, as assayed with ethanol [1]) dissolved in 20 μl of the phosphate buffer. The mixture was stirred at 4°C for 45 min and then at room temperature for 1 h. The reaction progress was monitored by TLC on silica gel F_{254} developed with 20% ethyl acetate in benzene (R_F 0.82 for **4b** and 0.50 for **4a**). Aliquots (0.1 ml) were withdrawn at time intervals and then immediately extracted with hexane (0.5 ml each) in the presence of 30–40 mg of sodium chloride. After appropriate dilution with hexane, the organic layers were analysed by HPLC (Fig. 5).

RESULTS AND DISCUSSION

First, the resolution power of seven columns was investigated with $Cr(CO)_3$-complexed 2-methylbenzyl alcohol (**1a**) and its derivatives of different functionality (**1b–1d**). The Chiralcel OB, OC and OD and Chiralpak OT(+) columns resolved at least one of the four racemic compounds (Table I). The Chiralcel OA and OK and Chiralpak OP(+) columns did not show any clear resolution, although they retained the compounds ($4 < k' < 15$).

The remarkably high resolution given by the OD column is interesting in terms of the structure of the stationary phase. According to the maker's catalogue, the packing materials of the Chiralcel OA, OB, OK, OC and OD columns are coated with cellulose triacetate, tribenzoate, tricinnamate, tris(phenylcarbamate) and tris(3,5-dimethylphenylcarbamate), respectively. It may be reasonable to consider that the solutes are adsorbed on the OD stationary phase by hydrogen bonding to the carbamyl

TABLE I

OPTICAL RESOLUTION OF PLANAR CHIRAL ORGANOMETALLIC COMPOUNDS BY HPLC WITH FOUR CHIRAL COLUMNS[a]

Compound	Column					
	OC			OT(+)		
	k'[b]	α[c]	R_s[d]	k'	α	R_s
1a	*8.86*, 9.33	1.05	0.69	*1.39*, 1.50	1.08	0.51
1b	8.85			*1.85*, 2.07	1.12	0.82
1c	3.46			1.39		
1d	7.00			1.63		
	OB			OD		
	k'	α	R_s	k'	α	R_s
1a	5.31			9.30, *10.02*	1.08	1.20
1b	7.83			-[e]		
1c	3.04, *3.39*	1.12	0.56	*2.06*, 2.28	1.11	1.38
1d	*6.44*, 7.13	1.11	0.68	3.86, *4.39*	1.14	2.08
2a	4.77			*5.86*, 14.77	2.52	15.63
2b	6.43			-[e]		
2c	3.27			*2.39*, 3.48	1.46	5.81
2d	6.16, *6.73*	1.09	0.64	*2.82*, 3.01	1.07	1.08
3a	0.86			3.66, *3.88*	1.06	0.91
3b	1.80			-[e]		
3c	0.68			*0.72*, 0.96	1.33	2.31
3d	0.98			0.99, *1.10*	1.10	1.21
4a	0.83			*2.48*, 3.71	1.50	5.90
4b	1.83			-[e]		
4c	0.78			*1.27*, 1.50	1.18	2.03
4d	0.95			*0.83*, 0.88	1.06	0.70
5a	1.01			2.27, *2.58*	1.14	1.81
5b	1.45			-[e]		
5c	0.65			*0.63*, 0.88	1.39	2.94
6a	0.96			*1.77*, 1.99	1.12	1.46
6b	1.46			-[e]		
6c	0.80			*0.99*, 1.35	1.35	3.41

[a] Chiralcel OB, OC and OD and Chiralpak OT(+) columns. Mobile phase, 1.3 *M* 2-propanol in hexane; flow-rate, 0.5 ml/min.

[b] Capacity factor. Values in italics are for the 1*R*-enantiomer. The enantiomeric assignment is based on the chromatography of the optically active or enantiomerically enriched specimen, except for **1c**. The assignment for **1c** was done by HPLC of the alcohol obtained by $LiAlH_4$ reduction of the ester resolved by the OD column.

[c] Separation factor.

[d] Resolution. Calculated with the width at the peak bottom by the equation $R_s = 2$ (difference between two retention times)/(sum of two peak widths).

[e] Not eluted. The aldehydes were also tested on the OT(+) column (1.3 *M* 2-propanol in hexane) but no resolution was observed for any aldehyde except **1b**.

group, as suggested by Okamoto *et al.* [19] in a study with other chiral compounds and various triphenylcarbamyl cellulose adsorbents. However, the chiral recognition on this phase must be mainly due to a steric effect from the 3,5-dimethyl groups of the phenyl moiety, as the unsubstituted triphenylcarbamate column (OC) was less effective than the OD column for the optical resolution of the present compounds. The dimethyl groups may depress the adsorption by steric hindrance of the adsorbate molecule [20] or modify the size and shape of the spaces in the adsorbent [21] so as to increase the slight difference between the adsorption modes of two enantiomers.

One unsatisfactory result with the OD column was the irreversible binding of aldehyde **1b**. The adsorption was so strong that **1b** was not eluted even with 100% 2-propanol.

The resolving power of the OD column was further studied with other planar chiral organometallic compounds (**2a–6c**). The results are summarized in Table I together with those given by the OB column for comparison. The OD column resolved, partly or completely, all compounds except for the aldehydes (**2b**, **3b**, **4b**, **5b** and **6b**). The resolution was considerably influenced by the difference in the metal atom and/or the structure around it. However, the elution order of enantiomers was definite in each of three series of compounds. The 1*R*-enantiomers of all 2-methyl alcohols and acetates (**1a**, **1d**, **3a**, **3d** and **5a**) were eluted after the corresponding 1*S*-enantiomer, and the reverse was found for all 3-methyl alcohols and acetates (**2a**, **2d**, **4a**, **4d** and **6a**). The enantiomers of all methyl esters (**1c**, **2c**, **3c**, **4c**, **5c** and **6c**) were eluted in the order 1*R* > 1*S*. These regularities suggest that the spatial arrangement of two ring substituents (*i.e.*, planar chirality) is the predominant factor in controlling the binding mode, probably through steric interactions with the substituents of the adsorbent.

The separation factor (α) for (±)-**1a**, -**1d**, -**2a** and -**2d** on the OD column was hardly affected by changing the concentration of 2-propanol or ethanol in the mobile phase, whereas the capacity factor (k') and resolution (R_s) increased with decreasing concentration of the alcohols. A typical result for (±)-**1a** is shown in Fig. 2. The

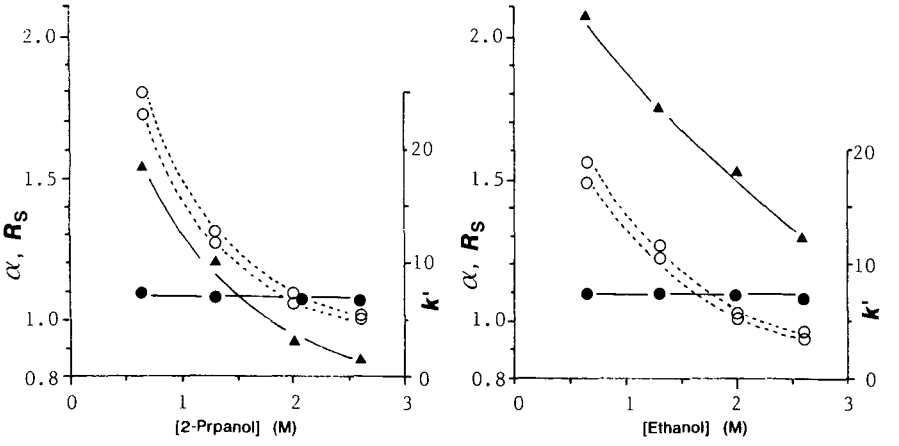

Fig. 2. Effect of the solvent on HPLC of (±)-**1a**. Column, Chiralcel OD (250 mm × 4.6 mm I.D.); flow-rate, 0.5 ml/min; solvent, hexane containing 2-propanol or ethanol. (○) Capacity factor (k'); (●) separation factor (α); (▲) resolution (R_s).

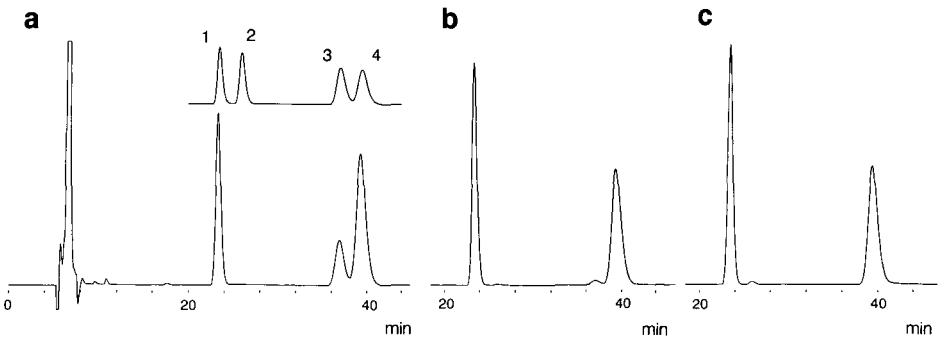

Fig. 3. HPLC of reaction mixtures of (±)-**1a** with lipase P and vinyl acetate after (a) 1 h, (b) 2 h and (c) 3 h. Column, Chiralcel OD; mobile phase, 2.0 *M* 2-propanol in hexane; flow-rate, 0.5 ml/min. The inset is the chromatogram (20–44 min) for an authentic mixture of (1*S*)-**1d** (peak 1), (1*R*)-**1d** (peak 2), (1*S*)-**1a** (peak 3) and (1*R*)-**1a** (peak 4).

alcohols in the mobile phase must work as hydrogen bonding modifiers. The aforementioned effect of the alcohol concentration on the chromatographic parameters supports the idea that the solutes are adsorbed on the OD phase via hydrogen bonding to the carbamyl group, but that this bonding would not be essential to the chiral recognition represented by α. In addition, the analysis with (±)-**1a** showed that ethanol was better than 2-propanol in obtaining high R_s (Fig. 2). This relationship was the reverse, however, for (±)-**1d**, -**2a** and -**2d** (data not shown).

HPLC with the OD column was applied to study the stereoselectivity of two enzymic transformations of planar chiral organometallic compounds. The chromatograms in Fig. 3 show that the (1*S*)-acetate (**1d**) formed by the lipase-catalysed acetylation of (±)-**1a** was optically very pure after 1 h of reaction (Fig. 3a), but the purity decreased to 98.2% e.e. after 2 h (Fig. 3b) and the remaining (1*R*)-**1a** became optically pure after 3 h (Fig. 3c). This result indicates that the optimum chemical and optical yields for both enantiomers are achieved after 2–3 h under the reaction condi-

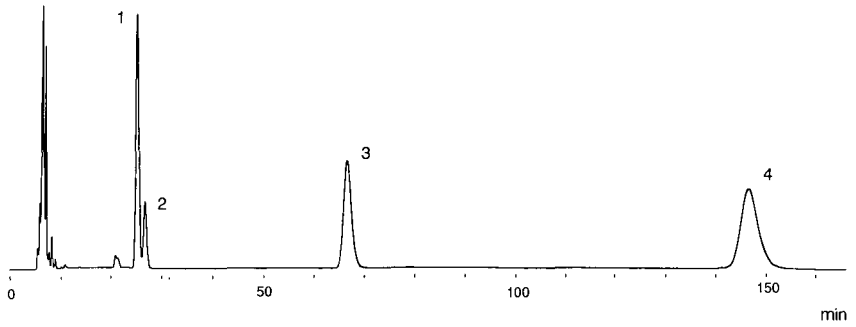

Fig. 4. HPLC of the reaction mixture of (±)-**2a** with lipase P and vinyl acetate after 4 h. Column, Chiralcel OD; mobile phase, 0.65 *M* ethanol in hexane; flow-rate, 0.5 ml/min. Peaks 1, 2, 3 and 4 were assigned as (1*R*)-**2d**, (1*S*)-**2d**, (1*R*)-**2a** and (1*S*)-**2a**, respectively. The ratio of peak areas is 24.0:7.2:26.2:42.5 in the above order.

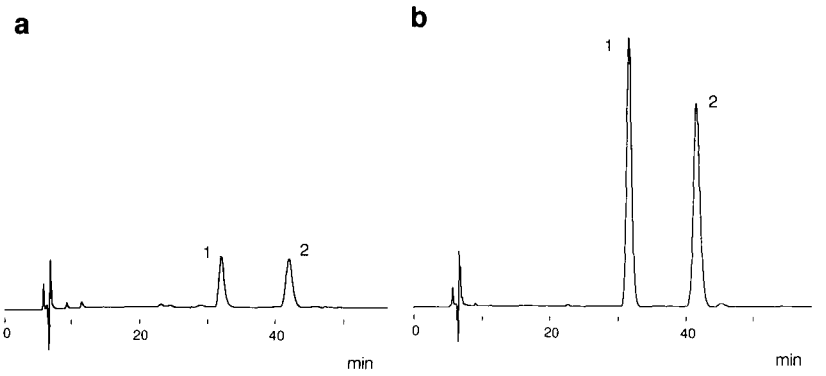

Fig. 5. HPLC of the reaction mixture of (±)-**4b** with HLADH, NADH and ethanol in an ice-bath (a) after 30 min and (b) after standing at room temperature for 1 h. Chromatographic conditions as in Fig. 4. Peaks 1 and 2 are assigned as (1*R*)-**4a** and (1*S*)-**4a**, respectively, and the ratio of the peak areas [(1*S*)-**4a**/(1*R*)-**4a**] is 1.235 ± 0.029 (n = 6) for (a), obtained in three separate runs, and 0.999 ± 0.003 (n = 6) for (b).

tions used. In any case, the 2-methylbenzyl alcohol complex (**1a**) is efficiently resolved by the lipase reaction. This reaction was, however, less enantioselective for the 3-methylbenzyl alcohol complex (**2a**). The chromatogram in Fig. 4 shows that the enantiomeric purity of the product [(1*R*)-**2d**] was 54% e.e. at a conversion rate of about 30%.

The enantioselectivity of HLADH-catalysed reduction was found to be low for the $Mn(CO)_3$-complexed 3-methyl aldehyde (**4b**) [5]. Determination of the small E value (an index of enantioselectivity [22]) was tried using HPLC (Fig. 5). E is given by the equation $E = \ln[1 - c(1 + ee_p)]/\ln[1 - c(1 - ee_p)]$, where c and ee_p are conversion rate and optical purity (e.e.) of the product, respectively. It was evidenced by TLC that the reaction had been completed before sampling for Fig. 5b. The conversion rate for the sample in Fig. 5a was calculated to be 22.5% by comparison with Fig. 5b. The enantiomeric purity of the alcohol [(1*S*)-**4a**] found in Fig. 5a was 11.5% e.e., and hence E was determined to be 1.30.

In conclusion, HPLC with the Chiralcel OD column is a convenient method for determining the optical purity of planar chiral organometallic alcohols and esters, and will serve for studies of the bioconversion of this special class of compounds.

REFERENCES

1 Y. Yamazaki, M. Uebayasi and K. Hosono, *Eur. J. Biochem.*, 184 (1989) 671–680.
2 Y. Yamazaki and K. Hosono, *Biotechnol. Lett.*, 11 (1989) 679–684.
3 Y. Yamazaki and K. Hosono, *Ann. N.Y. Acad. Sci.*, 613 (1990) 738–746.
4 Y. Yamazaki and K. Hosono, *Tetrahedron Lett.*, 30 (1989) 5313–5314.
5 Y. Yamazaki, M. Uebayasi, J. Someya and K. Hosono, *Agric. Biol. Chem.*, 54 (1990) 1781–1789.
6 Y. Yamazaki and K. Hosono, *Tetrahedron Lett.*, 31 (1990) 3895–3896.
7 N. W. Alcock, D. H. G. Crout, C. M. Henderson and S. E. Thomas, *J. Chem. Soc., Chem. Commun.*, (1988) 746–747.
8 S. Top, G. Jaouen, J. Gillois, C. Baldoli and S. Maiorana, *J. Chem. Soc., Chem. Commun.*, (1988) 1284–1285.
9 A. Solladié-Cavallo and J. Suffert, *Magn. Reson. Chem.*, 23 (1985) 739–743.
10 R. Eberhardt, C. Glotzmann, H. Lehner and K. Schlögl, *Tetrahedron Lett.*, (1974) 4365–4368.

11 D. W. Armstrong, W. DeMond and B. P. Czech, *Anal. Chem.*, 57 (1985) 481–484.
12 K. Schlögl, *J. Organomet. Chem.*, 300 (1986) 219–248.
13 H. Sotokawa, A. Tajiri, N. Morita, C. Kabuto, M. Hatano and T. Asao, *Tetrahedron Lett.*, 28 (1987) 5873–5876.
14 A. Tajiri, N. Morita, T. Asao and M. Hatano, *Angew. Chem., Int. Ed. Engl.*, 24 (1985) 329–330.
15 A. Casoli, A. Mangia, G. Predieri, E. Sappa and M. Volante, *Chem. Rev.*, 89 (1989) 407–418.
16 J. Blagg, S. G. Davies, N. J. Holman, C. A. Laughton and B. E. Mobbs, *J. Chem. Soc., Perkin Trans. 1*, (1986) 1581–1589.
17 H. Gowal and K. Schlögl, *Monatsh. Chem.*, 98 (1967) 2302–2314.
18 N. Tomizuka, Y. Ota and K. Yamada, *Agric. Biol. Chem.*, 30 (1966) 576–584.
19 Y. Okamoto, M. Kawashima and K. Hatada, *J. Chromatogr.*, 363 (1986) 173–186.
20 Y. Okamoto, K. Hatano, R. Aburatani and K. Hatada, *Chem. Lett.*, (1989) 715–718.
21 T. Shibata, I. Okamoto and K. Ishii, *J. Liq. Chromatogr.*, 9 (1986) 313–340.
22 C.-S. Chen and C. J. Sih, *Angew. Chem., Int. Ed. Engl.*, 28 (1989) 695–707.

Journal of Chromatography, 542 (1991) 137–143
Elsevier Science Publishers B.V., Amsterdam

CHROM. 23 034

High-performance liquid chromatographic assay of thiomersal (thimerosal) as the ethylmercury dithiocarbamate complex

J. E. PARKIN

School of Pharmacy, Curtin University of Technology, Kent Street, Bentley, Western Australia 6102 (Australia)

(First received September 12th, 1990; revised manuscript received December 11th, 1990)

ABSTRACT

A high-performance liquid chromatographic (HPLC) assay has been developed for the ethylmercury ligand of thiomersal (thimerosal) as either the morpholine or piperidinedithiocarbamate complexes. The assay has been compared with a previously reported HPLC assay of thiomersal for organomercurical degraded both thermally and photochemically, and significant differences are noted.

INTRODUCTION

Thiomersal (thimerosal, TM), the sodium salt of the complex formed between thiosalicylic acid (TSA) and ethylmercury (EtHg) (compound I, Fig. 1), is used as a

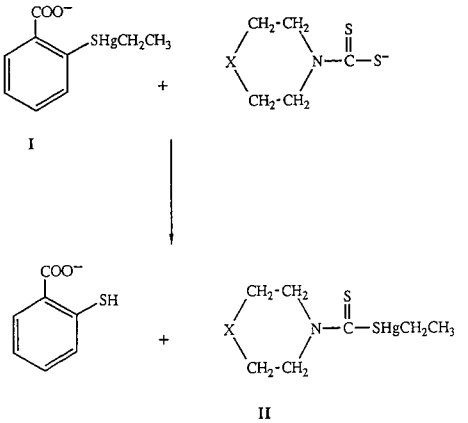

Fig. 1. Reaction of MDTC (X = O) and PIDTC (X = CH_2) with thiomersal (I) to form thiosalicylic acid and the MDTC or PIDTC complex of ethylmercury (II).

0021-9673/91/$03.50

topical antiseptic and antimicrobial preservative [1]. It is unstable to light [2–4] and can be adsorbed by plastics [4–6] both of which influence the potential shelf-life of pharmaceutical products. In studies of these problems and for routine analytical purposes a number of analytical methods have been reported using colorimetry [3,5,7], atomic absorption spectroscopy [8,9], polarography [10] and high-performance liquid chromatography (HPLC) [2–4, 11–14]. In studies where these analytical methods have been compared using identical degraded samples of TM, considerable differences have been noted [2–4].

In keeping with other mercurial antiseptics and antimicrobial preservatives the antimicrobial activity of TM probably resides in the EtHg ligand [15–17]. Should the two components of the complex (TSA and EtHg) decompose at different rates assessment of total EtHg (intact TM and free EtHg) may afford a better chemical assessment of active antimicrobial activity. All the reported HPLC methods are designed to detect and quantitate intact TM cognizance having not been given to the consequence of losses of TSA resulting in a reduced level of measured TM due to changes in the stoichiometric ratio of TSA and EtHg in the mixture. It is known that the major decomposition products of TM are 2,2′-dithiosalicyclic acid formed by oxidation of TSA, EtHg and, in the presence of light, elemental mercury [4]. Further, it has been shown that degraded samples of TM possess enhanced levels of antimicrobial activity, and it has been suggested that this may be due to EtHg formed during degradation [17].

The development in these laboratories of a range of dithiocarbamate (DTC)-complexing agents and their application to the quantitation of phenylmercuric nitrate [18–20] makes possible the development of an EtHg ligand-specific assay for TM. This paper reports the development of two such assays using morpholinedithiocarbamate (MDTC) and piperidinedithiocarbamate (PIDTC) and compares the results of this type of assay to the conventional HPLC method [13] using thermally and photochemically degraded samples of TM.

EXPERIMENTAL

Materials

TM and TSA (Sigma, St. Louis, MO, U.S.A.) and EtHgCl (TCI, Tokyo, Japan) were used as supplied. All other chemicals were analytical or HPLC grade. The morpholinium salt of MDTC and piperidinium salt of PIDTC were prepared as reported previously [18,19].

Preparation of derivatives

The MDTC and PIDTC reagents were prepared by dissolving 10, 20, 60 and 100 mg of the corresponding salts in 100 ml of acetonitrile–water (75:25) and 100% acetonitrile, respectively. Of this reagent, 1 ml was added to 1 ml of sample in a glass vial followed by mixing. For routine analytical purposes a concentration of 60 mg of reagent salt per 100 ml of solvent is appropriate.

Chromatographic equipment and conditions

The liquid chromatograph consisted of a Model 501 pump (Waters Assoc., Milford, MA, U.S.A.), Rheodyne Model 7125 loop injector (Cotati, CA, U.S.A.),

Model 484 variable-wavelength absorbance detector (Waters Assoc.) and Model 3396A integrating recorder (Hewlett-Packard, Palo Alto, CA, U.S.A.) together with a column of octadecyl silica (Waters Assoc.), 30 cm × 3.9 mm I.D., 10 μm particle size. The solvent consisted of $1 \cdot 10^{-4}$ *M* disodium ethylenediaminetetraacetate in 70 or 85% methanol (for the MDTC and PIDTC reagents, respectively) at a flow-rate of 1.5 ml min^{-1} and monitoring at 258 nm. The injection volume used was 20 μl.

Degradation of Thiomersal

Samples of TM at a concentration of 0.01% (w/v) were submitted to degradation in Pyrex flasks in direct sunlight in the presence or absence of 0.5% (w/v) sodium chloride or under reflux in 0.5% sodium chloride either protected from light or in subdued room lighting. Samples were withdrawn at regular intervals for analysis.

RESULTS AND DISCUSSION

The addition of excess DTC-complexing reagents to a solution of TM leads to rapid ligand exchange to form either the EtHg–MDTC or the EtHg–PIDTC com-

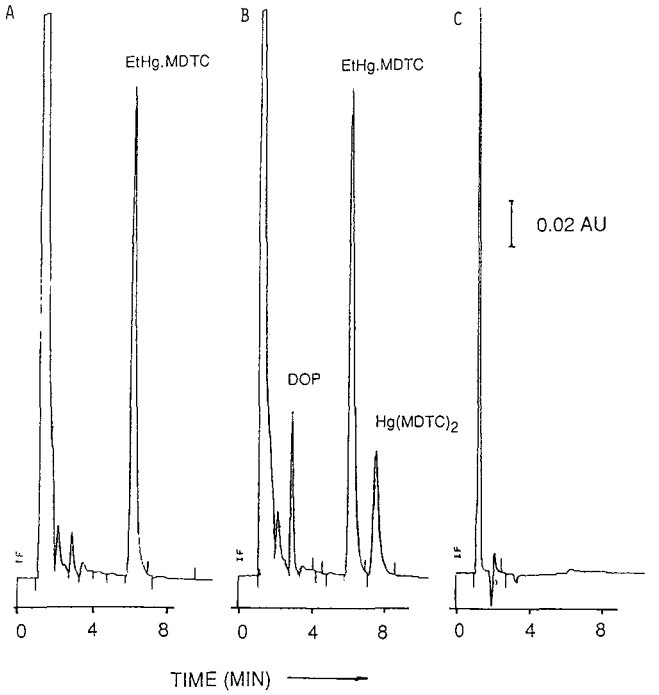

Fig. 2. Chromatograms of thiomersal assay using morpholinedithiocarbamate. (A) $6 \cdot 10^{-3}$% (w/v) thiomersal (1 ml) plus 0.06% (w/v) MDTC reagent (1 ml); (B) $6 \cdot 10^{-3}$% (w/v) thiomersal containing $1 \cdot 10^{-3}$% (w/v) mercuric acetate (1 ml) plus 0.06% (w/v) MDTC reagent (1 ml); (C) $6 \cdot 10^{-3}$% (w/v) thiomersal diluted 1:2 with acetonitrile. Peaks: 6.16 min, EtHg–MDTC; 7.48 min, $Hg(MDTC)_2$; 2.87 min, disulphide oxidation product (DOP) of derivatising agent. Excess MDTC thiosalicylic acid and dithiosalicylic acid elute at the void volume (1.5 min).

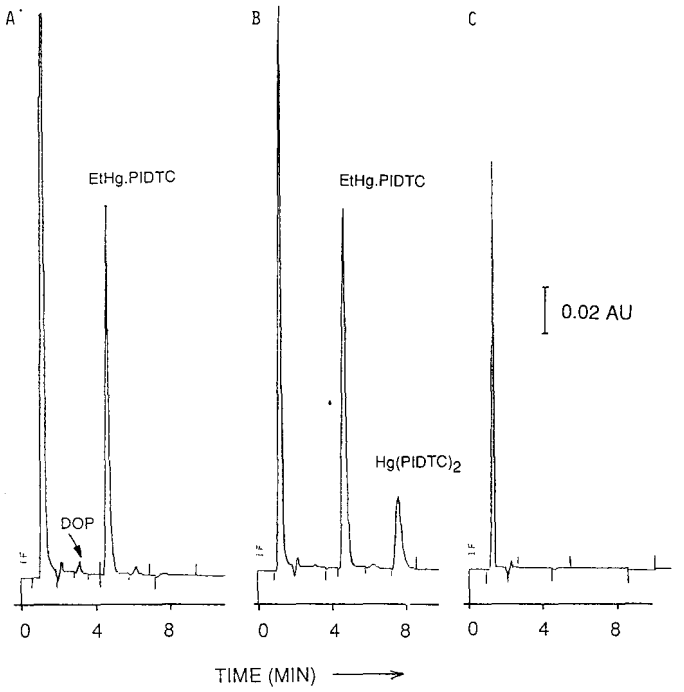

Fig. 3. Chromatograms of thiomersal assay using piperidinedithiocarbamate. (A) $6 \cdot 10^{-3}$% (w/v) thiomersal (1 ml) plus 0.06% (w/v) PIDTC reagent (1 ml); (B) $6 \cdot 10^{-3}$% (w/v) thiomersal containing $1 \cdot 10^{-3}$% (w/v) mercuric acetate (1 ml) plus 0.06% (w/v) PIDTC reagent (1 ml); (C) $6 \cdot 10^{-3}$% (w/v) thiomersal diluted 1:2 with acetonitrile. Peaks: 4.67 min, EtHg–PIDTC; 7.49 min, $Hg(PIDTC)_2$; 3.15 min, disulphide oxidation product (DOP) of derivatising agent; 6.08 min, unidentified contaminant of PIDTC agent which does not interfere with the assay. Excess PIDTC, thiosalicylic acid and dithiosalicylic acid elute at the void volume (1.5 min).

plexes (compound II, Fig. 1) which elute as clean peaks without interference (Figs. 2 and 3). The identity of the peaks ascribed to EtHg–MDTC, EtHg–PIDTC and TSA have been confirmed with an authentic sample of TSA and with the complexes formed between EtHg–Cl and MDTC and PIDTC reagents. Previous studies of the stability of TM have demonstrated the presence of elemental mercury as a major degradation product [4] and, under the chromatographic conditions employed in these assays, the $Hg(MDTC)_2$ and $Hg(PIDTC)_2$ complexes do not coelute with the peaks arising from the EtHg–DTC complexes (Figs. 2B and 3B). Also shown are the chromatographic traces obtained following dilution of TM with acetonitrile without the addition of derivatising agents (Figs. 2C and 3C). Disodium ethylenediaminetetraacetate has been added in low concentration to the HPLC mobile phases to minimise the possiblity of interference from other metal ions in the system [21].

Both reagents afford a linear relationship between area response and concentration which pass through the origin for the concentration range $0–1.2 \cdot 10^{-2}$% (w/v) of TM and allow quantitation of TM with reasonable precision (Table I). To show that the reaction proceeds rapidly to completion, studies have been undertaken to confirm that the peak-area responses of the EtHg–DTC complexes are indepen-

TABLE I

DATA FROM ASSAYS OF THIOMERSAL

Area response = slope × concentration (%, w/v) + intercept.

Compound	Slope	Concentration range (%, w/v)	Intercept	r	n	C.V. at $6 \cdot 10^{-3}$% (w/v) ($n = 6$) (%)
MDTC	$1.298 \cdot 10^{9}$	$0–1.2 \cdot 10^{-2}$	$7.73 \cdot 10^{4}$	0.9998	7	0.82
PIDTC	$1.316 \cdot 10^{9}$	$0–1.2 \cdot 10^{-2}$	$1.038 \cdot 10^{5}$	0.9998	7	0.65

TABLE II

AREA RESPONSE AS A FUNCTION OF THE TIME FOLLOWING MIXING

Data obtained using PIDTC reagent; thiomersal concentration was 0.01% (w/v).

Time following mixing (min)	Area response relative to that at 0.5 min
0.5	1.000
2.0	0.999
5.0	0.992
10.0	1.003

TABLE III

AREA RESPONSE AS A FUNCTION OF REAGENT CONCENTRATION

Data obtained using MDTC reagent; thiomersal concentration was 0.01% (w/v).

Concentration (%, w/v)	Response relative to that at 0.060% ((w/v)
0.010	0.989
0.020	1.005
0.060	1.000
0.100	0.996

dent of both complexing reagent concentration [0.01–0.1% (w/v) MDTC] (Table II) and time following mixing (0.5–10.0 min) (Table III). The complexation reaction occurs rapidly, the complex, once formed, is stable and the formation is independent of the concentration of complexing reagent [0.01–0.1% (w/v) corresponds to a 1.6–16 *M* excess of complexing agent]. For all subsequent studies a concentration of 0.06% (w/v) of complexing agent was used which corresponds to a ten-fold excess when TM is present at a concentration of 0.01% (w/v) in the sample.

To assess the assay, it has been compared with the previously reported HPLC method of Lam *et al.* [13] for samples degraded both thermally and photochemically

TABLE IV

COMPARISON OF LITERATURE HPLC ASSAY FOR THIOMERSAL WITH THIS ASSAY PROCEDURE

Time (h)	Percent remaining	
	Assay using PIDTC	Literature assay [13]
Under reflux in 0.5% sodium chloride in darkness		
0	100.0	100.0
5	99.6	98.3
20	99.2	97.8
24	100.2	96.8
Under reflux in 0.5% sodium chloride in subdued lighting		
0	100.0	100.0
5.5	98.3	95.1
20	95.7	85.1
25	92.9	78.5
Direct sunlight in plain solution		
0	100.0	100.0
0.25	96.3	96.7
0.5	89.6	88.5
1.0	72.6	71.0
2.0	37.6	30.3
Direct sunlight in 0.5% sodium chloride		
0	100.0	100.0
0.25	97.5	95.9
0.5	91.6	85.0
1.0	79.2	57.3
2.0	54.0	<1.0

(Table IV). A fully degraded sample of TM (direct sunlight for 12 h) when submitted to both methods of analysis afforded a flat baseline at the retention time of the EtHg–DTC complexes thus demonstrating that the degradation products do not interfere with either analytical method.

Refluxing in darkness in 0.5% sodium chloride indicated that the EtHg is stable thermally but the method of Lam *et al.* [13] demonstrated losses of TM. This is probably due to the slow atmospheric oxidation of the TSA to 2,2′-dithiosalicylic acid [4] altering the stoichiometry of the mixture of EtHg and TSA. When refluxed in subdued lighting losses of EtHg also occurred but at a considerably lower rate than indicated for TM by the literature method.

When TM solution was placed in direct sunlight destruction was rapid. Previous studies have suggested that halide ions promote the photochemical destruction of TM [22–24] and this is reflected in the results obtained using the HPLC method of Lam *et al.* [13]. However, when EtHg is measured using the DTC reagent it is demonstrated that the presence of the chloride enhances the stability of the EtHg ligand probably due to its tendency to complex with the organomercury ligand to form

EtHg–Cl [25,26]. The displaced TSA may then undergo more rapid decomposition by oxidation.

From these observations it is obvious that TM may be measured as EtHg and that the results obtained differ markedly from a more conventional method in which TM is quantitated directly. The availability of at least two alternative DTC-complexing agents makes possible the selection of reagents which may avoid interference from product components in more complex pharmaceutical formulations, and these assays may more correctly reflect the true antimicrobial activity of the TM in such formulations.

REFERENCES

1 R. G. Kimpton, *Aust. J. Hosp. Pharm.*, 17 (1987) 191.
2 B. J. Meakin and Z. M. Khammas, *J. Pharm. Pharmacol.*, 30 (1978) 52P.
3 S. N. Ibrahim, N. Stroud and B. J. Meakin, *J. Pharm. Pharmacol.*, 33 (1981) 7P.
4 M. J. Reader and C. B. Lines, *J. Pharm. Sci.*, 72 (1983) 1406.
5 N. E. Richardson, D. J. G. Davies, B. J. Meakin and D. A. Norton, *J. Pharm. Pharmacol.*, 29 (1977) 717.
6 C. M. McTaggart, J. Ganley, T. Eaves, S. E. Walker and M. J. Fell, *J. Pharm. Pharmacol.*, 31 (1979) 60P.
7 A. R. Neurath, *Cesk. Farm.*, 10 (1961) 75; *C.A.*, 61 (1964) 11854 g.
8 B. J. Meakin and Z. M. Khammas, *J. Pharm. Pharmacol.*, 31 (1979) 653.
9 W. Holak, *J. Assoc. Off. Anal. Chem.*, 66 (1983) 1203.
10 S. Pinzauti and M. Casini, *Farmaco, Ed. Prat.*, 35 (1980) 92; *Anal. Abstr.*, 39 (1980) 3E 66.
11 C. C. Fu and M. J. Sibley, *J. Pharm. Sci.*, 66 (1977) 738.
12 R. C. Meyer and L. B. Cohn, *J. Pharm. Sci.*, 67 (1978) 1636.
13 S. W. Lam, R. C. Meyer and L. T. Takahashi, *J. Parenter. Sci. Technol.*, 35 (1981) 262.
14 G. C. Visor, R. A. Kenley, J. S. Fleitman, D. A. Neu and I. W. Partridge, *Pharm. Res.*, 2 (1985) 73; *Anal. Abstr.*, 48 (1986) 3E 53.
15 A. R. Martin, in R. F. Doerge (Editor), *Wilson and Gisvold's Textbook of Organic, Medicinal and Pharmaceutical Chemistry*, Lippincott, Philadelphia, PA, 8th ed., p. 145.
16 V. M. Trikojus, *Nature (London)*, 158 (1946) 472.
17 D. J. G. Davies, Y. Anthony and B. J. Meakin, *Expo. Congr. Int. Technol. Pharm. 3rd*, 4 (1983) 238.
18 J. E. Parkin, *J. Chromatogr.*, 407 (1987) 389.
19 J. E. Parkin, *J. Chromatogr.*, 472 (1989) 401.
20 J. E. Parkin, *J. Chromatogr.*, 511 (1990) 233.
21 S. R. Hutchins, P. R. Haddad and S. Dilli, *J. Chromatogr.*, 252 (1982) 185.
22 K. Horworka, B. Horworka and R. Meyer, *Pharmazie*, 28 (1973) 136.
23 E. Lüdtke, H. Darsow and R. Pohloudek-Fabini, *Pharmazie*, 32 (1977) 99.
24 E. Lüdtke and R. Pohloudek-Fabini, *Pharmazie*, 32 (1977) 625.
25 R. B. Simpson, *J. Am. Chem. Soc.*, 83 (1961) 4711.
26 D. L. Rabenstein, *Acc. Chem. Res.*, 11 (1978) 100.

Journal of Chromatography, 542 (1991) 145–159
Elsevier Science Publishers B.V., Amsterdam

CHROM. 23 008

Determination of plant triacylglycerols using capillary gas chromatography, high-performance liquid chromatography and mass spectrometry

T. ŘEZANKA*
Institute of Microbiology, Czechoslovak Academy of Sciences, Videňská, 142 20 Prague 4 (Czechoslovakia)
and
P. MAREŠ[a]
Lipid Research Laboratory, IV Department of Medicine, Charles University, U Nemocnice 2, 128 08 Prague (Czechoslovakia)
(First received October 15th, 1990; revised manuscript received November 20th, 1990)

ABSTRACT

Molecular species of triglycerides (TG) were determined in plant fats and oils, both qualitatively and quantitatively, by means of capillary gas chromatography (CGC) on a "polarizable" column, reversed-phase C_{18} high-performance liquid chromatography (RP-HPLC) and desorption chemical ionization mass spectrometry (DCI-MS). For the qualitative analysis values of the equivalent carbon number (ECN) and equivalent chain length (ECL) were used for the identification of individual molecular species of TG by means of RP-HPLC or CGC. Plant oils including cocoa butter with smaller numbers of double bonds can be determined without any problems by means of CGC, RP-HPLC and DCI-MS. The determination by CGC and partially also RP-HPLC failed only with oils with either a complex distribution of chain lengths, *i.e.*, rape seed oil (high erucic acid) or a high unsaturation index (linseed oil and blackcurrant oil). However, with complementary results from all three methods it was possible to identify numerous molecular species of triglycerides in various plant oils.

INTRODUCTION

In the last decade, triglyceride (TG) analysis has become almost routine. Its rapid development has mainly been induced by requirements of the food industry, *i.e.*, determination of TG in cocoa butter or dietetic values of polyene TG, *e.g.*, in blackcurrant oil.

The use of reversed-phase high-performance liquid chromatography (RP-HPLC) for the determination of TG has recently been reviewed [1]. The determination of molecular species of TG from plant and animal fats and oils has been performed many times [2–19], mainly by RP-HPLC [2–15] and occasionally by capillary gas chromatography (CGC) [16–19]. Detection of TG is complicated as the ester bond

[a] Author deceased. This article was compiled from unpublished work of the late Dr. P. Mareš.

0021-9673/91/$03.50

absorbs only at low wavelengths, which limits the selection of a suitable mobile phase. All possible detection methods have been used, *i.e.*, refractive index [2–4,6,7], infrared, ultraviolet absorption [4,9,15], light scattering [8,12,14] and mass spectrometry (MS) [10]. Mass spectrometry appears to be the most suitable; however, the method is not commonly available. Therefore, we used UV detection at 222 nm; UV detectors are common and also facilitate the simple collection of individual fractions.

The use of a "polarizable" capillary column that has recently become commercially available is another method for the determination of TG. Determinations of TG on this column have been described several times [16–19], but an exact quantification of TG is not yet available. It has been stated that during CGC [16,19] and GC–MS [21], thermal degradation of polyene TG takes place, so that CGC is not suitable for plant oils such as linseed oil. Unfortunately, also in rape seed oil conclusive results could not be obtained. Therefore, in connection with previous work [22], we tried to quantify the losses. We were also surprised by the fact that data concerning the equivalent chain length (ECL) of individual triglycerides are scarce [23]. Therefore, we tried to determine ECL values at least roughly.

Direct chemical ionization (DCI) MS is a further method that can be used for the identification and quantification of TG. The method has also been applied several times [24,25] primarily to plant oils.

All the above methods have their advantages and shortcomings. However, suitable combinations can be used, with due caution, for the qualitative and quantitative determination of molecular species in any plant fats or oils.

EXPERIMENTAL[a]

Materials

Triglycerides [purified by thin-layer chromatography with silica gel H plates, 20 × 20 cm (Merck, Darmstadt, Germany), using hexane–diethyl ether (90:10)] (MMM, PPP, SSS, AAA, BeBeBe, LgLgLg, PoPoPo, OOO, GaGaGa, ErErEr, LLL, LnLnLn, MMP, PPM, SSM, SSP, OOP, PPO. OOS, SSO, POS) were obtained from Sigma (St. Louis, MO, U.S.A.). Mixed TG (SSA and SAA) were synthesized by interesterification between SSS and AAA using sodium methoxide as catalyst. The reaction was performed at 120°C for 20 min under vacuum with continuous stirring according to Ohshima *et al.* [21]. Analytical-reagent grade solvents were purchased from Lachema (Brno, Czechoslovakia) and Merck.

Plant oils and fats [cocoa butter, olive oil, palm oil, rape oil (high erucic acid), peanut oil, soyabean oil, sunflower oil and linseed oil] were obtained from a local pharmacy (in accordance with the Czechoslovak Pharmacopoeia No. 4) or isolated by cold pressing from plant seeds obtained from special drugstores [grape seeds, cotton seeds, blackcurrant seeds and corn (maize) seeds].

---

[a] Nomenclature: M = myristic acid, 14:0; P = palmitic acid, 16:0; Po = palmitoleic acid, 9–16:1; Mg = margaric acid, 17:0; S = stearic acid, 18:0; O = oleic acid, 9–18:1; L = linoleic acid, 9,12–18:2; Ln = linolenic acid, 9,12,15–18:3; A = arachidic acid, 20:0; Ga = gadoleic acid, 11–20:1; Be = behenic acid, 22:0; Er = erucic acid, 13–22:0; Lg = lignoceric acid, 24:0; SSS = triglyceride tristearin; PSO = triglyceride palmitostearoolein.

Capillary gas chromatography of intact triglycerides

Total TG were analysed on a fused-silica capillary column (25 m × 0.25 mm I.D.) with a 0.1-μm layer of triacylglycerol phase (TAP) (Chrompack, Middelburg, The Netherlands) with a flame ionization detector at 375°C. The carrier gas was hydrogen at 100 cm/s. The column temperature was programmed from 320 to 350°C at 1.5°C/min. An OCI-3 injector (SGE, Kensington, Australia) adapted to the "moveable on-column" injection technique [22] was used. A Model PU 4900 chromatographic system (Pye Unicam, Cambridge, U.K.) was used for the analysis.

High-performance liquid chromatography

HPLC was performed using a G-I gradient LC system (Shimadzu, Kyoto, Japan) with two LC-6A pumps (0.5 ml/min), an SCL-6A system controller, an SPD ultraviolet detector (222 nm), a SIL-1A sample injector and a C-R3A data processor. A 250 mm × 4 mm I.D. analytical column packed with SGX C_{18} (5-μm particles) was used (Tessek, Prague, Czechoslovakia). After injection of 1 μl of TG solution (5 mg/ml), a convex propionitrile (PCN)–methyl *tert.*-butyl ether (MTBE) gradient from 75:25 to 25:75 for 30 min was applied.

Mass spectrometry

A Finnigan MAT 90 mass spectrometer was used with an ion-source temperature of 200°C and a heating rate of 1°C/s. Ammonia (3×10^{-4} bar) was the most suitable reaction gas of three gases tested (methane, isobutane and ammonia). The equivalent carbon number (ECN) and ECL values were obtained using an IBM PC-compatible computer; ECL values were calculated by means of the Statgraphics program (Statistical Graphics, Rockville, MD, U.S.A.).

RESULTS AND DISCUSSION

Qualitative analysis

In principle, there are two possible methods for the identification of TG. The first consists in correlation between the chromatographic behaviour and structure of a compound, and the second in a direct identification of TG, either intact (*e.g.*, by means of GC–MS [21] or LC-MS [10]) or after transesterification by means of fatty acids [2,3,6,15]. TG in individual plant oils have so far been predominantly identified on the basis of data for TG content presented earlier [16] and on the basis of acid analysis obtained by transesterification of fractions resulting from RP-HPLC [2,3,6,9], and also according to values for quasi-molecular ions (QM^+) in DCI-MS [24,25].

Values of ECL, commonly used for the identification of fatty acids [26] and diglycerides [27], are useful for the identification of TG by CGC. However, for TG, ECL values were applied more than 10 years ago and only packed column was used [23]. Table I presents ECL values for more than 60 molecular species of TG, both synthetic (see Experimental) or contained in plant oils. The reproducibility was better than 0.03 unit. The ECL values of saturated TG were determined in agreement with fatty acids. For the determination of ECL values in other TG, the relationship between log (retention time) and number of carbon atoms was used. The values were calculated (and illustrated) using the Statgraphics program (see Experimental). As shown in Table I, TG differing by a single double bond can be separated, and in some instances

TABLE I

EQUIVALENT CHAIN LENGTH VALUES OF SOME TRIGLYCERIDES

TG	ECL[a]	TG	ECL[a]
MMM	42.00	OLL	55.26
MMP	44.00	OOLn	55.40
MPP	46.00	LLL	55.85
MMO	46.15	LLLn[b]	56.02[c]
PPP + MPS	48.00	LLnLn[b]	56.48[c]
MPO	48.15	Γ-LnLnLn	57.03[c]
MPL	48.45	α-LnLnLn	57.12[c]
PoPoPo	48.51	SSA	56.00
PPS	50.00	SOA + POBe	56.17
PPO	50.16	OOA + SOGa + POEr	56.24
MOO	50.21	OLA + SLGa + PLEr	56.61
PPoO	50.22	OLGa	56.85
PPL	50.47	LLA	57.11
PPoL	50.61	LLGa	57.27
MOL	50.64	SAA	58.00
MLL	51.10	PoLGa + SOBe + SSEr	58.17
PSS	52.00	PGaEr + SOEr + OOBe	58.24
PSO	52.17	PLLg + OOEr	58.51
POO	52.23	OLBe + SLEr	58.61
PSL	52.48	OLEr	58.86
PoOO	52.51	LLBe	59.11
POL	52.63	LLEr	59.28
PSLn	52.67	AAA	60.00
PoOL	52.87	SOLg	60.17
PLL	53.12	OOLg + PErEr + SGaEr	60.24
PoLL	53.25	OGaEr + GaGaGa	60.51
PLLn	53.50	LAEr + LGaBe + OLLg	60.61
SSS	54.00	LGaEr	60.86
SSO	54.17	LLLg	61.11
SOO	54.23	LnGaEr	61.40
SSL + OOO	54.50	SErEr	62.24
SOL	54.60	OErEr	62.51
OOL	54.85	LErEr	62.86
SLL	55.12	LnErEr	63.40

[a] Each value represents the mean ± S.D. (no greater than ±0.02) from five chromatograms.
[b] Triglycerides with α-Ln and Γ-Ln are not separated.
[c] This TG_{54} are eluted after SSA (TG_{56}).

even TG having identical numbers of carbon atoms and double bonds, *e.g.*, POO and PSL or OLL and OOLn. This is demonstrated in Fig. 1, in which the gas chromatogram of sunflower oil is shown.

Unfortunately, several critical pairs were identified, first SSL and OOO, as also has been reported elsewhere [16–18]. During the analysis of blackcurrant oil, TG with one or two positional isomers of 18:3 acid (*i.e.*, α-18:3 and Γ-18:3 acids) could not be separated. The third type of critical pairs was found in TG differing in the length of critical acyl groups bound to individual glycerol carbons, *e.g.*, $TG_{56:2}$ (type 011; AOO and/or SOGa and/or POEr). In these TG a similar phenomenon to that occurring in

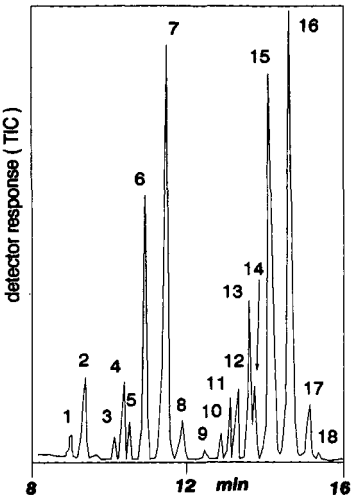

Fig. 1. Triacylglycerol profile (CGC) of soyabean oil. Peaks: 1 = POP, 2 = PLP, 3 = POS, 4 = POO, 5 = PLS, 6 = PLO, 7 = PLL, 8 = SOS, 10 = SOO, 11 = OOO + SLS, 12 = SLO, 13 = OOL, 14 = SLL, 15 = OLL, 16 = LLL, 17 = LLLn, 18 = probably LLnLn. TIC = total ion current.

wax esters [28] could be observed. The results given in Table I are summarized in Table II. The ECL values presented here thus make the identification of common plant oils possible, but unfortunately peak identification is only tentative.

For the analysis of TG by means of RP-HPLC, reproducible values of ECN, thanks mainly to studies by Podlaha and Töregård [29,30], make the identification of TG on the basis of their retention characteristics possible. In this work we utilized their program and equations [29,30] in order to calculate ECN values from our experimental data. The results are presented in Table III.

TABLE II

DIFFERENCES IN EQUIVALENT CHAIN LENGTH WITH CHANGES IN DOUBLE BOND(S) THROUGH THE CHANGE FROM LOWER TO HIGHER UNSATURATED FATTY ACIDS IN TRIGLYCERIDES

TG	Change in ECL[a]	TG	Change in ECL[a]
001	+0.16 ± 0.01 (6)	122	+1.27 ± 0.01 (2)
011	+0.22 ± 0.02 (6)	113	+1.40 ± 0.00 (3)
002	+0.47 ± 0.02 (4)	023	+1.50
111	+0.51 ± 0.00 (5)	222	+1.85
012	+0.62 ± 0.02 (5)	223	+2.02
003	+0.67	233	+2.48
112	+0.86 ± 0.01 (4)	333	+3.03[b]
022	+1.11 ± 0.01 (5)	333	+3.12[c]

[a] Value ± S.D. (number of determinations in parentheses).
[b] Γ-LnLnLn.
[c] α-LnLnLn.

TABLE III

EQUIVALENT CARBON NUMBER VALUES OF SOME TRIGLYCERIDES

TG	ECN[a]	TG	ECN[a]	TG	ECN[a]
α-LnLnLn	31.21	OOL	43.88	LLLg	49.21
β'-LnLnLn	31.52	PoOO	44.38	PSO	49.27
LLnLn	33.59	POL	44.40	LGaEr	49.37
LLLn	35.96	MOO	44.84	OOEr	49.93
OLnLn	37.56	PPL	45.00	PPS	50.00
PLnLn	38.09	MPO	45.38	OLBe	50.09
LLL	38.52	LLA	45.59	POEr	50.51
LnLnGa	39.38	OLGa	45.70	SOGa	50.60
PoLL	39.52	MPP	46.00	OOA	50.71
OLLn	39.53	OOO	46.26	SLA + PLBe	50.84
SLnLn	39.91	SOL	46.32	LErEr	51.22
MLL	40.08	POO	46.80	SSO + POA	51.23
PLLn	40.29	PSL	46.95	GaGaGa	51.72
LnLnEr	41.23	SSLn	47.07	OGaEr	51.75
OLL	41.40	PPO	47.33	PSS	52.00
PLL	41.91	LLBe	47.40	OOBe	52.68
OOLn	41.91	LnGaEr	47.40	SLBe + PLLg	52.78
PoOL	42.06	OLEr	47.55	OErEr	53.60
SLLn	42.11	PPP	48.00	SSS	54.00
MOL	42.46	OOGa	48.08	OOLg	54.63
PPoL	42.48	PLEr	48.10	SLLg	54.72
POLn	42.49	OLA	48.21	OAA + POLg	55.13
MPL	43.04	SLGa	48.29	SSA	56.00
LLGa	43.32	POGa	48.66	SOLg	57.09
MMO	43.42	SOO	48.75	SAA	58.00
SLL	43.74	SSL + PLA	48.90	AAA	60.00

[a] Each value represents the mean ± S.D. (no greater than ±0.01) from six chromatograms.

Even here critical pairs are formed, but different pairs to those in CGC are involved, *e.g.*, LLBe and LnGaEr have identical ECN, whereas their ECL differ by 2.29. Unfortunately the overlap of critical pairs and position isomers is more serious in RP-HPLC than in GC. The results are summarized in Tables IV and V, and a characteristic RP-HPLC record for soyabean oil is also shown in Fig. 2, indicating an excellent separation of individual TG.

TABLE IV

DIFFERENCES IN EQUIVALENT CARBON NUMBER WITH CHANGES OF TWO METHYLENE UNITS IN DIFFERENT GROUPS OF TRIGLYCERIDES

TG group	Change in ECN[a]
000 (by definition)	2.00
001 or 011 or 002	1.95 ± 0.01 (24)
012	1.91 ± 0.03 (8)
111 or 112 or 122 or 022 or 133 or 023 or 033	1.84 ± 0.04 (22)

[a] Value + S.D. (number of determinations in parentheses).

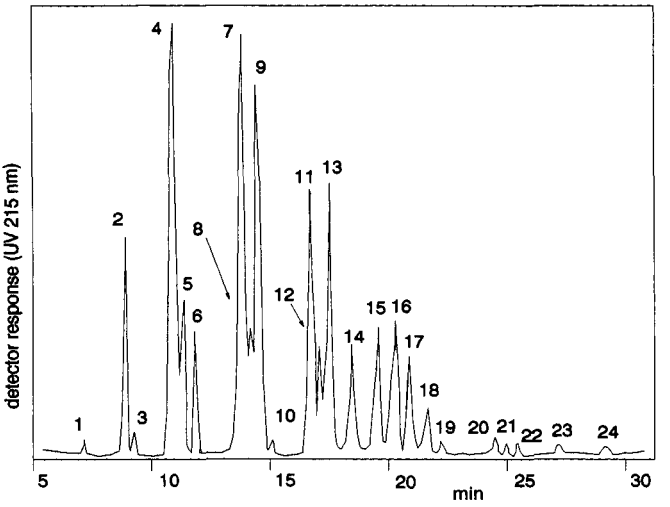

Fig. 2. RP-HPLC analysis of soyabean oil TGs using the gradient mode. Peaks: 1 = LLnLn 2 = LLLn, 3 = OLnLn, 4 = LLL, 5 = OLLn, 6 = PLLn, 7 = OLL, 8 = OOLn, 9 = PLL, 10 = POLn, 11 = OOL, 12 = SLL, 13 = POL, 14 = PPL, 15 = OOO, 16 = SOL, 17 = POO, 18 = PSL, 19 = PPO, 20 = SOO, 21 = SSL, 22 = PSO, 23 = PPS, 24 = SSO.

Podlaha and Töregård [29] gave a value of δ-ECN = 1.94 for an increase in carbon number of 2 in unsaturated TG, where as in this present study (see Table IV) an agreement with this value was only found in TG groups 001 or 011 or 002. For more unsaturated TG a lower δ-ECN value was found. However, Podlaha and Töregård [29] also obtained lower values, *e.g.*, for a change from PoPoPo to OOO a δ-ECN value of 1.89 for a single acid was reported and for a change from OOO to GaGaGa a δ-ECN value of 1.78 for a single acid. However, they did not include these results in their final table and did not even discuss them. In spite of this, we know that minor differences can be influenced by, *e.g.*, different columns, operating conditions, instruments and operators. The reproducibility of ECL values was better than 0.03 unit; for statistical values, see Tables III, IV and V.

The δ-ECN values presented in Tables IV and V are scattered. Even in this instance we are partially in agreement with literature data [29,30] where values higher by a maximum of 0.3 δ-ECN were presented, probably owing to the use of different chromatographic conditions. For instance, for a change of groups from 000 to 001 a difference of ECN between 2.99 and 3.32 was reported, compared with a value of 2.77 $\pm$ 0.05 in this work (see Table V). Almost the same holds for a change of groups from 111 to 112, where a value of δ-ECN of 2.38 was reported compared with a value of 2.36 $\pm$ 0.04 in this work. On the basis of Tables III–V and from a knowledge of the total fatty acid composition and the assumption of a random distribution, it is possible to predict relatively accurately the structure of individual peaks, without their time-consuming collection and without using the expensive LC–MS method.

However, for an accurate and error-free qualitative determination of molecular species, we also used the method DCI-MS (see also Fig. 3, in which a partial record of the QM^+ region of soyabean oil TG is presented) which makes it possible to determine

TABLE V

DIFFERENCES IN EQUIVALENT CHAIN LENGTH WITH CHANGES IN DOUBLE BOND(S) THROUGH THE CHANGE FROM LOWER TO HIGHER UNSATURATION (CARBON NUMBER CONSTANT)

Value ± S.D. (number of determinations in parentheses) (values only for one double bond in square brackets).

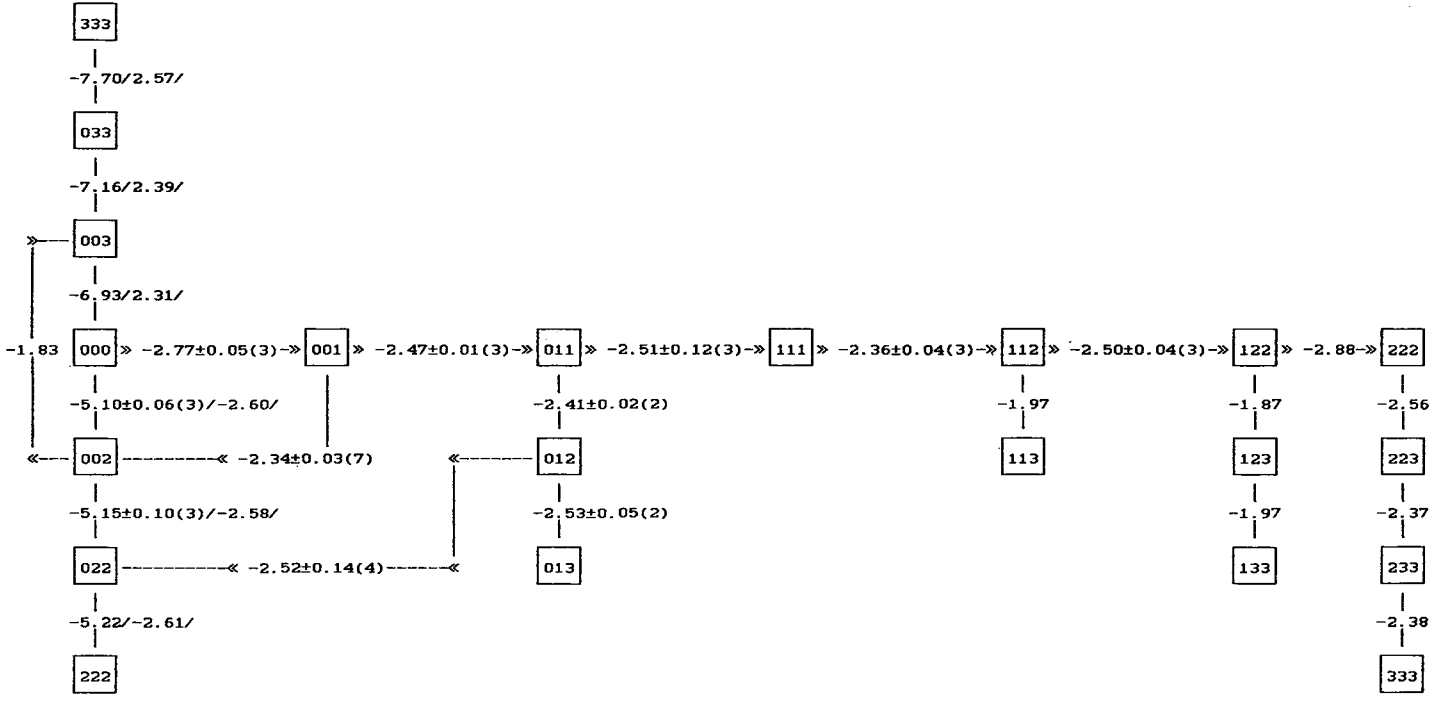

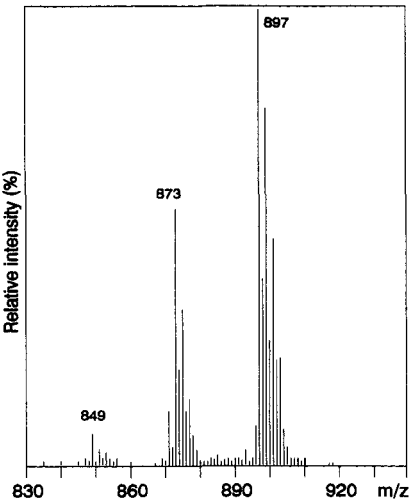

Fig. 3. DCI-MS of soyabean triacylglycerols. Only the range QM^+ is shown.

molecular weight of individual TG directly. This method was used for total mixture(s) of triglycerides. Therefore, this method does not confirm the stucture of TG in peak(s) but in the total mixture. Ammonia appeared to be the most suitable ionization gas, mainly owing to the formation of very intensive QM^+. The structures of TG presented in Tables VII–XI were thus verified by three independent methods.

TABLE VI

QUANTITATIVE YIELDS (RESPONSES) FROM A STANDARD MIXTURE OF TRIGLYCERIDES BY MEANS OF DIFFERENT TECHNIQUES (DETECTORS)

TG[a]	Relative response		
	CGC	RP-HPLC	DCI-MS
PPP	1.00	1.00	1.00
SSS	1.00	1.00	1.00
AAA	0.98	0.99	0.99
BeBeBe	0.90	0.99	0.99
LgLgLg	0.73	0.98	0.95
PoPoPo	1.00	1.00	1.00
OOO	0.98	0.99	0.99
GaGaGa	0.93	0.98	0.98
ErErEr	0.85	0.97	0.96
SSS	1.00	1.00	1.00
SSO	1.00	1.01	0.99
SOO	1.00	1.04	0.97
OOO	0.98	1.08	0.95
LLL	0.83	1.17	0.92
LnLnLn	0.14	1.74	0.86

[a] Intact TG were mixed in equal amounts (by weight).

TABLE VII

RELATIVE COMPOSITION (%) OF TRIGLYCERIDES FROM COCOA BUTTER, CORN, COTTON AND GRAPE OIL

For experimental conditions, see Experimental.

TG	Cocoa			Corn			Cotton			Grape		
	GC	LC	MS	GC	LC	MS	GC	LC	MS	GC	LC	MS
MPL	0	0	0	0	0	0	1.7	0.6	1.1	0	0	0
MPO	0.6	0	0.5	0	0	0	0.6	0	0.5	0	0	0
PPP	0.6	0	0.6	0	0	0	0.5	0	0.4	0	0	0
MLL	0	0	0	0	0	0	1.1	0	0.7	0	0	0
PPoL + MOL	0	0	0	0	0	0	0.8	0	0.4	0	0	0
PPL	1.7	3.3	2.1	0	0	0	8.1	7.7	7.9	0.8	0.3	0.6
PPO	23.3	18.0	19.7	3.9	1.5	2.7	6.2	1.5	3.1	0.5	0	0.3
PPS	0.8	0	0.7	1.9	0.4	1.2	0.1	0	0.1	0	0	0
PMgO	0.6	0	0.5	0	0.2	0.1	0	0	0	0	0	0
PPLn	0	0	0	0	0.1	0.1	0	1.4	0.5	0	0	0
PoLL	0	0	0	0	0	0	0.1	0.3	0.1	0	0	0
PLL + PoOL	0	0	0	17.1	16.4	16.8	20.8	24.5	21.3	15.7	17.6	16.1
POL	0.3	1.0	0.9	13.8	10.4	12.1	9.6	10.9	10.0	16.1	15.5	15.2
POO	2.5	6.3	"[a]	4.0	2.5	"	4.4	2.0	4.9	1.8	1.4	1.9
PSL	3.0	5.1	7.1	1.9	2.8	5.6	2.3	1.1	"	0.4	0.1	"
PSO	36.0	30.8	33.6	0.5	0.1	0.3	1.2	0.5	0.8	0.3	0.3	0.2
PSS	1.4	0	1.3	0	0	0	0	0	0	0	0	0
MgSO	0.5	0	0.5	0	0	0	0	0	0	0	0	0
LLLn	0	0	0	0.3	1.2	0.8	0	1.5	0.4	0	0	0
LLL	0	0	0	17.7	25.6	22.3	15.9	23.2	17.1	30.1	32.6	30.8
OLLn	0	0	0	0	0.6	"	0	0	0	0	0	0
OLL	0	0	0	18.8	22.5	21.4	14.1	15.4	14.8	18.9	19.1	18.7
OOLn	0	0	0	0	0.3	"	0	0	0	0	0	0
OOL	0	0	0	11.2	10.9	13.0	6.1	5.1	6.4	4.2	3.4	12.3
SLL	0	0	0	2.1	1.9	"	1.7	1.1	"	7.1	6.9	"
OOO[b]	1.3	1.7	3.5	4.1	3.1	4.9	2.6	1.6	3.1	0	0	0
SOL	0.3	1.3	"	1.7	1.2	"	1.3	0.9	"	2.4	1.9	3.5
SSL[b]	?	1.6	?	0	0	0	0	0	0	0.9	0.7	"
SOO	2.6	7.9	5.1	0.7	0.3	0.6	0.6	0.7	0.6	0.6	0.2	0.3
SSO	22.4	22.0	22.0	0.3	0	0.1	0.2	0	0.1	0.2	0	0
SSS	0.7	0	0.6	0	0	0	0	0	0	0	0	0
SLA	0.1	0	0.3	0	0	0	0	0	0	0	0	0
OOA	0.3	1.0	"	0	0	0	0	0	0	0	0	0
SOA	0.9	0	0.8	0	0	0	0	0	0	0	0	0
OAA	0.2	0	0.2	0	0	0	0	0	0	0	0	0

[a] The symbol " expresses the sum of the value above and in this line because the TG have the equal M.W. (*e.g.*, PLL and POLn have the same M.W. and in DCI-MS they show QM^+ with the same value).
[b] Peaks are not separated by CGC.

Quantitative analysis

As during the analysis of standards the responses of the detectors in all three methods were very similar up to triglyceride 222 (LLL), in a further analysis the response of the detectors was used directly without any calibration (Table VI). It

TABLE VIII

RELATIVE COMPOSITION (%) OF TRIGLYCERIDES FROM OLIVE, PALM, SOYABEAN AND SUNFLOWER OIL

For experimental conditions, see Experimental.

TG	Olive			Palm			Soyabean			Sunflower		
	GC	LC	MS	GC	LC	MS	GC	LC	MS	GC	LC	MS
MMO	0	0	0	1.0	0	0.5	0	0	0	0	0	0
MPP	0	0	0	0.6	0	0.3	0	0	0	0	0	0
MLO	0	0	0	0.3	0.6	0.4	0	0	0	0	0	0
MPL	0	0	0	0.4	0.6	0.5	0	0	0	0	0	0
MPO	0	0	0	2.8	0.5	1.4	0	0	0	0	0	0
PPP	0	0.4	0.4	11.6	7.1	9.0	0	0	0	0	0	0
MOO	0	0	0	0.6	0	0.3	0	0	0	0	0	0
PPL	1.4	2.6	1.4	10.3	10.7	10.5	3.9	1.4	1.2	3.8	1.2	3.3
PPO	7.3	4.2	5.3	27.0	24.0	26.3	1.2	0.2	0.4	1.0	0	0.7
PPS	0	0	0	0.5	0.2	0.4	0	0.2	0.2	0	0	0
PLLn	0	0	0	0	0	0	1.6	2.6	2.0	0	0	0
PLL + PoO	0.4	2.4	1.8	1.6	4.1	3.1	17.1	13.8	14.6	15.8	16.8	15.9
POLn	0	0	0	0	0	0	0	0.1	"	0	0	0
PoOO	7.8	2.1	9.0	0	0	0	0	0	0	0	0	0
POL	"[a]	8.2	"	8.1	10.8	9.8	12.1	10.7	8.8	6.9	6.0	6.1
POO	28.3	20.1	24.4	19.2	22.1	20.9	4.2	1.9	2.8	3.2	0.6	4.0
PSL	0	0	0	2.5	2.4	2.4	2.8	1.0	"	3.9	1.0	"
PSO	1.9	1.3	1.6	5.7	4.9	5.2	1.0	0.4	0.2	1.1	0.6	0.8
PSS	0	0	0	0.3	0	0.2	0	0	0	0	0	0
LLnLn	0	0	0	0	0	0	0	0.4	0.4	0	0	0
LLLn	0	0	0	0	0	0	2.5	8.4	7.4	0	0	0
OLnLn	0	0	0	0	0	0	0	0.4	"	0	0	0
LLL	0	1.0	0.6	0	0	0	16.5	16.8	24.5	22.8	28.0	26.1
OLLn	0	2.8	1.3	0	0	0	0	4.6	"	0	0	0
OLL	1.5	3.7	2.9	0.4	1.0	0.7	15.4	15.0	19.4	22.2	23.1	22.3
OOLn	0.6	0	"	0	0	0	0	1.9	"	0	0	0
OOL	0	0	0	1.0	2.6	1.9	8.7	10.1	12.4	5.3	7.5	15.0
SLL	0	0	0	0	0.6	0.3	3.9	4.0	"	7.9	10.2	"
OOO[b]	32.5	31.6	32.0	2.4	4.7	3.0	4.5	2.3	4.8	0.9	1.4	4.1
SOL	0	0	0	0.6	0.5	0.5	2.3	2.9	"	3.2	2.4	"
SSL[b]	0	0	0	0	0	0	?	0.2	"	0.6	0.4	1.7
SOO	4.9	4.9	4.9	2.0	1.7	1.8	0	0.5	0.6	1.4	0.8	"
SSO	0.4	0.7	0.6	0.7	0	0.4	1.3	0.2	0.3	0	0	0
OOGa	0.4	0	0.3	0	0	0	0	0	0	0	0	0
OOA	0.5	0	0.2	0.2	0	0.1	0	0	0	0	0	0
SOA	0	0	0	0.2	0	0.1	0	0	0	0	0	0

[a] See Table VII.

[b] Peaks are not separated by CGC.

follows from Tables VII–XI that the values obtained by means of the three independent methods are often different; for an explanation, see below.

Quantification by CGC, RP-HPLC and DCI-MS failed with three of the above twelve oils, especially linseed oil and blackcurrant oil. In these two oils problems with quantification of individual molecular species were clearly apparent. It follows from

TABLE IX

RELATIVE COMPOSITION (%) OF TRIGLYCERIDES FROM BLACKCURRANT OIL

TG	CGC	RP-HPLC	DCI-MS
PLLn	0.2	4.3	4.4
PLL	12.1	2.7	6.5
POLn	13.2	3.4	"[a]
POL	37.1	1.7	1.3
LnLn?[b]	0	0.9	0.8
LnLnLn	0	3.0	11.7
LnLnLn[c]	0	9.8	"
LLnLn[c]	0	20.2	20.5
LLLn[c]	0	21.8	25.5
OLnLn[c]	0	3.3	"
LLL	0.1	11.9	20.1
OLLn[b]	0	6.1	"
SLnLn[b]	0	1.6	"
OLL	1.3	2.2	5.3
OOLn[b]	2.1	3.0	"
OOL	13.8	1.8	3.9
SLL	20.1	2.3	"

[a] See Table VII.
[b] Probably TG with 18:4w3 acid.
[c] Indistinguishable between 18:3w3 and 18:3w6 acids in TG.

Table IX and even better from Table XI that the results obtained by determination by CGC and by RP-HPLC are contradictory, sometimes differing by two orders of magnitude. Only the DCI-MS method is reasonably satisfactory. As reported by Geeraert [20], in polyene TG discrimination occurs. However, in contrast to his study, we were able to analyse commonly available plant oils under optimum conditions

TABLE X

RELATIVE COMPOSITION (%) OF TRIGLYCERIDES FROM LINSEED OIL

TG	CGC	RP-HPLC	DCI-MS
PLnLn	5.2	4.2	4.3
PLLn	4.6	3.1	3.2
PLL	5.6	0.6	0.7
POL	10.7	0.8	1.0
LnLnLn	8.6	50.7	49.3
LLnLn	5.8	19.2	18.9
LLLn	5.9	3.6	13.0
OLnLn	12.9	9.2	"[a]
LLL	4.8	2.4	5.6
OLLn	7.6	3.2	"
OLL	8.1	1.4	2.9
SLLn	4.2	0.8	"
OOL	5.6	0.5	0.8
OOO	10.4	0.3	0.3

[a] See Table VII.

TABLE XI

RELATIVE COMPOSITION (%) OF TRIGLYCERIDES FROM PEANUT OIL

TG	CGC	RP-HPLC	DCI-MS
PPL	3.9	2.0	3.1
PPO	4.6	1.2	2.8
PLL	5.3	6.1	5.4
POL	9.9	11.6	10.3
POO	10.5	7.6	10.7
PSL	2.5	0.8	"[a]
PSO	1.9	0.9	1.4
LLL	1.7	3.6	3.0
OLL	9.6	17.5	14.5
OLO	10.8	17.3[b]	15.9
SLL	0.9	1.2	"
OOO	12.4[c]	8.1	13.6
PLGa	0	1.1[d]	"
SOL	5.6	2.1	"
POGa	0	1.2[e]	5.1
SOO	3.8	3.3	"
PLA + SSL	?[c]	0.9	"
POA + SSO	1.0	0.8	1.1
LLGa	0.4	?[b]	"
OLGa	1.0	0.6	0.9
LLA	0.5	?[d]	"
OOGa	1.5	0.5	2.1
OLA	1.4[f]	?[e]	"
OOA	1.6	2.5	2.0
SLA + PLBe	?[f]	0.8	"
SOA + POBe	1.6	0.7	0.9
LLBe	0.8	1.5	1.3
OLBe	1.8	1.6	1.6
OOBe	2.3	1.2	1.7
SLBe + PLLg	0.3	0.5	"
SOBe + POLg	0.6	0.5	0.5
LLLg	0.2	0.6	0.4
OLLg	0.5	0.8	0.7
OOLg	0.8	0.7	0.8
SLLg	0	0.2	"
SOLg	0.3	0	0.2

[a] See Table VII.
[b–f] Peaks are not separated by CGC and/or RP-HPLC.

without calibration. The results obtained were within the range of experimental error and within the range of quantitative differentiation caused by cultivation, treatment or storage.

A specific problem occurred with rape seed (high erucic acid) oil. Of the oils investigated, the distribution of chain lengths is most pronounced here (from TG_{50} to TG_{62}). In addition, TG with seven double bonds, *e.g.*, LnLnEr are present. Owing to the large number of fatty acids present (P, S, A, Be, Lg, O, Ga, Er, L and Ln), individual molecular species are not separated, being eluted in a single peak, *e.g.*, in

CGC as POEr + SOGa + OOA (and probably also others) and in RP-HPLC as LGaGa + POO + SSLn + OLEr (and others). Also in DCI-MS there is one QM^+, *e.g.*, of *m/z* 930, in several molecular species of TG. When scanning the region *m/z* 200–300, *i.e.*, for values that are manifested by ions of the types RCO^+ and $(RCO - 1)^+$, we detected ions corresponding to the acids P, S, A, O, Ga, Er and L. By combination of QM^+ (*m/z* 930) and the above-mentioned acids, the presence of, *e.g.*, molecular species PLEr, SLGa, OLA and OOGa can be assumed, positions and other isomers naturally not being considered.

From the above data, it can be clearly concluded that for the identification of such complicated mixtures of TG, a combination of two, better three, methods, must be used. For determination a much more effective column (with a higher number of plates) must be used both in CGC and particularly in RP-HPLC. When using CGC thermal dégradation causes a limitation (polyene TG and TG with more than 63 carbon atoms).

When using RP-HPLC a value of 45 000 plates for SSS was obtained (the manufacturer stated a value of 50 000 plates for toluene as a reference sample), but even this number was not sufficient for a complete separation of some critical pairs.

For the above reasons we do not present a table of quantitative results for rape seed oil as the correlation among values obtained by means of CGC, RP-HPLC and DCI-MS is very poor. Therefore, we also do not present ECN and ECL values.

CONCLUSIONS

It can be concluded that the main contribution to qualitative analysis is represented by the determination of ECL and ECN values (see Tables I and III), and particularly their differences (Tables II, IV and V). These δ-ECN and δ-ECL values make it possible to identify almost any plant fat or oil. The use of a combination of three independent techniques, *i.e.*, CGC, RP-HPLC and DCI-MS, made it possible to identify more than 80 molecular species of triglycerides in a dozen plant oils.

In quantitative analysis, the relative responses of the individual detectors, *i.e.*, of the flame ionization detector in CGC, UV detector in RP-HPLC and mass spectrometer in DCI-MS, were investigated with model mixtures. By optimizing the analytical conditions it was possible to avoid correction factors up to TG of the group 222 (*i.e.*, LLL), so that individual molecular species of TG could be detected in nine common oils without any problems. Certain difficulties occurred during the analysis of linseed, blackcurrant and rape seed oils. It can be concluded that by means of a combination of CGC, RP-HPLC and DCI-MS the qualitative and quantitative analysis of most plant oils and fats is feasible.

ACKNOWLEDGEMENTS

The authors thank Drs. J. Novák and J. Zima for the DCI-MS measurements.

REFERENCES

1 M. J. Wojtusik, P. R. Brown and J. G. Turcotte, *Chem. Rev.*, 89 (1989) 397.
2 G. Sempore and J. Bezard, *J. Chromatogr.*, 366 (1986) 261.

3 L. J. R. Barron, M. V. Celaá, G. Santa-Maria and N. Corzo, *Chromatographia*, 25 (1988) 609.
4 M. W. Dong and J. L. DiCesare, *J. Am. Oil Chem. Soc.*, 60 (1983) 788.
5 B. Herslöf and G. Kindmark, *Lipids*, 20 (1985) 783.
6 B. Petersson, O. Podlaha and B. Töregård, *J. Am. Oil Chem. Soc.*, 58 (1981) 1005.
7 E. Geeraert and D. De Schepper, *J. High Resolut. Chromatogr. Chromatogr. Commun.*, 6 (1983) 123.
8 A. J. Palmer and F. J. Palmer, *J. Chromatogr.*, 465 (1989) 369.
9 J. A. Singleton and H. E. Pattee, *J. Am. Oil Chem. Soc.*, 64 (1987) 534.
10 L. Marai, J. J. Myher and A. Kuksis, *Can. J. Biochem. Cell Biol.*, 61 (1983) 840.
11 T. Grossberger and E. Rothschild, *LC · GC*, 7 (1989) 437.
12 J. L. Perrin, A. Prevot, H. Traitler and U. Bracco, *Rev. Fr. Corps Gras*, 34 (1987) 221.
13 C. Merritt, M. Vajdi, S. G. Kayser, J. W. Halliday and M. L. Bazinet, *J. Am. Oil Chem. Soc.*, 59 (1982) 422.
14 A. Stolyhwo, H. Colin and G. Guiochon, *Anal. Chem.*, 57 (1985) 1342.
15 L. J. R. Barron and G. Şanta-Maria, *Chromatographia*, 28 (1989) 183.
16 E. Geeraert and P. Sandra, *J. High Resolut. Chromatogr. Chromatogr. Commun.*, 8 (1985) 415.
17 J. V. Hinsfaw and W. Seferovic, *J. High Resolut. Chromatogr. Chromatogr. Commun.*, 9 (1986) 731.
18 E. Geeraert and P. Sandra, *J. Am. Oil Chem. Soc.*, 64 (1987) 100.
19 H. J. Chaves Das Neves and A. M. P. Vasconcelos, *J. High Resolut. Chromatogr.*, 12 (1989) 226.
20 E. Geeraert, in A. Kuksis (Editor), *Chromatography of Lipids in Biomedical Research and Clinical Diagnosis*, Elsevier, Amsterdam, 1987, p. 48.
21 T. Ohshima, H. S. Yoon and C. Koizumi, *Lipids*, 24 (1989) 535.
22 P. Mareš, T. Řezanka and M. Novák, unpublished results.
23 T. Takagi and Y. Itabashi, *Lipids*, 12 (1967) 1062.
24 T. Řezanka, P. Mareš, P. Hušek and M. Podojil, *J. Chromatogr.*, 355 (1986) 265.
25 E. Schulte, M. Höhn and U. Rapp, *Fresenius' Z. Anal. Chem.*, 307 (1981) 115.
26 R. G. Ackman, in H. K. Mangold, G. Zweig and J. Sherma (Editors), *CRC Handbook of Chromatography, Lipids*, Vol. I, CRC Press, Boca Raton, FL, 1986, p. 95.
27 A. Kuksis, in H. K. Mangold, G. Zweig and J. Sherma (Editors), *CRC Handbook of Chromatography, Lipids*, Vol. I, CRC Press, Boca Raton, FL, 1986, p. 381.
28 T. Řezanka and M. Podojil, *J. Chromatogr.*, 362 (1986) 399.
29 O. Podlaha and B. Töregård, *J. Chromatogr.*, 482 (1989) 215.
30 O. Podlaha and B. Töregård, *J. High Resolut. Chromatogr. Chromatogr. Commun.*, 5 (1982) 553.

Journal of Chromatography, 542 (1991) 161–172
Elsevier Science Publishers B.V., Amsterdam

CHROM. 23 005

Gas chromatographic separation of stereoisomeric esters of α-amino acids and α-alkyl-α-amino acids on chiral stationary phases

HANS BRÜCKNER* and MATTHIAS LANGER[a]
Institute of Food Technology, University of Hohenheim, W-7000 Stuttgart 70 (Germany)
(First received September 5th, 1990; revised manuscript received November 22nd, 1990)

ABSTRACT

The separations of stereoisomers of (a) N-pentafluoropropionyl (PFP)-(*R,S*)-α-amino acid (AA) (*R,S*)-alkyl esters and (b) N-trifluoroacetyl (TFA)-(*R,S*)-α-alkyl-α-amino acid (AAA) (*R,S*)-α-alkyl esters were investigated by capillary gas chromatography on Chirasil-L-Val, and Chirasil-D-Val, respectively. The order of elution of the four possible stereoisomers (a) was found to be *R–S* < *R–R* < *S–R* < *S–S* for PFP-(*R,S*)-AA 2-butyl and 2-octyl esters, and *R–S* < *S–R* < *R–R* < *S–S* for PFP-(*R,S*)-AA 3-methyl-2-butyl esters (the first letter in the diastereomers refers to the configuration of the amino acid and the second to the configuration of the alcohol). For (b) it was found that the *S–S* diastereomers eluted first and the *R–S* diastereomers last (fourth) from the column. In the few instances in (b) in which all four stereoisomers were separated, with the TFA-(*R,S*)-α-butyl-Ala (*R*)-2-butyl esters the *S–R* diastereomer eluted second and the *R–R* diastereomer eluted third whereas with the TFA-(*R,S*)-α-butyl-Ala (*R*)-2-octyl esters and TFA-(*R,S*)-α-methylleucine (*R*)-2-octyl esters, the *R–R* diastereomers eluted second and the *S–R* diastereomers third. Further, the temperature dependence of the elution order of the four stereoisomers of PFP-(*R,S*)-Ala (*R,S*)-2-octyl esters on Chirasil-D-Val showed that the *S–R* diastereomer eluted first and the *R–R* diastereomer last (fourth) at all temperatures; however, at 125°C *S–S* eluted before *R–S* and at 150°C *S–S* and *R–S* eluted together, whereas at 175°C *R–S* eluted before *S–S*. The order of elution of stereoisomeric derivatives of AA and AAA from chiral stationary phases is rationalized by superimposed diastereomeric and enantiomeric resolution effects on the chiral stationary phase. That the chiral alcohol contributes to the resolution of stereoisomeric N-acyl-(*R,S*)-AA (*R,S*)-2-alkyl esters on a chiral phase is demonstrated by the resolution of enantiomeric TFA-Gly (*R*)-alkyl esters and TFA-Gly (*S*)-alkyl esters on Chirasil-D-Val.

INTRODUCTION

For the separation of enantiomers of volatile amino acid (AA) derivatives by gas chromatography (GC), a number of chiral stationary phases have been described [1–9]. In order to increase the thermal stability of the stationary phases, Bayer *et al.* [10] coupled L-Val *tert.*-butylamide as a chiral selector to a copolymer of dimethylpolysiloxane together with (2-carboxypropyl)methylsiloxane and named this phase

[a] M. L. is also at the Untersuchungsinstitut des Sanitätsdienstes der Bundeswehr, W-7000 Stuttgart 50, Germany.

0021-9673/91/$03.50

Chirasil-L-Val. Saeed *et al.* [11,12] synthesized chiral phases by coupling L-Val *tert.*-butylamide to modified polycyanopropylmethyl phenylmethyl silicone, and König and Benecke [13] coupled benzyloxycarbonyl(Z)-L-valine and Z-L-leucine to functionalized OV-225.

Optical isomers of AA are also separable as diastereomeric derivatives [14–17], preferably diastereomeric N-acyl AA alkyl esters, on non-chiral stationary phases such as alkylpolysiloxanes. For the determination of AA enantiomers as diastereomeric esters, derivatization with amino alcohols of the highest optical purity is essential in order to achieve satisfactory accuracy, as enantiomeric AA esters are not resolved on non-chiral columns. It was shown, however, that the enantiomeric and the diastereomeric approach can be combined by use of suitable chiral stationary phases and that mixtures of the two enantiomeric and two diastereomeric esters (*i.e.*, four stereoisomers), as obtained by esterification of (*R,S*)-AA by (*R,S*)-alkanols, are completely separable by capillary GC.

Using this approach, König [18,19] resolved the four possible stereoisomeric N-pentafluoropropionyl (PFP)-DL-Leu DL-3-methyl-2-butyl esters on the chiral phases N-trifluoroacetyl (TFA)-L-phenylalanyl-L-aspartic acid bis(cyclohexyl ester) (TFA-L-Phe-L-Asp(OcHex)-OcHex) and TFA-DL-Val (±)-3-methyl-2-butyl esters as well as PFP-DL-Leu (±)-3-methyl-2-butyl esters on the chiral phase XE-60-L-Val-(*S*)-α-phenylethylamide [XE-60-L-Val-(*S*)-PEA]. König determined and rationalized [18] the retention times of the isomers as D/*S*(+) < L/*R*(−) < D/*R*(−) < L/*S*(+) (*i.e.*, *R–S* < *S–R* < *R–R* < *S–S*; the first letter refers to the configuration of the AA). Liu [20] separated the isomers of TFA-DL-Leu (and Ala) (±)-2-butyl esters on the chiral stationary phase Chirasil-L-Val and used the method for the determination of the enantomeric purity of a sample of L-Ala. He found the retention times to increase in the order D–D < D–L < L–L < L–D (*i.e.*, R–S < R–R < S–R < S–S). This is the same elution order for the diastereomeric pairs *R–S* and *S–S* and the opposite elution order for the diastereomeric pairs *R–R* and *S–R* on an L-stationary phase.

The separation of diastereomeric N-acyl-AA esters on chiral stationary phases had been demonstrated for the few AA and chiral alcohols mentioned above; the elution orders of the *S–R* and *R–R* diastereomers of 2-butyl esters on Chirasil-L-Val were found to be the opposite of those of the 3-methyl-2-butyl esters on TFA-L-Phe-L-Asp(OcHex)-OcHex and XE-60-L-Val-(*S*)-α-PEA. No satisfactory explanation has been given for this phenomenon so far, nor has the a possible contribution of the chiral alcohol in the diastereomeric N-acyl-AA esters or a possible temperature dependence of the elution order of stereoisomers been discussed [18–20]. We have therefore determined the resolution and elution order of the stereoisomers of a series of N-PFP-(*R,S*)-AA (*R,S*)-2-alkyl esters on Chirasil-Val. Moreover, in continuation of our work on the chiral resolution of diastereomeric esters of non-protein α-alkyl-α-amino acids (AAA) [21–24] we have investigated the question of whether the stereoisomers of various TFA-(*R,S*)-AAA (*R,S*)-2-alkyl esters are resolvable on Chirasil-Val.

EXPERIMENTAL

Gas chromatography

GC was carried out on a Carlo Erba Model HRGC 5160 gas chromatograph with a flame ionization detector, a Shimadzu C-R3A integrator and (a) a Chirasil-L-Val column (25 m × 0.25 mm I.D.; Macherey–Nagel. Düren, Germany) or (b) a Chirasil-D-Val fused-silica capillary column (25 m × 0.25 mm I.D.; made by G. J. Nicholson, University of Tübingen). The carrier gas was hydrogen at 50 kPa (0.5 bar), the splitting ratio *ca.* 1:30 and the injector and detector temperatures 250°C with both columns.

α-Amino acids, α-alkyl-α-amino acids and reagents

DL-and L-α-amino acids (AA) were purchased from Fluka (Buchs, Switzerland). The (*R,S*)-α-alkyl-α-amino acids (AAA) α-amino-*n*-butyric acid (Abu), norvaline (Nva), norleucine (Nle) and α-aminooctanoic acid (Aoc) were synthesized in our laboratory according to the Strecker procedure, and optically pure and enantiomerically enriched AAA were obtained by enzymic digestion with acylase I or carboxypeptidase A [25]. AAA ar considered as being formally derived from protein α-amino acids by C^{α}-hydrogen substitution by alkyl groups [24]: α-Ethylalanine, "isovaline" (α-Et-Ala), α-butylalanine (α-But-Ala), and α-methylleucine (α-Me-Leu).

(*R,S*)- and (*S*)(+)-2-butanol, (*R,S*)- and (*S*)(+)-2-octanol and (*R,S*)-3-methyl-2-butanol were purchased from Fluka and (*S*)(+)-3-methyl-2-butanol from Chemical Dynamics (South Plainfield, NJ, U.S.A.). Esterification of AA and AAA with acetyl chloride and the respective alcohol and acylation with pentafluoropropionic anhydride were carried out as described previously [24]. The elution orders of amino acid stereoisomers were determined with the help of enantiomerically enriched AA (AAA) and 2-alkanols.

RESULTS AND DISCUSSION

Separation of N-PFP-(R,S)-2-alkylesters of α-amino acids on Chirasil-L-Val

Sections of selected gas chromatograms, taken on Chirasil-L-Val, of the separation of PFP-(*R,S*)-α-amino acid (*R,S*)-alkyl esters are shown in Fig. 1a–l. Net retention times at isothermal temperatures, resolution factors α and the number of stereoisomers resolved are shown in Table I. With the PFP-(*R,S*)-AA (*R,S*)-2-butyl esters, four stereoisomers are completely (Fig. 1a–d) or partially (Fig. 1e) resolved with the elution order *R–S* < *R–R* < *S–R* < *S–S*, or the *R–R* and *S–R* diastereoisomers are eluted together (Fig. 1f).

It is of interest that with the use of racemic AA and 2-alkanols the peak areas of the *R–S* and *S–R* derivatives are equal to each other, as also are those of the *R–R* and *S–S* derivatives. However, the peak areas of the *R–S* (*S–R*) derivatives were found to be significantly larger than those of the *R–R* (*S–S*) derivatives. This is attributed to kinetic (steric) discrimination in the course of the esterification process. The relative percentage of *R–S* with respect to *R–S* plus *S–S* was found to be 52.4% for PFP-AA 2-butyl esters on average.

For PFP-(*R,S*)-AA (*R,S*)-3-methyl-2-butyl esters the elution orders of the

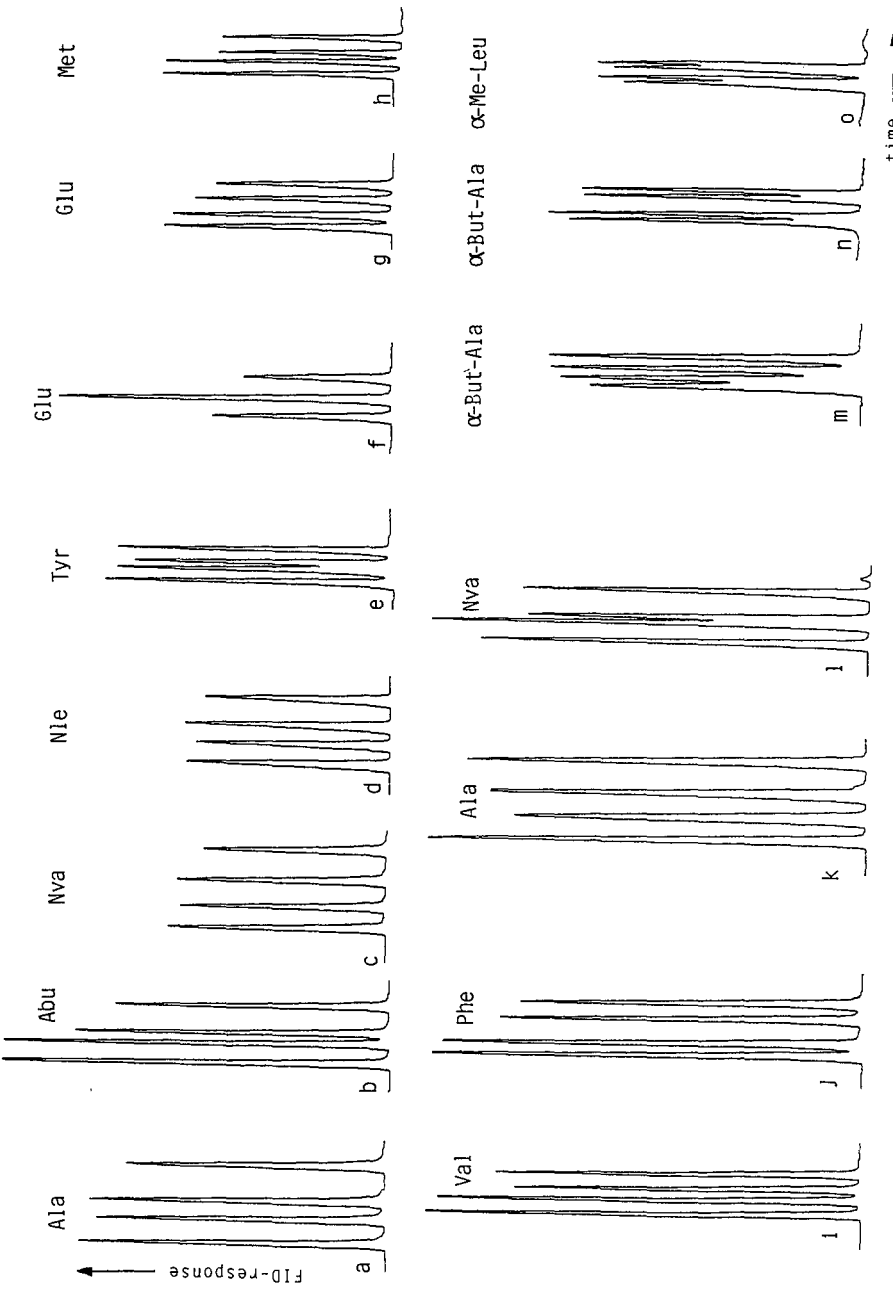

Fig. 1. Sections of gas chromatograms of the separation of stereoisomers of (a–l) PFP-(*R*,*S*)-AA (*R*,*S*)-2-alkyl esters and (m–o) TFA-(*R*,*S*)-AAA (*R*,*S*)-2-alkyl esters. (a–f) 2-Butyl esters; (g–j) 3-methyl2-butyl esters; (k and l), 2-octyl esters; (m) 2-butyl esters; (n and o) 2-octyl esters. Column, (a–l) Chirasil-L-Val, (m–o) Chirasil-D-Val. For GC conditions, retention times and elution orders see Tables I and II.

TABLE I

ELUTION ORDER OF STEREOISOMERS OF PFP-(*R,S*)-AA (*R,S*)-ALKYL ESTERS ON CHIRASIL-L-VAL

Net retention times, t (min), isothermal temperatures, T (°C), resolution factors, α, and number, n, of separated stereoisomers are given. For GC conditions, see Experimental.

Alkyl group in alkyl ester	(*R,S*)-AA	t (min)				T (°C)	α			n
		R–S	*R–R*	*S–R*	*S–S*		*S–S*/*R–S*	*S–R*/*R–S*	*S–S*/*R–R*	
2-Butyl	Ala	8.87	9.39	9.78	10.55	80	1.19	1.10	1.12	4
	Abu	7.69	8.11	8.34	8.92	90	1.16	1.08	1.10	4
	Nva	10.27	10.72	11.29	11.96	95	1.16	1.10	1.12	4
	Nle	9.69	10.12	10.53	11.10	105	1.14	1.09	1.10	4
	Aoa	9.98	10.33	10.58	11.02	125	1.10	1.06	1.07	4
	Val	8.18	8.58	8.58	9.02	90	1.10	1.05	1.05	3
	Leu	7.79	8.18	8.65	9.23	105	1.19	1.11	1.13	4
	Met	10.25	10.61	10.78	11.22	135	1.10	1.05	1.06	4
	Ser	9.80	10.08	10.08	10.47	100	1.07	1.03	1.04	3
	Glu	11.18	11.58	11.58	12.02	150	1.08	1.04	1.04	3
	Phe	9.64	9.96	9.96	10.37	145	1.08	1.03	1.04	3
	Tyr	8.81	9.08	9.23	9.51	160	1.08	1.05	1.05	4
		R–S	*S–R*	*R–R*	*S–S*					
3-Methyl-2-butyl	Ala	8.04	8.70	8.88	9.84	90	1.22	1.08	1.11	4
	Abu	8.84	9.58	9.71	10.68	95	1.21	1.08	1.10	4
	Nva	8.68	9.36	9.36	10.29	105	1.19	1.08	1.10	3
	Nle	10.88	11.72	11.72	12.83	110	1.18	1.08	1.09	3
	Aoa	10.67	11.23	11.41	12.12	130	1.14	1.05	1.06	4
	Val	7.29	7.60	7.85	8.16	100	1.12	1.04	1.04	4
	Leu	8.72	9.54	9.54	10.67	110	1.22	1.09	1.12	3
	Met	7.18	7.45	7.65	7.98	150	1.11	1.04	1.04	4
	Ser	8.39	8.51	8.90	9.19	110	1.10	1.01	1.03	4
	Glu	9.69	9.95	10.29	10.61	165	1.10	1.03	1.03	4
	Phe	10.27	10.53	11.06	11.41	150	1.11	1.03	1.03	4
	Tyr	8.89	9.09	9.71	9.99	165	1.12	1.02	1.03	4
		R–S	*R–R*	*S–R*	*S–S*					
2-Octyl	Ala	9.91	10.38	10.91	11.59	120	1.17	1.10	1.12	4
	Abu	7.91	8.18	8.48	8.99	130	1.14	1.07	1.10	4
	Nva	9.50	9.91	10.05	10.62	135	1.12	1.06	1.07	4
	Nle	10.90	11.25	11.25	11.97	140	1.10	1.03	1.06	3
	Aoa	9.85	10.05	10.05	10.40	160	1.06	1.02	1.03	3
	Leu	11.75	12.41	12.41	13.42	135	1.14	1.06	1.08	3
	Met	9.97	10.19	10.19	10.52	170	1.06	1.02	1.03	3
	Phe	11.78	11.95	12.31	12.56	175	1.07	1.04	1.05	4
	Tyr	9.23	9.55	9.55	9.81	190	1.05	1.03	1.04	3

respective stereoisomers are *R–S* < *S–R* < *R–R* < *S–S*, or *R–S* < *S–R* together with *R–R* < *S–S*; (*cf.*, Table I). The elution order *S–R* before *R–R* for the 3-methyl-2-butyl esters is the opposite of that found for 2-butyl esters (*cf.*, Table I).

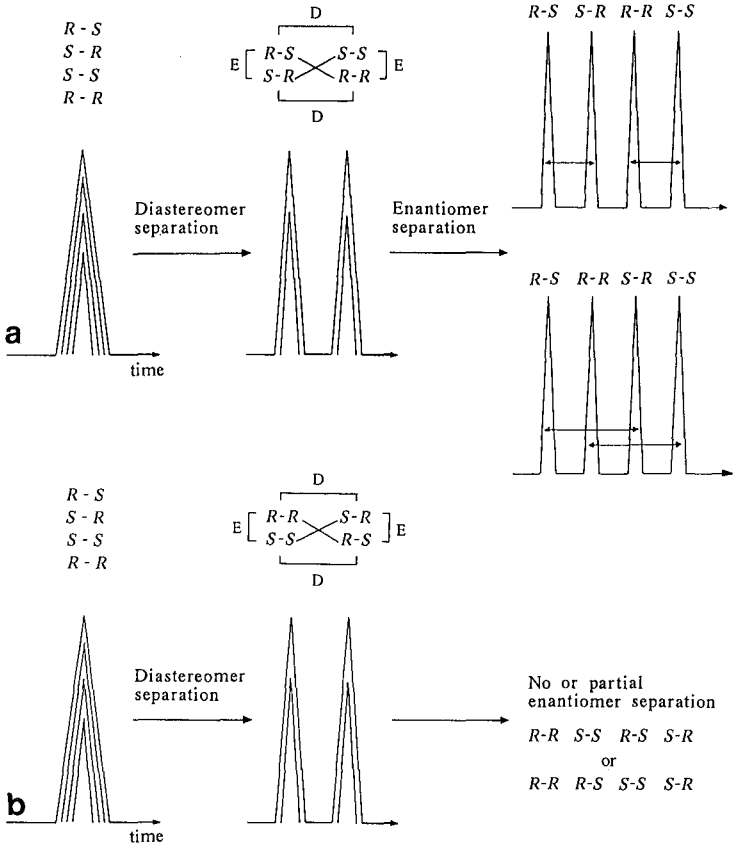

Fig. 2. Scheme of the GC separation on chiral L-α-amino acid phase (Chirasil-L-Val) of stereoisomers of (a) PFP-(*R,S*)-AA (*R,S*)-2-alkyl esters and (b) TFA-(*R,S*)-AAA (*R,S*)-2-alkyl esters. The first letter in the abbreviations of the stereoisomers (*e.g.*, *R–S*) refers to the configuration of the amino acid and the second to that of the alcohol. (*R*)- and (*S*)-α-amino amino acids correspond to D- and L-α-amino acids, and (*S*)(+)- and (*R*)(−)-2-alkanols to D- and L-2-alkanols [18–20]; diastereomers (D) and enantiomers (E) are assigned in the scheme.

3-Methyl-2-butanol also exerts an increased kinetic (steric) discrimination effect as compared with 2-butanol. The relative percentage of *R–S*, calculated with respect to *R–S* plus *S–S*, was found to be 55.7% for PFP-AA 3-methyl-2-butyl esters on average.

For PFP-(*R,S*)-AA (*R,S*)-2-octyl esters, the diastereomeric pairs *S–S* and *R–S* show smaller resolution factors than to 2-butyl and 3-methyl-2-butyl esters (*cf.*, Table I and Fig. 1k and l), and the diastereomeric pairs *S–R* and *R–R* of the 2-octyl esters of Nle, Aoa, Leu, Met and Tyr are eluted together (*cf.*, Table I). In summary, however, the selection of an appropriate ester makes the resolution of all four stereoisomers of the PFP-AA 2-alkyl esters possible (*cf.*, Table I).

The elution order of stereoisomers on Chirasil-L-Val is, in agreement with an explanation given by König [18] for other L-phases, rationalized as follows (Fig. 2a). On esterification with (*R,S*)-2-alkanols (*R,S*)-AA form two diastereomeric and two enantiomeric derivatives. On an appropriate non-chiral stationary phase the diaster-

eomeric esters, but not the enantiomeric esters, are separable, whereas on a chiral stationary phase, in principle, both the diastereomeric esters and the enantiomeric esters are separable. Therefore, if optimally separated, four baseline-resolved peaks of the respective stereoisomers should appear in the chromatograms. The elution order of the four possible stereoisomers on Chirasil-L-Val is explained below (*cf.*, Fig. 2a).

The stationary phase Chirasil-L-Val can be considered to consist of a non-chiral backbone of dimethylpolysiloxane to which the chiral selector L-Val *tert.*-butylamide has been covalently bonded via a spacer group [10,26].

On a non-chiral stationary phase diastereomeric, but not enantiomeric, PFP-AA esters are separated. This leads to the resolution of *R–S* and *S–S* diastereomers and of *S–R* and *R–R* diastereomers, respectively. The enantiomeric pair *R–S* and *S–R* will elute together and first; *S–S* and *R–R* also elute together but second (cf. Fig. 2a). This resolution effect is called the "diastereomeric resolution effect" in the following discussion. Diastereomers of AAA show the opposite elution order to AA, *i.e.*, *R–R* and *S–S* are eluted first and together, and *S–R* and *R–S* are eluted second and together (*cf.* Fig. 2b; for discussion, see below).

On a chiral stationary phase, such as Chirasil-L-Val, the diastereomeric resolution effect will be superimposed by an "enantiomeric resolution effect", and therefore simultaneously the separation of the enantiomeric pairs *R–S* and *S–R* or *S–S* and *R–R* will occur. As a result of chiral interactions on Chirasil-L (= *S*)-Val [and also other chiral phases composed of L (= *S*)-AA], (*R*)-AA derivatives are less retarded than (*S*)-AA derivatives. AAA enantiomers show the same elution order as AA enantiomers. The diastereomeric and enantiomeric effects are additive for the diastereomeric pairs *S–S* and *R–S*. For the diastereomeric pair *S–R* and *R–R* both effects are opposite. Depending on the dominance of the diastereomeric or the enantiomeric resolution effect (which is dependent on the alcohol used; *cf.* Table I), S–R is eluted before *R–R* or *vice versa*. It might also be possible that *S–R* and *R–R* are eluted together from the column or are incompletely resolved.

As neither a contribution of the chiral alcohol in N-acyl-AA 2-alkyl esters nor a possible temperature dependence on the resolution and elution order of stereoisomers on chiral stationary phases had been discussed previously [18–20], we investigated the separation of N-TFA-Gly (*R,S*)-2-alkyl esters and N-PFP-(*R,S*)-Ala (*R,S*)-2-octyl ester on the Chirasil-D-Val column. Achiral Gly was used in order to eliminate the influence of the chiral AA on resolution, and a laboratory-made, fused-silica Chirasil-D-Val column was selected as it showed exceptionally high resolution coefficients or DL-AA. [In agreement with the literature [3] and from our experience with the determination of D-AA in food [27,28], commercially available Chirasil-L-Val columns from various manufacturers (Macherey-Nagel; Chrompack, Middelburg, The Netherlands; C.G.C. Analytic, Mössingen, Germany; laboratory-made fused-silica and glass capillar columns) showed different selectivities for amino acid derivatives.] It was found that TFA-Gly (*R,S*)-2-alkyl esters (alkyl = 2-butyl, 3-methyl-2-butyl and 2-octyl) were significantly resolved on Chirasil-D-Val, the (*S*)(+)-derivative eluting before the (*R*)(−)-derivative (Fig. 3a); with a Chirasil-L-Val column the opposite elution order is to be expected. Therefore a (minor) contribution of the chiral alcohol to the resolution of AA enantiomers on chiral column also has to be taken into account.

On an L-stationary phase for the enantiomeric pair *R–S* and *S–R*, the

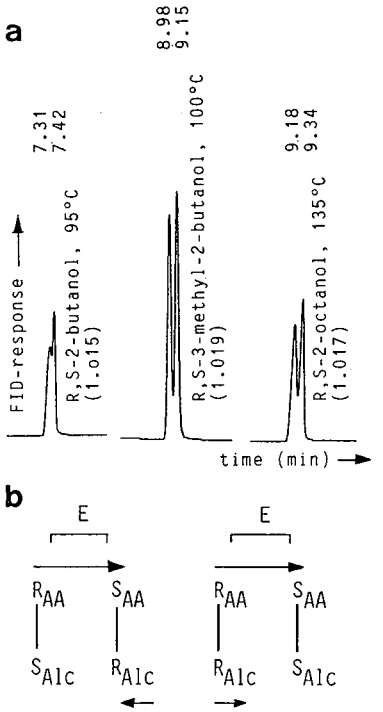

Fig. 3. (a) Resolution of TFA-Gly (*R,S*)-2-alkyl esters on Chirasil-D-Val. Alcohols used for esterification, net retention times (min), isothermal temperatures and resolution factors α are given. Derivatives with (*S*)(+)-alcohol elute before those with (*R*)(−)-alcohol on Chirasil-D-Val and the opposite on Chirasil-L-Val. Carrier gas, hydrogen at 0.5 bar. (b) Scheme of the influence (indicated by direction and size of the arrows) of the chiral alcohol in the N-acyl-(*R,S*)-AA (*R,S*)-2-alkyl esters on the separation of the enantiomeric pairs on Chirasil-L-Val. E, Enantiomers; R_{AA} and S_{AA}, S_{Alc} and R_{Alc}, configurations of the amino acid (AA) and alcohol (Alc), respectively, in diastereomers (*e.g.*, R_{AA}–S_{Alc}, arranged vertically in scheme).

contributions of the chiral AA and chiral alcohol are opposite with respect to the elution order, and for the enantiomeric pair *S–S* and *R–R* they are additive. This is shown schematically in Fig. 3b.

A comparison of resolution factors α for PFP-(*R,S*)-AA 2-alkyl esters (*cf.*, Table I) shows that in most instances the α-values of the enantiomeric pairs *S–S* and *R–R* are higher than those of the pairs *S–R* and *R–S*. In a few instances equal α-values were found; it is assumed that in these instances the chiral alcohol does not affect he resolution of enantiomers. In no case does the enantiomeric pair *S–R* and *R–S* show a higher α-value than the pair *S–S* and *R–R* (*cf.*, Table I).

Further, in order to determine a possible temperature dependence of the elution order of stereoisomers on the chiral stationary phase, the resolution of PFP-(*R,S*)-Ala (*R,S*)-2-octyl esters [enriched with PFP-(*S*)-Ala (*S*)-2-octyl ester] was investigated on Chirasil-D-Val at the isothermal temperatures 125, 150 and 175°C (Fig. 4). It was found that at all temperatures *S–R* eluted first and *R–R* last, but at 125°C *S–S* eluted

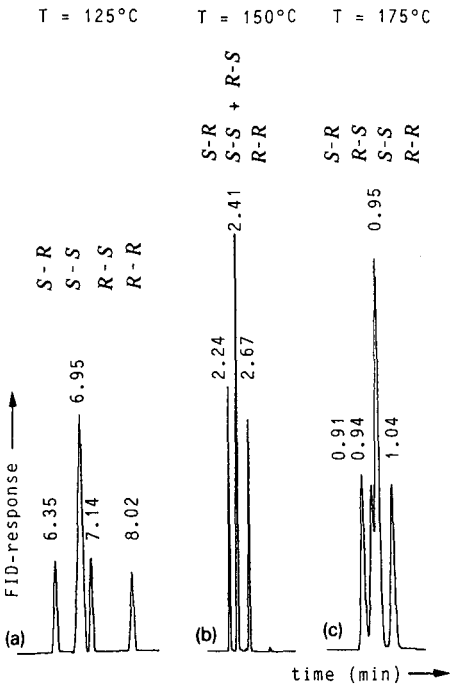

Fig. 4. Temperature dependence of the elution order of the diastereomeric pair *S–S* and *R–S* of PFP-(*R,S*)-Ala (*R,S*)-2-octyl esters on Chirasil-D-Val [sample enriched with PFP-(*S*)-Ala (*S*)-2-octyl ester]. (a) *S–S* is eluted before *R–S*; (b) *S–S* and *R–S* are eluted together; (c) *R–S* is eluted before *S–S*. Isothermal temperatures *T* and net retention times (min) are given; carrier gas, hydrogen at 0.5 bar.

before *R–S* and at 150°C *S–S* and *R–S* eluted together whereas at 175°C *R–S* eluted before *S–S*.

In summary, the resolution of (*R,S*)-AA as diastereomeric 2-alkyl esters on a chiral L-phase (Chirasil-L-Val) ideally will lead to the separation of four stereoisomers, *R–S* being eluted first and *S–S* last (fourth) in all instances. The elution order on an L-phase of the second and third stereoisomers (*i.e.*, *S–R* before *R–R* or *vice versa*) depends mainly on the structure of the chiral alcohol. The *S–R* and *R–R* diastereomers might also elute together or might be incompletely resolved (*cf.*, Fig. 1), depending on the selectivity of a certain stationary phase. A temperature dependence of the elution order has been demonstrated so far for the example PFP-(*R,S*)-Ala 2-octyl ester (*cf.*, Fig. 4).

Separation of TFA-α-alkyl-α-amino acid 2-alkyl esters on Chirasil-D-Val

In previous investigations it was found [22] that enantiomeric N-acyl-AAA *n*-propyl esters were satisfactorily resolved on commercial fused-silica capillary columns coated with Chirasil-L-Val, although the resolution coefficients in general were lower than those of AA. In spite of these findings, it was of interest to determine whether or not stereoisomers of representative AAA, in analogy with AA, were separable as 2-alkyl esters on Chirasil-Val, as in particular diastereomeric PFP-AAA

TABLE II

ELUTION ORDER STEREOISOMERS OF TFA-(*R,S*)-AAA (*R,S*)-ALKYL ESTERS ON A 25-m CHIRASIL-D-VAL CAPILLARY COLUMN

Net retention times, t (min), isothermal temperature, T (°C), number, n, of separated stereoisomers and resolution factors, α, are given. For GC conditions, see Experimental.

Alkyl group in alkyl ester	(*R,S*)-AAA[a]	t (min)				T (°C)	α (*R–S/S–S*)	n
		1st peak (*S–S*)	2nd peak	3rd peak	4th peak (*R–S*)			
2-Butyl	α-Et-Ala	6.46	6.46	6.57	6.65	75	1.029	3
	α-Bu-Ala	10.73	10.92[b]	11.13[c]	11.38	85	1.061	4
	α-Me-Leu	8.06	8.06	8.19	8.30	85	1.030	3
	α-Me-Met	9.60	9.60	9.77	9.87	115	1.028	3
	α-Me-Ser	8.12	8.12	8.22	8.22	85	1.012	2
	α-Me-Phe	9.11	9.11	9.11	9.11	130	1.000	1
3-Methyl-2-butyl	α-Et-Ala	6.72	6.72	6.88	6.88	85	1.024	2
	α-Bu-Ala	8.10	8.30	8.30	8.55	100	1.056	3
	α-Me-Leu	6.58	6.58	6.68	6.75	90	1.026	3
	α-Me-Met	8.92	8.92	9.24	9.24	130	1.036	2
	α-Me-Ser	7.68	7.68	7.97	7.97	95	1.038	2
	α-Me-Phe	8.76	8.76	8.76	8.76	140	1.000	1
2-Octyl	α-Et-Ala	7.63	7.73	7.73	7.86	120	1.030	3
	α-Bu-Ala	7.75	7.89[c]	8.27[b]	8.41	135	1.085	4
	α-Me-Leu	8.77	8.88[c]	9.10[b]	9.20	125	1.049	4
	α-Me-Met	7.86	7.86	8.57	8.57	160	1.090	2
	α-Me-Ser	7.11	7.11	7.56	7.56	130	1.063	2
	α-Me-Phe	8.78	8.78	8.91	8.91	170	1.015	2

[a] Et = Ethyl; Bu = butyl; Me = methyl.
[b] *S–R*.
[c] *R–R*.

(*S*)(+)-3-methyl-2-butyl esters and PFP-AAA (*S*)(+)-2-octyl esters showed good resolution properties on achiral methylpolysiloxane (CP-Sil-5) [24].

The laboratory-made Chirasil-D-Val column, specially designed for the highest resolution of TFA-DL-AA 1-propyl esters, achieved the resolution of the four possible stereoisomers of selected TFA-(*R,S*)-AAA (*R,S*)-2-alkyl esters, namely for TFA-(*R,S*)-α-But-Ala (*R,S*)-2-butyl ester, TFA-(*R,S*)-α-But-Ala (*R,S*)-2-octyl ester and TFA-(*R,S*)-α-Me-Leu (*R,S*)-2-octyl ester (Table II; Fig. 1m–o). If separated, the highest values were found for the diastereomeric pair *R–S* and *S–S* (*cf.*, Table II).

The elution order of stereoisomers of TFA-(*R,S*)-AAA (*R,S*)-2-alkyl esters is explained as follows. On non-chiral stationary phases *S–S* diastereomers are eluted before *R–S* diastereomers and *R–R* diastereomers before *S–R* diastereomers. This is the opposite elution order to that found for AA [21,24]. In contrast, on chiral stationary phases AAA and AA derivatives show the same elution order [21]. With Chirasil-D-Val *S–S* diastereomers are eluted before *R–R* diastereomers and *S–R* diastereomers before *R–S* diastereomers. (The possible elution order of stereoisomers of AAA on Chirasil-L-Val and Chirasil-D-Val as compared with those of AA is shown in Table III; see also Fig. 2b.)

TABLE III

POSSIBLE ELUTION ORDERS (WITH INCREASING RETENTION TIME FROM LEFT TO RIGHT) BY SUPERIMPOSITION OF THE DIASTEREOMERIC AND ENANTIOMERIC RESOLUTION EFFECTS FOR AA AND AAA ON CHIRASIL-L-VAL AND CHIRASIL-D-VAL

Acids	Chirasil-L-Val	Chirasil-D-Val
AA	*R–S* < *S–R* < *R–R* < *S–S* or	*S–R* < *R–S* < *S–S* < *R–R* or
	R–S < *R–R* < *S–R* < *S–S*	*S–R* < *S–S* < *R–S* < *R–R*
AAA	*R–R* < *S–S* < *R–S* < *S–R* or	*S–S* < *R–R* < *S–R* < *R–S* or
	R–R < *R–S* < *S–S* < *S–R*	*S–S* < *S–R* < *R–R* < *R–S*

As with AA, diastereomeric and enantiomeric resolution effects for AAA are additive for *S–S* and *R–S* diastereomers; of the four possible stereoisomers *S–S* is eluted first and *R–S* is eluted last (fourth) in all instances. The elution order of the second- and third-eluted stereoisomers is *R–R* before *S–R* or *vice versa*. With TFA-(*R,S*)-α-But-Ala (*R*)-2-butyl ester *S–R* is eluted before *R–R*, and with TFA (*R,S*)-α-But-Ala (*R*)-2-octyl ester and TFA-(*R,S*)-α-Me-Leu (*R*)-2-octyl ester *R–R* is eluted before *S–R* at the temperatures used (*cf.*, Table II).

The results presented are of interest for (a) the separation and determination of (*R,S*)-AA and (*R,S*)-AAA as diastereomeric esters on chiral stationary phases, in particular when the esterification reagent is not optically pure, (b) for the chromatographic determination of the absolute configuration of non-protein AAA and (c) for obtaining an insight into chromatographic resolution mechanisms of stereoisomers.

REFERENCES

1 E. Gil-Av, B. Feibush and R. Charles-Sigler, *Tetrahedron Lett.*, (1966) 1009.
2 B. Feibush, *J. Chem. Soc., Chem. Commun.*, (1971) 544.
3 E. Gil-Av, R. Charles and S.-C. Chang, in C. W. Gehrke, K. C. T. Kua and R. W. Zumwalt (Editors), *Amino Acid Analysis by Gas Chromatography*, Vol. II, CRC Press, Boca Raton, FL, 1987, pp. 1–34, and references cited therein.
4 B. Feibush and E. Gil-Av, *J. Gas Chromatogr.*, 5 (1967) 257.
5 B. Feibush and E. Gil-Av, *Tetrahedron*, 26 (1970) 1361.
6 N. Ôi, K. Moriguchi, M. Matsuda, H. Shimada and O. Hiroaki, *Bunseki Kagaku*, 27 (1978) 637.
7 N. Ôi, in C. W. Gehrke, K. C. T. Kua and R. W. Zumwalt (Editors), *Amino Acid Analysis by Gas Chromatography*, Vol. III, CRC Press, Boca Raton, FL, 1987, pp. 47–63.
8 G. Schomburg, I. Benecke and G. Severin, *J. High Resolut. Chromatogr. Chromatogr. Commun.*, 8 (1985) 391.
9 G. Palla, A. Dossena and R. Marchelli, *J. Chromatogr.*, 349 (1985) 9.
10 E. Bayer, G. Nicholson and H. Frank, in C. W. Gehrke, K. C. T. Kua and R. W. Zumwalt (Editors), *Amino Acid Analysis by Gas Chromatography*, Vol. II, CRC Press, Boca Raton, FL, 1987, pp. 35–53, and references cited therein.
11 T. Saeed, P. Sandra and M. Verzele, *J. Chromatogr.*, 186 (1980) 611.
12 T. Saeed, P. Sandra and M. Verzele, *J. High Resolut. Chromatogr. Chromatogr. Commun.*, 3 (1980) 35.
13 W. A. König and I. Benecke, *J. Chromatogr.*, 209 (1981) 91.
14 E. Gil-Av, R. Charles and G. Fischer, *J. Chromatogr.*, 17 (1965) 408.
15 J. W. Westley, B. Halpern and B. L. Karger, *Anal. Chem.*, 40 (1968) 2046.
16 G. S. Ayers, R. E. Monroe and J. H. Mossholder, *J. Chromatogr.*, 6 (1971) 259.
17 W. A. König, W. Rahn and J. Eyem, *J. Chromatogr.*, 133 (1977) 141.
18 W. A. König, *Chromatographia*, 9 (1976) 72.
19 W. A. König, *The Practice of Enantiomer Separation by Capillary Gas Chromatography*, Hüthig, Heidelberg, 1987, p. 72.

20 D.-M. Liu, *Chromatographia,* 25 (1988) 393.
21 H.Brückner, G. J. Nicholson, G. Jung, W. Kruse and W. A. König, *Chromatographia,* 13 (1980) 209.
22 H. Brückner, I. Bosch, T. Graser and P. Fürst, *J. Chromatogr.,* 395 (1987) 569.
23 H. Brückner, M. Langer, A. Esna-Ashari, A. Labudda, Z. J. Kamiński, M. T. Leplawy and R. Jöster, in G. Lubec and G. A. Rosenthal (Editors), *Amino Acids: Chemistry, Biology and Medicine*, Escom, Leiden, 1990, pp. 159–165.
24 H. Brückner and M. Langer, *J. Chromatogr.,* 521 (1990) 109.
25 H. Brückner, S. Kühne, S. Zivny and M. Currle, in T. Shiba and S. Sakakibara (Editors), *Peptide Chemistry 1987*, Protein Research Foundation, Osaka, pp. 175–178.
26 V. Schurig, Angew. Chem., 96 (1984) 733; *Angew. Chem., Int. Ed. Engl.*, 23 (1984) 747.
27 H. Brückner and M. Hausch, *J. High Resolut. Chromatogr.*, 12 (1989) 680.
28 H. Brückner and M. Hausch, *Milchwissenschaft*, 45 (1990) 421.

Journal of Chromatography, 542 (1991) 173–183
Elsevier Science Publishers B.V., Amsterdam

CHROM. 23 004

Impact of experimental parameters on the resolution of positional isomers of aminobenzoic acid in capillary zone electrophoresis

M. W. F. NIELEN

Akzo Research Laboratories Arnhem, Corporate Research, Chemical and Structure Analysis Department, P.O. Box 9300, 6800 SB Arnhem (The Netherlands)

(First received September 24th, 1990; revised manuscript received November 28th, 1990)

ABSTRACT

The separation process in capillary zone electrophoresis is governed by many experimental parameters, such as the choice of the electrolyte, field strength, ionic strength, pH, temperature and additives (including organic modifiers). Positional isomers of substituted benzoic acids were used as model compounds in order to study the contributions of pH, electrolyte, ionic strength, addition of alcohols, the choice of the counter ion and the temperature to the electrophoretic separation and the magnitude of the electroosmotic flow. The results thus obtained were compared critically with those of previous studies, in which only the modifier content had been varied. Obviously, pH was the most effective parameter in optimizing the resolution. However, thermostating of the capillary at elevated temperatures turned out to be a very effective additional feature; the resolution was increased and the analysis time was shortened considerably. Other options, such as the addition of alcohols or the choice of the counter ion, will also increase the resolution but also increase the analysis time. The improvement in the concentration sensitivity was studied using the technique of sample stacking. Volumes of up to 15 nl could be introduced in this way without serious separation problems, yielding a detection limit of 10^{-6} *M*.

INTRODUCTION

Capillary zone electrophoresis (CZE) offers fast and efficient separations of ionic and ionizable compounds [1,2]. The separation is primarily based on the different mobilities of analytes in an electric field. For a given set of experimental parameters, the effective mobility depends on the net charge, size and conformation of a molecule. For each separation, the experimental parameters have to be optimized in order to exploit fully the potential of CZE. Some of these parameters are pH, ionic strength, buffer additives (including organic solvents), counter ion, capillary material and temperature.

We studied the effects of these parameters on resolution, plate number, electroosmosis and electrophoresis, using positional isomers of aminobenzoic acid as model compounds. The dissociation constants of these model compounds are similar: *p*-aminobenzoic acid, $pK_1 = 2.41$ and $pK_2 = 4.85$; *m*-aminobenzoic acid, $pK_1 = 3.12$ and $pK_2 = 4.74$ [3]. Fujiwara and Honda [4] were able to improve the resolution of

0021-9673/91/$03.50

these compounds by the addition of methanol (resolution from 0.8 to 1.5) or acetonitrile (from 0.8 to 2.2). In addition to their work, we have also studied other parameters as mentioned above. Particularly the impact of temperature and the counter ion on the resolution in CZE have been neglected in the past. We also studied the potential of sample stacking [5] in order to improve the concentration sensitivity of the model compounds.

EXPERIMENTAL

Apparatus

An Applied Biosystems (San Jose, CA, U.S.A.) Model 270A capillary electrophoresis system [5] was used, equipped with a variable wavelength UV absorbance detector, operated at either 200 or 254 nm. CZE was performed in a 72 cm × 50 μm I.D. fused-silica capillary (Applied Biosystems) at 25 kV (constant-voltage mode). The capillary was thermostated at 30.0 ± 0.1°C unless indicated otherwise. Data were recorded using a Nelson Analytical Model 4400 integration system.

Chemicals

Distilled water was purified in a Milli-Q apparatus (Millipore, Bedford, MA, U.S.A.). Morpholinoethanesulphonic acid (MES) was obtained from Sigma (St. Louis, MO, U.S.A.), *p*- and *m*-aminobenzoic acid from laboratory stock and mesityl oxide from Aldrich (Steinheim, Germany). All the other chemicals were of analytical-reagent grade from J. T. Baker (Deventer, The Netherlands).

Methods

Buffers were prepared in Milli-Q water and adjusted to a specific pH using a Philips (Cambridge, U.K.) Model PW 9409 pH meter. Stock solutions of *p* and *m*-aminobenzoic acid (10^{-2} *M*) were prepared in methanol. Each day, samples were freshly diluted with buffer solution or mixtures of the buffer solution with Milli-Q water, yielding 10^{-4} *M* sample solutions. Buffers and samples were filtered through 0.45-μm Spartan 30/B filters (Schleicher & Schüll, Dassel, Germany) prior to use.

Samples were introduced to the capillary via a controlled vacuum system. Unless stated otherwise, the injection time was 1.0 s, which corresponds to a volume of *ca.* 3.0 nl. The coefficient of electroosmotic flow was calculated using mesityl oxide as a neutral marker.

RESULTS AND DISCUSSION

The coefficient of electroosmotic flow, μ(eo) in cm^2 V^{-1} s^{-1}, and the effective electrophoretic mobility, μ(ep) in cm^2 V^{-1} s^{-1}, were calculated as follows:

$$\mu_{(eo)} = \frac{L_{(d)}L_{(t)}}{t_{(eo)}V} \tag{1}$$

$$\mu(ep) = \frac{L_{(d)}L_{(t)}}{V}\left[\frac{1}{t_{(m)}} - \frac{1}{t_{(eo)}}\right] \tag{2}$$

where $L_{(t)}$ (cm) is the total length of the capillary, $L_{(d)}$ the distance between the inlet of the capillary and the detector (50 cm), V (V) the applied voltage $t_{(eo)}$ (s) the migration time of the neutral marker and $t_{(m)}$ (s) the migration time of the analyte. The resolution, R_s, was calculated using

$$R_s = 0.25\, N^{0.5} \left[\frac{\mu_{(ep1)} - \mu_{(ep2)}}{\mu_{(epm)} + \mu_{(eo)}} \right] \tag{3}$$

where $\mu_{(epm)}$ (s) is the mean value of $\mu_{(ep1)}$ and $\mu_{(ep2)}$. The plate number, N, was determined using the equation

$$N = \left[\frac{t_{(m)}}{\sigma_{(t)}} \right]^2 \tag{4}$$

in which $\sigma_{(t)}$ (s) represents the peak half-width at 0.6 of the peak height.

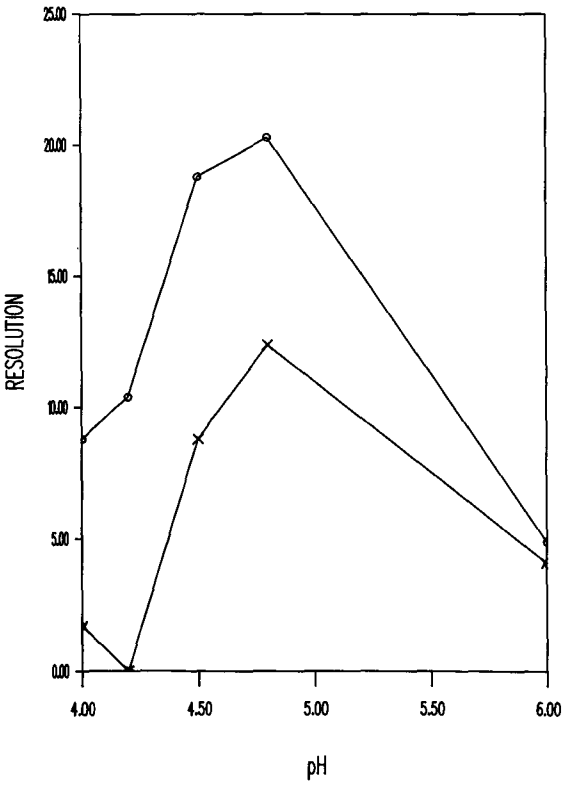

Fig. 1. Influence of pH on the resolution of *p*- and *m*-aminobenzoic acid. Conditions: CZE at 25 kV in 40 m*M* ammonium acetate buffer. Capillary thermostated at (×) 30.0°C and (○) 60.0°C.

Influence of pH

The pH of a 40 m*M* ammonium acetate buffer was varied between 4.0 and 6.0. As expected [6], the resolution was found to be optimum at a pH value close to the p*K* values of the analytes (Fig. 1). A minimum was found at pH 4.2 (co-migration). Below pH 4.2, a reversal of the migration order of *p*- and *m*-aminobenzoic acid was observed, following their p*K* values (*p*-aminobenzoic acid, $pK_1 = 2.41$ and $pK_2 = 4.85$; *m*-aminobenzoic acid, $pK_1 = 3.12$ and $pK_2 = 4.74$). Typical plate numbers ranged between 170 000 and 200 000 throughout the pH range investigated. Both $\mu_{(eo)}$ and $\mu_{(ep)}$ were reduced on decreasing the pH from 6 to 4, owing to the increased neutralization of the capillary wall and the decreased ionization of the analytes, respectively.

Similar experiments were carried out using 40 m*M* phosphate buffers between pH 5.8 and 6.8. In contrast with ref. 4, baseline separation could easily be obtained at pH 6.8 (Fig. 2). Probably band broadening due to Joule heating was significantly higher in that study (current 100 μA *versus* 38 μA in our phosphate system).

Influence of ionic strength

The ionic strength was varied using 10–100 m*M* MES buffers at pH 6.0. At lower buffer concentrations, both $\mu_{(eo)}$ and $\mu_{(ep)}$ increased owing to an increase in the zeta potential. This increase was found to be more pronounced for $\mu_{(eo)}$, yielding up to twice as fast separations at 10 m*M*. The plate number, however, decreased dramatically (from 210 000 to 40 000) and the resolution was lost completely at 10 m*M* (Fig.

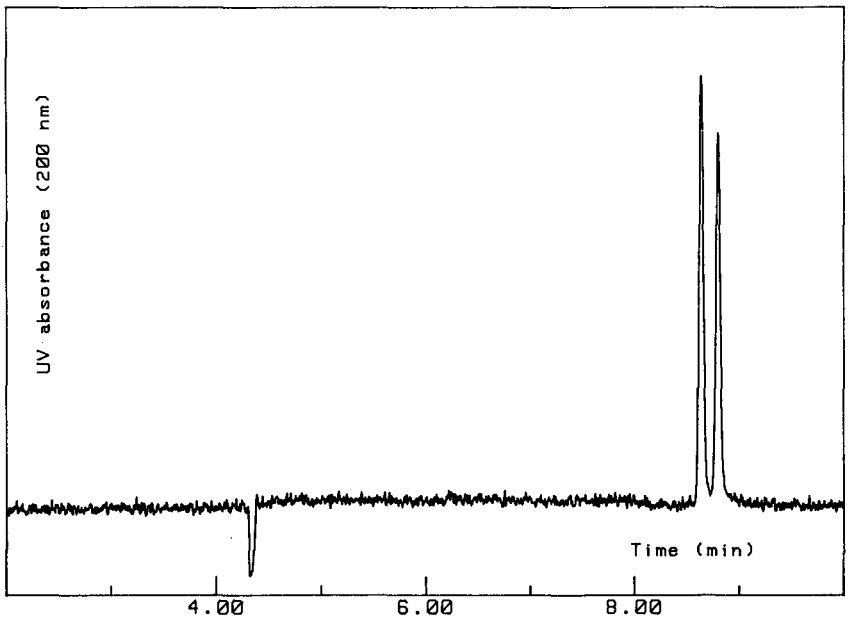

Fig. 2. CZE separation of *p*- and *m*-aminobenzoic acid at 25 kV in 40 m*M* sodium phosphate buffer (pH 6.8). Capillary thermostated at 30.0°C.

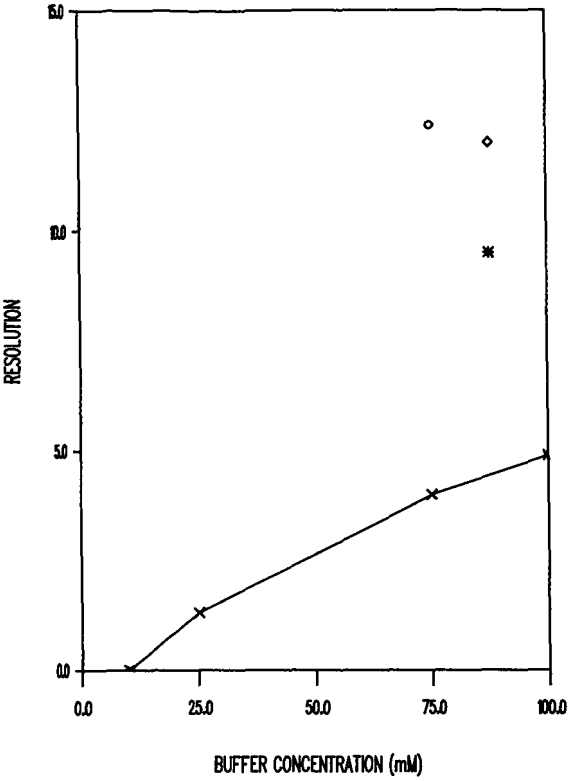

Fig. 3. Influence of buffer concentration on the resolution of *p*- and *m*-aminobenzoic acid. (×) MES buffer (pH 6.0); (○) MES buffer–methanol (75:25); (∗) MES buffer–isopropanol (87.5:12.5). Capillary thermostated at 30.0°C, except for (◇) MES buffer–isopropanol (87.5:12.5) at 60.0°C.

3). A similar trend was observed in a series of experiments using phosphate buffers at pH 6.8.

The decrease in plate number might be attributed to band broadening caused by the sample volume, migrational dispersion [7], inhomogeneous electroosmosis or time constants, etc.

Influence of alcohols

Only a few organic solvents are compatible with the materials used in our CZE apparatus. We investigated the addition of both methanol and isopropanol (IPA) to phosphate (Table I) and MES (Table II) buffer systems.

The resolution obtained with a 40 m*M* phosphate buffer (pH 6.8)–methanol (75:25) system did not differ from that obtained with a purely aqueous system. The analysis time, however, was doubled owing to a strong decrease in $\mu_{(eo)}$ and a minor decrease in $\mu_{(ep)}$. The decrease in plate number from 200 000 to 74 000 can be explained at least partially by the impact of the decreased apparent mobility [$\mu_{(ep)} + \mu_{(eo)}$] on the diffusion. Similar results were obtained with phosphate–IPA (87.5:12.5). In addition to the different wetting characteristics, the stronger effect of IPA can be attributed to its higher viscosity.

TABLE I

EFFECT OF THE ADDITION OF ALCOHOLS ON THE CZE SEPARATION OF AMINOBENZOIC ACID ISOMERS

Conditions: 40 m*M* phosphate buffer (pH 6.8); 25 kV constant voltage; samples, 3 nl, 10^{-4} *M*; capillary thermostated at 30°C; detection by UV absorbance at 200 nm. Analytes: P = *p*-aminobenzoic acid; M = *m*-aminobenzoic acid. Other conditions are given under Experimental.

Parameter	Aqueous phosphate	Phosphate–methanol (75:25)	Phosphate–IPA (87.5:12.5)
$\mu_{(ep,P)}$ (10^{-3} cm^2 V^{-1} s^{-1})	−0.269	−0.189	−0.185
$\mu_{(ep,M)}$ (10^{-3} cm^2 V^{-1} s^{-1})	−0.274	−0.193	−0.189
$\mu_{(eo)}$ (10^{-3} cm^2 V^{-1} s^{-1})	+0.546	+0.333	+0.320
N	200 000	74 000	64 000
i (μA)	38	23	24
R_s	2.0	2.0	1.9
Analysis time (min)	9	20	20

Generally, the influence of alcohols was found to be much more pronounced than reported in ref. 4. This discrepancy can be explained by the smaller I.D. of our capillary and hence the larger impact on electroosmosis.

With regard to the analysis time, *and* with regard to $\mu_{(ep)}$, *and* with regard to $\mu_{(eo)}$, Table II shows similar trends for the MES–methanol system as for the phosphate systems in Table I. The plate number decreased from 210 000 to 120 000. The resolution between *p*- and *m*-aminobenzoic acid, however, was improved considerably (see also Fig. 3). Substituting 12.5% IPA for methanol yielded similar results and again an improved resolution (asterisk in Fig. 3).

Although a direct comparison of the phosphate and the MES buffer systems is not allowed (slightly different ionic strengths and pH conditions), it is clearly suggested that zwitterionic buffers, such as MES, not only are beneficial because of their lower conductivity at relatively high concentrations, but also might have a significant

TABLE II

EFFECT OF THE ADDITION OF ALCOHOLS ON THE CZE SEPARATION OF AMINOBENZOIC ACID ISOMERS

Conditions: 100 m*M* MES buffer (pH 6.0); detection by UV absorbance at 254 nm. Other conditions as in Table I.

Parameter	Aqueous MES	MES–methanol (75:25)	MES–IPA (87.5:12.5)
$\mu_{(ep,P)}$ (10^{-3} cm^2 V^{-1} s^{-1})	−0.256	−0.161	−0.160
$\mu_{(ep,M)}$ (10^{-3} cm^2 V^{-1} s^{-1})	−0.266	−0.179	−0.174
$\mu_{(eo)}$ (10^{-3} cm^2 V^{-1} s^{-1})	+0.480	+0.294	+0.304
N	210 000	120 000	140 000
i (μA)	21	12	13
R_s	4.9	12.4	9.5
Analysis time (min)	11	19	18

TABLE III

EFFECT OF THE COUNTER ION ON THE CZE SEPARATION OF AMINOBENZOIC ACID ISOMERS

Conditions: 40 m*M* acetate buffer (pH 5.4); 25 kV constant voltage; samples 1.5 nl, 10^{-4} *M*; the mobility data are mean values of duplicate experiments; other conditions as in Table I.

Parameter	Lithium (μ^a = 0.401)	Sodium (μ^a = 0.519)	Potassium (μ^a = 0.762)
$\mu_{(ep,P)}$ (10^{-3} cm^2 V^{-1} s^{-1})	−0.228 ± 0.001	−0.242 ± 0.001	−0.250 ± 0.001
$\mu_{(ep,M)}$ (10^{-3} cm^2 V^{-1} s^{-1})	−0.245 ± 0.001	−0.260 ± 0.001	−0.268 ± 0.001
$\mu_{(eo)}$ (10^{-3} cm^2 V^{-1} s^{-1})	+0.486 ± 0.001	+0.464 ± 0.002	+0.442 ± 0.001
N	200 000	170 000	165 000
i (μA)	22	26	27
R_s	7.6	8.7	10.0
Analysis time (min)	10	12	14

[a]Cationic mobility at infinite dilution (10^{-3} cm^2 V^{-1} s^{-1}).

impact on the selectivity of the CZE system. However, more data will be required to support this statement statistically.

Influence of the counter ion

Lithium, sodium and potassium acetate buffers at pH 5.4 were applied to the separation of *p*- and *m*-aminobenzoic acid. The results are given in Table III.

As shown by the data in Table III, the choice of the counter ion does have an important effect on the electrophoretic mobility of the analytes: the $\mu_{(ep)}$ values of *p*- and *m*-aminobenzoic acid increase in the order lithium < sodium < potassium. Actually, one would expect a reversed order as the absolute ionic mobilities (at infinite dilution) of these cations increase from lithium to potassium. The cationic environment around the anionic analytes would yield enhanced relaxation and retardation forces [8] and, consequently, a diminished electrophoretic mobility of the anionic analytes, instead of the observed increase.

In order to exclude possible effects caused by the dissociation equilibria of the weakly acidic analytes, the experiment was repeated using the strongly aromatic acid, *p*-toluenesulphonic acid. However, the results given in Table IV clearly show the same trends as in Table III.

Another possible explanation, namely an increase in electrophoretic mobility due to the increase in current and increased Joule heating, is not supported by the

TABLE IV

EFFECT OF THE COUNTER ION ON THE CZE DATA FOR *p*-TOLUENESULPHONIC ACID

Conditions as in Table III.

Parameter	Lithium	Sodium	Potassium
$\mu_{(ep)}$ (10^{-3} cm^2 V^{-1} s^{-1})	−0.305 ± 0.001	−0.317 ± 0.001	−0.327 ± 0.001
$\mu_{(eo)}$ (10^{-3} cm^2 V^{-1} s^{-1})	+0.485 ± 0.001	+0.448 ± 0.001	+0.431 ± 0.001
Analysis time (min)	14	19	24

observed trend in the $\mu_{(eo)}$ values. Obviously, this experimental set-up is far from the theoretical requirement for infinite dilution, but apart from that we did not find a sound explanation for the discrepancies observed.

From a practical point of view, the choice of the counter ion might be used to optimize the resolution of the anionic analytes. Despite the slightly lower plate number obtained with the potassium acetate system, an increased resolution between *p*- and *m*-aminobenzoic acid was observed, owing to the increased matching of $\mu_{(epm)}$ and $\mu_{(eo)}$ (*cf.*, eqn. 3). However, the analysis time will increase from lithium to potassium, because of the reduced electroosmotic flow and the increased electrophoretic mobility (in the opposite direction).

Influence of temperature

In CZE, temperature is usually considered in a negative context, *e.g.*, in terms of Joule heating. However, temperature can also be exploited as a selectivity parameter. It has been observed that an increased temperature will shorten the analysis time, owing to a lower viscosity. It has also been suggested that chemical equilibria can be influenced by temperature [9] or pH gradients can be thermally generated [10]. In this study, we used the temperature dependence of chemical equilibria as a selectivity parameter. Ammonium acetate buffer (40 m*M*) was used at 30.0 and 60.0°C in the pH range 4.0–6.0. The results at 60.0°C are included in Fig. 1. It can be seen that the resolution improved over the entire pH range investigated. A resolution of more than 20 could be obtained for the positional isomers of aminobenzoic acid. In contrast to the experiments at 30.0°C (see *Influence of pH*), co-migration and a reversal of the migration order did not occur within this pH range, but they probably will below pH

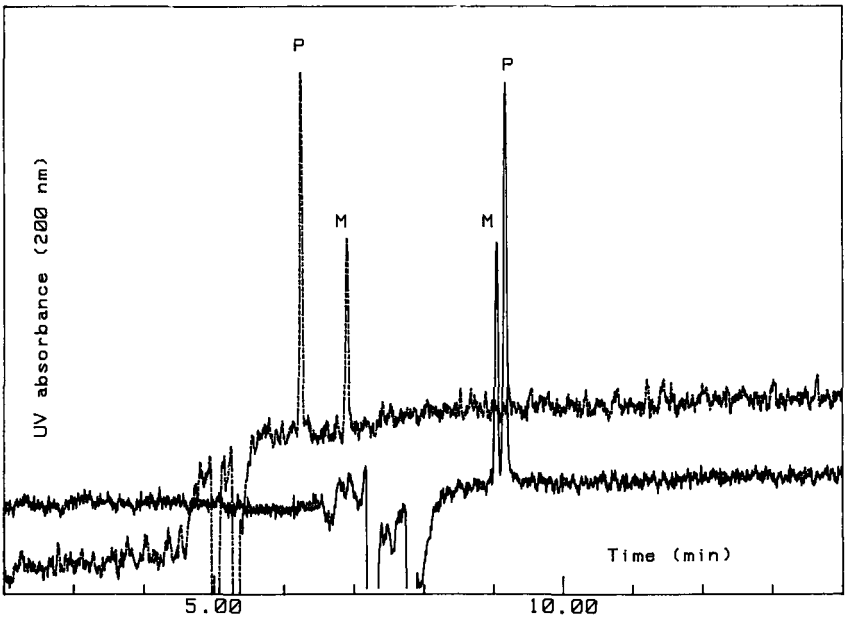

Fig. 4. CZE separation of *p*- (P) and *m*-aminobenzoic acid (M) at 25 kV in 40 m*M* ammonium acetate buffer (pH 4.0). Solid line, 30.0°C; dashed line, 60.0°C.

4.0. The migration order at pH 4.0 can be completely reversed, *i.e.*, the original migration order can be restored, just by increasing the temperature (Fig. 4).

The increase in resolution over the pH range investigated and the restoring of the original migration order at elevated temperatures can be explained by the temperature dependence of the chemical equilibria involved. Both positional isomers show increased effective mobilities, $\mu_{(ep)}$, owing to the lowered viscosity and the increase in their dissociation constants (lower pK values). However, only the *meta* isomer will be subjected to an additional chemical equilibrium. The analytes will exist either in the zwitterionic form or in the deprotonated zwitterionic form. Two molecules of the *meta* isomer will be able to form a dimer because of the electrostatic interaction and/or hydrogen-bonding ability between each other's amino and carboxyl groups. This additional equilibrium will result in a decrease in the effective mobility of *m*-aminobenzoic acid at 30.0°C. At 60.0°C, however, this chemical equilibrium will be much less pronounced, resulting in a much larger increase (relative to the *para* isomer) of $\mu_{(ep)}$ than would be expected from the viscosity and acid–base equilibrium alone. Thus an increase in selectivity and resolution will be obtained and the point of co-migration and peak reversal will be shifted towards a pH value below 4.0. The validity of this explanation was supported by the separation of the corresponding N-acetamides of *p*- and *m*-aminobenzoic acid. Obviously, these molecules will not be able to form a zwitterion, and the *meta* isomer would not be subjected to the above-mentioned additional chemical equilibrium. Indeed, an increase in temperature did not result in any increase in selectivity or resolution. The $\mu_{(ep)}$ values for the respective isomers increased exactly to the same extent.

At 60.0°C, the analysis time was reduced by only 30%. A larger reduction would have been expected, based on the dependence of viscosity on temperature ($-2\%°C^{-1}$). However, the reduced viscosity will influence both $\mu_{(eo)}$ and $\mu_{(ep)}$ in opposite directions. Additionally, it should be noted that our apparatus allows only $L_{(d)}$ to be thermostated, *i.e.*, about 70% of $L_{(t)}$. Improved resolution at higher temperature was also observed with the MES–IPA buffer system (Fig. 3).

Influence of sample volume

The influence of the sample volume on peak broadening has been emphasized recently [11,12]. On the other hand, when the sample is dissolved in a buffer of much lower ionic strength than that of the run buffer, peak compression will occur (sample stacking) [5] at the interface between the sample plug and the run buffer.

p-Aminobenzoic acid was dissolved in 40 mM ammonium acetate buffer and separated using 40 mM ammonium acetate at pH 4.8. The sample volume was varied between 0 and 90 nl and the calibration graphs thus obtained are shown in Fig. 5. The peak area was found to increase linearly within the range tested. A plot of the peak height, on the other hand, showed that serious band broadening occurred at larger injection volumes.

From the point of view of improvement of the concentration sensitivity, a volume of up to 15 nl can be introduced, thereby still obtaining a reasonable increase in peak height, provided that the ionic strength of the sample is only one-tenth of that of the run buffer. Using the sample stacking technique, the detection limit of *p*- and *m*-aminobenzoic acid was found to be 10^{-6} M.

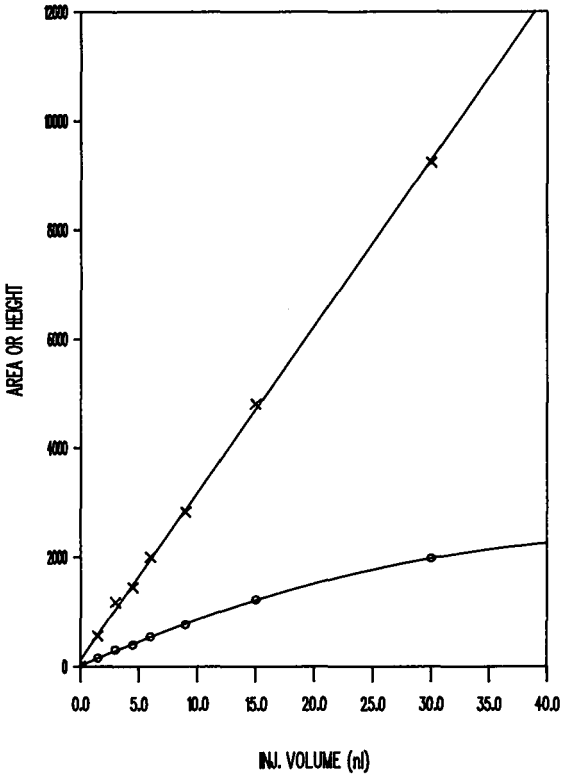

Fig. 5. Calibration graphs for *p*-aminobenzoic acid (sample stacking). (×) Peak area; (○) peak height in arbitrary units.

CONCLUSION

The influence of several experimental parameters on the resolution of *p*- and *m*-aminobenzoic acid has been investigated. Not surprisingly, pH had the strongest impact on resolution and selectivity. However, an increase in the temperature of the thermostated capillary was also very beneficial. The resolution improved and the analysis time was shortened considerably.

Unexpected results were obtained on varying the counter ion in acetate buffers. The electrophoretic mobilities of both strongly and weakly acidic aromatic model compounds increased significantly in the (cationic) order lithium < sodium < potassium. An improved resolution was obtained using potassium acetate; however, the analysis time increased by up to 40%.

The addition of alcohols resulted in an improved resolution at the expense of an increase in analysis time. Addition of 12.5% of IPA yielded similar results to those obtained with 25% of methanol. For the alcohol and cation experiments, the improved resolution is mainly due to an increased matching of $\mu_{(eo)}$ and $\mu_{(ep)}$.

The detection limit of *p*- and *m*-aminobenzoic acid in aqueous samples could successfully be lowered to 10^{-6} *M* using the sample stacking technique while maintaining the separation of the two positional isomers.

REFERENCES

1 J. Jorgenson and K. D. Lukacs, *Anal. Chem.*, 53 (1981) 1298.
2 R. A. Wallingford and A. G. Ewing, *Adv. Chromatogr.*, 29 (1989) 1.
3 A. Albert and E. P. Serjeant, *Ionization Constants of Acids and Bases*, Methuen, London, 1962.
4 S. Fujiwara and S. Honda, *Anal. Chem.*, 59 (1987) 487.
5 S. E. Moring, J. C. Colburn, P. D. Grossman and H. H. Lauer, *LC · GC Int.*, 3 (1990) 46.
6 S. Terabe, T. Yashima, N. Tanaka and M. Araki, *Anal. Chem.*, 60 (1988) 1673.
7 F. E. P. Mikkers, F. M. Everaerts and Th. P. E. M. Verheggen, *J. Chromatogr.*, 169 (1979) 11.
8 F. M. Everaerts, J. L. Beckers and Th. P. E. M. Verheggen, *Isotachophoresis —Theory, Instrumentation and Applications*, Elsevier, Amsterdam, 1976.
9 R. J. Nelson, A. Paulus, A. S. Cohen, A. Guttman and B. L. Karger, *J. Chromatogr.*, 480 (1989) 111.
10 C. H. Lochmuller, S. J. Breiner and C. S. Ronsick, *J. Chromatogr.*, 480 (1989) 293.
11 K. Otsuka and S. Terabe, *J. Chromatogr.*, 480 (1989) 91.
12 X. Huang, W. F. Coleman and R. N. Zare, *J. Chromatogr.*, 480 (1989) 95.

Journal of Chromatography, 542 (1991) 184–188
Elsevier Science Publishers B.V., Amsterdam

CHROM. 23 094

Short Communication

High-performance liquid chromatographic separation of bile acids and bile alcohols diastereoisomeric at C-25

ASHOK K. BATTA* and GERALD SALEN

Department of Medicine and Sammy Davis Jr. National Liver Center, University of Medicine and Dentistry of New Jersey, New Jersey Medical School, Newark, NJ 07103 and Veterans Administration Medical Center, East Orange, NJ 07019 (U.S.A.)

RENU ARORA and SARAH SHEFER

Veterans Administration Medical Center, East Orange, NJ 07019 (U.S.A.)

and

MANJU BATTA

Department of Medicine and Sammy Davis Jr. National Liver Center, University of Medicine and Dentistry of New Jersey, New Jersey Medical School, Newark, NJ 07103 (U.S.A.)

(First received September 14th, 1990; revised manuscript received December 27th, 1990)

ABSTRACT

The high-performance liquid chromatographic separation of the 25*R* and 25*S* diastereoisomers of the bile alcohols 5β-cholestane-3α,7α,26-triol and 5β-cholestane-3α,7α,12α,26-tetrol and the bile acids, 3α,7α-dihydroxy-5β-cholestan-26-oic acid and 3α,7α,12α-trihydroxy-5β-cholestan-26-oic acid is described. A Radial-Pak μBondapak C_{18} reversed-phase cartridge was used for the separations and elutions were carried out with acetonitrile–water–methanol–acetic acid mixtures. All eight diastereoisomeric compounds showed baseline separation when up to 200 μg of the isomeric mixtures were injected into the column and the method can be used for isolation of pure diastereoisomers of these bile acids and bile alcohols.

INTRODUCTION

5β-Cholestane-3α,7α-diol and 5β-cholestane-3α,7α,12α-triol (Fig. 1) are considered obligate intermediates in the biosynthesis of chenodeoxycholic acid and cholic

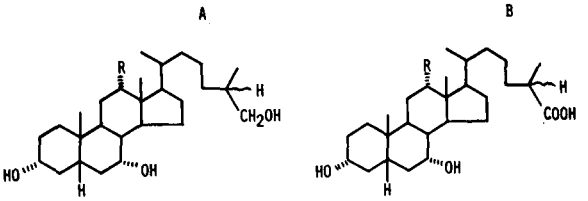

Fig. 1. Structures of bile acids and bile alcohols diastereoisomeric at C-25. (A) 25*R* and 25*S* diastereoisomers of 5β-cholestane-3α,7α,26-triol (R = H) and 5β-cholestane-3α,7α,12α,26-tetrol (R = OH); (B) 25*R* and 25*S* diastereoisomers of DHCA (R = H) and THCA (R = OH).

0021-9673/91/$03.50

acid, respectively, from cholesterol in vertebrates [1]. Shefer *et al.* [2] have recently shown that the biosynthesis of cholic acid involves hydroxylation of 5β-cholestane-3α,7α,12α-triol at C-25 as the initial step, while the classical pathway for the biosynthesis of both primary bile acids is considered to involve intermediates hydroxylated at C-26 [1]. The 26-hydroxylated bile alcohols are then oxidized to 3α,7α-dihydroxy-5β-cholestan-26-oic acid (DHCA) and 3α,7α,12α-trihydroxy-5β-cholestan-26-oic acid (THCA) (Fig. 1), respectively. Further hydroxylation of these C_{27} bile acids at C-24 followed by cleavage of the C-24,25 bond results in the formation of chenodeoxycholic acid and cholic acid, respectively [1]. Traces of the 26-hydroxylated bile alcohols and the cholestanoic acids are present in human bile [3,4]. Large quantities of THCA have been found in the bile of patients with intrahepatic bile duct anomalies [5,6] and Zellweger's syndrome [7]. THCA is also the major biliary bile acid of the alligator [8]. We have recently shown that THCA in both alligator mississippiensis and humans exists as the 25*R* diastereoisomer [9,10] which suggests stereospecificity of the hepatic 26-hydroxylating enzymes. Since, synthetic C_{27} bile acids and bile alcohols are all mixtures of the 25*R* and 25*S* diastereoisomers, it is important to have analytical methods to differentiate between the diastereoisomers of these bile acid intermediates and isolate them in pure form in order to be able to study the stereospecificity of 26-hydroxylation of bile alcohols and metabolism of the pure isomers.

We have developed solvent systems for the thin-layer chromatographic (TLC) separation of the 25*R* and 25*S* diastereoisomers of 5β-cholestane-3α,7α,26-triol,5β-cholestane-3α,7α,12α,26-tetrol and THCA [9,11]. However, the TLC separation requires two or three developments of the TLC plate in the solvent system and bands tend to overlap when larger amounts of compounds are applied on the plate [11]. We report herein separation of these diastereoisomeric bile alcohols and bile acids by high-performance liquid chromatography (HPLC). Diastereoisomers of all compounds are well resolved and the method can be used to isolate quantities of the pure diastereoisomers which may be used as substrates or reference standards to test the substrate specificity of the hepatic 26-hydroxylating enzymes.

EXPERIMENTAL

Materials

25*R* and 25*S* diastereoisomers of 5β-cholestane-3α,7α,26-triol and 5β-cholestane-3α,7α,12α,26-tetrol were synthesized from chenodeoxycholic acid and cholic acid, respectively, as described before [12,13]. Chromic acid oxidation of (25*R* or 25*S*)3α,7α-diformyloxy-5β-cholestane-26-ol [prepared during the synthesis of (25*R* or 25*S*)5β-cholestane-3α,7α,26-triol] followed by alkaline hydrolysis yielded the 25*R* and 25*S* diastereoisomers of DHCA. The 25*R* and 25*S* diastereoisomers of THCA were isolated from the bile of alligator mississippiensis via rigorous hydrolysis of the bile with 25% sodium hydroxide (which resulted in partial isomerization of the 25*R* into the 25*S* diastereoisomer) followed by fractional crystallization [9]. All compounds were >98% pure as judged by TLC and HPLC.

High-performance liquid chromatography

HPLC of the bile acids and bile alcohols was performed on a Waters Assoc. (Millford, MA, U.S.A.) Model M-6000 reciprocating pump and a Model UK6

septumless loop injector. A Waters Assoc. Model 401 differential refractometer was used and the detector response was recorded with a Spectra-Physics (San Jose, CA, U.S.A.) Model SP 4290 integrator. A Waters Assoc. Radial-Pak μBondapak C_{18} reversed-phase column (100 × 8 mm I.D., 5 μm particle size) was employed for all separations. A guard column (Waters Assoc.) prepacked with C_{18} reversed-phase material was placed before the separation column.

A 10–200-μg amount of the bile acid or bile alcohol dissolved in 5–20 μl of methanol was injected into the HPLC column. Solvent systems containing the following proportions of acetonitrile–water–methanol–acetic acid (v/v) were used for analysis: 60:70:20:1 (solvent system A); 70:70:20:1 (system B); 75:70:20:1 (system C) and 80:70:20:1 (system D). The solvents used were HPLC grade and were purchased from Waters Assoc. The flow-rate was maintained at 2.5–3.0 ml/min (operating pressure, *ca.* $13.8 \cdot 10^3$ KPa).

RESULTS AND DISCUSSION

Fig. 2 shows the HPLC analysis of the 25*R* and 25*S* diastereoisomers of the bile acids and bile alcohols with solvent system C as the mobile phase. As is seen from the figure, the diastereoisomers of all four compounds were well resolved in approximately 40 min at a solvent flow-rate of 3 ml/min. 5β-Cholestane-3α,7α,12α,26-tetrol and THCA with three hydroxyl groups in the ring system were eluted significantly earlier than 5β-cholestane-3α,7α,26-triol and DHCA which have two hydroxyl groups in the

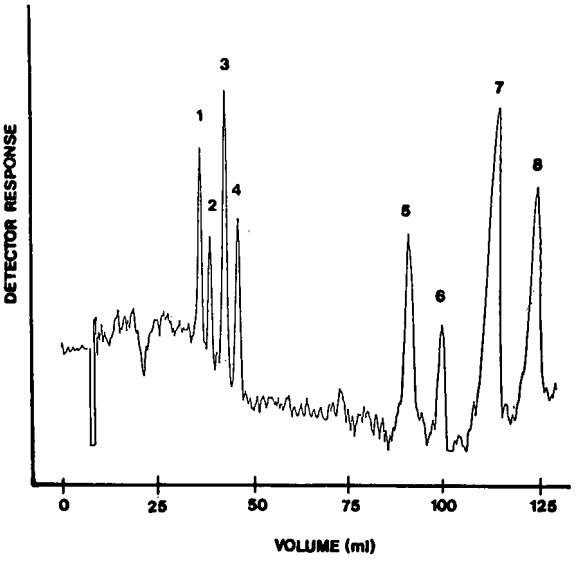

Fig. 2. HPLC of diastereoisomeric bile acids and bile alcohols. Column: 100 × 8 mm I.D. Radial-Pak μBondapak C_{18} reversed-phase cartridge (5 μm). Eluent: acetonitrile–water–methanol–acetic acid (75:70:20:1, v/v). Flow-rate: 3 ml/min. The bile acids and bile alcohols were dissolved in methanol and 20 μl of the solution containing 10–100 μg of each compound was injected into the column. Peaks: 1 = (25*S*)THCA; 2 = (25*R*)THCA; 3 = (25*S*)5β-cholestane-3α,7α,12α,26-tetrol; 4 = (25*R*)5β-cholestane-3α,7α,12α,26-tetrol; 5 = (25*S*)DHCA; 6 = (25*R*)DHCA; 7 = (25*S*)5β-cholestane-3α,7α,26-triol; 8 = (25*R*)5β-cholestane-3α,7α,26-triol.

ring system. Thus, introduction of an hydroxyl group in the ring system greatly increased the polarity of the compound. On the other hand, the retention volume changed only slightly when a bile alcohol and the corresponding bile acid were injected. The retention volumes were highly reproducible and remained within a 2% range when fresh solvent system was used for analysis. Less than 2 μg of the bile acid or bile alcohol could be detected and the detection limit for THCA and 5β-cholestane-3α,7α,12α,26-tetrol was as low as 0.5 μg. In order to isolate bile acids or bile alcohols for biological experiments, 200 μg of each compound could be injected onto the column without appreciable loss of resolution.

It was found that the polarity of the solvent system had profound effect on the retention volumes of the various compounds and the effect was more pronounced for the less polar compounds which were eluted later. Thus, as shown in Table I, reducing the volume of acetonitrile from 75 ml in the solvent system C to 70 ml in system B substantially increased the retention volumes for all compounds and 25*S* and 25*R* diastereoisomers of 5β-cholestane-3α,7α,26-triol were eluted at approximately 143 and 157 ml, respectively. Although the two diastereoisomers of 5β-cholestane-3α,7α,26-triol were very well resolved in this system, the large retention volumes resulted in broad peaks. Further reduction in the amount of acetonitrile in the solvent system (system A) resulted in very high retention volumes for both 5β-cholestane-3α,7α,26-triol and DHCA but the system was quite suitable for the resolution of the diastereoisomers of 5β-cholestane-3α,7α,12α,26-tetrol and THCA. Obviously, larger retention volumes resulted in better resolution between the two diastereoisomers of all compounds. We found that although systems C and D could be employed for the

TABLE I

HPLC RETENTION VOLUMES OF THE DIASTEREOISOMERIC BILE ACIDS AND BILE ALCOHOLS

Bile acids and bile alcohols were subjected to HPLC on a μBondapak 5 μm reversed-phase C_{18} column. For HPLC operating conditions, see Experimental. Solvent systems: (A) acetonitrile–water–methanol–acetic acid (60:70:20:1, v/v), flow-rate, 2.5 ml/min; (B) acetonitrile–water–methanol–acetic acid (70:70:20:1, v/v), flow-rate, 2.5 ml/min; (C) acetonitrile–water–methanol–acetic acid (75:70:20:1, v/v), flow-rate, 3 ml/min; (D) acetonitrile–water–methanol–acetic acid (80:70:20:1, v/v), flow-rate, 3 ml/min.

Compound	HPLC retention volume (ml)			
	A	B	C	D
5β-Cholestane-3α,7α,26-triol (25*R*)	–	157.1	123.1	108.1
5β-Cholestane-3α,7α,26-triol (25*S*)	–	143.0	112.3	98.8
5β-Cholestane-3α,7α,12α,26-tetrol (25*R*)	79.5	52.0	42.8	37.6
5β-Cholestane-3α,7α,12α,26-tetrol (25*S*)	72.4	47.6	39.4	34.7
DHCA (25*R*)	–	124.2	96.8	82.5
DHCA (25*S*)	–	112.2	87.8	74.6
THCA (25*R*)	68.6	43.8	35.5	31.1
THCA (25*S*)	63.1	40.4	32.9	28.7

resolution and characterization of all compounds, systems A and B were more suited for the isolation of pure diastereoisomers of 5β-cholestane-3α,7α,12α,26-tetrol and THCA and baseline resolutions were obtained when 10–200 μg of the diastereoisomeric mixtures were injected into the column.

ACKNOWLEDGEMENTS

This work was supported by U.S. Public Health Service grants HL-17818, DK-18907 and DK-26757.

REFERENCES

1 H. Danielsson, in P. P. Nair and D. Kritchevsky (Editors), *The Bile Acids, Vol. 2, Physiology and Metabolism*, Plenum Press, New York, 1973, p. 1.
2 S. Shefer, F. W. Cheng, B. Dayal, S. Hauser, G. S. Tint, G. Salen and E. H. Mosbach, *J. Clin. Invest.*, 57 (1976) 897.
3 S. Kurori, K. Shimazu, M. Kuwabara, M. Une, K. Kihira, T. Kuramoto and T. Hoshita, *J. Lipid Res.*, 26 (1985) 230.
4 J. B. Carey, Jr. and G. A. D. Haslewood, *J. Biol. Chem.*, 238 (1963) 855.
5 R. F. Hanson, J. N. Isenberg, G. C. Williams, D. Hachey, P. Szczepanik, P. D. Klein and H. L. Sharp, *J. Clin. Invest.*, 56 (1975) 577.
6 H. Eyssen, G. Parmentier, F. Compernolle, J. Boon and E. Eggermont, *Biochim. Biophys. Acta*, 273 (1972) 212.
7 B. F. Kase, I. Bjorkhem, P. Haga and J. I. Pedersen, *J. Clin. Invest.*, 75 (1984) 427.
8 G. A. D. Haslewood, *J. Biol. Chem.*, 52 (1952) 583.
9 A. K. Batta, G. Salen, F. W. Cheng and S. Shefer, *J. Biol. Chem.*, 254 (1979) 11907.
10 A. K. Batta, G. Salen, S. Shefer, B. Dayal and G. S. Tint, *J. Lipid Res.*, 24 (1983) 94.
11 A. K. Batta, G. Salen, J. F. Blount and S. Shefer, *J. Lipid Res.*, 20 (1979) 935.
12 B. Dayal, A. K. Batta, S. Shefer, G. S. Tint, G. Salen and E. H. Mosbach, *J. Lipid Res.*, 19 (1978) 191.
13 B. Dayal, A. K. Batta, S. Shefer, G. S. Tint and G. Salen, *Steroids*, 32 (1978) 337.

Journal of Chromatography, 542 (1991) 189–192
Elsevier Science Publishers B.V., Amsterdam

CHROM. 23 083

Short Communication

Stereochemical analysis of a leukotriene related hydroxypentadecadiene using a chiral high-performance liquid chromatography column and diode array detection

DAVID M. RACKHAM* and GEORGINA A. HARVEY
Lilly Research Centre Ltd., Eli Lilly & Co., Erl Wood Manor, Windlesham, Surrey GU20 6PH (U.K.)
(First received October 5th, 1990; revised manuscript received December 11th, 1990)

ABSTRACT

A high-performance liquid chromatographic separation of the chiral isomers of a leukotriene related hydroxypentadecadiene has been achieved using a chiral protein column which permits low levels of the undesired distomer to be measured in the eutomer. Diode array and proton magnetic resonance analytical methods were used to confirm their diene stereochemistry and that of a related impurity produced in trace amounts in the synthesis.

INTRODUCTION

The chiral hydroxypentadecadiene **Ia** is a leukotriene antagonist which is potentially useful in the treatment of asthma [1].

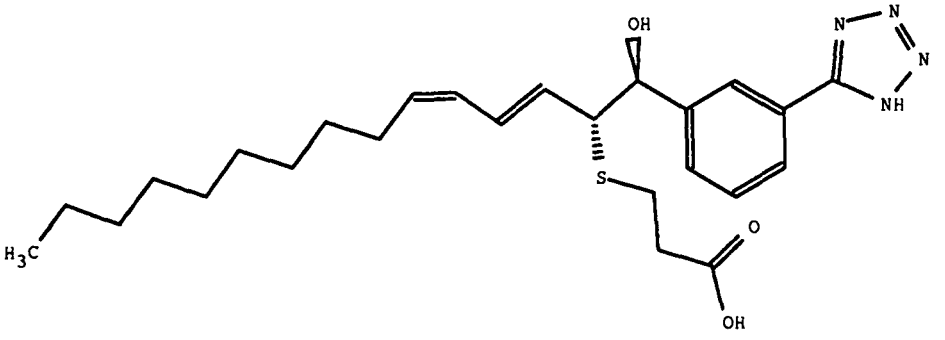

a. 5-(3-[2(R)-(carboxyethylthio)-1(S)-hydroxypentadeca-3(E),5(Z)-dienyl]-phenyl-1H-tetrazole.

0021-9673/91/$03.50

With the current importance [2,3] of the chiral purity of new drug substances in mind we have developed a high-performance liquid chromatographic procedure which separates the enantiomeric forms of this *cis–trans* diene (**Ia,b**) and allows the pharmacologically undesirable (distomer) impurity (**Ib**) in the eutomer (**Ia**) to be monitored to less than 0.5%. The HPLC analysis also shows the presence of any of the analogous *trans–trans* diene isomer **II** which has the same 2(*R*),1(*S*) configuration as **Ia** and is the most likely geometrical impurity.

Early attempts to separate the underivatised chiral isomers of **Ia,b** using α-, β- or γ-cyclodextrin columns were unsuccessful. Chemical derivatisation with diazomethane to mask the acid function was also unhelpful and led only to a complex mixture of methylation products. A more successful derivatisation of **Ia,b** was performed by reaction of the carboxyl group with chiral α-methylbenzylamine [4] and separation of the resultant diastereomeric mixture with a non-chiral, unbonded silica column. The latter method, however, involves an overnight chemical reaction followed by a 40-min HPLC analysis time. In addition it does not offer an absolute method of determining low distomer impurity levels because of the uncertain chiral purity of commercial α-methylbenzylamine and the risk of epimer formation during derivatisation.

EXPERIMENTAL

High-performance liquid chromatography

The chromatographic system consisted of a Spectra-Physics SP 8800 pump and Spectra 200 detector (Spectra-Physics, Hemel Hempstead, U.K.). The eluent (acetonitrile–water (50:50) with 0.1% acetic acid) was pumped at 0.9 ml/min. The column was a chiral AGP (Chrom Tech, Norsborg, Sweden; dimensions 100 × 4 mm) and the analyte concentration was 100 μg/ml (2 μg injected on column).

Diode array detection

The diode array detector was a Hewlett-Packard Model 1040A (Hewlett-Packard, Wokingham, U.K.) consisting of 205 diodes together with a Hewlett-Packard series 9000/300 computing system.

Proton magnetic resonance spectra

The spectra were measured on a Bruker AM 300 spectrometer at 300 MHz using [$^2H_4$]methanol as solvent (Bruker Spectrospin, Coventry, U.K.).

RESULTS AND DISCUSSION

Experiments with the recently developed α_1-acid glycoprotein chiral column (Chiral AGP) [5] on the underivatised hydroxypentadecadienes were immediately successful. Using the conditions described above, a mixture containing 66.0% of the eutomer **Ia** and 30.8% of the distomer **Ib** was baseline resolved and clearly separated from the *trans–trans* diene chiral impurity (**II**, 3.2%). The total HPLC run time was less than 5 min.

The diene stereochemistries in **Ia,b** and **II** were clearly revealed by the vicinal alkene couplings in their high field (300 MHz) proton magnetic resonance spectra and by a diode array analysis of the three peaks marked in Fig. 1.

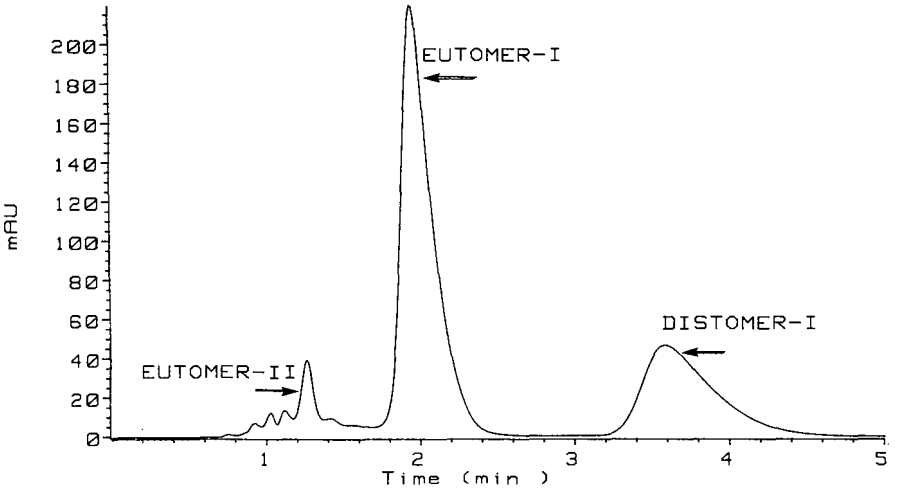

Fig. 1. HPLC separation of the eutomer and distomer of **I** (**Ia,b**) and of the related diene impurity **II** using Chiral AGP column. Eluent, acetonitrile–water (50:50) with 0.1% acetic acid.

The wavelength maxima for the two chiral isomers of **Ia,b** were, as expected, identical but the maximum for the diene stereoisomer **II** showed a small hypsochromic shift of 2 nm (Fig. 2). This shift agrees well with that reported for pairs of *cis–trans* and *trans–trans* diene systems [6].

Typical synthesised batches of the pure chiral hydroxypentadecadiene **Ia** were found to contain less than 1% of the distomer (**Ib**) and less than 1% of the *trans–trans* diene **II**.

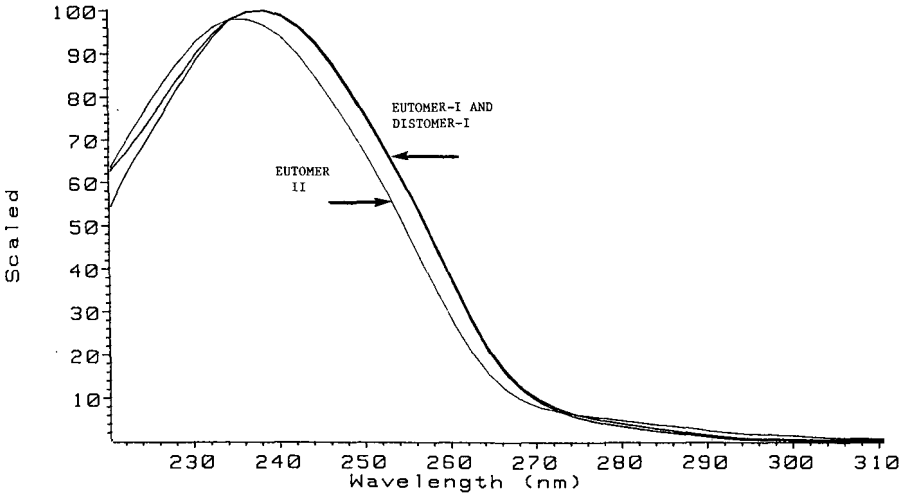

Fig. 2. Diode array analysis of the eutomer and distomer of **I** (**Ia,b**) and the related diene impurity **II** using a Hewlett-Packard 1040A detector.

ACKNOWLEDGEMENTS

We thank members of the Anti-Allergy group for supplying samples of the hydroxypentadecadienes and Ms. C. Burt for discussion of the chemical derivatisation.

REFERENCES

1 J. R. Boot, A. Bond, R. Gooderham, A. O'Brien, M. Parsons and K. Thomas, *Br. J. Pharmacol.*, 98 (1989) 259.
2 W. H. De Camp, *Chirality*, 1 (1989) 2.
3 D. B. Campbell, *Eur. J. Drug. Metab. Pharmacokinet.*, 15 (1990) 109.
4 S. W. McKay, D. N. B. Mallen, P. R. Shrubsall, B. P. Swann and W. R. N. Williamson, *J. Chromatogr.*, 170 (1979) 482.
5 J. Hermansson, *Trends Anal. Chem.*, 8 (1989) 251.
6 R. Grinter and T. L. Threlfall, *Tetrahedron*, 35 (1979) 1543.

Journal of Chromatography, 542 (1991) 193–199
Elsevier Science Publishers B.V., Amsterdam

CHROM. 23 014

Short Communication

Determination of isoquinoline alkaloids in *Chelidonium majus* L. by ion-pair high-performance liquid chromatography

CHANG-QUN NIU* and LI-YI HE
Institute of Materia Medica, Chinese Academy of Medical Sciences, 1 Xian Nong Tan Street, Beijing 100050 (China)
(First received June 6th, 1990; revised manuscript received November 30th, 1990)

ABSTRACT

A simple and precise method using ion-pair high-performance liquid chromatography was developed for the simultaneous determination of eight isoquinoline alkaloids, namely chelidonine, berberine, protopine, coptisine, tetrahydrocoptisine, 6-methoxydihydrochelerythrine, 6-methoxydihydrosanguinarine and dihydrosanguinarine, in *Chelidonium majus* L.. A reversed-phase system consisting of a chemically bonded ODS silica gel column and 0.05 *M* tartaric acid–methanol–acetonitrile (44:10:46) containing 0.5% sodium dodecyl sulphate as the mobile phase was used. The eight alkaloids were completely separated within 40 min. The analytical results for various samples are presented.

INTRODUCTION

Chelidonium majus L. is one of the most important medicinal plants in the Papaveraceae, owing to its chemically and pharmacologically interesting alkaloids. Its biologically active components are mainly isoquinoline alkaloids [1]. The clinical use of *C. majus* dates back to 1896 when Botkin reported two cases of carcinoma which responded to treatment with *C. majus* extracts [10]. Subsequent clinical reports include the use of chelidonine sulphate for gastric cancer and *C. majus* extracts for breast cancer, and in other clinical trials [2]. In China, *C. majus* has intensive clinical used. It is used to cure whooping cough and chronic bronchitis and as an analgesic, the effective rates being 94.5%, 95.3% and 96%, respectively [3]. Each individual alkaloid has its own medical uses. Therefore, the determination of the individual alkaloids is important in evaluating the quality and developing and utilizing the resources of *C. majus*.

To data, there have beeen only three reports on the separation and determination of isoquinoline alkaloids in *C. majus* by high-performance liquid chromatogra-

0021-9673/91/$03.50

phy (HPLC). Freytay [4] put forward two alternative methods and analysed only three alkaloids, chelidonine, sanguinarine and chelerythrine. For the determination of quaternary alkaloids in *C. majus*, Bugatti *et al.* [5] employed several methods, including reversed-phase and ion-pair chromatography, but the results were not satisfactory. Finally they chose normal-phase HPLC to determine berberine, sanguinarine and chelerythrine. Dzido [6] used di(2-ethylhexyl) orthophosphate as the ion-pair reagent in reversed-phase HPLC and separated allocryptopine, protopine and chelidonine, but the resolution was not complete. Other methods have also been employed to determine analyse *C. majus*, such as thin-layer chromatography (TLC) [7], high-performance, TLC [8] and capillary isotachophoresis [9]. All these methods can determine only three or four alkaloids. In order to determine the content of more alkaloids rapidly and precisely, it is necessary to establish a new method.

EXPERIMENTAL

Plant materials

C. majus was collected in the Botanical Garden of the Institute of Medicinal Plant Development, Chinese Academy of Medical Sciences, Beijing, and other locations in July, 1989.

Apparatus

A Shimadzu 4A liquid chromatograph equipped with an SPD-2AS UV spectrophotometric detector and linked to a C-R_2AX data processor was used. A stainless-steel column (250 mm × 4 mm I.D.) packed with chemically bonded ODS silica gel (YWG-C_{18}, 10 μm) (Tianjin Second Chemical Reagent Factory, Tianjin, China) was employed.

Reagents

Eight alkaloid standards were provided by Professor Qi-cheng Fang of this Institute. The ion-pair reagents, namely sodium decyl sulphate, sodium dodecyl sulphate (SDS) and tetradecyl sulphate, were supplied by Wako (Osaka, Japan) and stilbene (internal standard) by Beijing Chemical Factor (Beijing, China). Acetonitrile of chromatographic grade was used.

HPLC conditions

Acetonitrile–methanol–0.05 *M* tartaric acid (46:10:44) containing 0.5% SDS was used as the mobile phase. The temperature was ambient (20–25°C) and the flow-rate was 1.0 ml/min. The substances eluted were detected with a UV detector operated at 290 nm.

Assay procedure

C. majus dry powder (0.5 g) was immersed in 5 ml of chloroform–ethanol (1:1), then macerated for 12 h and ultrasonicated for 30 min. After clarification (lay aside), the upper solution was retained and internal standard (2 ng/μl) was added. A 1-μl volume of this solution was injected into the HPLC system. The content of each alkaloid was calculated by the internal standard method.

Calibration graphs, precision and detection limits

A set of eight standard solutions containing between 0.01 and 0.28 mg/ml of each alkaloid were prepared. These were injected into the HPLC system to obtain data for calibration graphs, precision and detection limits.

RESULTS AND DISCUSSION

HPLC conditions

Elution parameters such as the organic content of the mobile phase, the kind and concentration of the counter ion and pH were varied to establish the optimum elution conditions on chemically bonded ODS silica gel.

When only buffer solution and acetonitrile were used as mobile phase components, complete resolution could not be achieved. It was found that a certain amount of methanol was necessary. As acetonitrile exerted the main role in the mobile phase, its concentration was examined (see Fig. 1). An increase in acetonitrile concentration caused a decrease in the capacity factors of eight alkaloids. The optimum separation was obtained at 46% acetonitrile.

As regards the kind of counter ion, alkyl sulphates were examined. Sodium decyl sulphate could not separate two alkaloids (coptisine and tetracoptisine), and sodium tetradecyl sulphate required too long a time and gave unsatisfactory peak shapes. The optimum separation was obtained with SDS (Fig. 2). The SDS concentration in the mobile phase was varied from 0.3 to 0.6%. As the SDS concentration

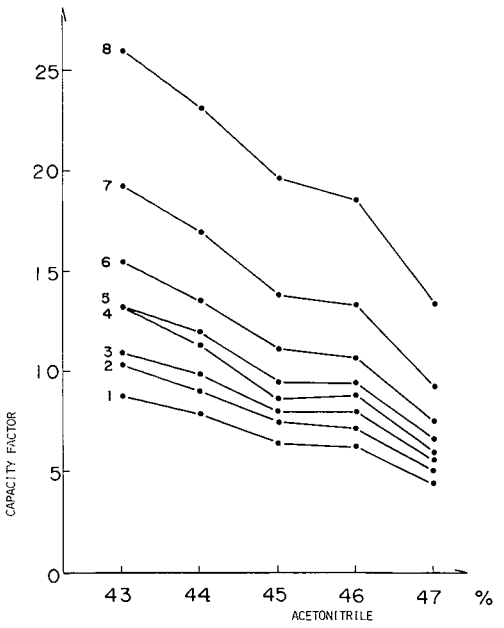

Fig. 1. Effect of acetonitrile concentration on capacity factor. 1 = Protopine; 2 = chelidonine; 3 = coptisine; 4 = tetrahydrocoptisine; 5 = 6-methoxydihydrosanguinarine; 6 = berberine; 7 = 6-methoxydihydrochelerythrine; 8 = dihydrosanguinarine.

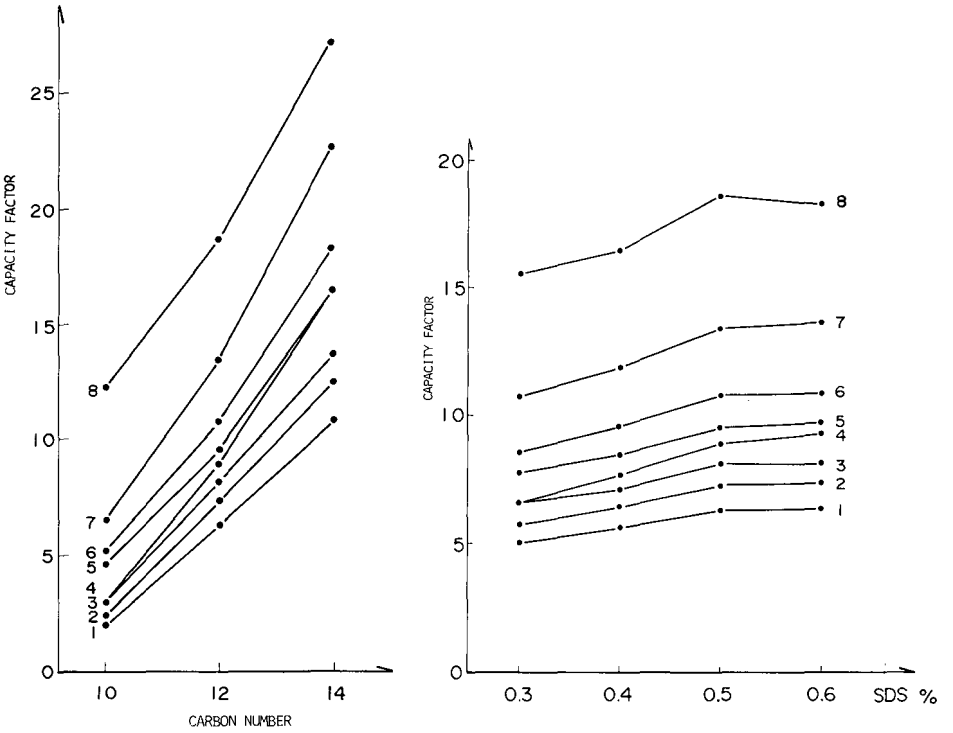

Fig. 2. Effect of the carbon number of alkyl sulphate on capacity factor. 1 = Protopine; 2 = chelidonine; 3 = coptisine; 4 = tetrahydrocoptisine; 5 = 6-methoxydihydrosanguinarine; 6 = berberine; 7 = 6-methoxydihydrochelerythrine; 8 = dihydrosanguinarine.

Fig. 3. Effect of SDS concentration on capacity factor. 1 = Protopine; 2 = chelidonine; 3 = coptisine; 4 = tetrahydrocoptisine; 5 = 6-methoxydihydrosanguinarine; 6 = berberine; 7 = 6-methoxydihydrochelerythrine; 8 = dihydrosanguinarine.

increased, the capacity factors became larger. The most suitable concentration was 0.5% SDS (Fig. 3).

The pH of the mobile phase strongly affected the retention times. When the concentration of tartaric acid changed from 0.05 to 0.04 *M*, the capacity factors became too large and caused incomplete separation of several alkaloids. It was proved that a decrease in acid concentration was not favourable for the separation, but a suitable pH of the chemically bonded ODS column is 2–8. When 0.05 *M* tartaric acid was added to the mobile phase in the proportion of 44%, the pH of the mobile phase was 2.1, so we selected 0.05 *M* tartaric acid for use in the mobile phase.

Finally, a mobile phase consisting of 0.05 *M* tartaric acid–methanol–acetonitrile (44:10:46) containing 0.5% SDS was selected optimum for the separation of these alkaloids.

Extraction conditions

The extraction efficiency for the eight isoquinoline alkaloids was examined us-

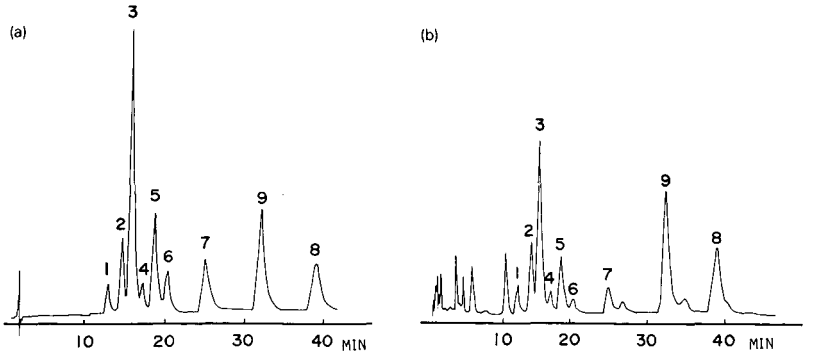

Fig. 4. Chromatograms of (a) standards and (b) alkaloid extract of subterrean parts from *C. majus*. 1 = Protopine; 2 = chelidonine; 3 = coptisine; 4 = tetrahydrocoptisine; 5 = 6-methoxydihydrosanguinarine; 6 = berberine; 7 = 6-methoxydihydrochelerythrine; 8 = dihydrosanguinarine. Mobile phase: 0.05 *M* tartaric acid–methanol–acetonitrile (44:10:46) containing 0.5% SDS. Flow-rate: 1 ml/min. Injection volume: 1 μl.

ing different solvents, *viz.*, chloroform, ethanol and chloroform–ethanol (1:1, v/v). The most efficient solvent was found to be chloroform–ethanol (1:1, v/v). Using this extraction solvent, we then compared the heating extraction method with the macerating extraction method. The two methods gave the same extraction efficiency for four isoquinoline alkaloids, but not for tetrahydrocoptisine, 6-methoxydihydrochelerythrine, 6-methoxydihydrosanguinarine and dihydrosanguinarine. As these alkaloids are readily oxidized to the quaternary analogues, the heating extraction efficiency was lower than that of the macerating method.

Finally, we compared different times of ultrasonic irradiation. The optimum extraction conditions were chosen, namely chloroform–ethanol (1:1, v/v) as extraction solvent, then macerating for 12 h and ultrasonicating for 30 min. This extraction method was applied under neutral conditions (pH 7). The recoveries of berberine, coptisine, protopine, chelidonine, 6-methoxidihydrocherythrine, tetrahydrocoptisine, 6-methoxydihydrosanguinarine and dihydrosanguinarine were 102, 101, 103, 102, 97, 95, 96 and 97%, respectively.

TABLE I

DATA FOR CALIBRATION GRAPHS

Alkaloid	Regression equation[a]	Correlation coefficient, *r*	Linear range (μg/ml)
Protopine	$y = 4.983x - 0.01596$	0.9997	15–150
Chelidonine	$y = 1.670x + 0.03617$	0.9997	28–256
Coptisine	$y = 9.111x - 0.00562$	0.9995	29–260
Tetrahydrocoptisine	$y = 4.925x - 0.00423$	0.9999	15–150
6-Methoxydihydrosanguinarine	$y = 17.20\ x - 0.3340$	0.9997	18–180
Berberine	$y = 9.216x - 0.2810$	0.9995	15–150
6-Methoxydihydrochelerythrine	$y = 14.40\ x - 0.3825$	0.9999	16–160
Dihydrosanguinarine	$y = 25.60\ x - 0.3750$	0.9998	13–130

[a] x = Content (μg/ml); y = peak area.

TABLE II

PRECISION AND DETECTION LIMITS FOR THE EIGHT ALKALOIDS

Alkaloid	Mean ± S.D. (μg) (n = 8)	Relative standard deviation (%)	Detection limit	
			Standard (ng)	Sample (μg)[a]
Protopine	0.304 ± 0.0056	1.8	10	102
Chelidonine	0.549 ± 0.0098	1.8	24	245
Coptisine	1.938 ± 0.0240	1.2	5	50
Tetrahydrocoptisine	2.215 ± 0.0420	1.9	10	105
6-Methoxydihydro-sanguinarine	1.422 ± 0.0150	1.1	6	63
Berberine	0.791 ± 0.0260	3.3	5	50
6-Methoxydihydro-chelerythrine	0.956 ± 0.3490	3.7	5	52
Dihydrosanguinarine	1.053 ± 0.0190	1.8	4	42

[a] Per gram of plant material.

Analytical results

Fig. 4 illustrates the chromatograms of standards and extracts of subterranean parts of *C. majus*. The data for the calibration graphs and precision are shown in Tables I and II. The detection limits were determined at a signal-to-noise ratio of 3:1 for the peak heights (Table II). Table III gives the analytical results for samples collected in different locations. The results indicate that the individual contents of the alkaloids differ widely with plant location. The total amounts of alkaloids vary from 0.8 to 2.0%. Chelidonine and coptisine are the main components of the subterranean parts of *C. majus*, the others being minor components.

TABLE III

ALKALOID CONTENTS (%) OF SUBTERRANEAN PARTS OF *C. MAJUS* COLLECTED IN DIFFERENT LOCATIONS

Alkaloid	Jilin	Liaoning	Chengde	Juyongguan	Beijing
Protopine	0.022	0.020	Trace	0.029	0.114
Chetidonine	1.020	0.503	0.889	1.010	0.767
Coptisine	0.578	0.155	0.394	0.415	0.336
Tetrahydrocoptisine	Trace	Trace	0.064	Trace	Trace
6-Methoxydihydrosanguinarine	0.107	0.081	0.117	0.151	0.110
Berberine	0.035	Trace	Trace	0.034	0.038
6-Methoxydihydrochelerythrine	0.123	0.081	0.106	0.198	0.142
Dihydrosanguinarine	0.051	0.019	0.095	0.042	0.053
Total alkaloids	1.936	0.859	1.665	1.879	1.560

CONCLUSIONS

The reversed-phase ion-pair HPLC method developed is simpler, faster and more accurate than previous methods. It has several advantages over other methods: first, it is an isocratic HPLC system; second, no pretreatment is required except for extraction; and third, for the first time, eight alkaloids with very different polarities have been separated and determined. This method will be important and useful in developing and utilizing the resources of *C. majus*.

ACKNOWLEDGEMENT

The authors thank Professor Tong-hui Zhou, the Director of the Department, for comments on the manuscript.

REFERENCES

1 J. Slavik and L. Slavikova, *Collect. Czech. Chem. Commun.*, 42 (1977) 2686.
2 G. A. Cordell and N. R. Farnsworth, *Heterocycles*, 4 (1976) 406.
3 C.-C. Zhang, *J. Chin. Med. Mater.*, 5 (1987) 46.
4 W. E. Freytay, *Dtsch. Apoth.-Ztg.*, 126 (1986) 1113.
5 C. Bugatti, M. L. Colombo and F. Tome, *J. Chromatogr.*, 393 (1987) 312.
6 T. Dzido, *J. Chromatogr.*, 439 (1988) 257.
7 C. Scholz, R. Haensel and C. Hille, *Pharm. Ztg.*, 121 (1976) 1571.
8 W. E. Freytag, *Planta Med.*, 40 (1980) 278.
9 D. Walterova, V. Preininger and V. Simanek, *Planta Med.*, 50 (1984) 149.
10 H. P. Pim, N. R. Farmsworth, R. N. Blomster and H. H. S. Fong, *J. Pharm. Sci.*, 58 (1969) 372.

Journal of Chromatography, 542 (1991) 200–203
Elsevier Science Publishers B.V., Amsterdam

CHROM. 23 036

Short Communication

High-performance liquid chromatographic determination of the antibiotic cortalcerone

JIŘÍ GABRIEL*, OLDŘICH VACEK, ELENA KUBÁTOVÁ and JINDŘICH VOLC
Institute of Microbiology, Czechoslovak Academy of Sciences, Vídeňská 1083, 142 20 Prague 4 (Czechoslovakia)
(First received September 13th, 1990; revised manuscript received November 28th, 1990)

ABSTRACT

Cortalcerone (2-hydroxy-6*H*-3-pyrone-2-carboxaldehyde hydrate) is an antibacterial antibiotic produced by a number of basidiomycetous fungi. Its biosynthesis is connected with C-2 oxidation of D-glucose. A method for the reliable determination of this antibiotic is required for the study of the mechanism of its biosynthesis and for the determination of its pharmacological properties. The high-performance liquid chromatographic determination of cortalcerone in the presence of D-glucose, D-fructose, D-*arabino*-2-hexosulose, D-gluconic acid and D-*arabino*-2-hexulosonic acid on an amino-phase column with 70% aqueous acetonitrile (pH 5.00) and UV detection at 195 nm is reported. A linear relationship between response and cortalcerone concentration was found in the range 0.25–10.00 mg/ml. The detection limit is 6.5 μg/ml.

INTRODUCTION

Cortalcerone, an antibacterial antibiotic produced by a number of basidiomycetous fungi [1,2], is a β-pyrone compound unusual in nature, 2-hydroxy-6*H*-3-pyrone-2-carboxaldehyde hydrate (Fig. 1). Its biosynthesis starts from D-glucose and consists of two enzymatic steps; in the first step; *D*-glucose is oxidized by the action of the enzyme pyranose 2-oxidase into D-*arabino*-2-hexosulose (D-glucosone) [3], which is then dehydrated to cortalcerone by a new enzyme, pyranosone dehydratase [4] via putative unstable intermediates that have not yet been identified.

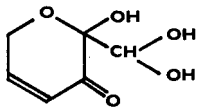

Fig. 1. Structure of cortalcerone.

0021-9673/91/$03.50

A method for the reliable determination of cortalcerone is required for the study of the mechanism of its biosynthesis. High-performance liquid chromatography (HPLC) on silica [5], ion-exchange [6], reversed-phase [7] or amino-phase [8] columns has often been used for the determination of sugars and/or their derivatives in natural samples. The separation of sugars on various stationary phases has been reviewed and discussed in detail [9,10]. For cortalcerone, only a qualitative thin-layer chromatographic assay is available [2].

A simple HPLC method has been devised for the determination of cortalcerone in the presence of D-glucose, D-fructose, D-*arabino*-2-hexosulose, D-gluconic acid and D-*arabino*-2-hexulosonic acid using an amino-phase column and UV photometric detection. The method was used to examine the time course of cortalcerone production by the washed intact mycelium of the basidiomycete *Phanerochaete chrysosporium* during incubation with a solution of pure D-glucose.

EXPERIMENTAL

Chemicals

Cortalcerone was isolated [11] from submerged cultures of the basidiomycete *Phanerochaete chrysosporium* (CCBAS 571, Culture Collection of Basidiomycetes, Institute of Microbiology, Prague (Czechoslovakia) by a procedure described by Baute *et al.* [1]. D-*arabino*-2-hexosulose was synthesized enzymatically [12] from D-glucose. D-Glucose was obtained from Fluka (Buchs, Switzerland), D-fructose was of analytical-reagent grade from Lachema (Brno, Czechoslovakia), sodium D-gluconate was purchased from Koch-Light Labs. (Haverhill, U.K.) and calcium D-*arabino*-2-hexulosonate from Merck (Darmstadt, Germany).

Sample preparation

All standards were prepared as aqueous solutions of concentration 10 mg/ml unless noted otherwise. The time course of cortalcerone production was studied as follows: 10 g of washed intact mycelium of the basidiomycete *Phanerochaete chrysosporium* were suspended in 50 ml of a 2% aqueous solution of D-glucose. The suspension was shaken at 20°C for 48 h, than 100-μl samples of liquid were taken and, after filtration through an Acrodisc 13 disposable filter unit (Gelman Sciences, Ann Arbor, MI, U.S.A.), 10-μl aliquots were chromatographed.

Column liquid chromatography

An HP 1090 liquid chromatograph with a diode-array detector (Hewlett-Packard, Amstelveen, The Netherlands) was used. For quantitative purposes compounds were detected at 195 nm. The separation was performed on an analytical column (200 mm × 4 mm I.D.) packed with Separon SGX NH_2, 7 μm (Tessek, Prague, Czechoslovakia). The mobile phase was acetonitrile–water (70:30) of pH 5.0 adjusted by addition of 0.1 *M* phosphate buffer (1 ml of buffer to 1 l of the mobile phase), at a flow-rate of 1.5 ml/min. Quantification was performed by recording the ratio of the peak area to that of calibration standards of cortalcerone injected directly into the HPLC column.

Precision and reproducibility studies

The precision and linearity were validated by analysing ten calibration standards containing 0–10.00 mg/ml of cortalcerone in triplicate over 48 h. The reproducibility of the peak-area ratios over the calibration range, expressed as relative standard deviation (R.S.D.), ranged from 5.2 to 7.0%. The R.S.D. of the peak-area ratio was determined at each concentration level of the calibration graph. The slope and the correlation coefficient of the calibration graphs were also calculated.

RESULTS AND DISCUSSION

Cortalcerone is a relatively unstable compound that recyclizes spontaneously to 2-furylglyoxal. In the pH range 5.0–7.0 cortalcerone forms an equilibrium mixture with 2-furylglyoxal which contains 85.6% of cortalcerone. These solutions are stable for 2 days under laboratory conditions. The heat lability of cortalcerone precludes the use of ion-exchange columns which are usually operated at elevated temperatures. For this reason and the earlier successful separation of D-*arabino*-2-hexosulose on an amino-bonded column [8], this type of stationary phase was chosen. The formation of Schiff bases of carbonyl compounds with the column packing [13] can be overcome by using a mobile phase buffered on the acidic side.

Dicarbonyl sugars in solution possess a number of tautomeric forms [14,15]. To check possible complications resulting from different chromatographic behaviours of different forms of D-*arabino*-2-hexosulose, we sampled aliquots of solutions prepared in 0.1 *M* acetate buffers of pH 4.0, 4.5, 5.0, 5.5, 6.0 and 6.5 after equilibration for 2 h. Comparison of the chromatograms showed that negligible changes in the retention time and peak area of D-*arabino*-2-hexosulose occurred. As D-*arabino*-2-hexosulose decomposes in the presence of trace amounts of a base [16], the mobile phase should be buffered on the acidic side.

D-Glucose and D-*arabino*-2-hexosulose coelute when the mobile phase is not buffered or when phosphate buffer of pH 6.0 is used. Considering the stability of cortalcerone and D-*arabino*-2-hexosulose, a mobile phase of pH 5.0 was adopted. In the concentration region between 60 and 80% of acetonitrile in the mobile phase, the best resolutions of both D-glucose–D-*arabino*-2-hexosulose and cortalcerone–2-furyl-

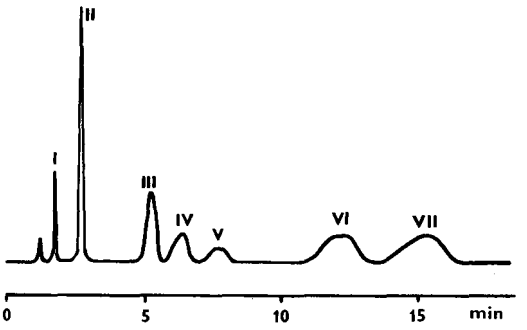

Fig. 2. Chromatogram of (I) 2-furylglyoxal, (II) cortalcerone, (III) D-fructose, (IV) D-glucose, (V) D-*arabino*-2-hexosulose, (VI) D-*arabino*-2-hexulosonic acid and (VII) D-gluconic acid using UV detection at 195 nm.

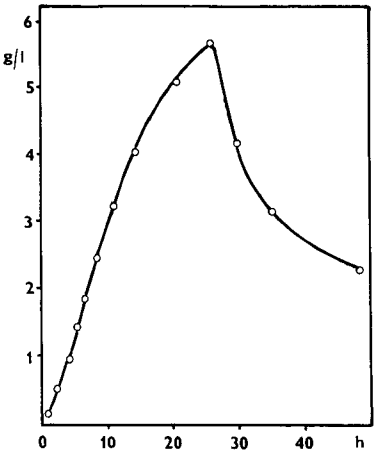

Fig. 3. Production curve of cortalcerone by the washed intact mycelium of the basidiomycete *Phanerochaete chrysosporium*.

glyoxal were obtained when 70% of acetonitrile of pH 5.0 was used; reliable measurements were then achieved.

Fig. 2 shows the measurement of cortalcerone using UV detection at 195 nm in the presence of D-glucose, D-fructose, D-*arabino*-2-hexosulose, D-gluconic acid and D-*arabino*-2-hexulosonic acid. These compounds could play a role in the biochemical oxidation of D-glucose in fungi. A linear relationship was found between the peak area at 195 nm and the cortalcerone concentration in the range 0.25–10.00 mg/ml (slope 0.267 absorbance/μg, correlation coefficient 0.9995, R.S.D. 6.3% from five parallel determinations). At a signal-to-noise ratio of 3, the detection limit was found to be 6.5 μg/ml.

The method was used to determine the time course of cortalcerone production by the washed intact mycelium of the basidiomycete *Phanerochaete chrysosporium*. The production curve is shown in Fig. 3. The maximum cortalcerone concentration was found after incubation for 26 h.

REFERENCES

1 R. Baute, M. A. Baute, G. Deffieux and M. J. Filleau, *Phytochemistry*, 15 (1976) 1753.
2 M. A. Baute and R. Baute, *Phytochemistry*, 23 (1984) 271.
3 J. Volc and K. E. Eriksson, *Methods Enzymol.*, 161 (1988) 316.
4 R. Baute, M. A. Baute and G. Deffieux, *Phytochemistry*, 26 (1987) 1395.
5 M. B. Blanc, G. E. Davis, J. M. Parchet and R. Viani, *J. Agric. Food Chem.*, 37 (1989) 926.
6 D. P. Lee and M. T. Bunker, *J. Chromatogr. Sci.*, 27 (1989) 496.
7 R. B. Meagher and A. Furst, *J. Chromatogr.*, 117 (1976) 211.
8 J. Geigert, D. S. Hirano and S. L. Neidleman, *J. Chromatogr.*, 202 (1980) 319.
9 L. A. Th. Verhaar and B. F. M. Kuster, *J. Chromatogr.*, 220 (1981) 313.
10 K. Robards and M. Whitelaw, *J. Chromatogr.*, 373 (1986) 81.
11 J. Gabriel, J. Volc, E. Kubátová and V. Musílek, *Czech. Pat.*, PV 5172-90 (1990).
12 J. Volc, P. Sedmera and V. Musílek, *Czech. Pat.*, 175 897 (1978).
13 B. B. Wheals and P. C. White, *J. Chromatogr.*, 176 (1979) 421.
14 C. E. Becker and C. E. May, *J. Am. Chem. Soc.*, 71 (1949) 1491.
15 R. S. Shallenberger and W. J. Wienen, *J. Chem. Educ.*, 66 (1989) 67.
16 B. Ericsson, B. O. Lindgren and O. Theander, *Cellulose Chem. Technol.*, 7 (1973) 581.

PUBLICATION SCHEDULE FOR 1991

Journal of Chromatography and Journal of Chromatography, Biomedical Applications

MONTH	D 1990	J	F	M	A	M	
Journal of Chromatography	535/1 + 2	536/1 + 2 537/1 + 2 538/1	538/2 539/1 539/2	540/1 + 2 541/1 + 2 542/1	542/2 543/1	543/2 544/1 + 2 545/1	The publication schedule for further issues will be published later
Cumulative Indexes, Vols. 501–550							
Bibliography Section				560/1			
Biomedical Applications		562/1 + 2 563/1	563/2	564/1	564/2 565/1 + 2	566/1 566/2	

INFORMATION FOR AUTHORS

(Detailed *Instructions to Authors* were published in Vol. 522, pp. 351–354. A free reprint can be obtained by application to the publisher, Elsevier Science Publishers B.V., P.O. Box 330, 1000 AH Amsterdam, The Netherlands.)

Types of Contributions. The following types of papers are published in the *Journal of Chromatography* and the section on *Biomedical Applications:* Regular research papers (Full-length papers), Review articles and Short Communications. Short Communmications are usually descriptions of short investigations, or they can report minor technical improvements of previously published procedures; they reflect the same quality of research as Full-length papers, but should preferably not exceed six printed pages. For Review articles, see inside front cover under Submission of Papers.

Submission. Every paper must be accompanied by a letter from the senior author, stating that he/she is submitting the paper for publication in the *Journal of Chromatography*.

Manuscripts. Manuscripts should be typed in double spacing on consecutively numbered pages of uniform size. The manuscript should be preceded by a sheet of manuscript paper carrying the title of the paper and the name and full postal address of the person to whom the proofs are to be sent. As a rule, papers should be divided into sections, headed by a caption (*e.g.*, Abstract, Introduction, Experimental, Results, Discussion, etc.). All illustrations, photographs, tables, etc., should be on separate sheets.

Introduction. Every paper must have a concise introduction mentioning what has been done before on the topic described, and stating clearly what is new in the paper now submitted.

Abstract. All articles should have an abstract of 50–100 words which clearly and briefly indicates what is new, different and significant.

Illustrations. The figures should be submitted in a form suitable for reproduction, drawn in Indian ink on drawing or tracing paper. Each illustration should have a legend, all the *legends* being typed (with double spacing) together on a *separate sheet*. If structures are given in the text, the original drawings should be supplied. Coloured illustrations are reproduced at the author's expense, the cost being determined by the number of pages and by the number of colours needed. The written permission of the author and publisher must be obtained for the use of any figure already published. Its source must be indicated in the legend.

References. References should be numbered in the order in which they are cited in the text, and listed in numerical sequence on a separate sheet at the end of the article. Please check a recent issue for the layout of the reference list. Abbreviations for the titles of journals should follow the system used by *Chemical Abstracts*. Articles not yet published should be given as "in press" (journal should be specified), "submitted for publication" (journal should be specified), "in preparation" or "personal communication".

Dispatch. Before sending the manuscript to the Editor please check that the envelope contains four copies of the paper complete with references, legends and figures. One of the sets of figures must be the originals suitable for direct reproduction. Please also ensure that permission to publish has been obtained from your institute.

Proofs. One set of proofs will be sent to the author to be carefully checked for printer's errors. Corrections must be restricted to instances in which the proof is at variance with the manuscript. "Extra corrections" will be inserted at the author's expense.

Reprints. Fifty reprints of Full-length papers and Short Communications will be supplied free of charge. Additional reprints can be ordered by the authors. An order form containing price quotations will be sent to the authors together with the proofs of their article.

Advertisements. Advertisement rates are available from the publisher on request. The Editors of the journal accept no responsibility for the contents of the advertisements.

Artificial Intelligence in Chemistry

Structure Elucidation and Simulation of Organic Reactions

by **Z. Hippe,** *Department of Physical and Computer Chemistry, I. Lukasiewicz Technical University, Rzeszów, Poland*

(Studies in Physical and Theoretical Chemistry, 73)

Coedition with and distributed in the East European Countries, China, Cuba, Mongolia and Vietnam by ARS POLONA Warsaw, Poland

This comprehensive overview of the application of artificial intelligence methods (AI) in chemistry contains an in-depth summary of the most interesting achievements of modern AI, namely, problem-solving in molecular structure elucidation and in syntheses design.

The book provides a brief history of AI as a branch of computer science. It also gives an overview of the basic methods employed for searching the solution space (thoroughly exemplified by chemical problems), together with a profound and expert discussion on many questions that may be raised by modern chemists wishing to apply computer-assisted methods in their own research. Moreover, it includes a survey of the most important literature references, covering all essential research in automated interpretation of molecular spectra to elucidate a structure and in syntheses design. A glossary of basic terms from computer technology for chemists is appended.

This book is intended to make the emerging field of artificial intelligence understandable and accessible for chemists, who are not trained in computer methods for solving chemical problems. The author discusses step-by-step basic algorithms for structure elucidation and many aspects of the automated design of organic syntheses in order to integrate this fascinating technology into current chemical knowledge.

Contents: **Part 1. Introduction to problem-solving in artificial intelligence.** 1. Historical and bibliographical remarks. 2. Problem-solving and artificial intelligence. 3. Knowledge and state-space representation. Unordered search methods. 4. Problem reduction. Ordered search methods. 5. Expert systems. **Part 2. Problem-solving in structure elucidation.** 6. Heuristic interpretation of one spectrum. 7. Heuristic interpretation of set of spectra. **Part 3. Problem-solving in synthesis design.** 8. Basic concepts in computer-assisted design of synthesis. Principal components of CASD systems. 9. Structure perception. 10. Selection of strategy in CASD. Evaluation of reactions and synthetic pathway. **Appendix A. Glossary of terms. Appendix B. Compilation of references on computer systems for structure elucidation and prediction of organic reactions.**

1991 xiv + 272 pages
Price: Dfl. 240.00 / US$137.00
ISBN 0-444-98746-0

Elsevier Science Publishers

P.O. Box 211, 1000 AE Amsterdam, The Netherlands
P.O. Box 882, Madison Square Station, New York, NY 10159, USA